Nobel Metal Nanoparticles and their Application in Electrochemical Studies

Inauguraldissertation

Zur Erlangung der Würde eines

Doktors der Philosophie

vorgelegt der

Philosophisch-Naturwissenschaftlichen Fakultät der Universität Basel

von

Ulrike Fluch

aus

Thal/Graz, Österreich

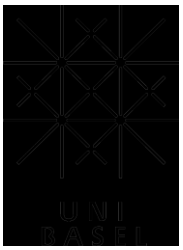

Deutschland, 2014

Genehmigt von der Philosophisch-Naturwissenschaftlichen Fakultät auf Antrag von

Prof. Dr. Marcel Mayor

Prof. Dr. Catherine Housecroft

Basel, den 22. 4. 2014

Prof. Dr. Jörg Schibler

Dekan

Namensnennung-Keine kommerzielle Nutzung-Keine Bearbeitung 3.0 Schweiz
(CC BY-NC-ND 3.0 CH)

Sie dürfen: **Teilen** — den Inhalt kopieren, verbreiten und zugänglich machen

Unter den folgenden Bedingungen:

Namensnennung — Sie müssen den Namen des Autors/Rechteinhabers in der von ihm festgelegten Weise nennen.

Keine kommerzielle Nutzung — Sie dürfen diesen Inhalt nicht für kommerzielle Zwecke nutzen.

Keine Bearbeitung erlaubt — Sie dürfen diesen Inhalt nicht bearbeiten, abwandeln oder in anderer Weise verändern.

Wobei gilt:

- **Verzichtserklärung** — Jede der vorgenannten Bedingungen kann **aufgehoben** werden, sofern Sie die ausdrückliche Einwilligung des Rechteinhabers dazu erhalten.
- **Public Domain (gemeinfreie oder nicht-schützbare Inhalte)** — Soweit das Werk, der Inhalt oder irgendein Teil davon zur Public Domain der jeweiligen Rechtsordnung gehört, wird dieser Status von der Lizenz in keiner Weise berührt.
- **Sonstige Rechte** — Die Lizenz hat keinerlei Einfluss auf die folgenden Rechte:
    - Die Rechte, die jedermann wegen der Schranken des Urheberrechts oder aufgrund gesetzlicher Erlaubnisse zustehen (in einigen Ländern als grundsätzliche Doktrin des **fair use** bekannt);
    - Die **Persönlichkeitsrechte** des Urhebers;
    - Rechte anderer Personen, entweder am Lizenzgegenstand selber oder bezüglich seiner Verwendung, zum Beispiel für **Werbung** oder Privatsphärenschutz.
- **Hinweis** — Bei jeder Nutzung oder Verbreitung müssen Sie anderen alle Lizenzbedingungen mitteilen, die für diesen Inhalt gelten. Am einfachsten ist es, an entsprechender Stelle einen Link auf diese Seite einzubinden.

Quelle: http://creativecommons.org/licenses/by-nc-nd/3.0/ch/ Datum: 12.11.2013

Was du mir sagst, das vergesse ich.
Was du mir zeigst, daran erinnere ich mich.
Was du mich tun lässt, das verstehe ich.
Konfuzius

Acknowledgements

First of all, I would like to thank my supervisor Professor Dr. Marcel Mayor for the possibility to work in his research group perusing a very interesting project and constantly being further educated in the understanding of organic chemistry and the freedom in my research. I enjoyed our conversations, and I feel honored for having worked with you.

I thank Professor Dr. Catherine Housecroft for co-refereeing this thesis and to Prof. Dr. Thomas Pfohl for chairing the examination.

Thanks goes to Dr. Thomas Wandlowski and Nataraju Bodappa for performing and helping to interpret the electrochemical and STM.

I would like to thank the golden boys and girls Dr. Jens Hermes, Dr. Carla Cioffi and Dr. Fabian Sander for the nice team spirit. Especially, I thank Fabian Sander for the interesting discussions, fun at conferences and non-chemical topics. I thank Pascal Hess for the nice time as lab neighbor, climbing partner and fun we had. Also I want to thank Lukas Jundt for fruitful chemical discussion and the nice time in the working group. As well, I thank Dr. Michal Juríček, Dr. Almudena Gallego and Mario Lehmann for proofreading this work.

I thank all past and present members of the Mayor group for the nice atmosphere not only for working but also for the nice coffee breaks and some memorable time. I dedicate a special thanks all lab mates in Lab 8. The atmosphere was great within the whole department and I thank all past and present coworkers for the nice time during work and beyond that.

I am very grateful for all the support within the department: Dr. Heinz Nadig for performing EI mass measurements. Sylvie Mittelheiser is acknowledged for performing the elemental analysis. The Werkstatt Team, Roy Lips and Markus Hauri for technical support. The endless support of our secretary staff Brigitte Howald, Marina Mambelli-Johnson and Beatrice Erismann is also gratefully acknowledged.

I thank my dearest Simon for the understanding and support, also in the last year when he was not physically present.

Especially I thank my parents and family for their love and support.

Table of Contents

1 Introduction

1.1 Gold Nanoparticles

Gold nanoparticles were the first time verifiable used in the 4th or 5th century AD in Egypt and in the Ancient Rome. One of the most impressive examples for this use is the Lycurgus Cup.[1,2] The making and use of this powerful dye fall into oblivion. In the Baroque the Cranberry Glass (Figure 1**Error! Reference source not found.**) was reinvented and mainly used for church windows, expensive tumblers and carafes. At that time people did not know that they were preparing and using nanoparticles and their properties.

Figure 1. Cranberry Glas glasses (left), church window (right).

The first one who reported the preparation of gold nanoparticles, at that time called colloidal gold was Faraday in 1857, by reducing an aqueous solution of chloroaurate ($AuCl_4^-$) solution with phosphorus in carbon disulfide.[3] His particles were so well stabilized that they survived till this day. It took about hundred years before the technology had progressed so far that Thomas, in 1988 could verify the presence of nanoparticles by the use of transmission electron microscopy (TEM).[4]

Since that time the synthesis of nanoparticles has been refined and applied to other, mostly coinage but also to some transition metals.[5] In the 20th century the prediction and the understanding of the optical properties of nanoparticles was enabled by new physical descriptions, such as the Mie theory.[6]

The term nanoparticle means small objects that behave like a unit. The size of nanoparticles ranges from 1 to 100 nm in diameter and among those, particles with a diameter smaller than 10 nm hold

an exceptional position due to the fact that they behave neither like single atoms nor like bulk material.[7] The word nanocluster means particles with a narrow size distribution between 1-20 nm with well-defined composition.[8]

1.1.1 Physical and Chemical Properties

Surface Plasmon Resonance

Nanoparticles have completely different physical and chemical properties than the bulk metal they are made of.[9] For example the melting point is lower,[10,11] they can show phosphorescence,[12] surface plasmon resonance[13] (SRP) or their charging can be quantized single electronevents.[14,15] The color spectrum of nanoparticles is related to the collective oscillation of the surface electrons excited by the electrical field of the impinged light. The excitation of such a surface occurs in metallic particles in a broad frequency band, mostly in the UV part of the spectrum.[16] For gold, silver and other noble metals nanoparticles, this surface plasmon resonance (SPR) band is shifted to the visible part of the spectrum. In these metals the conducting band electrons can move freely, independently from the ion background. The ions serve only as scattering centers for the electromagnetic waves.[17,18] This is the reason why the electrons of noble metals are easily polarizable and their SRP is therefore shifted to lower frequencies with a sharp bandwith.[11] For particles with a diameter below ~2-3 nm no such resonance band is observed.[19,20] For particles with diameter between 2 and 20 nm the SPR is well defined by the Mie theory[21,22] and therefore a UV/Vis spectrum is used as evidence for the concentration and size distribution of nanoparticles (Figure 2).

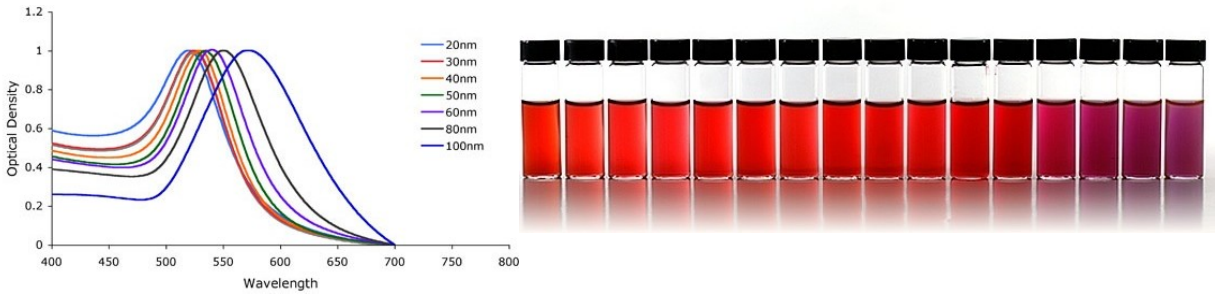

Figure 2. UV/Vis spectrum of gold nanoparticles with sizes between 20 and 100 nm[23] and aqueous solution of gold nanoparticles with different sizes starting from 5 nm (left) to 100 nm (right).[24]

The origin of the SPR can be explained as follows. If the number of atoms in a solid matter is continuously decreased, at one point the particle does not anymore behave like a small copy of the corresponding bulk solid.[25,26] In bulk materials, the valence and the conduction band of metals overlap and therefore exhibit quasi-delocalized electronic states and conductivity, see Figure 3. If one

decreases the size from bulk to nanoparticles the density of states decreases in both, the conduction and the valence band. As a final consequence, the energy bands split into quantized levels. When the size of the nanoparticles is further decreased down to a few atoms, localized bonds have defined orbitals. In other words the splitting of the energy levels and therefore also the physical properties are directly dependent on the size of a nanoparticle.[11,26,27]

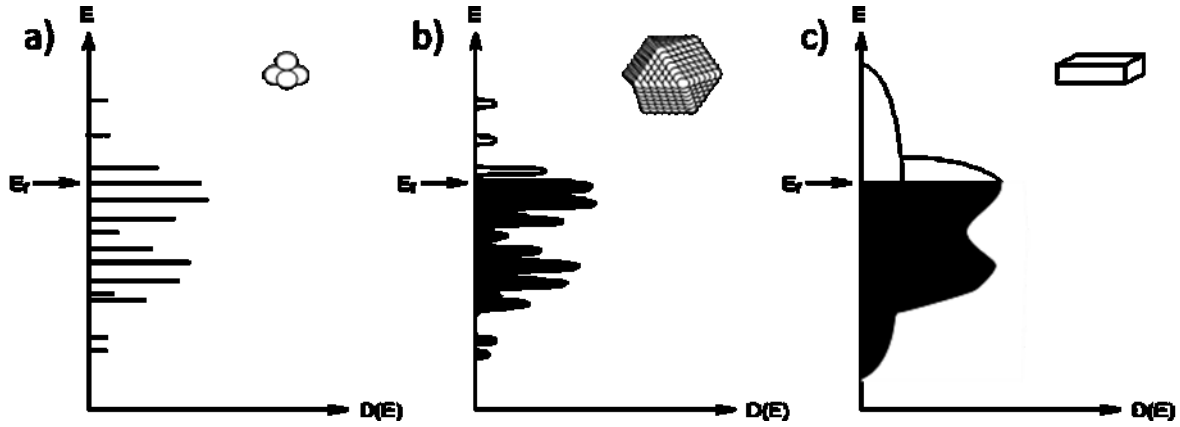

Figure 3. Distribution of energy states in a) molecules, b) nanoparticles and beginning at a certain size c) bulk metal. From Ref 27

In case the particle diameter is in the size range of the impression depth of an electromagnetic wave into metal, the exciting light can penetrate the particle. The electromagnetic field shifts the conducting electrons collectively, relative to the fixed positive charges of the lattice ions (Figure 4). These electrons build up a negative charge at one side of the surface of the nanoparticle. If the frequency of the exciting wave correlates with the eigenfrequency of the collective oscillation of the electron cloud inside the particle, already small fields will lead to a strong oscillation.[11]

Figure 4. Schematic representation of the plasmon oscillation of a metal nanoparticles.[28]

Coulomb-Quantum Size Effect and Electron Tunneling

The energy needed to add one electron to a system is known as Coulomb charging energy ($E_c = e^2/2C$), and is close to 0 for bulk metals. For very small particles the electrons are restricted to distinct levels what leads to strong Coulomb repulsion and to the increase of the Fermi energy (E_F).

When a single nanoparticle (NP) is trapped between two electrodes a double tunneling junction can be observed due to the small size of the cluster and the band splitting, see Figure 5. The Coulomb charging energy is the energy that must be applied to the system to enable the tunneling of an electron from the source to the drain.

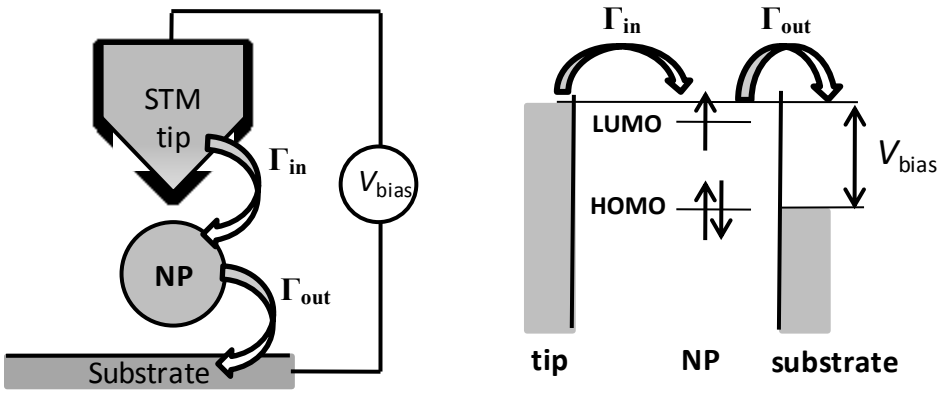

Figure 5. Schematic drawing of tunneling spectroscopy of a NP using an STM: the STM tip is fixed above the NP and the current is measured as a function of the bias voltage between the tip and the substrate (left). Energy level diagram of the STM set-up: showing how electron transport is possible if the tip Fermi level aligns with an energy level of the NP. Γ_{in} and Γ_{out} denote the tunneling rates in and out of the nanoparticles (NP) (right).[29]

If a NP is addressed by a probe tip that undergoes stepwise increase of the tip-substrate bias, Coulomb staircases of NPs can be observed as tunneling currents. [30–34] The core size dependency of the observed Coulomb staircases (see Figure 6) points towards quantized electronic levels. [14] At room temperature, solutions of monodisperse cores display an electrochemical "ensemble Coulomb staircase".[35]

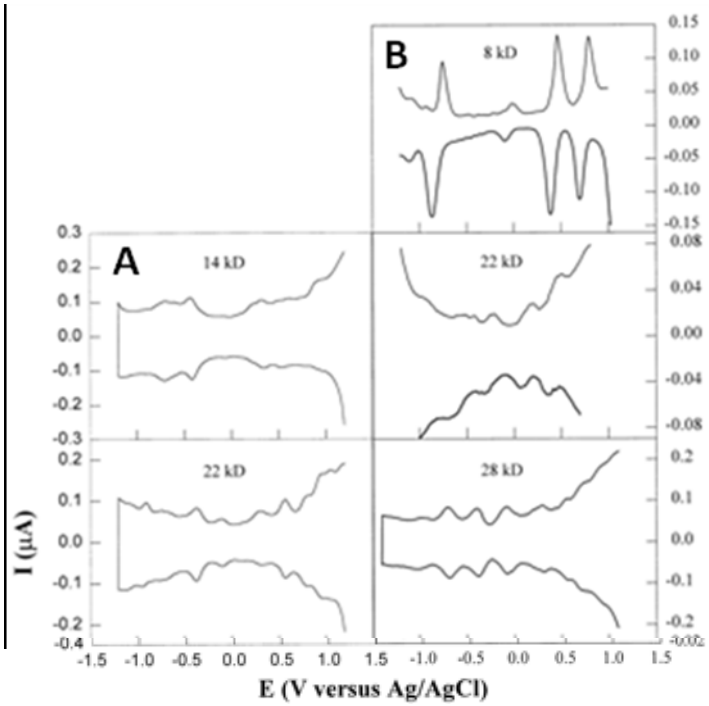

Figure 6. Differential pulse voltammograms for (A) butanethiolate (C4) and (B) hexanethiolate (C6) Au MPCs as a function of uniform core size, in 0.05 M Hex_4NClO_4/toluene/acetonitrile (2/1 v:v), at 9.5x10^{-3} cm^2,Pt electrode; DC potential scan 10 mV/s, pulse amplitude 50 mV. Concentrations are: (A) 14 kDa, 0.086 mM; 22 kDa, 0.032 mM; (B) 8 kDa, 0.30 mM; 22 kDa, 0.10 mM; 28 kDa, 0.10 mM.[14]

1.1.2 Synthesis of Gold Nanoparticles

For the synthesis of gold (Au) NPs usually Au(III) is being reduced with suitable reducing agents to give Au(0). Nonstabilized, naked Au(0) particles are however thermodynamically not stable and aggregate quite fast. To avoid this aggregation the particles can be stabilized with different, mostly organic ligands. Turkevich[36] invented in 1951 the synthesis of Au NPs with a diameter ranging from 16 to 140 nm by the reduction of $HAuCl_4$ with citric acid which is also the stabilizing agent.

At the beginning of the research investigations towards Au NPs mainly citric acid and triphenylphosphine[37,38] were used. In the last one to two decades a vast number of different organic compounds have been investigated as stabilizing agents for NPs. The explored substances vary from simple compounds as thiols, over polymers such as PMMA[39] and PVP[40] to quite complex molecules as DNA[41,42] and peptids.[43–45]

To obtain uniform particles with a small size distribution there are a few important things to take into account. It is crucial that the substances taking part in the formation and stabilization of the particles are homogeneous distributed in the solution and that the nucleation starts simultaneously. Soon after the nucleation started the concentration of the metal precursor should drop below the critical

level where the formation of new nuclei stops. At that time all the particles should be built that are present at the end of the reaction. From there on the particles grow through molecular addition until the equilibrium of metal precursor is reached where there is no further growth possible. In this growing process the small particles grow faster than the bigger ones due to the driving force of free energy that is bigger for smaller particles.[46]

In today's applications of NPs it is getting more and more important to know and understand the accurate composition of NPs. The first stoichiometric defined reports about phosphine stabilized Au_5 and Au_6 clusters were reported by Naldini and and coworkers.[47,48] In 1969 the first complete structural determination of the gold cluster $[Au_{11}(PPh_3)_7](SCN)$ with single crystal X-ray was achieved.[49] See Table 1

Magic number gold clusters can be regarded as super atom complexes. The exceptional stability of these particles arises from the shell closure of the orbitals. An total electron count of n* = 2,8,18, 34,58,92,… to fulfill this requirements must be given.[50,51] Thiols and other ligands can electrochemically stabilize the gold cluster by delocalizing or withdrawing electrons form the core of the particle into covalent bonds. The requirement of an electrochemically closed shell super atom has to fulfill the requirement ($[Au_M(SR)_N]^Z$) which can be calculated by the equation: n* = M – N – Z. The shell-closure electron count (n*) of the gold core has to correlate to one of the shell-closure numbers mentioned above.[52]

Table 1. Masses, formula and shell-closure electron count of different Au NP. From Zhang[50]

Core mass/kDa	Formula	Shell-closure electron count (n*)	References
5	$[Au_{25}(SR)_{18}]^-$	8	53–55
8	$[Au_{38}(SR)_{24}]^Z$	18	56–58
34	$[Au_{68}(SR)_{34}]$	34	59
58	$[Au_{102}(SR)_{44}]$	58	60,61
29	$[Au_{144}(SR)_{59}]^Z$	92	62–64

One of the most important publications towards the synthesis of AuNPs synthesis was published by Brust et al.[65] In this publication they reported the synthesis of thiol stabilized NPs. For the synthesis they used a two phase system where they transferred the Au(III) ions to the organic phase with the help of tetraoctylammonium bromide (TOABr). In the presence of dodecanthiol they reduced the gold precursor with the addition of sodium borohydrid ($NaBH_4$) to yield NPs in the size range of 1 to

3 nm. The NPs obtained with this synthetic method are very stable and can be dried and redissolved in a big variety of organic solvents.

This reaction procedure is not restricted to alkylthiols but can also be applied to a large variety of thiols bearing different functional groups.

In the course of this investigations $[N(C_8H_{17})_4][Au_{25}(SCH_2CH_2Ph)_{18}]$ (Figure 7) was characterized and the X-ray structure was reported.[54] Interestingly the cluster consists of a Au_{13} core with Au-Au bond length and coordination sphere in good agreement with the reports for bulk gold.[66] The outer shell of this Au_{25} cluster consists of 12 Au atoms that are arranged in a so called "staple" motif of RS-Au(I)-SR-Au(I) motifs. This leads to the assumption that this cluster should be better named as staple-protected Au_{13} than thiol protected Au_{25} cluster. This shows the major difference between clusters stabilized by thiol and clusters stabilized by other ligands than thiol.

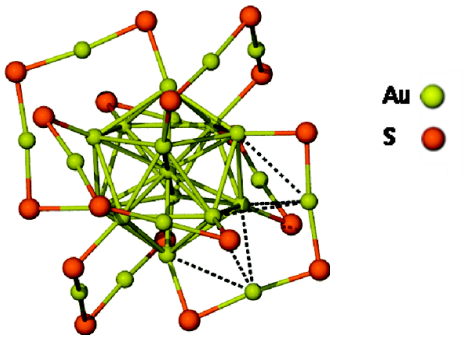

Figure 7. Solid state molecular structure for $[N(C_8H_{17})_4][Au_{25}(SCH_2CH_2Ph)_{18}]$ The green Au_{13} core is surrounded by 6 $Au_2(SR)_3$ staple motifs. Au is indicated green and sulfur red, all other atoms were omitted for clarity.[54]

1.1.3 Au–S Interface

It is a widely accepted concept that the formation of stable and covalent gold-sulfur interfaces requires the formation of gold-thiolate bindings. It is believed that the sulfhydryl group is deprotonated, generating formally a thiol radical ($RS^{\cdot}$).[67] The coordinative binding of the protonated SH group through the sulfur lone pair electron would just lead to weak interaction. The bond strength of RS-Au is in the same order as the Au-Au bond strength and can therefore modify the surface of gold at the gold-sulfur interface.[67]

The Brust-Schiffrin synthesis is still the ruling method towards thiol protected AuNPs. Thereby it can be distinguished in a one[68] and a two[65] phase method.

In the classical two phase system the Au(III) is being transferred to the organic solvent with quaternary ammonia salt NR_4X (Scheme 1). Then the thiol is added and the Au(III) is transferred to

Au(I). It was believed for a long time that the Au(I) and the thiol form polymers in the form of [Au(I)-SR]$_n$ in this two phase system. In the last years it could be shown that the complexes that are formed consist of Au(I) and the ion pair of the phase transfer catalyst (NR_4X) in the form of $[NR_4][AuX_2]$.[69] The Au(I) is in this case being incapsulated in inverse micelles of NR_4X. After the addition of $NaBH_4$ the gold precursor is getting reduced to Au(0) and the free, dissolved thiol molecules bind to the surface of the newly formed NPs.[70]

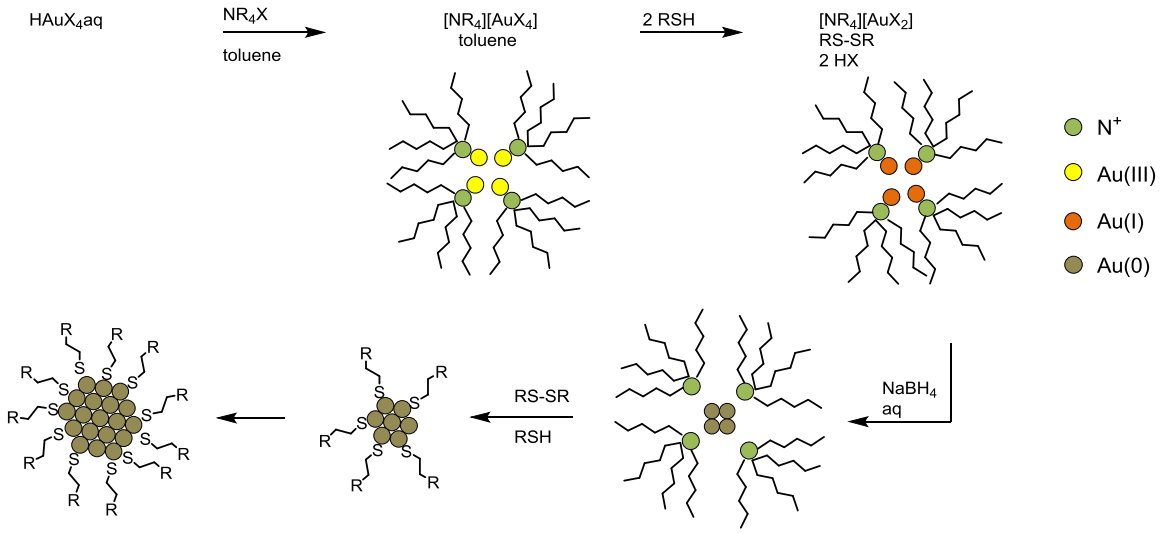

Scheme 1. Scheme of the reactions in two-phase Brust-Schiffrin method.[71]

In the one phase synthesis (Scheme 2) in contrast the Au(III) is reduced to Au(I) by the free thiol in polar solvents such as tetrahydrofuran (THF) or methanol (MeOH). The polymer has the form of [Au(I)–SR]$_n$ and is reduced to Au(0) by the addition of $NaBH_4$ to form monolayer protected NPs. The polymer that is formed under these conditions can be very stable and might not be fully reduced by the addition of the reducing agent.[72]

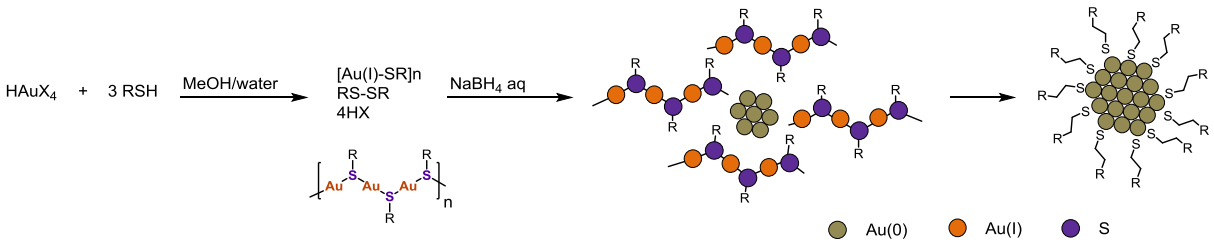

Scheme 2. Scheme of the reactions in one-phase Brust-Schiffrin method [71]

In Figure 8 the composition of a thiol protected Au_{102} particle in a core and a shell part is shown. The core consists of 79 Au atoms with a lot of Au–Au bonds and the surface consisting of several S–Au–S

bonds with one Au–S bond as anchor (c, d, f, g). Figure e) shows a close look on 2 different staple motifs: one is consisting of 2 ligands interlinked with one Au atom (small orange sphere) and the other shows a motive, where 3 ligands are interlinked with 2 Au atoms and anchored by two Au atoms (big orange spheres). Other fully characterized gold clusters are listed in Table 2.

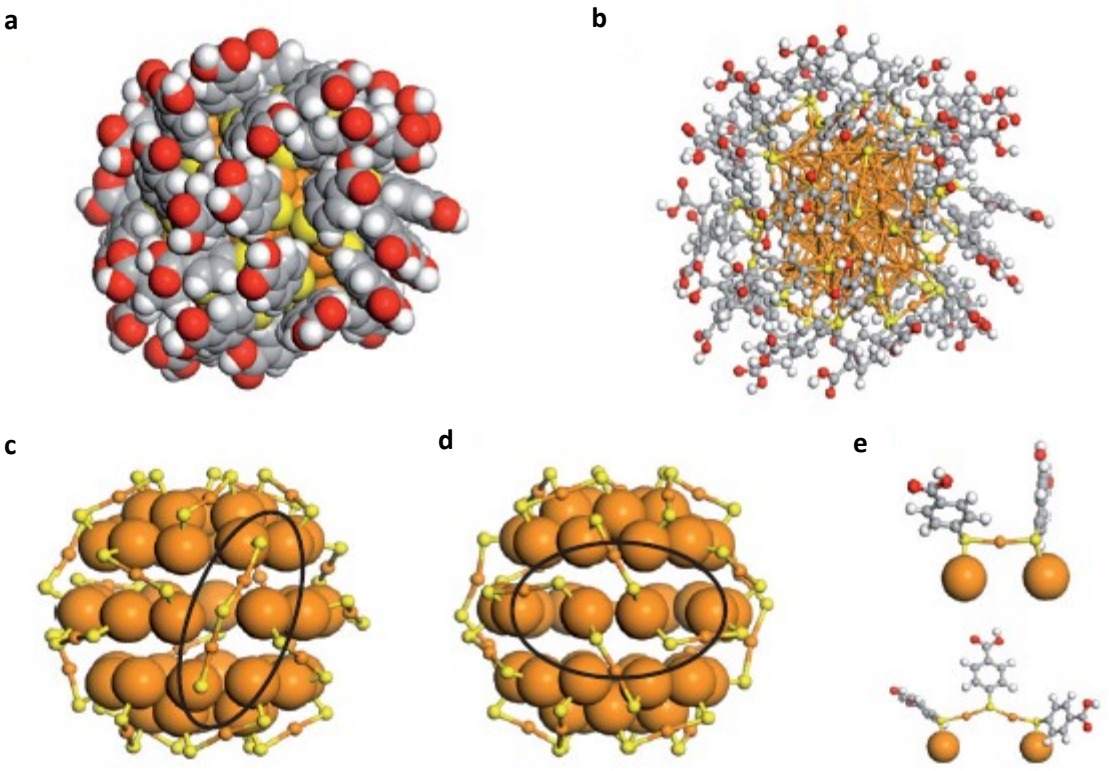

Figure 8. Analysis of the single-crystal X-ray structure of Au_{102}(p-MBA)44. a) Space-filling and b) ball-and-stick representations. c, d) two views on the 40 Au atoms at the surface together with the passivating Au_{23}(p-MBA) mantle. e) protecting (RS-Au-SR) unit with 1 and 2 repeating units. The Au(I) atoms are shown as small, the Au(0) atoms as big orange spheres. The sulfur is shown as yellow spheres. Au: orange; S: yellow; C: grey; O: red; H: white. Adapted from [52]

Table 2. Fully characterized gold clusters and their composition in core and shell

Au cluster in classical writing	Au cluster in core /shell writing	From reference
$Au_{25}(SR)_{18}$	$Au_{13}[RS(AuSR)_2]_6$	54,73
$Au_{38}(SR)_{24}$	$Au_{23}(RSAuSR)_3[RS(AuSR)_2]_6$	74,75
$Au_{102}(SR)_{44}$	$Au_{79}(RSAuSR)_{19}[RS(AuSR)_2]_2$	61
$Au_{144}(SR)_{60}$	$Au_{114}(RSAuSR)_{30}$	63,64,74

1.1.4 Post Synthetic Modifications

The direct synthesis of thiol capped NPs does not give a good control over the surface composition. Therefore post-synthetic modification and ligand exchange are used.

The post-synthetic modification is used to attach a molecule with desired characteristics to the present ligands. In these cases, reaction sites on the installed ligands are used such as bromine in a S_N2 reaction.[76] Terminal –COOH groups were reacted with –OH and $–NH_2$ groups to give the esters and amids.[77] Also modification of the NPs surface by polymerization[78] and peripheral group transformation[79] could be shown. The bulkiness of the attached functionality plays a crucial role in these modification reactions.[80]

1.1.4.1 Ligand Exchange

Ligand exchange is the most often used method to alter the composition and properties of NPs. The existing ligand shell can either be partly or completely exchanged with other ligands.[80–82]

For this approach, NPs with a week coordinating ligand shell are often used such as citrate or triphenylphosphine (PPh_3). The exchange can last between hours and days and can be accelerated by increasing the temperature.[80,83] After the desired rate of exchange, the particles must be separated from exchanged and excess ligands to disable further exchange. This is mostly achieved by washing and extraction with suitable solvents.

Phosphine Ligand Exchange

Triphenylphosphine and citric acid are not able to bind strongly to the gold surface and can therefore be rather easily exchanged with thiols. Woehrle et al.[80,84] reported ligand exchange of PPh_3 stabilized AuNPs with thiols. They described one and two phase exchange reactions of 1.4 nm particles where complete displacement of the PPh_3 with incoming thiols took place. Although a small loss of Au atoms was observed, the diameter of the particles did not change, indicating that the loss of Au atoms is negligible.[85,86] Au_{55} clusters were reported to be much more stable when the PPh_3 ligand was exchanged with thiols.[84] The thiol protected Au_{55} was stable for several days also if exposed to high salt concentration or extreme pH, the original PPh_3 protected clusters were stable for less than 3 hours.

In contrast to these findings, Qian and collaborators[87] reported etching and therefore size focusing of PPh_3 stabilized NPs upon ligand exchange. They used 1-3.5 nm AuNPs and stirred them with excess of

thiols for 12 hours at room temperature to give mainly $[Au_{25}(PPh_3)_{10}(SC_2H_4Ph)]^+$. This Au_{25} core is reported to consist of two Au_{13} units sharing one common vertex (13*2-1=25 Au atoms). "Five thiol ligands bridge two icosahedrons, the two chlorides bind to the apical Au atoms of the rod and the 10 PPh_3 ligands are terminally coordinated to the two Au_5 pentagonal rings."[87] The Au(I) byproduct in this reaction was shown to be $[Au_2(PPh_3)_2(SC_2H_4Ph)]^+$ although other compositions of Au(I) side products were expected as for example$(Au(I)SR)_n$ polymers.[87]

Thiol Ligand Exchange

NPs synthesized directly with thiol ligand shell are quite common due to their stability and well known synthesis. Nevertheless it remains challenging to introduce a certain number of ligands with special functionality in the direct synthesis. Also the tendency of thiols to form disulfides was mentioned to have an influence in the stability of the formed NPs.[88,89] Therefore thiol-thiol ligand exchange is often necessary to introduce distinct functionalities to the particles. Knowing that thiols are binding stronger to gold than PPh_3 also the exchange reaction is more difficult to realize.

The exchange reaction consists of a dissoziation[90] and a assoziation[91–93] pathway where the incoming ligand protonates the sulfur of the leaving ligand.[94,95] Thiol–capped NPs offer a diversity of ligand binding sites — vertex, edges and terraces, see Figure 9 — with different electron density and sterical accessibility and therefore a vast diversity in ligand exchange kinetics.[94]

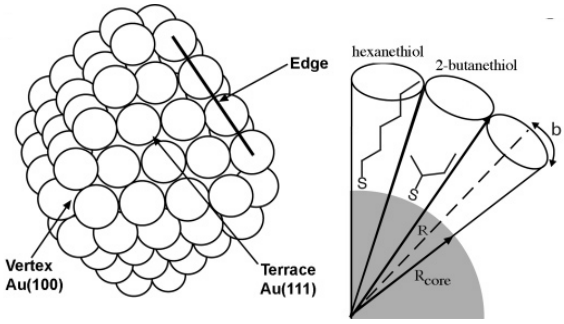

Figure 9. A model of an Au_{140}nanocluster with a truncated octrahedral geometry. Schematic diagram of a gold cluster (radius = R_{core}) protected with a branched and non-branched alkanethiolate; R is the radial distance of the conical packing constraint. Adapted from[96]

Assuming a spherical shape for a 1.3 nm Au particle, 88% of its atoms are on the surface and 2 nm particles still have 58% surface atoms.[96] Up to 45% of these surface sites are located on edges and vertexes. Furthermore the surface of NPs has high radium of curvature and therefore a packaging gradient density.[94,96]

To conclude, ligand exchange is faster at edges and corners due to lower density in packaging of the ligand than on terraces. At first the incoming ligand penetrates the monolayer at less crowded nonterrace sites and protonates the leaving ligand to form a free thiol there.[94,95] Oxidative formation of disulfide does not occur due to the ligand exchange but was proved to come from the presence of ozone.[97]

The ligand exchange rates depend strongly on the concentration of the incoming and exiting ligand. The exchange rate decreases with the size of the incoming ligand and the chain length of the stabilizing ligand. Some sites like interior terraces are nearly unexchangeable. After the exchange at the edge and vertex sites the rate determining step is the very slow exchange of thiols at terraces or the slow migration of other thiols to the defect sites.[94]

1.2 Palladium Nanoparticles

The interest in the properties of other metal NPs than gold has been growing over the last decade.[98]In particular the high surface to volume ratio makes NPs potential catalysts.[99] In particular, palladium (Pd) is known to be one of the most potential metal for catalysis approaches.[100,101] It shows good performance in the fields of hydrogenation[102,103], oxidation[104,105], C–C bond formation[106,107], hydrogen storage[108,109] and sensing.[110,111]

For the use in such fields the size and the shape of the formed particles and their monodispersity is crucial.[112,113]

NPs are thermodynamically unstable and tend to aggregate, therefore the NPs are stabilized by either electrostatic or steric forces or both.[99] The interactions between the ligand and the NPs exist in different forms, such as electrostatic interactions, chemisorbed atoms (for example *via* lone pair) or covalent linkage, such as thiols.

Strong interactions of platinum group metals and sulfur have been reported that thiol protected NPs possess a high stability.[99] A drawback in the use of sulfur units as protecting ligands for PdNPs is that sulfur is known to poison the catalyst.[114] Nevertheless reports exist where thiol capped PdNPs were successfully used as catalysts for Suzuki-Miyaura C–C coupling[115] or in the hydrogenation of allylamine.[116]

1.2.1 Sulfur Based Ligands

Alkylthiol protected PdNPs can be synthesized according to the Brust-Schiffrin[65] method (see chapter 1.1.2). The two phase method is most widely used wherein the palladium precursor such as tetrachloropalladate (Na_2PdCl_4) is dissolved in water and the metal ions are then transferred to the organic phase with a quaternary ammonia salt (Scheme 3). After the ligand is added the reduction is started with the addition of aqueous $NaBH_4$. The size and the shape of the formed can be tuned by the reaction conditions[117] such as the surfactant, the reaction time, the stabilizing ligand[118] and the ratio of palladium precursor to reducing agent and ligand.[119]

Another synthetic approach was published by Ulman et al.[120] where they use Super-Hydride© (lithium trithylborohydride, $LiEt_3BH$) as reductant in a one phase system. The treatment of palladium acetate with octylthiol and Super-Hydride© in THF leads to the formation of NPs with a diameter of 2.3 nm.[120]

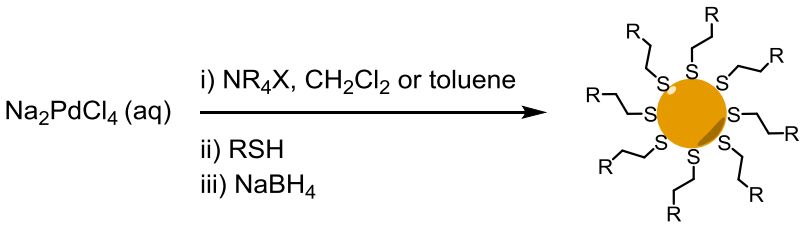

Scheme 3. Scematic reaction procedure towards the synthesis of PdNPs in a variation of the Brust-Schiffrin method.[121]

For the introduction of functionality to the PdNPs, the ligand exchange is a successful way without changing the size of the metal core.[80,122] With this reaction electrochemically active ferrocene containing particles could be obtained.[123] For details of the ligand exchange reaction see chapter 1.1.4.

View examples are reported where other thiol containing ligands than free thiols are used as stabilizing ligands. Two of these examples are thioether[124] and thioester[125] groups. These ligands bind to the NPs with weaker interactions than the free thiols. This can be an advantage in the use as catalyst and can gives rise to easy post-synthetic modifications *via* ligand exchange.[126] The use of thioethers gave rise to the formation of PdNPs in gram scale using palladium acetate as precursor. The NPs were obtained with a narrow size distribution and the particle size could be tuned by changing the length of the stabilizing polymer.

1.2.2 Phosphorus Based Ligands

Hyeon et al.[127] reported the formation of PdNPs by thermolysis. They first formed palladium-trioctylphosphine (TOP) complexes and treated them together with $Pd(acac)_2$ (acac = acetylacetone) at 300°C under an argon atmosphere. The particles had a diameter of 3.5 nm and could be made more monodisperse and enlarged up to 7.5 nm with the addition of oleylamine which served as solvent and stabilizer.[127]

Besides the direct formation of phosphine stabilized Pd NPs the ligand gives rise to easy to accomplish exchange reactions. The weakly bond phosphine shell of such NPs can be easily and successfully exchanged by stronger binding ligands. In one example Son et al. demonstrated the exchange reaction of TOP with a wide variety of mono and bidentate phosphines.[128]

In another example the two phase Brust-Schiffrin[65] method was adapted for the synthesis of Pd NPs. A tetrachloropalladate was therefore used as palladium precursor. The metal ion was transferred to

the organic phase using TOABr and was reduced to Pd(0) with $NaBH_4$.[37,129] As ligand the optical active bidentate BINAP (2,2'-bis(diphenylphosphino)-1,1'-binaphthyl) was used, what led to the formation of chiral NPs. These chiral NPs were effective catalysts in the hydrosilylation of styrene with trichlorsilane.

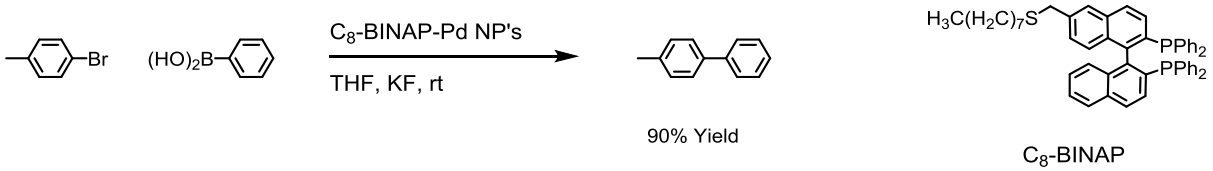

Scheme 4. Reported C–C coupling using BINAP thioether stabilized Pd NP as catalyst.[130]

BINAP-thioether derivative stabilized NPs were used in the C–C coupling of boronic acids.[130] An example is illustrated in Scheme 4. The Pd NPs were very good stabilized by BINAP throughout the reaction and could be reisolated without any loss of catalytic activity.

1.2.3 Nitrogen Based Ligands

The lone pair of the nitrogen is able to bind strongly to the metal surface and the organic rest of such ligands hinder agglomeration through steric repulsion.

Mazumder et al.[131] demonstrated the synthesis of monodispers PdNPs by reduction of $Pd(acac)_2$ in oleylamine with boron tributylamine (BTB). Oleylamine served in this reaction as solvent, stabilizing ligand and reduction agent with BTB as co-reductant. The reaction without BTB lead to the formation of larger NPs with a less narrow monosispersity.[127]

It was shown in general that the choice of the primary amine used as stabilizer gives rise to NPs of different size and quality. This led to the suggestion that not just the lone pair of the amine is stabilizing the formed particles but that the double bond present in the oleylamine plays an important role in the growth of the NPs.[99] It is also likely that the palladium precursor used for the formation has an influence on the particle growth. $Pd(acac)_2$ gave in general more monodispers particles than the use of nitrate and chloride precursors.[127] The size of the Pd particle can be changed *via* changing the ratio of Pd precursor to amine. Also the length of alkylamines has an influence on the particle size, in general the size of the formed particles decreased with the increasing length of the alkyl chain.[132]

Other than aliphatic amines have been used for stabilizing Pd NPs such as aromatic amines[133], porphyrines[134], pyridyl groups[135] and imidazole derivatives.[136]

The readily available dimethylaminopyridine (DMAP) has been used for the synthesis of catalytic active Pd microcapsules. DMAP is a non bulky ligand, leading access to the surface of the NPs for organic reactions.[137]

DMAP stabilized Pd NP have been synthesized in different synthetic approaches like in the reduction of Na_2PdCl_4 with $NaBH_4$ in water or by a ligand exchange reaction.[135] In this reaction NPs were achieved by reducing the palladium precursor in the presence of tetraalkyl (TAA) ammonium bromide in a two phase system to give TAA stabilized particles. These were treated with an organic solution of DMAP to give fast and complete transfer of the NPs to the organic phase. See Scheme 5. The core size of the particles stayed unchanged in this ligand exchange reaction.

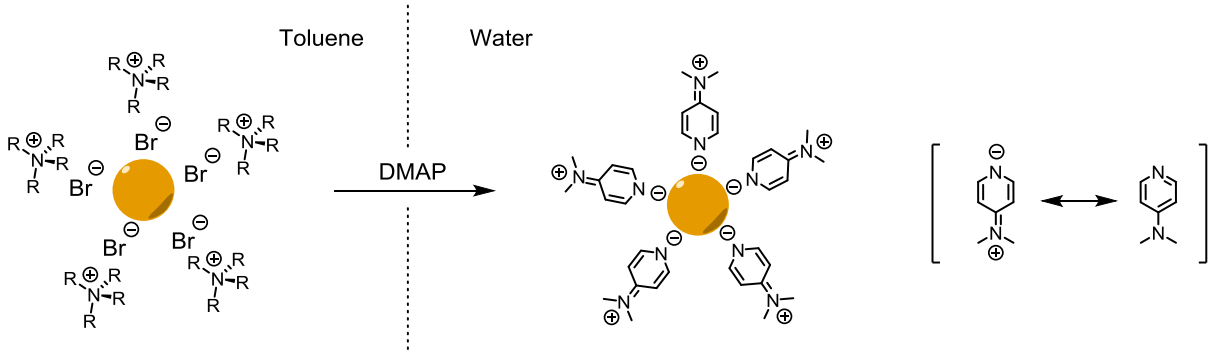

Scheme 5. Transformation of PdNPs from organic to aqueous solvent systems by using DMAP. The resonance structure of DMAP is shown in brackets.[99]

Imidazole derivatives areas well reported to serve as stabilizer for PdNPs and the subsequent deposition of these PdNPs onto activated carbon gives active catalysts for hydrogenations.[136]

1.2.4 Carbon Based Ligands

Ligands with heteroatoms can stabilize noble metal NPs with the formation of strong interactions with the metal surface. Recently particles stabilized by just carbon based ligands were reported.[138,139] The bond energy for such a Pd–C bond is 436 kJ/mol and therefore bigger than the S–Pd bond with 380 kJ/mol.[140] PdNPs have been stabilized by Pd–C covalent linkages with the use of diazonium derivatives as precursors.[140] As already described in subchapter 1.2.1 PdNPs can be synthesized with the use of Super-Hydride©. Simultaneously aliphatic radicals are generated by the reduction of the diazonium ligand. This radical can undergo a reaction with the metal surface and this leads to the formation of Pd–C linkage.[140]

1.2.5 Steric Stabilization

Besides the classical ligands, NPs can also be stabilized by the incorporation into organic matrixes such as flexible polymers or preorganized dendritic structures. Such stabilizing agents prevent NPs usually through their steric bulk very effective from agglomeration.[141,142]

Polymers

Polymers like poly(N-vinyl-2-pyrrolidone) (PVP) and poly(vinyl alcohol) (PVA) are widely used for the stabilization of different metal NPs. These polymers are commercially available at relatively low price and are soluble in various solvents including water.[143,144] Often the reduction in the presence of these polymers is carried out under elevated temperature with the use of ethylene glycol as reducing agent. This reduction usually takes several hours to come to completion although the reaction can be accelerated by the use of microwave irradiation.[145,146] The use of alcohols as reductant bears the benefit that the formed byproducts are organic compounds in contrast to the reduction with borohydrates.[147] PVP and polyurea stabilized PdNPs were successfully used in Suzuki–Miyamura reactions[148,149] and Stille reactions of aryl bromides and chlorides could be performed under mild conditions with the recovery of the catalytic NPs.[148]

Dendrimers

Dendrimers are big molecules like polymers but with a accurate defined molecular composition.[150,151] The inner cavities are so to say “molecular boxes” that can trap and stabilize NPs, especially when the dendrimers exhibit heteroatoms at the inner side of the cavities. Especially two kinds of dendrimers were extensively studies and used in a variety of NPs synthesis: Poly(amidoamine) (PAMAM) and poly(propyleneimine) (PPI), see Figure 10.[152,153]

In the first step of the synthesis the metal ions are sorbed by the macromolecule. Than the precursor is subsequently reduced and the NPs stay encapsulated in the dendrimers and therefore cannot aggregate.[154]

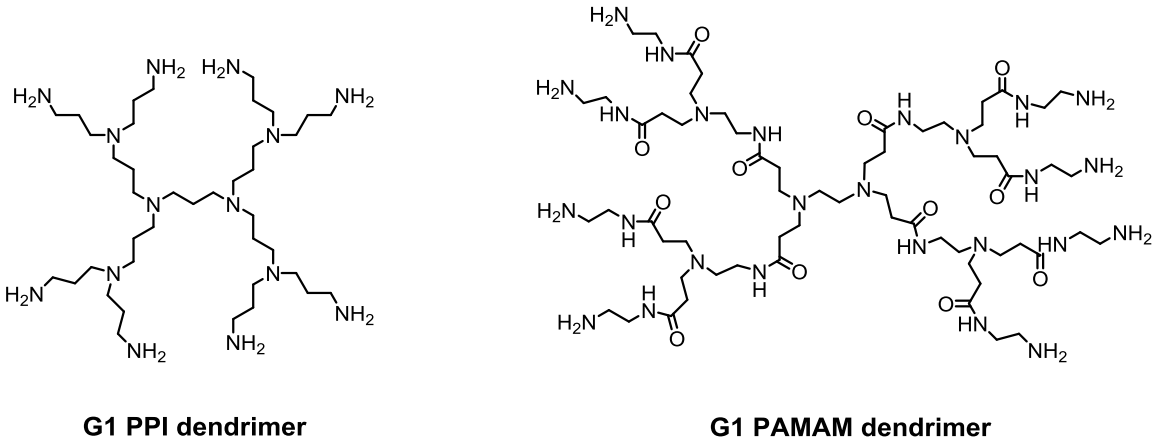

Figure 10. Structure of first generation PPI and PAMAM.

The size of the formed NPs is in this case depending on the metal ion loading into the dendritic structure and on the size of the dendrimer. Typically particles with a narrow size distribution between 1 to 3 nm are achieved.[155] This synthesis yields particles with a good accessability of the metal surface for catalysis, compare Figure 11. The cavity of dendrimeric macromolecules is highly porosive and allows the starting materials and the products to migrate from the media to the PdNPs and *vice versa*.[156,157] With the tuning of the porosity a selectivity can be achieved to a certain degree.[156,158]

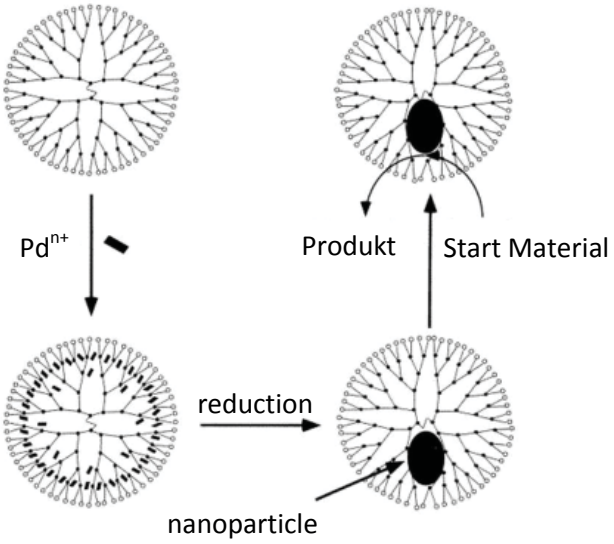

Figure 11. Scematic drawing of the formation of Pd NP within a dendritic structure and the use in catalysis.[157]

2 Research Project, Concept and Objective

The aim of this project was the development and investigation of novel concepts for the control of the size and the surface functionalization of noble metal NPs. The Control of the functionalization allows for adjusting of the chemical behavior while the control over the size allows for tuning of the physical behavior of the particles. The concept behind this approach is to synthesize NPs with a certain number of bifunctional ligands. The two functional groups in these ligands should be chosen such that one functional group, in most instances a thiol, is binding to the surface of the NPs. The second functional group is supposed to bind the NPs to a substrate. For this purpose the second functionality has to exhibit a strong binding affinity to the substrate surface but should not interact with the surface of the NPs. The final NPs should thus exhibit the potential to form self-assembled monolayers (SAM) on a metal substrate, as illustrated in Figure 12.

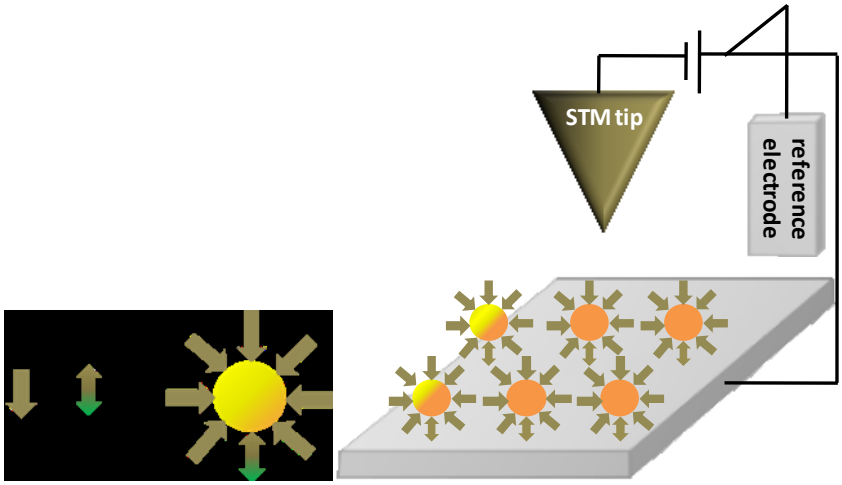

Figure 12. Illustration of a NP SAM on a metal substrate in a STM setup. brown arrow, single functionality; double arrow, bifunctionality, the metal core of the NPs is indicated as yellow ball. Right figure represents a SAM on a metal substrate in a STM setup.

The anchoring ligands should be rigid, so they cannot fold up and are notable to bind to the metal surface. The ligands should be conjugated to provide high conductivity in the investigation of their physical properties.

The physical behavior of the NPs is depending highly on the size of the particle, therefore a small size distribution of the NPs is required. Hence the synthesis of the NPs should either provide NPs of a very narrow size distribution or the polydisperse NPs mixture should be easily separated in to fractions of a small size distribution.

The length and conjugation motif of the bifunctional ligand influences the conductivity of the ligand, while the anchoring groups influence the conductivity over the interface between the metal core of the NPs and the ligand, and between the ligand and the substrate, respectively.

Scanning tunneling microscope (STM) (compare Figure 12) can be used to address single particles on a surface and thereby gain insight in the electrochemical behavior and quantum size effects.

The second part of this thesis is focused on the synthesis of ether ligands of different length and their potential for the stabilization of the NPs. The potential of thioether ligands to stabilize AuNPs has recently been investigated in the group of Marcel Mayor.[159–161] Theseimportant findings led to the design of similar ether–containing oligomers and opened the field for the stabilization of other noble metal NPs that could not be stabilized by the thioether ligands.

The focus of this part of the work lies in the exploration of the feasibility of the ether ligands as stabilizer for NPs in direct synthesis. The synthetic methodology for the formation of ether ligands had to be developed. Suitable ether ligands had to be synthesized and investigated concerning their ability to stabilize NPs made of different metals.

3 Thiol-Coated Gold Nanoparticles

3.1 Pyridine-Thiol Ligand Synthesis

The design of conjugated ligands bearing a thiol group and as a pyridine unit leads to a consideration from which side to start to build up the ligands. Especially for longer ligands this is an important question because it is known that sulfur (and pyridine) can lower the efficiency of cross-coupling reactions and hamper the purification of the product.

The synthetic strategy towards these ligands is based on typical cross-coupling reactions using palladium-based catalysts. The Sonogashira, Heck and Suzuki reactions were considered as cross–coupling reactions.

To elongate the ligand **1,** while maintaining its rigidity and conductivity, an acetylene bond was used as bridging between the pyridine and the phenyl unit (Figure 13). Two different approaches were tried to prepare **2**. On the other hand also molecule **3** was synthesized. It bears a double bond which makes the molecule not as rigid as the one with the triple bond (**1**) but shows better conductivity.

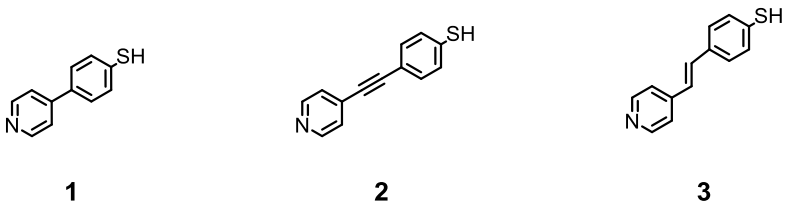

1 **2** **3**

Figure 13. The three desired ligands of different length and conductivity.

4-(Pyridin-4-yl)benzenethiol (**1**) was chosen as model ligand because it is the shortest ligand in this series and it can be synthesized in just two previously described steps.[162] The first step is a Suzuki reaction.4-Bromopyridine hydrochloride, 4-(methylthio)phenylboronic acid and potassium phosphate were placed in a microwave tube. DMF and water were used as solvents in a 5/1 ratio. Palladium acetate ($Pd(OAc)_2$) was used as a catalyst and X-Phos was used as a ligand for this Suzuki reaction (Scheme 6). The reaction mixture was heated by microwave irradiation at 140°C for 2 hours. After the reaction was quenched with saturated aqueous NH_4Cl solution, the crude was purified by column chromatography to yield the pure product as a white solid in 95% yield. The reaction could be performed on a 5 gram scale. Because the purification of such a big quantity by column chromatography is difficult, the product **4** was purified by “kugelrohr” distillation.

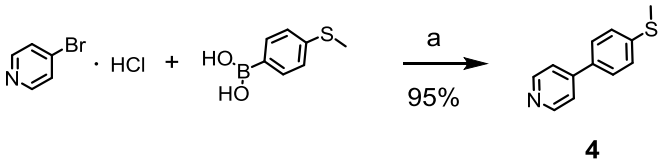

Scheme 6. Synthesis of protected ligand 4; a) $Pd(OAc)_2$, X-Phos, K_3PO_4 DMF, water, 140°C MW, 2 h, 95%.

For the deprotection reaction (Scheme 7) **4** was dissolved in DMF and put under an inert atmosphere. Sodium 2-methyl-2-propanethiolate was added in an excess of 2.8 equivalents before the reaction mixture was heated at 140°C for 4 hours. The reaction was poured on ice and neutralized with HCl (1M). The neutralization could easily be realized by the color change of the solution from white to yellow. After the aqueous solution was extracted with ethyl acetate, the crude product was purified by column chromatography and obtained in 51% yield.

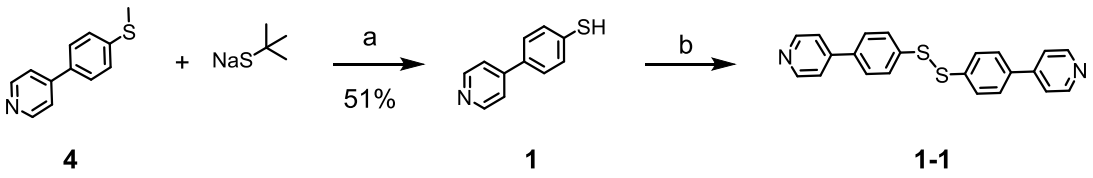

Scheme 7. Deprotection reaction of 1; a) DMF, 160°C, 4 h, 51%; b) oxygen.

The product was obtained as an orange liquid which turns into a pale yellow solid within one day at room temperature due to the formation of disulfide **1-1** (Scheme 7).

To increase the yield of this reaction, other solvents were tried, which have a better ability to stabilize the intermediate of the reaction. Solvents like DMSO did give lower or similar yields. When 1,3-Dimethyl-2-imidazolidinone (DMI) was used instead of DMF as solvent, interestingly the product of this reaction was not the desired product (**1**) but 4-(4-(*tert*-butylthio)phenyl)pyridine (**5**) (Scheme 8). This lead to the assumption that an ipso substitution took place if DMI was used as solvent.

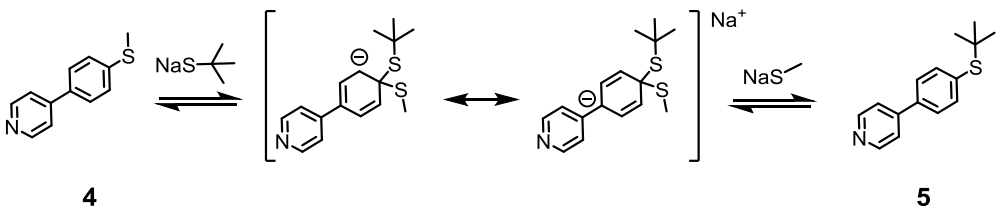

Scheme 8. Proposed Mechanism of the *ipso* Substitution.

For the synthesis towards the longer ligands **2** and **3** the thiol protecting group (methyl) was changed. This change was made because of the poor handability and the need of big excess of the deprotection agent for the deprotection reaction.

Acetyl is a widely used protecting group, which is easy to install, stable between pH 2 to 9 and can be cleaved under relatively mild conditions.[163] Therefore, *S*-(4-iodophenyl) ethanethioate (**6**) was synthesized according to literature (Scheme 9).[164] In brief, zinc dust and dichlorodimethylsilane were suspended in 1,2-dichloroethane. Pipsyl chloride and *N*,*N*-dimethylacetamide were added. The reaction mixture was heated at 75°C until the zinc dust was dissolved, and then the mixture was cooled to 50°C. Acetyl chloride was added and the solution was stirred for 20 minutes. The reaction was quenched with ice and the crude product was purified by column chromatography to yield the pure product as white solid in 50% yield.

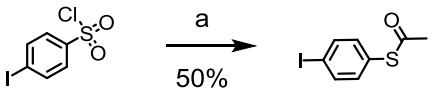

6

Scheme 9. Synthesis of 6; a) Zn, Me_2SiCl_2, $(ClH_3C)_2$, *N*,*N*-dimethylacetamide, 75°C, 50°C, AcCl, 20 min, 50%.

Due to the fact that 4-ethynylpyridine is known not to be stable under ambient conditions[165] ,the acetylene group was introduced on the phenylene unit of **2** first before the corresponding compound **7** (Scheme 10) was reacted with 4-bromo-pyridine.

In a Sonogashira reaction using tetrakis(triphenylphosphine)palladium ($Pd(PPh)_4$) as catalyst, triethylamine (Et_3N) as base and copper iodide (CuI), the starting material **6** was reacted with an excess of the trimethylsilyl acetylene to *S*-(4-ethynylphenyl) ethanethioate. An aqueous work-up was performed followed by the removal of the solvent. The residue was redissolved in methanol (MeOH). K_2CO_3 was added and the mixture was stirred for 30 minutes before the reaction was extracted with ethyl acetate. Purification by column chromatography afforded the pure product **7** in up to 55% yield as dark yellow oil.

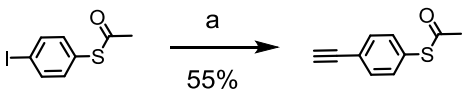

6 **7**

Scheme 10. Synthesis of 7; a) TMS-acetylene, $Pd(PPh)_4$,CuI, DMF, rt, 40 min; K_2CO_3, THF/MeOH, rt, 1 h, 55%.

The reaction of **7** with 4-iodopyridine was carried out at room temperature using $Pd(OAc)_2$ as a catalyst. The starting material was fully consumed within 3 hours as monitored by TLC. Unfortunately, the formation of not just one but two new products was observed. After purifying these two compounds by column chromatography, the second product formed was 4-((4-(pyridin-4-ylethynyl)phenyl)thio)pyridine (**9**) (Scheme 11). The ratio of the two products **8** and **9** was 1:3.

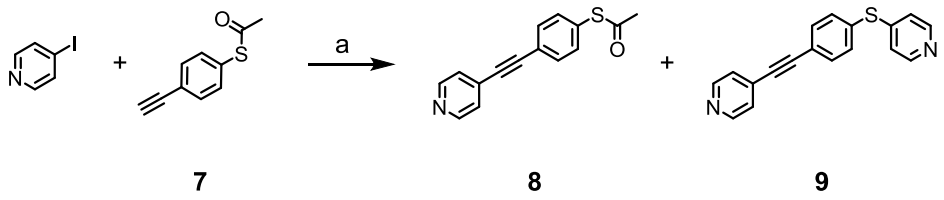

Scheme 11. Synthesis towards the product 7; a) $Pd(OAc)_2$, CuI, X-Phos, Et_3N, DMF, 140°C, MW, 1 h; 8:9 = 1:3.

This side reaction occurs because the base Et_3N is able to deprotect a thioacetate moiety (Scheme 12) under the employed reaction conditions and a free thiol reacts (Scheme 13) in the presence of a base and CuI with a iodo- or bromopyridine to form a phenylthiopyridine **9**.[166–169]

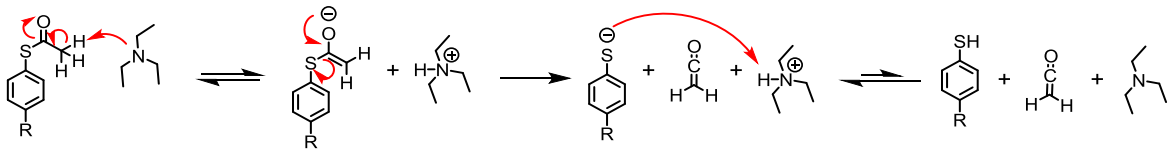

Scheme 12. Proposed deprotection mechanism of the S-acetyl group in the presence of Et_3N.

Changing the base from Et_3N to potassium phosphate and 1,8-diazabicyclo[5.4.0]undec-7-ene (DBU) did not lead to a more efficient cross-coupling reaction.

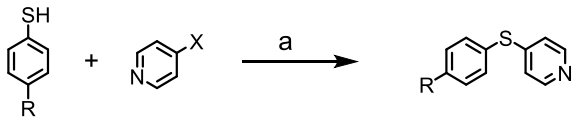

Scheme 13. Reaction of the free thiol with 4-iodopyridine; a) K_2CO_3, DMF, rt, 1.5 h.

The best results in this cross-coupling reaction were achieved by the combination of $Pd(OAc)_2$, 2-(dicyclohexylphosphino)-2',4',6'-triisopropylbiphenyl (X-Phos) and potassium phosphate in DMF at 140°C in the microwave for 1.5 hours. However, the product **8** was obtained in 14% after column chromatography.

The methyl and acetyl protective groups described above were either not fully stable under the reaction conditions they were exposed to or could not be easily deprotected. For this reason the not so widely known ethyl trimethylsilyl (ETMS) group was endeavored.

The installation of this group on 4-bromothiophenol was achieved according to a literature procedure.[170] The starting material was reacted with a small excess of vinyltrimethylsilane and di-*tert*-butylperoxide as radical initiator in a solvent-free setup (see Scheme 14). Fractionated distillation gave the desired (2-((4-bromophenyl)thio)ethyl)trimethylsilane (**10**) as colorless liquid in 76% yield.

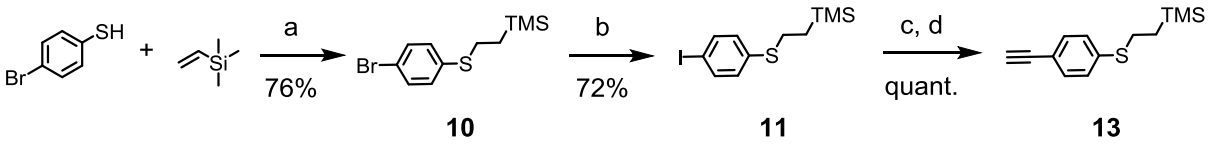

10 **11** **13**

Scheme 14. Introduction of the ETMS group, halogene exchange, introduction of the acetylene group; a) di-*tert*-butyl peroxide, 100°C, 18 h, 76%; b) I_2, *t*-BuLi, Et_2O, –70°C, 40 min, 72%; c) TMS-acetylene, $Pd(PPh_3)_2Cl_2$, CuI, $NHEt_2$, 50°C, 1.5 h, quant; d) K_2CO_3, THF/MeOH, rt, 1 h, quant.

The Sonogashira coupling of **10** with trimethylsilylacetylene did not proceed efficiently, therefore, the bromine atom was exchanged by a iodine atom by halogen exchange reaction using *tert*-butyllithium and iodine at -70°C following literature procedure,[170] see Scheme 14. Purification by column chromatography afforded the pure (2-((4-iodophenyl)thio)ethyl)trimethylsilane (**11**) in 72% yield.

The next two reaction steps also followed the procedure of Yu et al.[170] using bis(triphenylphosphine)palladium(II) chloride ($Pd(PPh_3)_2Cl_2$) as a catalyst. The base was changed to diethylamine (Et_2NH); all other conditions were kept the same as reported in the literature. The cleavage of the TMS group in the presence of an ethyl-TMS group was performed with potassium carbonate as the base. (2-((4-Ethynylphenyl)thio)ethyl)trimethylsilane (**13**) was obtained in quantitative yield over two steps as a yellow–brown solid.

In the final Sonogashira cross-coupling reaction (Scheme 15), **13** was reacted with a small excess of 4-iodopyridine to afford the intermediate **14**. The reaction was performed at 0°C, this temperature is sufficient for iodine to react in cross-coupling reactions. DMF and Et_2NH were used in a 3/2 ratio as solvents to increase the solubility of the starting materials. Aqueous work-up and column chromatography gave the pure product as a pale yellow solid in 71% yield.

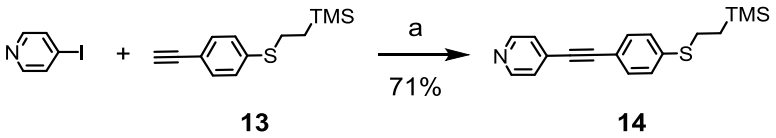

Scheme 15. Sonogashira coupling to the intermediate 14; a) $Pd(PPh_3)_2Cl_2$, CuI, Et_2NH, DMF, rt, 2 h, 71%.

The deprotection of the ETMS group with tetrabutylammonium (TBAF)[171] as well as the reaction with silver tetrafluoroborate[172,173] did not afford the desired product **2**, although these conditions are known to work well in similar systems throughout the literature (Scheme 16).

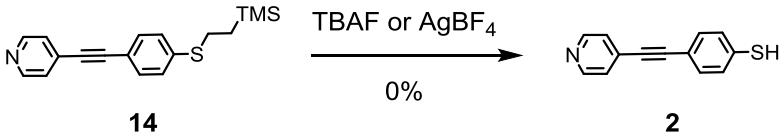

Scheme 16. Scheme of the deprtoection of the ETMS group towards the free thiol ligand 2.

A literature procedure using a mixture of TBAF and TFA[173] resulted in the decomposition of the product. The start material **14** was dissolved in THF and TBAF was added. The mixture turned orange after the addition of TBAF. The reaction was stirred for 30 minutes before it was transferred into degassed ethanol (EtOH) upon thereupon the color changed to yellow. The reaction was again stirred for half an hour before TFA was added. With the addition of TFA the solution lost color again. Aqueous work-up was performed, but no product could be found.

Because of these findings the sulfur-ETMS group was transprotect to the less stable acetyl group instead of the direct deprotection.[171] Compound **14** was dissolved in THF and treated with 20 equivalents of TBAF. After 1 hour the reaction mixture was cooled to 0°C and acetyl chloride was added, which was followed by a color change from yellow to colorless and after some minutes a white precipitate was formed. Basic work-up and purification by column chromatography gave the OPE-S-acetyl (**8**) as a pale yellow solid in 85% yield.

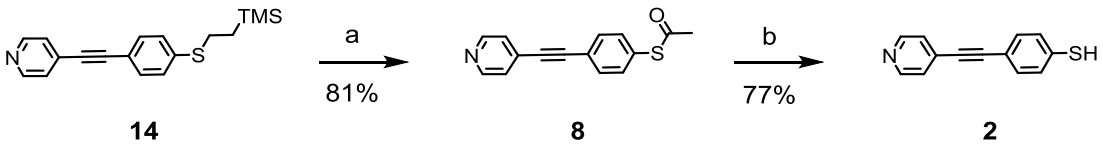

Scheme 17. Synthetic pathway of the synthesis towards the free thiol ligand 2; a) TBAF, THF, 0°C, 1 h, AcCl, EtOH, 20 min 81%; b) pyrrolidine, CH_2Cl_2, rt, 3 h, 77%.

Different reaction conditions were tested to deprotect **8** to give the free sulfur-OPE ligand **2**.

The first approach employed basis conditions.[163,174] Compound **7** was dissolved in a 1:1 mixture of THF and MeOH. Five equivalents of potassium hydroxide (KOH) were added and the mixture was stirred for 1 hour. The desired product was not, however, formed. Similar results were obtained when using TBAF, catalytic amounts of H_2SO_4[175,176] as well as Et_3N at elevated temperatures. The desired product was not formed even when the neat compound **8** was heated at 140°C.

8 was dissolved in CH_2Cl_2 and put under an argon atmosphere. To this mixture, 5 equivalents of pyrrolidine were added and the mixture was stirred at room temperature for 3 hours, see Scheme 17. The reaction progress was visualized by TLC. After an aqueous work-up the crude product was purified by column chromatography to give the pure product in 77% yield.

Acetylene bridges are very rigid bonds but double bonds exhibit better conductivity. To get a better understanding of the effect of both of these features, a ligand which has a similar length as ligand **3** but bears a double bond instead of the triple bond was designed.

For the synthesis of this ligand, the Heck reaction was the reaction of choice. The synthesis started with the building block **10** (Scheme 18). According to the literature procedure,[177] 4-vinylpyridine and **10** were suspended in an aqueous solution of potassium carbonate (0.38M). Triphenylphosphine, tributylamine and palladium chloride ($PdCl_2$) were added. The suspension was heated at 100°C for 10 hours before it was extraction with ethyl acetate. After the evaporation of the solvent the residue was filtered over a silica plug to remove the excess of vinyl pyridine, followed by sublimation at 120°C to give the pure product as a pale yellow solid in 65% yield.

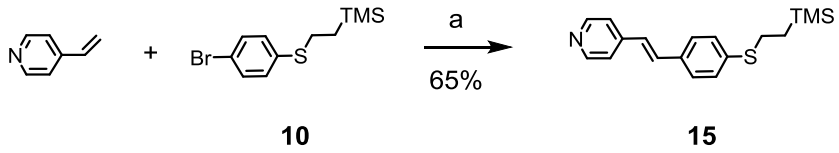

10 **15**

Scheme 18. Synthesis of the ETMS-OPV 15; a) $PdCl_2$, K_2CO_3, PPh_3, $N(Bu)_3$, 100°C, 10 h, 65%.

Because of the difficulties with the deprotection of **14** to the free thiol **2**, **15** was trans-protected to the acetyl protected compound **16**. For this reaction, the same conditions as described above did not afford the desired product. In most cases the starting material could be reisolated.

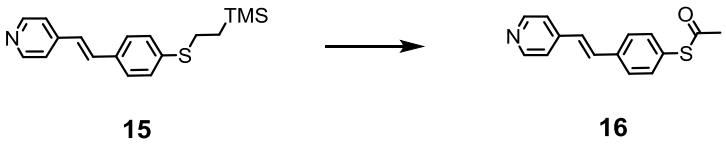

15 **16**

Scheme 19. Transprotection of 15 to the acetyl compound 16.

Reaction conditions that have not been tried for the deprotection of the OPE were investigated as for example to use silver tetrafluoroborate and acetyl chloride. Due to the strong color change upon the addition of the acetyl chloride the reaction looked promising but NMR showed that the ETMS group was still present. Also the reaction of cesium fluoride together with 18-crown-6 was not successful in terms of removing the protecting group. The reaction with a mixture of acetic acid and TBAF destructed the molecule. According to NMR no double bond was present in the molecule any more.

Besides the use of TBAF, as mentioned before, silver tetrafluoroborate and acetyl chloride as well as cesium fluoride together with 18-crown-6 and a mixture of acetic acid and TBAF were investigated in the trans-protection reaction towards the molecule **16**. None of this reaction conditions lead to the formation of the desired product **16**.

Because the trans-protection of the ETMS group was not successful, a different synthetic strategy was designed. In the new synthesis, the sulfur moiety was installed in the at last step and directly as *S*-acetyl group. Therefore the (E)-4-(4-bromostyryl)pyridine (**17**) was synthesized first, see Scheme 20.

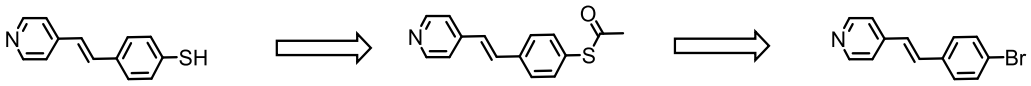

3 **16** **17**

Scheme 20. Retrosynthesis of the OPV ligand 17.

For the synthesis of **17** the procedure by Burdeniuk and Milstein[178] was found to be successful. 4-Vinylpyridine and 1-bromo-4-iodobenzene were reacted with triphenylphosphine and $Pd(OAc)_2$ in a pressure vessel (Scheme 21). The product could be purified by sublimation at 100°C and was obtained in 73% yield.

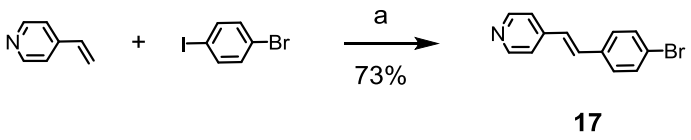

17

Scheme 21. Synthesis of 17; a) $PdCl_2$, PPh_3, Et_3N, 110°C, pressure vessel, 25 h, 73%.

The sulfur moiety was introduced according to literature[179] (Scheme 22) using 2 equivalents of potassium thioacetate in DIPEA and dioxane. Bis(dibenzylideneacetone)palladium ($Pd(dba)_2$) and 9,9-dimethyl-4,5-bis(diphenylphosphino)xanthene (Xantphos) were used as the catalytic system for the microwave reaction. After the reaction was finished the reaction mixture was poured into water and extracted with ethyl acetate. The crude product was purified by column chromatography to give the pure product **16** in 30% yield as a yellow solid.

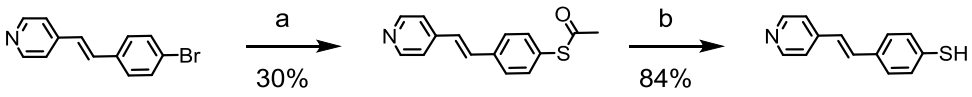

17 **16** **3**

Scheme 22. Synthesis towards3; a) KSAc, $Pd(dba)_2$, Xantphos, DIPEA, dioxane, 160°C, MW, 25 min, 30%; b) NH_4OH, THF, rt, 3 h, 84%.

The deprotection of the OPV-S-acetyl **16** with pyrrolidine, which worked in the case of the deprotection of **8**, was unsuccessful. Fortunately, the deprotection described by Röβler et al.[180] and de Boer etal.[181] were found to be successful.

For this reaction, **16** was dissolved in THF and 10 equivalents of ammonium hydroxide were added. After 3 hours, the pH of the solution was adjusted to 7 and the product was extracted with ethyl acetate. The pure product **3** was obtained in 84% yield without further purification.

3.2 Thiol Coated Gold Nanoparticles by Ligand Exchange Reaction

3.2.1 Introduction

Ligand exchange has been proven to be a powerful tool to introduce functionality to the ligand shell of thiol functionalized NPs.[80] By using this approach even water soluble NPs could be achieved.[81] Although this approach was used for a wide range of ligands it could not be used for the introduction of charged ligands.[182,183] Other challenges that arise with the exchange reaction is for example the control over the core size and driving the replacement to completion.[81] The direct synthesis of NPs with a mixed ligand shell is possible but shows drawbacks such as incompatibility of functionalized ligands with the reaction conditions or shows strong dependence of the core size on the used stabilizing ligand.[65,184]

Several reports about thiol–thiol exchange on monolayer protected clusters (MPC) can be found in literature.[94,95,185] The ligand exchange starts usually quite fast and the exchange rate drops down with ongoing reaction time.[95] This is attributed to the different reaction rates on terraces (slow exchange) and defect sites like edges and vertexes (fast exchange) of MPC, see Figure 14.[94,95] The slow exchange rate on Au(111) terraces is also a reason that some ligands usually remain unexchanged.[95] On the other hand it was also reported that ligand exchange reactions can lead to etching of the metal core, leading in some cases to the loss of the distinct size[185] and in some cases to more narrow sizes of the NPs.[87]

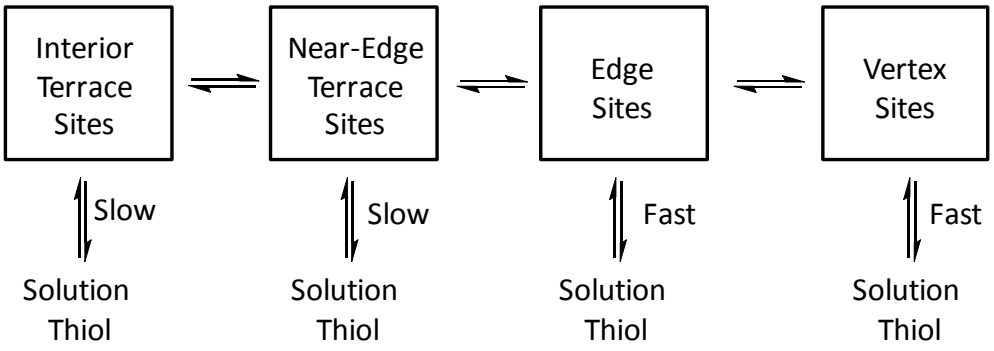

Figure 14. Processes of Place-Exchange Reactions on Au MPCs. From Ref 94

In the case of ligand exchange with 1,1'-binaphthyl-2,2'-dithiol (BINAS) as incoming ligand it is reported that the size of the particles is shifted.[186] The AuNPs consist before the exchange reaction of Au_{38} and Au_{40}NPs in a ratio of 88:12. With ongoing exchange reaction and saturation the ratio drops

to 70:30 which is a sign that the Au_{38} clusters decompose during the exchange reaction leading to the formation of Au-SR polymers.[187]

The place exchange reaction stoichiometry is

$$x(R'SH) + (RS)_m MPC \rightarrow x(RSH) + (RS)_{m-x}(R'S)_x MPC$$

and the exchanged ligands appear in the solution as free thiol (RSH) in the same ratio as the new ligand is bond to the surface (R'S). As was reported in the chapter 1.1 it is believed that the exchange reaction takes place at the surface of the nanoparticles, where the new ligand penetrates the ligand shell before the bond ligand (RS) is leaving the MPC.[94]

It seems also possible that the size and composition of the staple motifs have an influence on the exchange kinetics. For example the shell of Au_{38} consists of 3 (SR)–Au–(SR) (**M1**) and 6 (SR)–Au–(SR)–Au–(SR) (**M2**) motifs. In contrast to that Au_{40} consists of 6 **M1** and 4 **M2** units. Exchange studies showed that Au_{40} is more likely to undergo exchange and is also more stable under the exchange reactions.[186] Au_{144} is reported to be stabilized by 28 **M1** and just one **M2**.[74] It can be assumed that the smaller NPs, which have a larger curvature are more likely coated with the bend structure **M2** and larger MPCs are coated with the quite small **M1**. No matter which staple motive is exhibited in all cases the surface Au atoms on the core are bound via a thiolate at the end of the staple motif.[74]

3.2.2 Synthesis and Ligand Exchange

Au_{144}NPs were successfully synthesized according to literature[188]. In this publication they present the efficient synthesis and separation of Au_{144} from other sizes formed during the reaction by simple extraction and centrifugation. The reaction is carried out in methanol at room temperature under air. After the successful reduction with $NaBH_4$ the mixture is stirred for 4 hours to get so called particle ripening. After the separation of the formed particles from the reaction mixture they were washed several times with methanol to remove the phase transfer agent and the excess ligand. After that the particles were separated into different size fractions by subsequent centrifugation, see Figure 15.

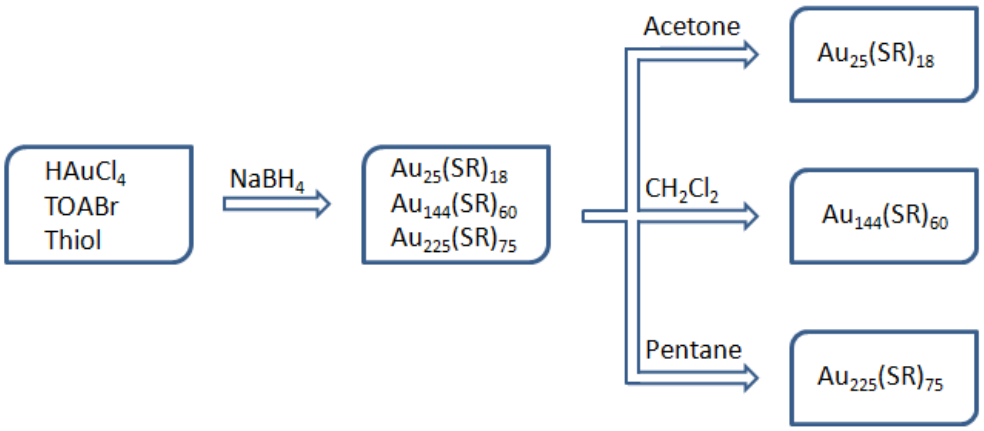

Figure 15. Schematic drawing of the synthesis and size separation of Au clusters.

The two main fractions in this synthesis were small Au particles around Au_{25} and particles around Au_{144}. Au_{25} particles were soluble in acetone while the bigger particles were not. So after dispersion in acetone and centrifugation, the supernatant contained Au_{25} particles and bigger particles formed a pellet. In the same way Au_{144} could now be separated from bigger particles and Au(I)–SR polymers using dichloromethane. Particles with a gold core-diameter of 2 nm (what corresponds to Au_{225})[189] and above were just soluble in apolar solvents such as pentane. After all the particles have been separated from the pellet a white insoluble solid was obtained. This solid corresponds to the so called Au(I)–SR polymers[187,188] that are not reduced to Au(0) during the reduction.

It is remarkable that although the reaction is performed in methanol and is therefore a one phase synthesis, the addition of TOABr is required to obtain Au_{144}NPs. The use of other phase transfer catalysts leads to different sizes and to less well defined sizes of NPs formed in the synthesis. It was discussed in section 1.1.3 that the use of a quaternary amine salt leads to the formation of a $[NR_4][AuX_2]$[69] complex that encapsulates the Au(I) and also stabilizes the freshly formed NPs to a certain extent before it is replaced by the thiol ligand. This method gives rise to bigger NPs and hampers the formation of Au(I)–SR polymers.

As reported in the section 1.1.2 the ligand shell of NPs can be altered after the synthesis by ligand exchange reaction. NPs with just a small number of anchoring ligands should be obtained. Therefore Au_{144}NPs where synthesized with hexyltiol as ligand.

Table 3. Diameter and number of Au atoms of NPs extracted with different solvents.

Solvent	Diameter	# Au atoms
Acetone		Au_{25}
Dichloromethane	1.7 nm	Au_{144}
Pentane	2.0 nm	Au_{225}
Insoluble		$(Au\text{-}SR)_{pol.}$

3.2.2.1 Ligand exchange

With the target molecule **1** in hand, ligand exchange experiments were performed using the previously prepared hexylthiol stabilized Au_{144} cluster. As mentioned before, the Au_{144} cluster is soluble in solvents with a similar or lower polarity than dichloromethane. Due to the fact that hexylthiol protected Au NPs and ligand **1** are both soluble in organic solvents such as CH_2Cl_2 no two-phase experiment could be performed. A benefit of the two-phase reaction is that it is easy to follow the change of the NPs form one phase to the other because of the intense color of AuNPs. Because of that, other methods had to be applied to verify the progress of the reaction. Therefore it was decided to follow the exchange progress by UV/Vis (Figure 16), because a change should be detectable due to the introduction of the highly fluorescent ligand **1**.

To get an idea about the exchange rate, a rough experiment was performed. Herein a small amount of Au_{144}NPs was dissolved in dichloromethane and a huge excess of **1** (1000 eq) was added and the mixture was stirred at room temperature for 3 days. To remove the excess ligand the mixture was dried, redissolved in EtOH and centrifuged for 15 minutes. This was performed twice. The pellet was redissolved in CH_2Cl_2 and UV studies were performed in this solvent. Unfortunately the strong fluorescence of the ligand **1** was cut off by the dichloromethane cut-off. The unchanged UV/Vis spectrum referred that the size of the NPs stayed constant during the exchange. The NMR did not show any evidence of ligand exchange. Also binding experiments (done at the University of Bern) with these NPs did not show any binding of the particles to the surface, indicating that the exchange reaction is not working in a reasonable amount.

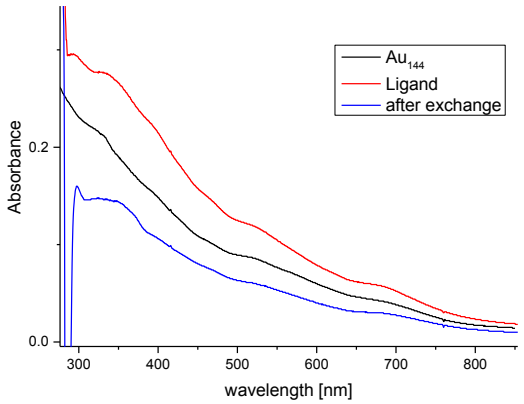

Figure 16. UV/Vis of reaction mixture (red), Au_{144} NPs before (black) and after exchange (blue) with ligand 1, all in CH_2Cl_2.

To further investigate the ligand exchange reaction and to gain an idea about the influence of the size of the ligand, three reactions were performed simultaneously with the ligands shown in Figure 17.

7.3 mg Au_{144} were dissolved in 3 ml of toluene and divided in 3 portions of 1 ml. 1 µmol of the ligand was added and the reaction mixture was degassed with argon for 10 minutes before sealed. After stirring for 5 days the samples were dried and extracted with acetone to remove the excess ligand. The residue could be separated in a methanol soluble and in a methanol insoluble part. UV/Vis and NMR measurements were performed. In the toluene soluble part, which was in all three cases the main part, no evidence could be found that an exchange of hexylthiol with the other ligand took place. In the methanol soluble part, which was the smaller fraction, a change in the UV/Vis could be detected in the case of ligand **1** but not in the case of the two other ligands **1-1** and **18**, (Scheme 17). Ligand **1-1** is the disulfide form of ligand **1**, which is formed quite fast under ambient conditions and within a view days in the freezer under argon atmosphere. In the case of ligand **1,** the reaction neither took place in a high degree, leading to the conclusion that the ligand exchange is not the way of choice to get to mixed-ligand stabilized AuNPs, compare Figure 18 to Figure 20.

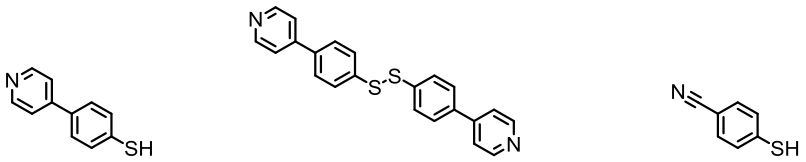

1 **1-1** **18**

Figure 17. Ligands used for the ligand exchange reactions.

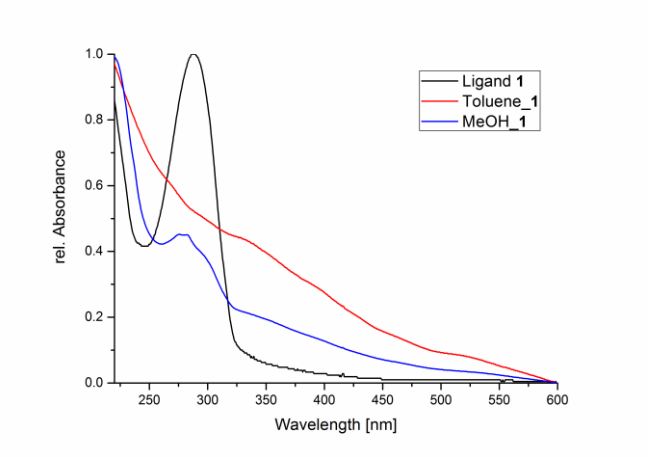

Figure 18. UV/Vis spectra of ligand exchange reactions with ligand 1.

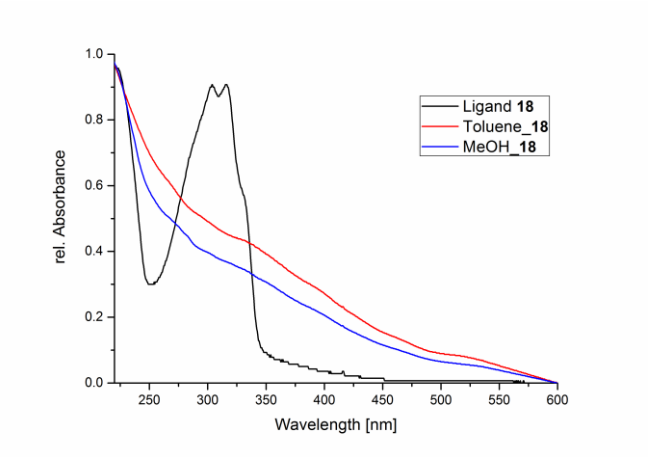

Figure 19. UV/Vis spectra of ligand exchange reactions with ligand 18.

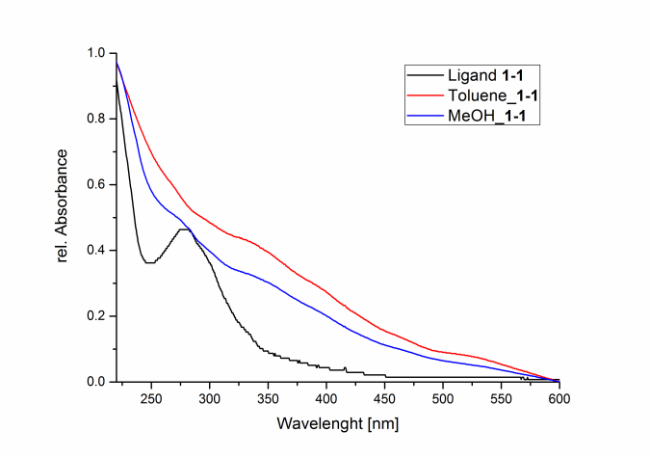

Figure 20. UV/Vis spectra of ligand exchange reactions with ligand 1-1.

3.2.2.2 Inverse ligand exchange

Because of the low exchange rate of hexylthiol with pyridine ligand **1**, the idea came up to stabilize particles with the pyridine ligand and exchange it with the hexylthiol. This exchange reaction is to be much more likely. The hexylthiol is known to be quite stable under ambient conditions without forming disulfides readily, the pyridine ligand **1** is bulky but rigid and can therefore encapsulate the particle not so densely as the hexylthiol that can rotate completely freely. The exchange should also not be working at 100% exchange because it is reported that the ligand exchange is much more likely at the edges and vertexes of a particle than at the terraces.[96]

As a test reaction, NPs were synthesized stabilized just by the pyridine ligand **1** according to the synthesis described above. Upon the addition of the ligand to the chloroaurate solution, the color of the solution turned from red to yellow. After the reduction the reaction mixture was stirred for 3 hours at room temperature. After that time the formed particles were collected and washed with methanol. The residue was not soluble in common organic solvents such as acetone, dichloromethane, ethyl acetate or acetonitrile.

It was hoped that a partial exchange of the ligand with hexylthiol would increase the solubility of the NPs. So the black solid was suspended in a mixture of toluene and ethyl acetate (2+2 ml) and hexylthiol was added. This mixture was stirred for 48 hours before the supernatant was separated and dried. Unfortunately just traces of the NPs were soluble after 2 days of ligand exchange indicating that the exchange reaction did not take place in a feasible degree.

3.2.3 Summary & Conclusion

It was shown that the exchange reaction of hexylthiol for pyridyl ligand **1** does not take place in a reasonable amount of Au_{144}NPs. Different reasons for this low exchange rate can be given. It is known that hexylthiol exhibits a strong binding to gold surfaces. Due to the low uniformity of the NPs surface, the package density is much smaller than for SAMs formed on Au(111) surfaces. This lower density makes it possible for the flexible alkyl chains to coil up and therefore hinders the attack of free ligands. On the other hand the pyridyl ligand **1** forms disulfides quite fast. Although cleavage of the disulfide bold is reported by literature, the exchange rate is lowered because of the hindered penetration of this disulfide ligand. Another disadvantage of this reaction was also the weak control over the exchange rate. Due to the fact that the exchange reaction could not be followed by NMR or UV/Vis it could not be easily followed if the exchange is occurring at all particles to a similar degree.

The formation of just ligand **1** stabilized NPs led to the formation of an insoluble black powder. The ligand exchange with hexylthiol did not lead to the increase of the solubility of the particles suggesting that the exchange did not work well. A reason for the low exchange rate might be the low solubility of the particles which hinders the attack of the hexylthiol.

3.3 Direct Synthesis with 2 Different Ligands

3.3.1 Introduction

As already mentioned on the introduction, the strategy developed by Brust and Schiffrin[65] is still the most widely used method for the synthesis of thiol capped NPs. Nowadays this method is not just used for the synthesis of gold-thiol but also of other thiol protected NPs such as silver[190,191], palladium[116,121] or copper.[191] Some advantages of this method are that it can be easily performed under ambient conditions and the easy separation of the formed NPs and the byproducts. A lot of publications describe the size focusing protocols that give rise to quite monodisperse NPs.[74,188,192] In most cases this size focusing is achieved by differentiating the ratio of gold precursor to ligand or phase transfer catalyst. Other reported parameters to tune the size of the particles are the reaction temperature and the reaction time. Especially the reaction time has a big influence on the particle size and the size distribution. It was reported in several publications that the particle size distribution is quite broad directly after the reduction of Au(I) to Au(0).[50,188,193,194] With longer reaction time, so called ripening, the size of the NPs narrows down and after a certain time (mostly 5-20 hours) just a few specific sizes of NPs are left.[188] Mostly but not always the concentration of smaller NPs decreases in this ripening process. In general the freshly formed NPs narrow their size to the magic numbers. These particles are reported to be more stable than other cluster numbers.

3.3.2 Synthesis

The synthesis of Au_{144} NP *via* ligand exchange reaction did not lead to the exchange of hexylthiol by the aromatic pyridine ligand in the desired degree. And also the fast formation of disulfide out of the pyridine ligand let to the change of the synthetic strategy.

The synthesis of Qian et al.[188] had already given rise to the effective and easy formation of Au_{144}NPs. To stay with this well working procedure it was tried to introduce the second ligand already at the stage of the NPs formation instead of performing a ligand exchange reaction on the previously formed NPs. This also seemed to be the more promising way due to possible size change of the particle core due to ligand exchange as has been discussed previously, see chapter Au–S Interface.

The ratio of thiol ligand to gold precursor was shown to be crucial for the synthesis of Au_{144} particles.[188] So the overall amount of thiol was kept constant. It was decided to use a 20:1 ratio of hexylthiol to pyridyl ligand. The pyridine ligand was used as disulfide compound due to the cleavage

of the S–S bond in the presence of gold.[195,196] The tetrachloroaurate was dissolved in NanoPure water and TOABr was added in methanol. Hexylthiol and ligand **1** dissolved in dichloromethane were added in an overall thiol to gold ratio of 5.3 to 1. Upon the addition of the thiols the solution turned cloudy. After stirring for 10 minutes at room temperature an aqueous solution of sodium borohydride was added. The mixture turned immediately black indicating the formation of NPs. After stirring for 4 hours at room temperature the particles were collected and the solvent was removed in a gas stream. The residue was suspended in methanol and centrifuged for 10 minutes. The supernatant was discarded and the pellet was again washed with methanol. This procedure was repeated until all excess thiol was removed. The amount of ligand **1** present in the formed NPs should be low what means that the solubility properties of this particles should not be influenced by the presence of a small amount of pyridine ligand **1**, so the size separation protocol of Qian was adopted.[188]

Thus the NPs were suspended in acetone and centrifuged. The brown supernatant was separated. It was containing small AuNPs such as Au_{25}. The pellet was suspended in dichloromethane and centrifuged for 10 minutes. This black supernatant solution contained Au_{144}NPs. The residue was again suspended in dichloromethane to extract also the remaining Au_{144} clusters. After drying under ambient temperature the NPs were analyzed by UV/Vis, NMR and TEM. In the NMR no clear signal in the region of the aromatic signals could be detected. It was hard to say if and how many pyridine ligands **1** were present in these NPs. So the hexylthiol to ligand **1** ratio was changed from 20:1 to 5:1 to enhance the possibility of ligand **1** to be bound to the NPs surface. But also under these conditions no clear evidence of the presence of the pyridine ligand **1** could be found by NMR. To investigate the presence of pyridine ligand and the become an idea about the binding behavior of the particles on a surface, the purified and characterized Au_{144}NPs were send to Bern for further investigations. The particles showed very limited surface binding indicating that pyridyl-ligands are present in the NPs but in a limited number.

The composition of Au particles of 1.7 nm in diameter is known to be about $Au_{144}SR_{60}$.[63,64] With a hexylthiol to pyridyl **1** ratio of 5 to 1 the composition of the ligand shell should be about 50 hexylthiol and 10 pyridyl ligands per particle. All experiments showed that the amount of pyridine ligand **1** is much lower than the theoretical amount, suggesting a much lower binding rate of the pyridine-thiol **1** compared with the binding of hexylthiol. This was already suggested upon the low ligand exchange in the exchange experiments above.

In another approach the gold salt was again dissolved in water and the phase transfer catalyst was added in methanol as well as the ligand **1**. The mixture was stirred for 5 minutes where upon the color changed from red to brown. Aqueous $NaBH_4$ was added and the mixture turned black. After 2 minutes also the hexylthiol was added and the mixture was stirred for 4 hours whereupon the

solution became brighter and was yellow at the end. More $NaBH_4$ was added, whereupon a slow reduction take place that yielded in NPs. Purification was performed as described above. The different sizes of NPs were separated by their different solubility in dichloromethane, toluene and cyclohexane. The dichloromethane fraction showed a much broader size distribution than in the other cases with a maximum peak above 2.0 nm. The toluene fraction showed a size distribution between 2.0 and 4.5 nm with a maximum peak at 3.0 nm.

This synthesis showed that the hexylthiol is able to dissolve the formed NPs if the stabilizing ligand is much weaker than the alkynthiol. The formed yellow oil was not further analyzed but the comparison with reported findings suggest that it was kind of a Au(I)SR polymer or staple motif.[61,71,197]

The tried procedures showed that the simultaneous addition of the two different ligands to the gold ions followed by reduction leads to low integration of ligand **1** in the ligand shell and the addition of hexylthiol after the reduction started, led to the decomposition of the already formed NPs. So the attempt was made to add the hexylthiol and the reducing agent at the same time. The reduction starts spontaneously and was stirred for 4 hours. The particles did not decompose in that time. After removal of the excess thiols the NPs were subjected to size separation by acetone and dichloromethane as described above. The purified NPs were analyzed by UV/Vis, NMR and TEM.

3.3.3 Analysis

TEM

One of the most widely used methods to directly observe the core of metallic NPs is Transmission Electron Microscopy (TEM). The precise core size of such NPs can be determined by directly measuring the diameter of the NPs which exhibit, due to the high density of the metallic core, a high contrast on the picture taken by this method.

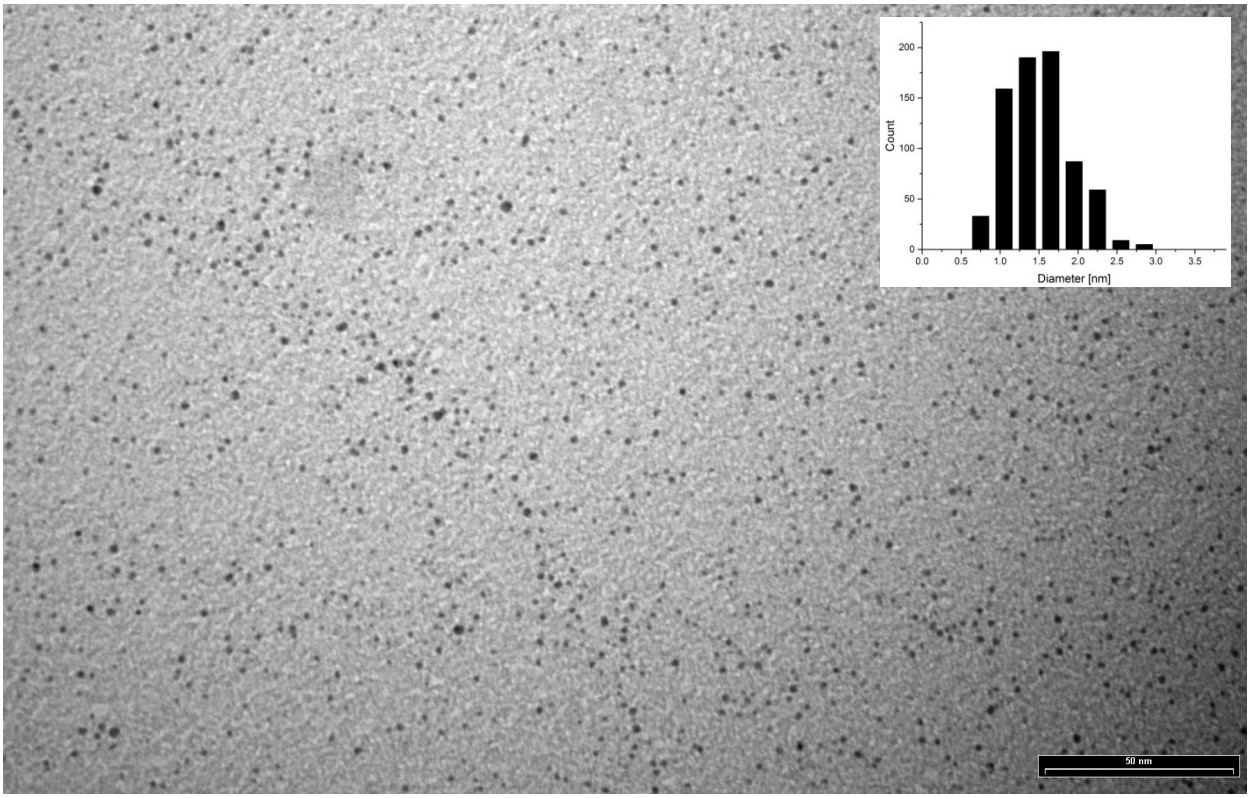

Figure 21. TEM picture and diagram of Au_{144}, the bar indicates 50 nm.

For the size distribution given by TEM measurements several pictures were used to investigate the diameter of the particles. The measurements were made by using the program *ImageJ* which gives the opportunity to determine the size of a large number of particles in a short time. The Figure 21 is such a representative picture taken by TEM. The inset gives the size distribution of the Au_{144}NPs containing CH_2Cl_2 fraction. The size of the particles is 1.7±0.6 nm and therefore in good agreement with a particle composition of about Au_{144}.

UV/Vis

UV/Vis is a nondestructive, fast and easy to handle method for determining the size of small (≤ 20 nm) NPs. As already mentioned in the section 1.1.1 NPs below 2-3 nm do not exhibit a plasmon resonance band, but still their UV/Vis spectrum (Figure 22) is quite significant and can therefore be used to investigate the size of AuNPs. The acetone soluble fraction exhibits two peaks at 400 and 450 nm which matches well with the literature for such small particles.[53,192,198] The dichloromethane soluble NPs exhibit a UV/Vis spectrum in good agreement with the literature reports.[189,199]

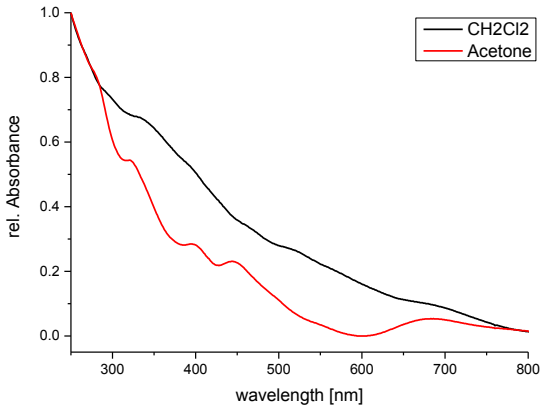

Figure 22. UV/Vis of the dichloromethane soluble (red) and the acetone soluble (black) fraction of the NPs.

MALDI-ToF MS

Matrix-assisted laser desorption/ionization (MALDI) time of flight (ToF) mass spectroscopy (MS) was proven in several publications to be a reasonable method for the size determination of metal NPs.[58,74,192,194,197] Qian and Jin[188] showed that not just the size of Au_{144} particles but also the monodispersity can be analyzed by MALDI-ToF-MS.

The achieved spectrum (Figure 23) proves nicely the size of the Au_{144}NPs containing fraction to be around 32 kDa. A similar mass for $Au_{144}(SR)_{60}$NPs was also reported by Qian and Jin[188]. They explain the mass difference between the calculated (35 kDa) and the found mass by partial loss of the thiol ligands under MALDI conditions. But also spectrum around 29 kDa are reported in literature to be related to Au_{140} – Au_{146}.[74,197,198] The MALDI spectrum achieved from the acetone soluble NPs fraction gave a distinct peak at 5.7 kDa (see Figure 24). This peak is related to particles of the size of $Au_{21}SR_{14}$ (where SR is a mixture of hexylthiol and ligand **1**) and in literature it is reported to be a fragment of $Au_{25}SR_{18}$ which has a mass around 7 kDa. This difference can be attributed to the subsequent loss of ligand and $Au_4(SR)_4$ units, where the mass of the ligand (SR) can in most cases be neglected in comparison with the high mass of gold. The loss of such small gold clusters was reported by several authors not just for MALDI but also for electrospray ionization (ESI).[59,63,194,193]

Figure 23. MALDI-ToF MS of the dichloromethane soluble fraction.

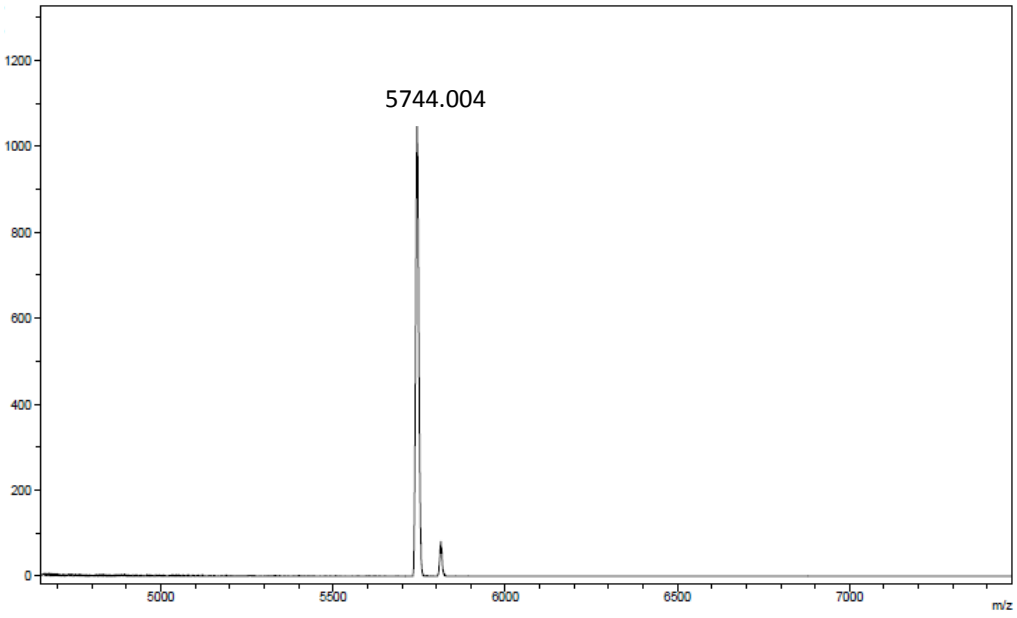

Figure 24. MALDI-ToF MS of the acetone soluble Au_{25} fraction.

High laser energy leads to splitting of the particles hence smaller masses are detected. As can be seen in Figure 25 the mass differences of the discrete signals matches the weight of an Au atom.

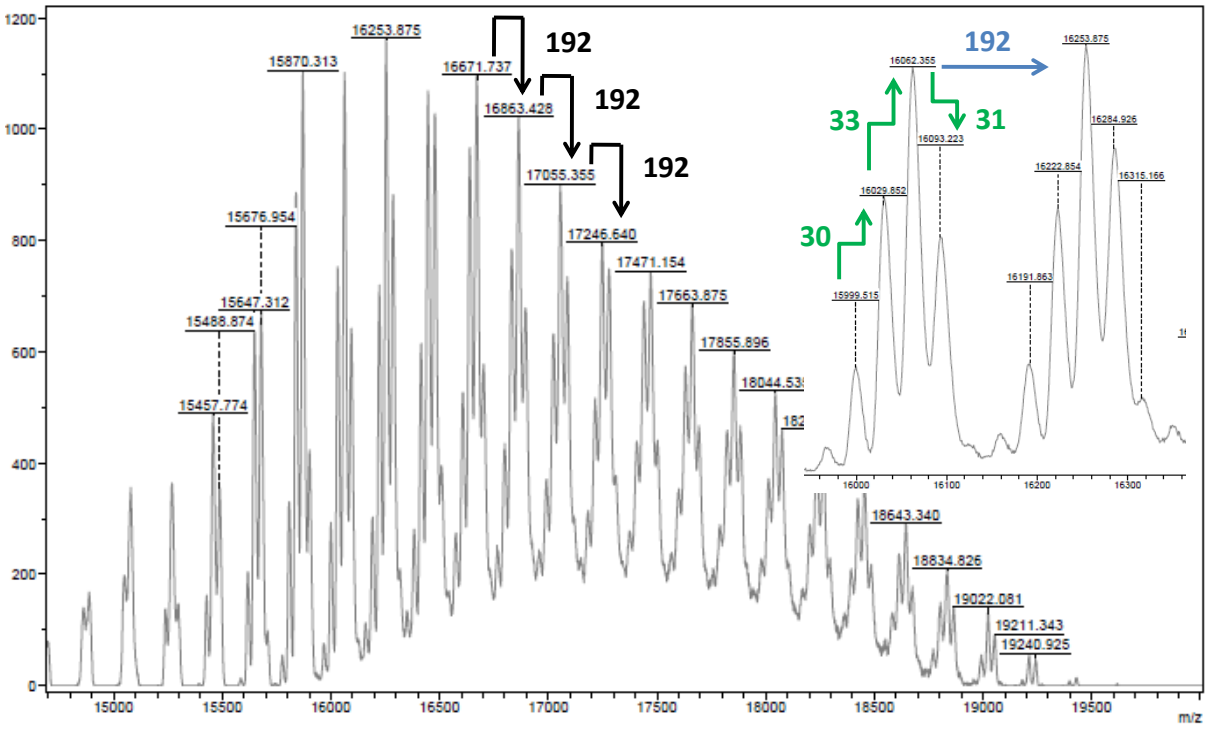

Figure 25. Masses detected by MALDI-ToF MS at high laser intensity of the Au_{144} fraction.

NMR

As already mentioned, the presence and the amount of the pyridine ligand **1** on the surface of the mixed AuNPs cannot be determined by NMR. The protons of the ligand are too close to gold surface and the system is too rigid to obtain a good resolution for the bound ligand. Because of this other ways to determine the composition of the ligand shell needed to be found. It was decided to investigate the NPs composition by elemental analysis (EA) and by thermogravimetric analysis (TGA). The EA gives the composition of the ligand shell on the element base and the TGA gives the percentage of organic compound and of inorganic residue.

Never the less NMR can be used to detect the presence of free ligand. The free ligand exhibits sharp signals that can be detected easily, even in small quantities.

EA

NMR reveals that all TOABr and excess ligand was removed from the NPs, so the sample is just consisting of the elements Au, C, H, S and N in an unknown composition. Apart from the AuNPs no other mass source was present. From the elements present in the sample (Au, C, S, H and N) EA allows merely the direct measurement of C, H and N content. The content of the other elements (Au

and S) can just be calculated. EA gave a composition of C 17.82%, H 3.09% and N 0.32%.The sulfur and gold content of the sample amount together the residue 78.7% of the sample. Both ligands consist out of C, H and S but just the pyridine ligand **1** also bears nitrogen. EA gives the mass percentage, out of which the molar percentage (Mol%) could be calculated (Formula 1), giving a ratio of C : H : N of 65 : 135 : 1 (Formula 2).

$$Mol\% = \frac{Sample\%}{MW}$$

Formula 1. Calculation of the mol% out of the found sample%; MW : molecular weight.

$$Ratio = \frac{Mol\%_x}{Mol\%_N}$$

Formula 2. Calculation of the elemental ratio with respect of N. $Mole_x$: Mol% of the element to be calculated; $Mol\%_N$: Mol% of nitrogen.

Table 4. Elemental composition of the ligands and calculation of the elemental ratio.

	MW	Atoms per Ligand Hexylthiol Ligand 1		Sample%	Mol%	Ratio
C	12.011	6	11	17.82	1.48	64.94
H	1.008	14	9	3.09	3.06	134.18
N	14.007	0	1	0.32	0.02	1.00
S	32.066	1	1			

The ratio of the elements for each ligand is given (see Table 4). Just the pyridine ligand **1** bears nitrogen and the calculation was normalized to N, so the composition of **1** (11 C, 9 H atoms) can be subtracted from the final ratio leaving a composition of 52 carbon and 126 hydrogen atoms which is exactly the composition of 9 hexylthiol ligands. The ratio of hexylthiol to pyridine ligand **1** can therefore be given with 9:1.

Calculating the amount of sulfur can, as mentioned, only be carried out theoretically and can just show if this result would fit with the found ligand composition. Both types of ligands contain one S atom what gives a ratio of (9+1) 10 and therefore the calculated S content is 7.32%. This leaves a gold residue of 71.44% which gives a Au : N ratio of 15.8:1 and a Au atom to ligand ratio of about 1.6:1.

In literature it is reported that Au_{144} particles are capped with 60 alkyl thiol ligands.[188] This gives a Auks ratio of 2.4:1 what is remarkable larger than the calculated ratio for the measured NPs.

TGA

The ligand ratio found by EA was used as given ratio of the NPs composition for a rough determination of the composition.

The TGA gave an overall loss of 24.89% where upon the major part (22.38%) was lost in the main step between 150 and 218°C, see Figure 26. The other 2.38% were lost in two minor steps at 410 and 590°C. TGA results fits very well with the molecular formula estimated from EA measurements, as 22.38% which corresponds nicely with the amount of hexylthiol, calculated as 21.16%. In that case the two minor steps could correspond to the loss of ligand **1** which is calculated to be 3.72% whereupon 2.38% were found by TGA.

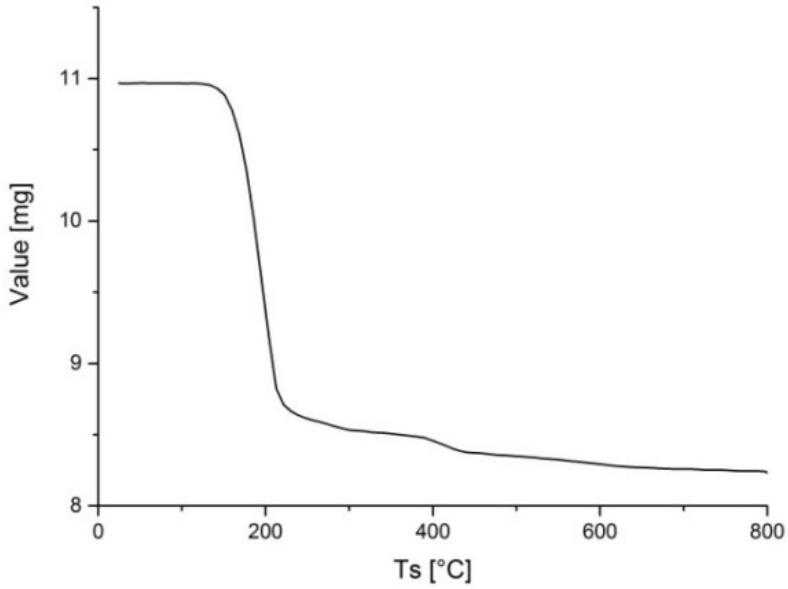

Figure 26. TGA mass loss of Au_{144} stabilized by hexylthiol and pyridine ligand 1.

A composition of $Au_{140}(SC_6H_{13})_{65\text{-}66}(SC_{11}H_8N)_7$ consists of 24.88% organic and 75.12% inorganic compound and fits the TGA results of 24.89% organic compound best. This finding is also in good agreement with the findings from EA that the ratio of gold to thiol is remarkable lower than calculated for the composition of $Au_{144}SR_{60}$.

3.3.4 Discussion

The synthesis and the analysis of mixed thiol ligand AuNPs with a metal core of 1.7 nm were performed. In the synthesis, not only the ratio of thiol to gold but also the time of the addition was a key step. The early addition of the hexylthiol leads to the expulsion of the ligand **1** whereupon the addition of hexylthiol after the started reduction of the gold leads to desorption of the already formed particles and probably to the formation of Au-SR oligomers. Only the simultaneously addition of the reducing agent and the hexylthoil leads to the formation of NPs that exhibit enough anchoring ligands to form stable SAMs.

The above mentioned measurements are all in a good agreement with the results found in literature and confirm the size of the dichloromethane fraction to be ~Au_{144}. The diameter is 1.7±0.6 nm and the literature given diameter of Au_{144} is given between 1.5 and 1.8 nm, depending on the publication and the performed measurement.[20,197,200] Although the UV/Vis spectrum of the dichloromethane fraction does not show the peaks at 500 and 700 nm it is still in good correlation with the reported spectrum for Au_{144}.[189,199] It does also not show a plasmon resonance band what would indicate particles with a diameter bigger than 2-3 nm. A mass of 32 kDa is in good agreement with the literature found mass for Au_{144} and the lower than the expected 35 kDa from theoretically calculations can be explained by the subsequent loss of ligands in the MALDI conditions. The destruction of the particles also explains the lower masses that can be found in MALDI exhibiting nicely gold pattern, see Figure 25.

EA and TGA indicate that the particles are slightly smaller than Au_{144} and are closer to Au_{140}. Furthermore both measurements reveal that the particles are covered by mixed ligands where hexylthiol is the main and pyridine **1** is the minor ligand present in the ligand shell. The composition of $Au_{144}(SC_6H_{13})_{54}(SC_{11}H_8N)_6$ fits well the results of the EA where upon a higher coverage or a smaller metal core is revealed by TGA.

3.4 Investigations

Investigations of the $Au_{144}(SC_6H_{13})_{54}(SC_{11}H_8N)_6$ towards their physical properties was performed in Prof. Wandlowski's group, at the University of Bern. Electrochemical measurements were performed which play a crucial role in the understanding of the NPs charging behavior, HOMO-LUMO gap and electron transfer kinetics.[201,202] Electrochemical techniques are limited to NPs assemblies and give therefore just an insight in the average response. To gain understanding of the electron transport of individual NPs the combination of electrochemical scanning tunneling microscopy (STM) and spectroscopic (STS) techniques was proven to be a useful technique.[203–205] These techniques provide an insight into the tunneling between a STM-tip a NPs and the substrate, see Figure 27.

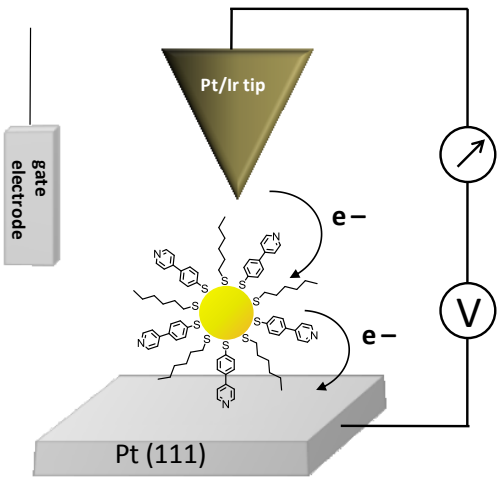

Figure 27. Schematic of the experimental setup in electrochemical STS.

The assembly of the NPs on a Au(111) surface led to the disintegration of the NPs and has driven to choose Pt(111) as surface for the SAM formation. As shown in Figure 27 the pyridine part of the ligand binds to the Pt surface and the sulfur binds to the metal core of the NPs.

The structure of the formed SAM depends significantly on the preparation of the Pt(111) surface. If the substrate was cooled down after the annealing in an argon atmosphere, the NPs formed densely packed hexagonal structures, see Figure 28 A. Upon cooling down in a water saturated mixture of hydrogen and argon the NPs formed individual, well separated clusters (Figure 28 C). Figure 28 D gives a typical cross-section profile of two individual NPs of Figure C. Figure e gives the height distribution histogram obtained from the cluster profiles as shown in Figure D. The measured height of the NPs is 3.6±0.3 nm and therefore in good relation to the theoretically calculated height of

3.2 nm (metal core + twice the length of the ligand). The STM measured height of the NPs is smaller than the NP diameter measured with the same method. This is attributed to the finite size of the STM tip and in agreement with literature.[206]

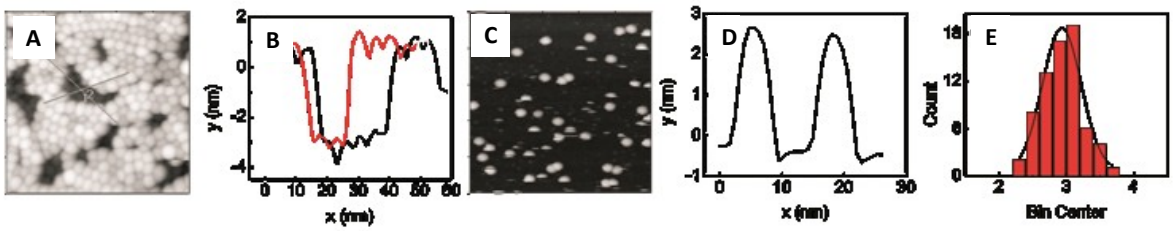

Figure 28. Ex-situ 100 x100 nm STM images of $Au_{144}(C_6S)_{50}(C_{11}H_8NS)_{10\text{-}15}$ NPs on Pt(111) surface cooled down in pure Ar (panel A) and H_2/Ar mixture (panel C). Panel B shows two characteristic profiles obtained from image A (see red and black lines). Typical cross-section profile obtained from micrograph shown in panel C (panel D). Panel E shows the height distribution histogram obtained from fifty individual cluster profiles as shown in D.

The electrochemical properties of the Au_{144}NPs were examined by using differential pulse voltammetry (DPV) in solution or as SAM on the electrode/electrolyte interface.

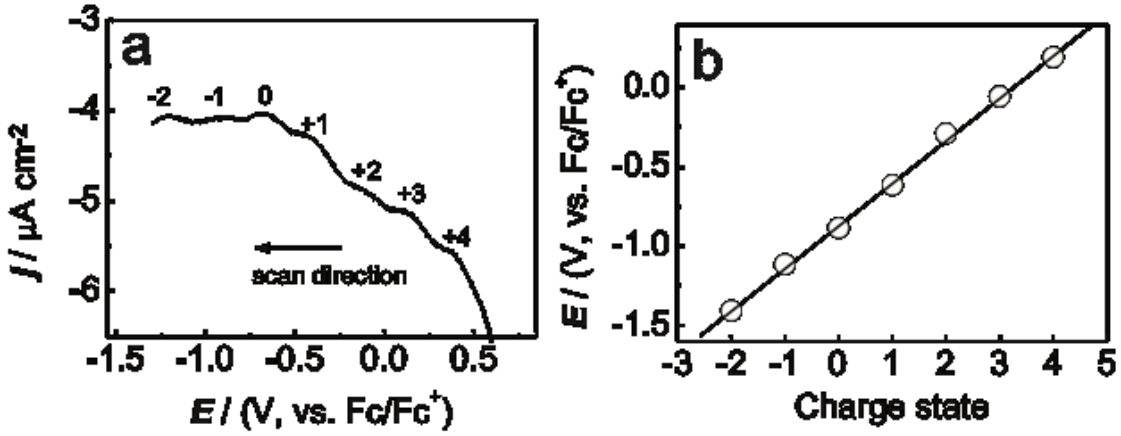

Figure 29. (A) DPV of Au_{144} clusters in SAM on Pt(111) electrode (0.1M $TBAPF_6/CH_2Cl_2$). (B) Relation between the peak potentials in (A) and the charge state of NPs.

The cathodic scan of DPV for self assembled NPs on a Pt(111) surface displays seven well defined maxima between -1.5 and +1.5 V vs. Fc/Fc^+. The maxima indicate discrete charging of the NPs within the SAM (Figure 29A). Figure 29 B shows that the position of the peaks exhibits a linear dependence on the charge state.

Scanning tunneling spectroscopy (STS) was carried out in ionic liquids because of their large electrochemical window one can address a lot of redox charging states compared to aqueous media.

Figure 30 A shows a DPV of a drop-cast NPs on Pt(111) between –0.6 and +0.8 V which is quite similar to the measurements reported in the literature for Au_{144}[207,208] with a peak to peak distance of about 0.194 V. Figure 30B shows a typical STS curve with the STS tip being kept at constant height on top of one NP. It can be clearly seen that the tunneling current increases strongly at some potentials and exhibits minima at others. The tunneling response is strongly dependent on the particle to particle distance and for closely packed NPs no double peaks can be observed. For more individually, separated particles double peaks can be found (Figure 30B, bracket indicate double peaks).

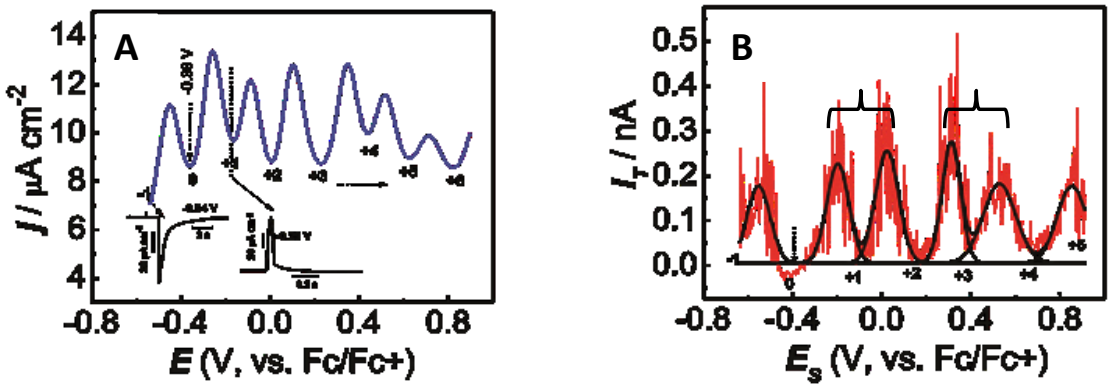

Figure 30. DPV (panel A) and constant bias tunneling current-voltage response (panel B) of a single NP on Pt(111) surface (i_{set} 50 pA, V_b = +0.1 V, E_s = –0.6 V, E_t = +0.7 V, sweep rate 0.6 V/s).

3.4.1 Summary and Conclusion

It was demonstrated that $Au_{144}(SC_6H_{13})_{54}(SC_{11}H_8N)_6$NPs form either densely packed SAM's or individual particles on a Pt(111) surface, depending on the cooling media for the Pt(111) substrate. It could be further proven that the NPs represent a multistate electronic switch at room temperature in ionic liquid. Further on it could be shown that the tunneling characteristics depend on the arrangement of the NPs on the substrate.

3.5 Elongated Pyridine Ligands for the Formation of Au NPs

Elongated conjugated ligands are expected to provide a better understanding of the effect of the anchoring ligand on the tunneling through the NPs. To test this hypothesis, ligand **1** was enlarged by inserting a triple bond (**2**) and a double bond (**3**) between the phenylene and the pyridine moiety (Figure 31). The acetylene-bearing ligand **2** is as rigid as the ligand **1,** while the double-bond-bearing ligand **3** is not as rigid as ligand **2** but should show a better performance during conductivity measurements.

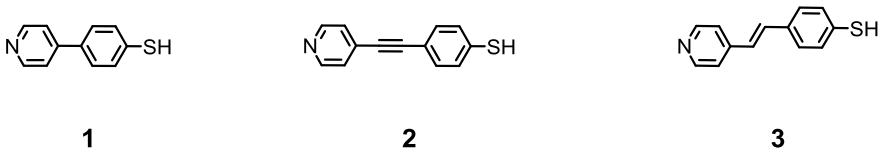

1 **2** **3**

Figure 31. Ligand 1 and the longer ligands 2 and 3.

The synthesis of Au_{144} was conducted with ligands **2** and **3** in the same way as was found to lead to reasonable results in the chapter 3.3.2. In these cases, the addition of the hexylthiol was found to be the crucial step for the formation of NPs with a mixed ligand shell. The cleaning and separation of the different sizes was performed as previously described using acetone, ethyl acetate, dichlorome

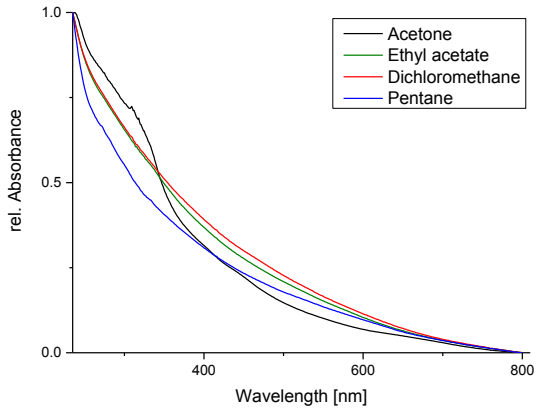

(

Figure 32) were performed to confirm the size of the isolated NPs.

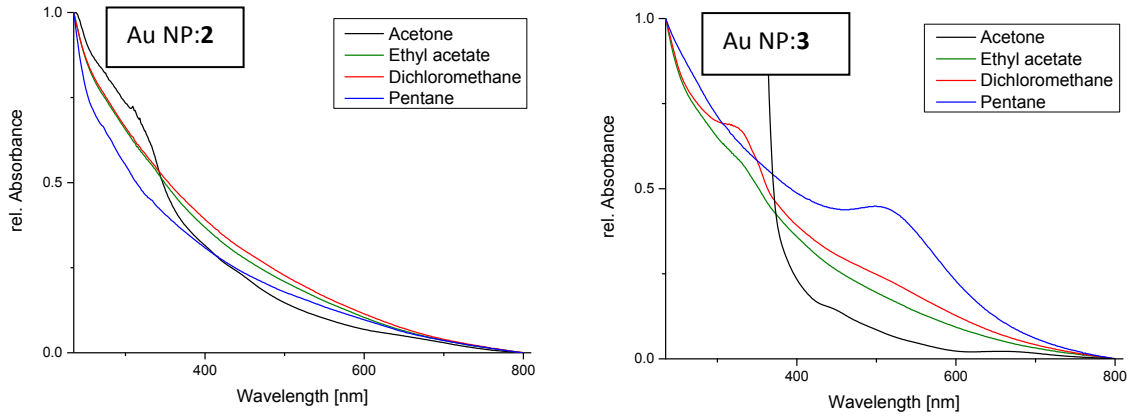

Figure 32. UV/Vis spectrum of the different fractions of Au NP with hexylthiol and ligand 2 and 3.

UV/Vis measurements show that the formed particles do not exhibit a Plasmon resonance band, except the pentane fraction of the NP containing ligand **3**. TEM of the main fraction (dichloromethane soluble) of the NPs exhibits in the case of ligand **2** a size between 1.5 and 2.1 nm, respectively, see Figure 33. The NPs bearing ligand **3** show a slightly bigger diameter with the main diameter being 2.1 ± 0.3 nm. These particles are slightly bigger than the ones formed with the ligand **1**, but should still show quantum size behavior.

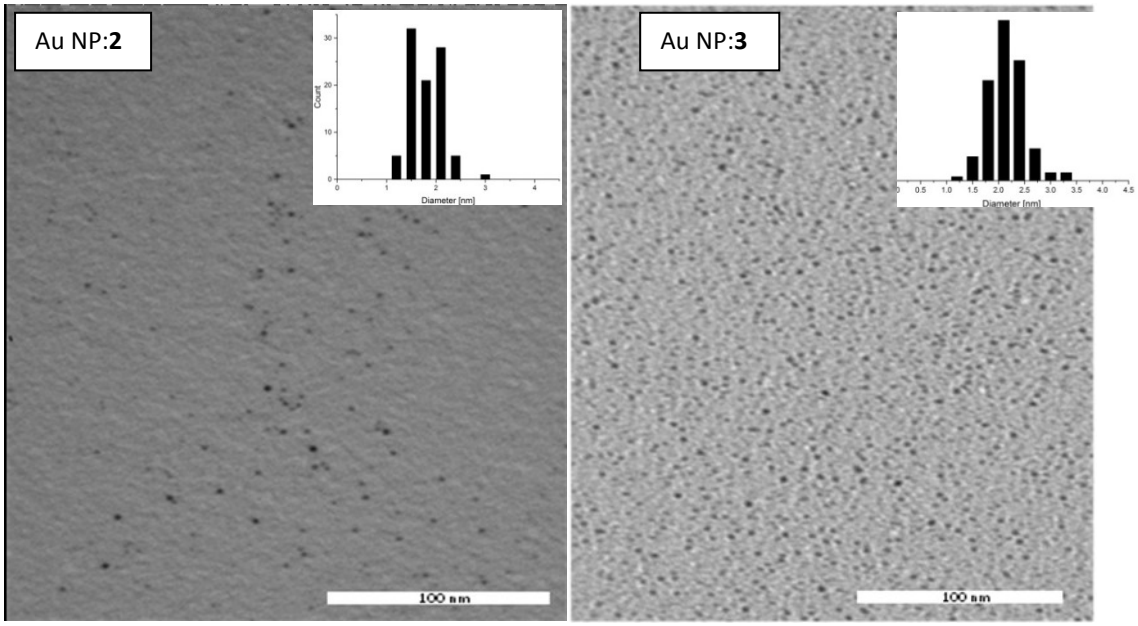

Figure 33. Representative TEM pictures of the CH_2Cl_2 fractions of the Au NPs with hexylthiol and ligand 2 and 3, respectively. The scale bare represents 100 nm.

These Au_{144}NPs were sent to the collaborators in Bern for further investigations as described in chapter 3.4.

4 Perfluoroalkylthiol Protected Gold NPs

4.1 Introduction

An important feature of the fluorine atom is its high molecular mass. The fluorine atom has a molecular weight of 18.998 g/mol which is considerably heavier than the hydrogen with a atomic molecular weight of 1.008 g/mol. Incorporation of the fluorine atoms into organic compounds by substituting hydrogen atoms like alkyl chains gives rise to molecules with a much higher molecular weight. For example, octanethiol has a mass of 146 g/mol, while 3,3,4,4,5,5,6,6,7,7,8,8,8-tridecafluorooctane-1-thiol (F-octylthiol), has a mass of 380 g/mol. In F-octylthiol 13 hydrogen atoms were replaced by fluorinated atoms. Besides the high mass of such fluorinated compounds, the flourine–carbon single bond is also much stronger than the corresponding carbon-hydrogen bond (485 kJ/mol and 425 kJ/mol). The high stability of this bond originates from the better overlap of the orbitals, which is also the reason for the remarkable thermal and chemical stability of fluorinated compounds. Fluorine atoms itself as well highly fluorinated compounds exhibit high volatility despite their high mass which arises from the low polarizability of the fluorine atoms and the low van der Waals interactions of fluorinated alkyl chains.

These unique properties of fluorinated compounds led to the idea to stabilize AuNPs with fluorinated alkyl chains and use these NPs for mater-wave experiments in the group of Prof. Arndt to reach new weight records.

4.2 Synthesis and Investigations

For the first attempt to synthesize AuNPs stabilized by perfluorinated alkyl chains, the slightly modified synthetic strategy developed by Brust et al.[209] was employed. Methanol was used as solvent to perform the synthesis in a one-phase system. The gold salt ($HAuCl_4$) was dissolved in water, two equivalent of tetraoctylammonium bromide and five equivalents of the ligand, in this case 3,3,4,4,5,5,6,6,7,7,8,8,8-tridecafluoro-1-octanethiol (F-octylthiol, Figure 34) were added. The mixture was stirred for 10 minutes before 10 equivalents of freshly dissolved sodium borohydride were added. The reaction mixture turned black indicating the formation of small NPs. The mixture was stirred at room temperature for 3 hours and during this time the solution turned brown and brighter

and it was clear and yellow at the end. The NPs had completely disappeared most likely due to polymer formation of the type Au–SR–Au–SR.

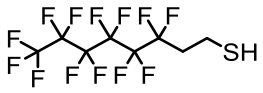

Figure 34. Stabilizing agent 3,3,4,4,5,5,6,6,7,7,8,8,8-tridecafluorooctane-1-thiol (F-octylthiol).

The synthesis was then changed to the procedure reported by Yonezawa et al.[210] In this publication, they report the synthesis of AuNPs stabilized by F-alkylthiols.

$HAuCl_4$ and F-octylthiol were mixed at a 1:1 ratio and dissolved in ethanol. The mixture was stirred at room temperature and an aqueous solution of 3 equivalents of $NaBH_4$ was added. The mixture turned immediately black and after some time a precipitate was formed. After 3 hours of stirring the precipitated particles were collected and washed.

TEM measurements show that the AuNPs stabilized by fluorinated ligands show a narrow size distribution with the particle size between 0.75 and 2.55 nm and a maximum peak at 1.5 nm. The size of the particles was also confirmed by UV/Vis spectroscopy where no plasmon resonance band could be detected, indicating that the size of the particles is below 3 nm. On the TEM picture it can be clearly seen that the particles have the tendency to pack in a well ordered manner, which is in agreement with the findings of Yonezawa et al.[210], who reported hexagonal packing of these NPs.

Due to the fact that the ligand density is not high enough to be seen in TEM the black dots in the picture (Figure 34) represent the cold core of the particle. Calculation of the Au atoms per particle with a diameter of 1.5 nm gives a result of 104 Au atoms. Particles in the range of 0.75 to 2.5 nm bear between 13 and 512 Au atoms.

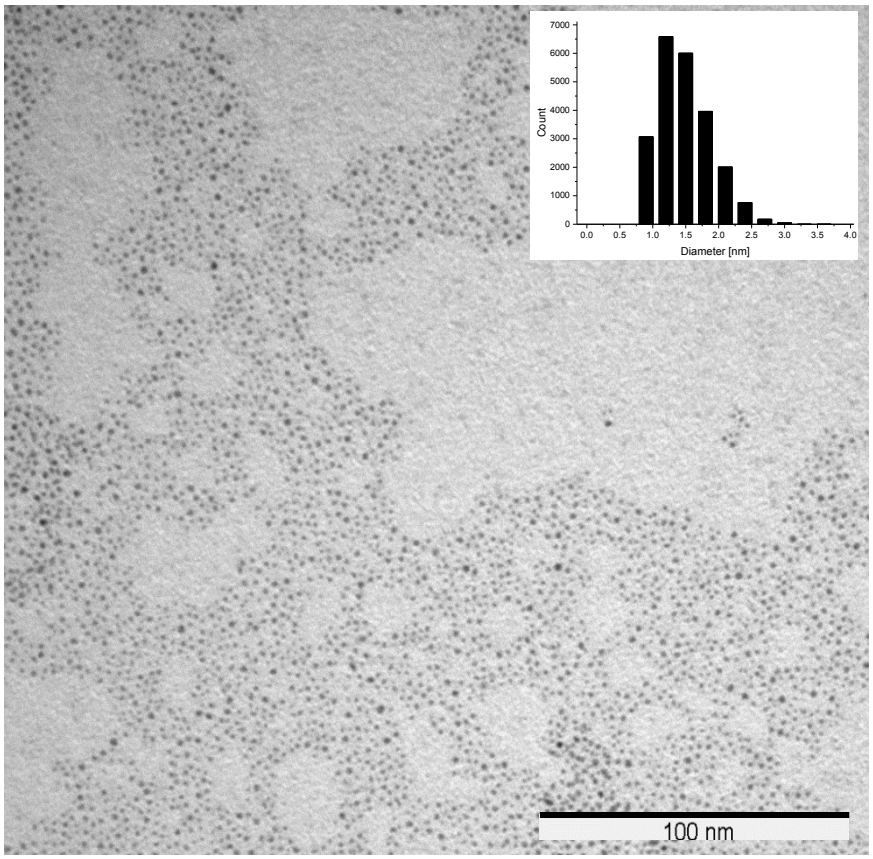

Figure 35. TEM image of F-octylthiol protected Au NP (Au:F-octylthiol).

TGA shows that the particles are stable up to 160°C with a fast release of ligands at 200°C, a second step between 230–242°C. In the heating process up to 800°C, an overall loss of mass of 56.86% was detected. This percentage means that the residual 43.14% is pure gold that does not evaporate up to 800°C. In MALDI-TOF MS an average mass of 35400 amu was found, see Appendix. Together with the TEM results, a composition of about Au_{78}(F-octylthiol)$_{53}$ is proposed. This would give particles with a diameter of 1.37 nm, a calculated mass of 35512 amu, 56.74% organic and 43.26% inorganic compound.

The NMR of these fluorinated particles was obtained in C_6F_6. Stabilization of the particles by the fluorinated legand was indicating by the broadening of the signals and the absence of any other signals in ^{1}H and ^{19}F NMR.

Conclusion

The AuNPs stabilized with perfluorinated alkylchains were synthesized and characterized by NMR, TGA and MALDI-ToF MS. The composition of the particles was determined to be about Au_{78}(F-octylthiol)$_{53}$ and have therefore a mass of about 35000 amu which is in good agreement with all measurements.

The NPs could unfortunately not be detected by mater-wave experiments. This might be due to the breaking of the thiol-gold bond under desorption conditions.

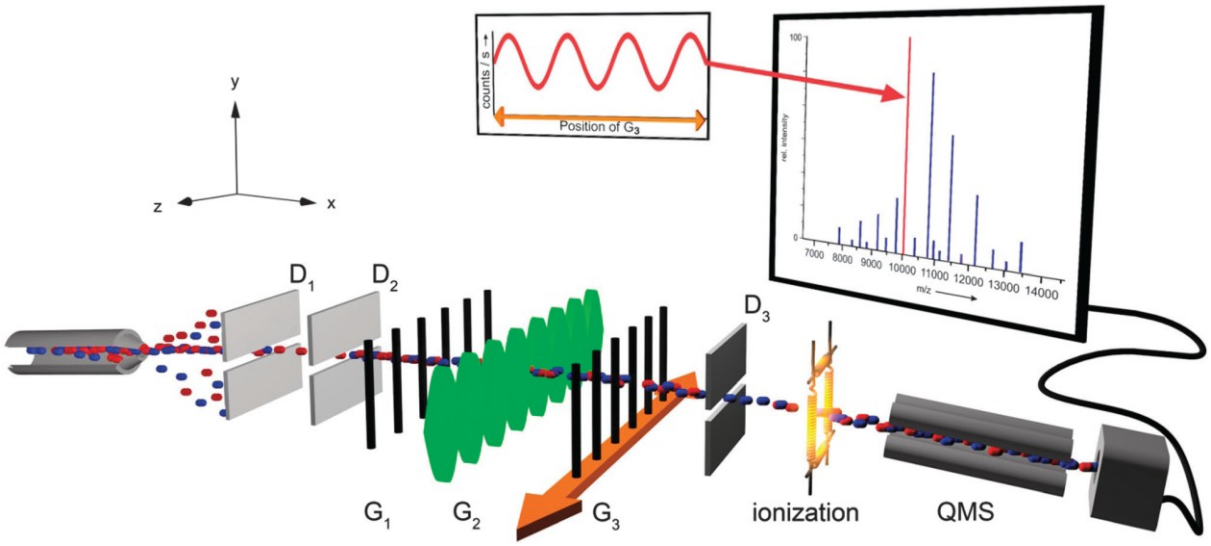

Figure 36. KDTL interferometer setup: the molecules are evaporated in a furnace. Three height delimiters, D1–D3, define the particle velocity by selecting a flight parabola in the gravitational field. The interferometer consists of three gratings with identical periods of d = 266 nm. G1 and G3 are SiN_x gratings, whereas G2 is a standing light wave which is produced by retro-reflection of a green laser at a plane mirror. The transmitted molecules are detected using electron ionization quadrupole mass spectrometry after their passage through G3, which can be shifted along the z-axis to sample the interference pattern. Adapted from Referenz 211.

The NPs were tried to be detected by a new type of interferometer which is similar to the one shown in Figure 36[211] The biggest particles detected in such a set-up have a mass of 10000 amu.[211,212] So the fluorinated Au NPs would have been by far the biggest “single molecules” and would have given rise to a big variety of easy to synthesize molecules with even bigger masses.

Further synthetic approaches towards fluorinated NPs for mater-wave experiments are made investigating different metals, ligands as well as binding motifs.

5 Gold NPs Stabilized by Au–C Bonds

5.1 Introduction

One of the main challenges in the nanoscale assembly of single molecules (or NPs) and electrodes is the formation of well-defined, stable and highly conducting contacts.[213] Many different chemical anchoring groups have been investigated to fulfill these requirements.[214–218] The most frequently used functional groups to bind organic molecules to metal surfaces are thiol (–SH)[214,219], amino (–NH_2),[220] and pyridyl.[221,222] For practical applications however, the robustness and stability of such stabilized particles needs to be enhanced and their electronic properties need to be chemically modified.[40]

High single-molecule junction conductance was reported for metal–carbon couplings, such as those in oligo(phenylene ethylene) (OPE) rods attached to the electrodes by acetylene moieties.[213] Several groups reported the binding between carbon and metal in case of Au, Fe and PdNPs.[40,139,223–225] These methods produce mainly NPs with diameters lager than 2 nm. Maity et al.[40,226] reported that AuNPs with terminal acetylene ligands smaller than 2 nm cannot be formed directly by synthesis from metal precursor (such as $HAuCl_4$) but via ligand–exchange reaction. Polyvinylpyrrolidone (PVP)-stabilized AuNPs were proved to be a suitable precursor for this exchange reaction because they gave rise to NPs with a diameter smaller than 2 nm.

Maity et al. reported that AuNPs with terminal acetylene ligands smaller than 2 nm cannot be formed by direct synthesis from an inorganic metal precursor ($HAuCl_4$), but instead from a PVP stabilized AuNPs via ligand exchange (Scheme 23).[40,226]

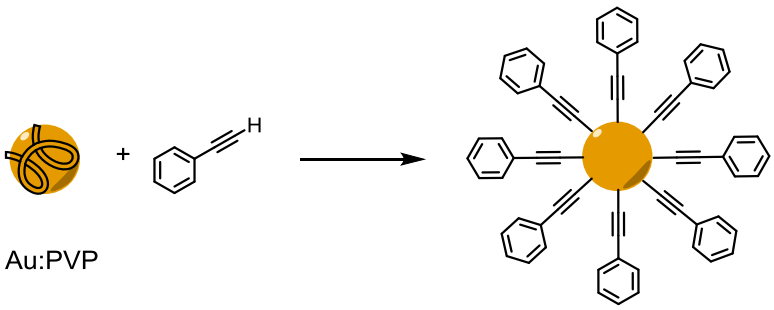

Scheme 23. Synthesis of phenylacetylene protected Au clusters.[40]

As reported by Maity et al.,[226] four binding motives (Figure 37) for an ethyne unit such as phenylacetylene to bind to a gold surface have been proposed.[223,227–232] In **type 1**, the dehydrogenated alkynyl group (R–C≡C–) is bound to the metal surface in an upright position by forming a bond.[223,227,229,230] In **type 2**, the alkynyl group is in a flat-lying orientation bound to the gold surface via a σ–π interaction.[231] In **type 3**, the alkyne moiety is transferred into a vinyliden group (RCH=C=) by intramolecular hydrogen transfer and is bound in a upright orientation.[223] In **type 4**, the intact ethynyl group is bound in a flat-lying fashion on the metal surface *via* π–π interactions.[232]

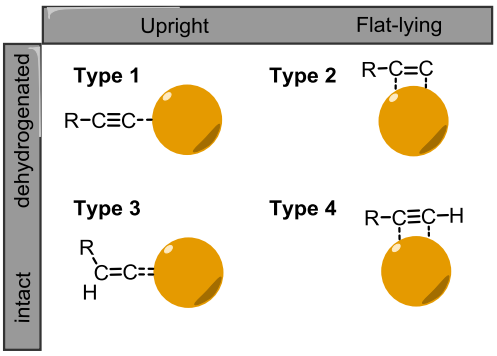

Figure 37. Proposed binding motifs of ethynyl to a gold surface.

As loss of H_2 was confirmed by IR and mass spectroscopy, **types 3** and **4** cannot be the favored binding motives.[223,226] Photoluminescence behavior as well as theoretical calculations confirmed that the upright binding motif of the ethynyl ligand in **type 1** is most favored with **types 2** and **3** as possible intermediates.[223]

5.2 Acetylene Ligands Synthesis

Figure 38shows the target ligands **19–21** synthesized for the exchange reaction towards Au NPs stabilized by Au–C bounds.

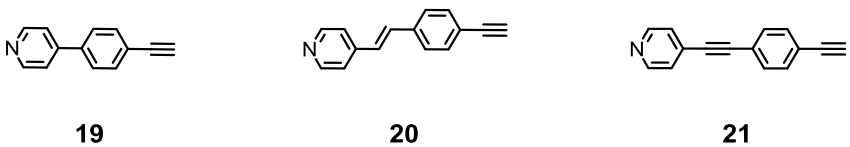

19 **20** **21**

Figure 38. Three different acetylene ligands for the ligand exchange reaction.

The synthesis towards ligand **19** started with a Suzuki cross-coupling to intermediate **22** following the procedure by Su et al.[233], see Scheme 24. In brief, pyridine-4-boronic acid and 1-bromo-4-iodobebzene were dissolved in toluene and EtOH. Potassium carbonate was added as a 2M solution. $Pd(Ph)_4$ was added and the mixture was heated to reflux for 24 hours. The crude was extracted with toluene and further purified by column chromatography to give the product as white solid in 73% yield.

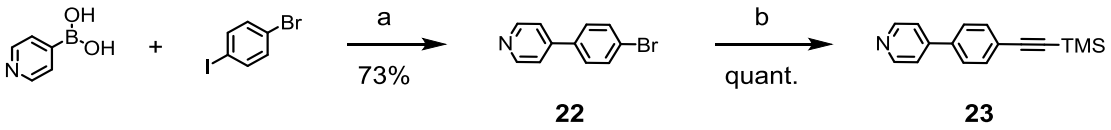

22 **23**

Scheme 24. Synthesis of 23; a) $Pd(PPh_3)_4$,2M K_2CO_3, toluene/EtOH, reflux, 24 h, 73%; b) TMS-acetylene, $Pd(PPh_3)_2Cl_2$, CuI,Et_3N, THF, 100°C, MW, 20 min, quant.

In a standard Sonogashira coupling reaction **22** was reacted in the microwave to the TMS-acetylene **23**. The product was purified by sublimation in quantitative yield. This product was dissolve in a mixture of MeOH and EtOAc and treated with 3 mol equivalent of potassium carbonate. After an aqueous work-up the crude was purified by column chromatography to give the free acetylene **19** in quantitative yield.

With the same procedure as used to synthesize **23**, **17** was reacted with TMS acetylene to (E)-4-(4-((trimethylsilyl)ethynyl)styryl)pyridine (**24**) in 57% yield. Deprotection of the TMS-acetylene was performed in a mixture of MeOH and THF with potassium carbonate to yield the desired product **20** in quantitative yield, see Scheme 25.

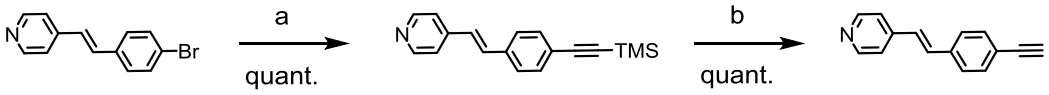

17 **24** **20**

Scheme 25. Synthesis of ligand 20; a) TMS-acetylene, $Pd(PPh_3)_2Cl_2$, CuI, Et_3N, THF, 100°C, MW, 20 min, quant.; b) K_2CO_3, MeOH, THF, rt, 1 h, quant.

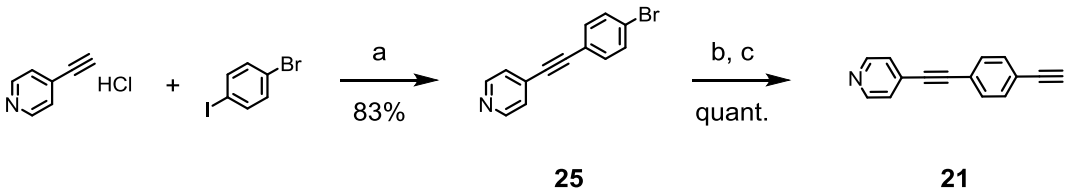

Scheme 26. Synthesis towards the ligand 21; a) $Pd(PPh_3)_2Cl_2$, Et_3N/DMF, rt, 30 min, 83%; b) $Pd(PPh_3)_4$, TMS-acetylene, CuI, Et_3N, DMF, 120°C, MW, 20 min, 80%; c) K_2CO_3, THF/MeOH, 1 h, rt, quant.

The synthesis towards ligand **21** was reported in literature[234] and started with a Sonogashira reaction of 4-ethynylpyridine hydrochloride and 1-bromo-4-iodobebzene in Et_3N and $Pd(PPh)_2Cl_2$ at room temperature to give the 4-((4-bromophenyl)ethynyl)pyridine **25** as white solid in 83% yield as shown in Scheme 26. In another Sonogashira reaction the TMS-acetylene was installed in the microwave at 120°C. Sublimation gave the acetylene protected product as white solid in 80% yield. This white solid was dissolved in a 1/1 mixture of THF and MeOH and treated with potassium carbonate for 1 hour to give the free acetylene compound **21** in quantitative yields.

5.3 Investigations of the Ligand Exchange Reaction

To enhance the conductivity between AuNPs and electrodes, the acetylene derivatives (Figure 39) of the thiol ligands investigated earlier (Chapter 1) were synthesized.

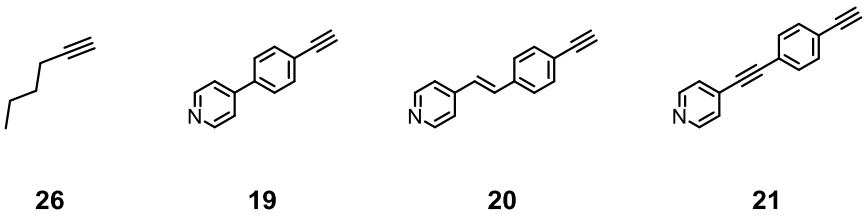

Figure 39.Ligands for the synthesis of acetylene protected Au NPs.

It is reported that polymers like polyvinylpyrrolidone (PVP) are able to stabilize NPs (Au NP:PVP).[235–237] PVP can be dissolved in water and a broad variety of organic solvents. This polymer is on one hand able to stabilize AuNPs quite efficiently and, on the other hand, the interactions between the polymer and the NPs are weak enough, so the particle surface can easily be modified by ligand exchange reactions.

PVP protected NPs could be easily synthesized in large quantities following a procedure reported by Tsunoyama and coworkers.[235] For this synthesis, $HAuCl_4$ and PVP were dissolved in water and stirred for 30 minutes at 0°C. With the addition of aqueous $NaBH_4$, the reaction towards NPs took place. The resulting reddish–brown NPs mixture was dried without further purification by lyophilization to prevent the particles from coagulation.

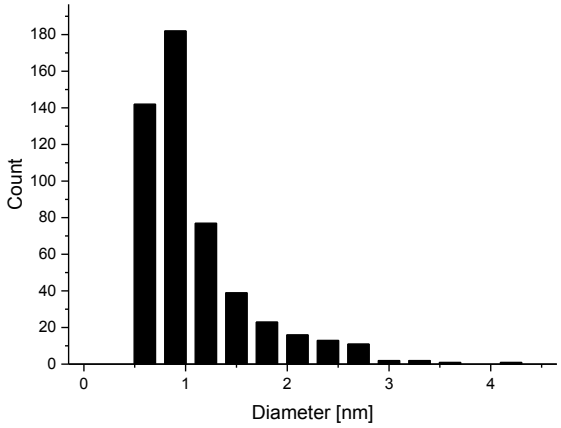

Figure 40. Size distribution of AuNP:PVP clusters.

For the preparation of acetylene–covered gold clusters out of PVP-stabilized NPs the procedure reported by Maity et al.[40] was applied. For this reaction the lyophilized PVP-stabilized AuNPs (Au NP:PVP) were redissolved in water. Molecule **26** was dissolved in toluene and added to the aqueous NPs solution. This two-phase system was stirred and heated at 60 °C for 2 hours. After this time, the toluene phase had turned brown and the aqueous phase had lost color, but was still slightly brown. The organic phase was concentrated and used for further analysis. Matrix-assisted laser desorption ionization time-of-flight (MALDI-TOF) mass spectrometry (MS) of the particles was obtained with the use of *trans*-2-[3-(4-tert-butylphenyl)-2-methyl-2-propenylidene]malononitrile (DCTB) as the matrix, see Figure 41. The comparison of the ^{1}H NMR spectrum of the PVP stabilized and the hexyne stabilized AuNPs shows clear changes. No peaks corresponding to PVP were detected after the ligand exchange reaction. The broader peaks in the aliphatic region, compared with the spectrum of the free hexyne indicate the linkage of the acetylene to the surface of the NPs.

5.4 Investigations and Calculations

The size of the particles obtained with this procedure was significantly more monodisperse than that of the PVP-stabilized particles.

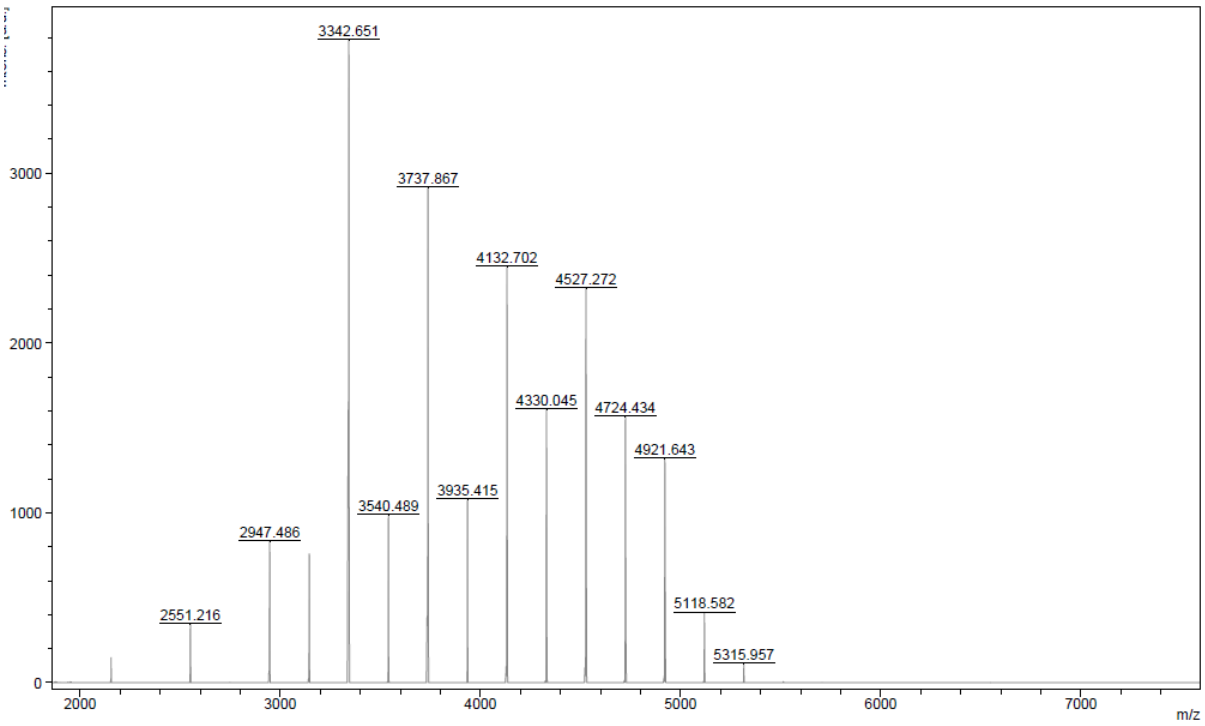

Figure 41. MALDI-TOF MS spectrum of Au NP:26 clusters.

Particles obtained with this procedure had a remarkable high monodisperisity according to MALDI-ToF MS. The size distribution was between 2500 and 5100 amu with 4 main peaks at 3342, 3737, 4132 and 4527 amu. These particles were too small to be measured by TEM, so the mass was determined just by the MALDI-ToF MS analysis, see Figure 41. To get an idea of the composition, a list of possible composition was calculated, see Table 5.

Table 5. Found and calculated masses of Au NP:26 clusters.

found		# hexyne			
m/z	**Au atoms**	5	7	12	17
2947.5	8	1981.4	2143.7	2549.4	2955.1
3145.3	9	2178.4	2340.7	2746.4	3152.1
3342.7	10	2375.4	2537.6	2943.3	3349.0
3540.5	11	2572.3	2734.6	3140.3	3546.0
3737.9	12	2769.3	2931.6	3337.3	3743.0
3935.4	13	2966.3	3128.5	3534.2	3939.9
4132.7	14	3163.2	3325.5	3731.2	4136.9
4330.0	15	3360.2	3522.5	3928.2	4333.9
4572.3	16	3557.2	3719.4	4125.1	4530.8
4724.4	17	3754.1	3916.4	4322.1	4727.8
4921.6	18	3951.1	4113.4	4519.1	4924.8
5118.6	19	4148.1	4310.3	4716.0	5121.7
5316.0	20	4345.0	4507.3	4913.0	5318.7
	21	4542.0	4704.3	5110.0	5515.7
	22	4739.0	4901.2	5306.9	5712.6
	23	4935.9	5098.2	5503.9	5909.6
	24	5132.9	5295.2	5700.9	6106.6
	25	5329.9	5492.1	5897.8	6303.5

As shown in Table 5the found masses from MALDI-ToF MS analysis fit the compositions with 8–22 Au atoms and 12 or 17 ligands reasonably well. These compositions fit the found mass best with differences lying between 3 and 9 amu. The difference between the calculated and the found mass is within the margin of error and considerably smaller than the one shown in the publication of Maity et al.[40] The composition bearing 5 and 7 hexyne ligands does not seem to be very likely. Mass differences between 14 and 21 amu and compositions as, for example 25 Au atoms stabilized by five, considerably small ligands seem to be unfavored. The main peaks seem therefore to have a composition of $Au_{12}hexyne_{12}$ or $Au_{10}hexyne_{17}$ for 3342, $Au_{14}hexyne_{12}/Au_{12}hexyne_{17}$for 3737, $Au_{16}hexyne_{12}/Au_{14}hexyne_{17}$ for 4132 and 4527 with a composition of $Au_{18}hexyne_{12}/Au_{16}hexyne_{17}$. The full list of calculated masses can be found in the appendix.

5.4.1 Investigations with Aromatic Ligands and TMS Protected Acetylene Ligands

Several attempts were made to get particles stabilized with a mixture of pyridine ligands **19** to **21** and hexyne **26**.The exchange reactions were performed in the same way as with hexyne. In the first attempt, the PVP stabilized AuNPs dissolved in water were treated with a 10:1 mixture of hexyne and pyridine ligand **19**. After a reaction time of 3 hours, the water and the organic phase were both light brown and none of the fractions was black to purple in color, as the presence of AuNPs would indicate. After drying the organic phase no particles, could be detected by TEM or MALDI-ToF MS. UV/Vis measurement was not performed due to the lack of purification possibilities.

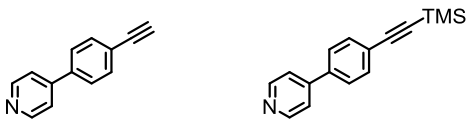

19 **23**

Figure 42. Ligand 19 and TMS protected acetylene ligand 23.

Because of these findings, the ligand exchange reaction was performed with only the pyridine ligand **19** to gain understanding if the mixing of the two ligands leads to the decomposition or if it is the pyridine ligand **19** itself, which causes the decomposition of the AuNPs. The exchange reaction with the ligand **19** led to fast decomposition of the NPs with a complete colorless aqueous phase and an organic phase in the light brown color, corresponds to the pyridine ligand **19**.

To verify whether the gold surface interacts with the free acetylene and not with the pyridine, the PVP-stabilized AuNPs were treated with the TMS-protected ligand **23** (Figure 42) in the same way as with the free acetylene ligand **19**. The PVP-stabilized Au NPs were dissolved in water and the ligand was dissolved in toluene. This mixture was heated at 60°C under vigorous stirring for 8 hours. No transfer of NPs to the organic phase could be detected indicating that the free acetylene and not the pyridine interact with the AuNPs surface in this case.

5.5 Summary & Conclusion

PVP protected Au NPs were successfully synthesized. The ligand-exchange using hexyne was successful and gave monodisperse although relatively quite small NPs. The MALDI-ToF MS analysis gave us information about the composition of the hexyne stabilized NPs although the final composition of the nanoclusters could not be determined.

The presence of any of the above mentioned aromatic acetylene ligands lead to the composition of the NPs. This happened also in the case of mixtures of hexyne and aromatic acetylene ligands. By exposing the PVP stabilized NPs to TMS protected ligand **23** it could be proven that the pyridine is not able to conduct a ligand exchange. This also means that the acetylene moiety and not the pyridine lead to the disintegration of the NPs in the ligand exchange reaction with the aromatic ligands.

6 Ether Ligands for the Inclusion of Nobel Metal Clusters

Reports about NPs stabilized by ether-containing molecules mostly described to ether-containing polymers.[238,239] In these cases the stabilization is usually not achieved by the interaction of the metal NPs with the ether moieties but by the bulkiness of the polymer and the resulting steric repulsion. One example of such a polymer is given in Figure 43.

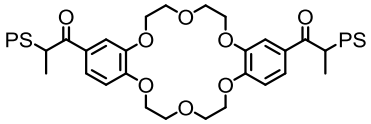

Figure 43. Chemical structure of a polymer with a crown ether; PS = polystyrene.[238]

Due to the fact that ether-containing polymers do not exhibit strong interactions with the surface of the NPs, the formed metal NPs exhibit usually quite a broad size distribution. This polydispersity makes these particles suitable as catalyst, but not a very good material for physical and electronical investigations.

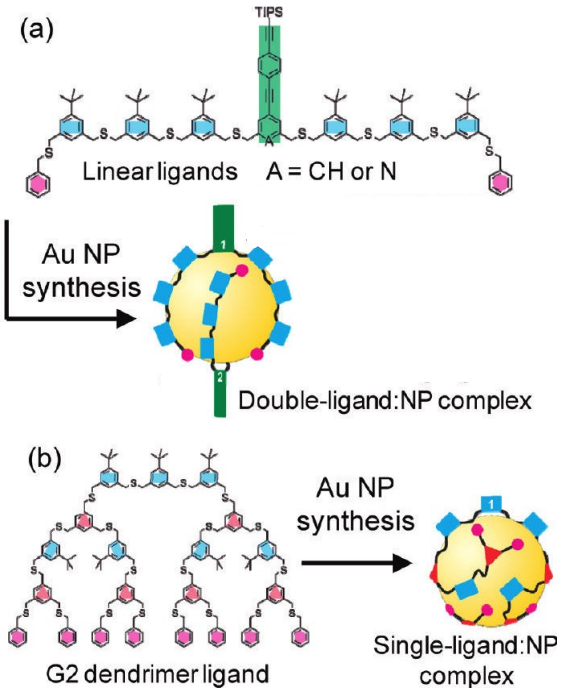

Figure 44. Illustration of the ligand-mediated nanoparticles synthesis, showing the key components and structural features. (a) Double-ligand particle complex formed using linear ligands. (b) Single-ligand particle complex formed using the second-generation dendrimer. Adapted from [240]

Previously in this research group, it was proven that thioether ligands like illustrated in Figure 44 are able to stabilize AU NPs and that the stabilization is due to the interaction of the sulfur in the ligand with the gold surface.[159,161] Computational studies proved that two heptameric ligands, each bearing eight sulfur atoms, are needed to enwrap one Au NP of 55 gold atoms (Figure 44 a). Just one ligand is needed to stabilize the same size of NP in the case of a brached ligand (Figure 44 b) bearing the same amount of sulfur moieties as two linear heptamer ligands.[240]

To broaden the scope of the metal NPs that can be stabilized by such ligand systems ether ligands should be synthesized and investigated (Figure 45).

6.1 Oxygen-Containing Ligand Synthesis

6.1.1 Synthesis of the Building Blocks

The symmetric design of the linear benzylether ligands **33** to **36** (Figure 45) allows for two synthetic strategies: one approach starting from the central monomer, where the monomeric units can be attached at each end simultaneously, or starting from the benzyl end of the linear ligand, to which the monomeric units are attached in a step-by-step fashion, see Scheme 27.

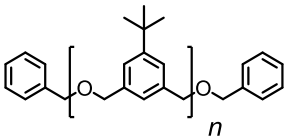

n = 7 Heptamer **33**
n = 5 Pentamer **34**
n = 3 Trimer **35**
n = 1 Monomer **36**

Figure 45. Linear ligands 33, 34, 35 and 36.

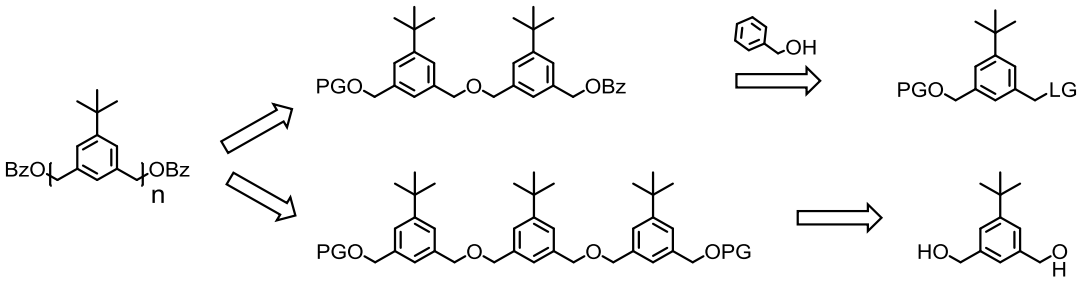

Scheme 27. Retrosynthetic pathways for the synthesis of linear ligands; Bz: benzyl, PG: protecting group, LG leaving group.

The synthetic strategy towards these ligands is based on nucleophilic substitution reactions, which *per se* require for one reactant to process as a leaving group and the other one to act as a nucleophile. One of the most common synthetic approaches towards ethers is *via* reacting benzylic halids with alcohols. Symmetric building blocks are required for the synthesis of such ligands and theirfore, a difunctional compound was required, carrying one benzylic leaving group and one protected benzylic alcohol.

The building block **37** can be easily obtained by radical bromination of the commercially available 5-*tert*-butyl-1,3-xylene with *N*-bromosuccinimide (NBS). A commonly used solvent for this type of

reaction is carbon tetrachloride. Due to the fact that this solvent is toxic, carcinogenic and ozone-layer damaging (see Material Safety Data Sheet), another solvent was chosen. Methyl formate was shown to work also very efficiently for bromination at the benzylic positions. A procedure that makes use of this solvent was therefore adapted for the synthesis of the dibromide **37** (Scheme 28). The radical reaction was initiated by 2,2'-azobis(2-methylpropionitrile) (AIBN) and illumination with a 500 W halogen lamp. The distance of the lamp and the reaction flask was chosen such that the heat emitted by the lamp also heated the mixture at reflux. After the reaction time of 3 hours, aqueous work-up and purification by recrystallization from cyclohexane afforded the pure product **37** as white crystals in 71 % yield on a multigram scale.

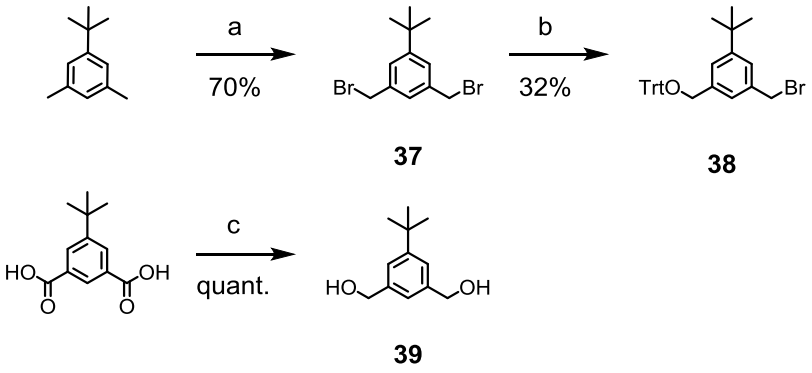

Scheme 28. Synthesis of 37, 38and 39. a) NBS, AIBN, HCOOMe, *hv*, reflux, 70%; b) TrtOH, NaH, THF, reflux, 18 h, 32%; c) $LiAlH_4$, THF,–20°C, 4 h, quant.

The central diol-building block **39** was synthesized starting from the commercially available 5-*tert*-butylisophthalic acid (Scheme 28). The starring material was dissolved in dry diethyl ether and cooled to –20°C to –35°C before lithium aluminum hydride ($LiAlH_4$) was added portion-wise.[224] The reduction agent was not added as a solution but as a powder due to the need of more than the double-molar amount of $LiAlH_4$in relation to the starting material and the large scale of the reaction. After the reaction time of 4 hours at –20°C and aqueous work-up, the pure product **39** was obtained in quantitative yield without further purification as a white waxy solid.

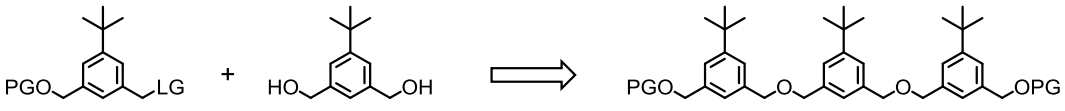

Scheme 29. Synthesis of the building block with dialcohol 39; PG protecting group; LG leaving group.

As mentioned above, the difunctional building block had to carry one protected benzylic alcohol and one leaving group, also in the benzylic position (Scheme 29). The alcohol protection group had to fulfill several requirements. It had to be stable under the conditions used for the nucleophilic

substitution reaction. The separation of the starting material, the desired, monoreacted product and the double reacted byproduct had to be easy to realize. Also the conditions used for the cleavage of the protecting group should not leave to the cleavage of the ether moieties. In addition to these requirements the protecting group precursor should be commercially available in large amounts, cheep, non-toxic and easy to handle.

Based on these requirements different protecting groups were tested, starting with the trityl group (Trt) which fulfilled the criteria stated above the best and was used to synthesize the target molecule **38**. Furthermore, tritylbromide is commercially available, cheep and cab be coupled with **37** to give the target molecule **38**. Trt-protected alcohols are stable under basic conditions and can be mildly cleaved in acidic media which should leave the benzylic ethers intact.[163]

The dibromide **37** was thus reacted in a nucleophilic substitution reaction with Trt-methanol to form the building block **38**. In literature, only a few methods can be found where tritylmethanol was reacted with benzylic bromides.[241] Due to the similar reaction and reactivity with the tritylthiol reported by Peterle et al.[159] the reaction conditions were adapted. So THF was used as solvent and K_2CO_3 was used as a relatively weak base (Scheme 30). The reaction of the starting material **37** and equimolar amounts of tritylalcohol in THF in the presence of 1.5 equivalents K_2CO_3 was monitored by thin-layer chromatography (TLC).

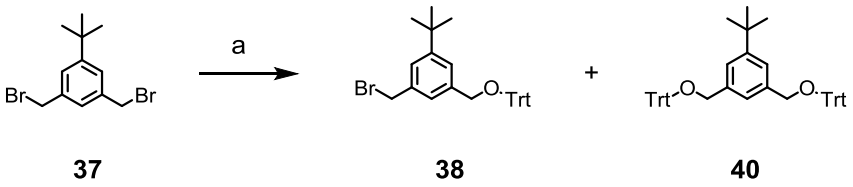

37 **38** **40**

Scheme 30. Synthesis of the building block 38; a) TrtOH, NaH, THF, reflux, 18 h, 38:32%; 40: 23%.

Unfortunately, the reaction under these conditions was too slow and even after several days no compounds other than the starting materials were detected by TLC. To increase the reaction rate, a considerably stronger base, sodium hydride (NaH) was used as a base. Furthermore, NaH is readily available and easy to handle as dispersion in mineral oil.

After 24 hours at reflux, the tritylmethanol was completely consumed and two new spots could be detected by TLC, the desired mono and the disubstituted byproduct. The difference in the R_f values of the three spots (dibromide **37**, mono-(**38**) and disubstituted byproduct **40**) was about 0.05 theirfore the purification by column chromatography had to be repeated several times.

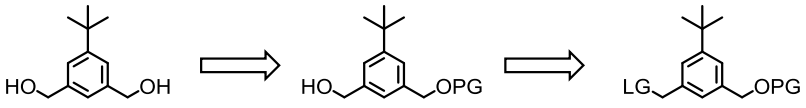

Scheme 31. Illustration of the reaction towards the building block starting with the introduction of the protecting group; PG protecting group; LG leaving group.

In order of elution, the starting material **37**, the desired monosubstituted building block **38** and the disubstituted compound were isolated in yields of 21%, 32% and 23% respectively.

Because of the purification problems the introduction order of the functional groups was reordered. At first the Trt-group was statistically introduced on the diol **39** followed by a reaction on the second side towards a leaving group (Scheme 31).

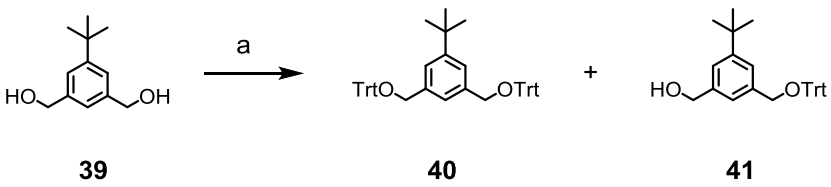

Scheme 32. Synthesis of the building block 40; a) TrtBr, NaH, THF, –40°C, reflux, 18 h, 41: 18%

To achieve this goal the starting material **39** was dissolved in THF, treated with 1.5 equivalents of NaH and an equimolar amount of tritylbromide. The reaction mixture was heated at reflux for 20 hours. TLC indicated clearly the consumption of tritylbromide and the formation of two new spots, corresponding to the di- and the mono-substituted building block **40** and **41**. These three spots appeared well separated on TLC. Purified by column chromatography gave the pure product **41** as white solid in 18% yield. In this case, the yield of the monosubstituted product is considerable lower than in the case of the introduction of the Trt-group on the dibromo building block **37**.

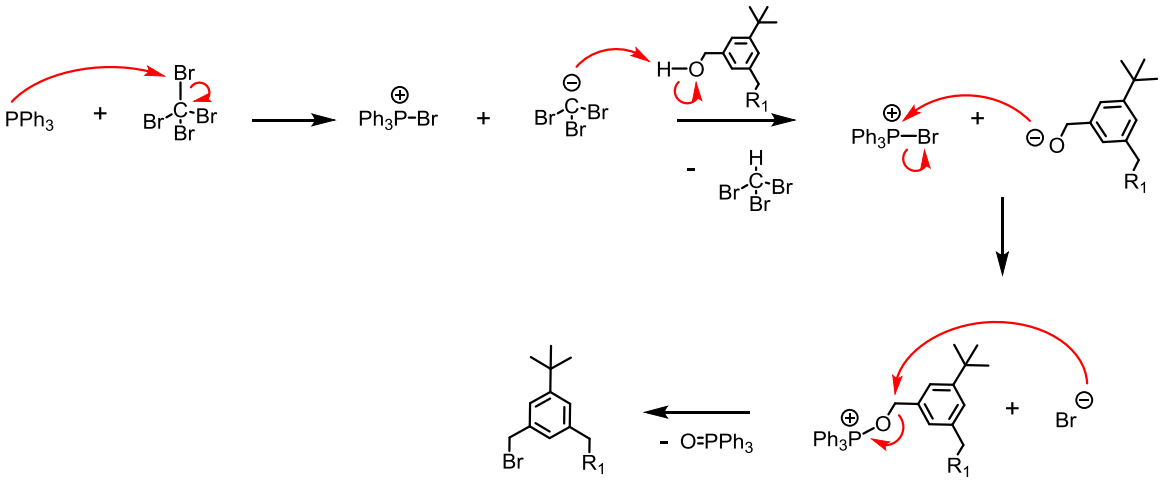

Scheme 33. Mechanism of the Appel reaction.

The remaining free alcohol needed to be transferred into a leaving group. Hence, an Appel-type reaction was performed, see Scheme 33, reacting a solution of compound **41** in THF with equimolar amounts of triphenylphosphine (PPh_3) in carbon tetrabromide. The reaction was quenched after 5 hours but unfortunately no Trt-group was present in the molecule anymore. The Trt-group might be cleaved during the aqueous work-up of the reaction.

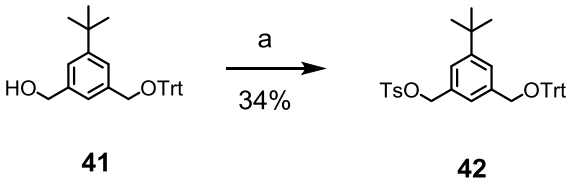

41 **42**

Scheme 34. Introduction of the tosyl leaving group, building block 42; a) TsCl, NaH, THF, reflux, 18 h, 34%.

The tosylate (Ts) group is known to be an excellent leaving group and can be easily introduced to benzylic alcohols.[242–244] The mono-protected building block **41** was,together with 1.2 equivalents of *p*-tosylsulfonyl chloride, dissolved in THF before an excess of NaH was added, see Scheme 34. The reaction mixture was stirred for 18 hours at reflux before the excess NaH was carefully quenched with water and an aqueous work-up was carried out. Column chromatography gave the clean product **42** in 34% yield. Unfortunately, this building block **42** turned out to decompose at room temperature within one week as a solid material and within two days in solution.

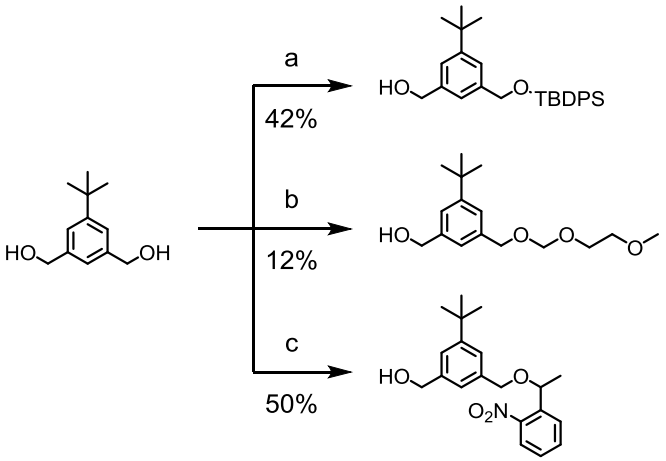

Scheme 35. Different protecting groups investigated. a) *t*BDPS Cl, DMAP, DIPEA, CH_2Cl_2 –20°C, rt, 18 h, 42%; b)MEM Cl, DIPEA, CH_2Cl_2rt, 2 h, 12%; c) 1-(2-nitrophenyl)ethan-1-ol, NaH, THF, 20 h, dark, 50%; MEM: 2-methoxyethoxymethyl; *t*BDPS: *tert*-butyldiphenylsilyl.

A silyl-protecting groups were investigated next. Bulky silyl protecting groups are known to be relatively stable under basic conditions which are used for the elongation of the desired ligands and they can be easily cleaved with trifluoroacetic acid (TFA). *tert*-Butyldiphenylsilyl (*t*BDPS) group was considered as a good protecting group due to its bulkiness, see Scheme 35. The reaction was carried out starting with dialcohol **39** which, was dissolved in dichloromethane (CH_2Cl_2), cooled to –20°C and treated with 3 equivalents of *N*,*N*-diisopropylethylamine (DIPEA). One equivalent of *t*BDPSCl and 15 mol% 4-dimethylaminopyridine (DMAP) were added. The reaction mixture was warmed to room temperature and stirred over night before the reaction was quenched with saturated ammonium chloride solution. The obtained crude product was purified by column chromatography affording the pure product **43** as colorless oil in 42% yield.

Although the building block **43** (see Scheme 35) was obtained in good yields for a statistical reaction, this protecting group was not used for the synthesis of the higher oligomers because of the low coupling efficiency with **37** and the very high stability of the protection group. Deprotection of the *t*BDPS group could not even for the monomer be achieved in reasonable yields.

Other protecting groups were also investigated, for example, the MEM group (Scheme 35). In this case, the dialcohol **39** was treated with 1.5 equivalent of DIPEA and 2-methoxyethoxymethyl chloride (MEMCl) in CH_2Cl_2.[245] The reaction mixture was stirred at room temperature for 2 hours. After this time, the TLC showed the total consumption of MEMCl and the formation of two new spots corresponding to the mono- and the di-substitution product. Two chromatographic columns gave the desired pure product **44** in 12% yield.

The next investigated protective group was a photo-labile group, *p*-nitrophenylethyl (NPE), was investigated. An equimolar ratio of monomer **39** and NPE-1-ol was added to a brown glass and dissolved in THF. NaH was added in excess and the reaction was stirred at room temperature for 18 hours. After aqueous work-up and evaporation of the solvent the crude product was purified by column chromatography to give the pure desired product **45** in 50% yield. Although the reaction towards the product **45** worked in good yield this building block was not used hereinafter, namely, because several test reactions showed that the handling of the building block as well as of the protected products was not as easy as expected and the yield was quite low. The product was very difficult to purify by column chromatography form the formed by-products.

These results showed the Trt-group to still deliver the best performance during the formation, the handling and the deprotection.

6.1.2 Synthesis of the Linear Ligands

The introduction of the trityl group to form **38** as well as the elongation reaction is a nucleophilic substitution reaction with an alcohol as the nucleophile and a benzylic bromide as the leaving group. The same reaction conditions were used for the introduction of the benzyl protecting group. An equimolar amount of **38**, benzyl methanol and NaH were reacted in refluxing THF (Scheme 36). In contrast to the analogous reaction with a thiol[159,160] which is finished within one hour applying these conditions, the reaction of the alcohol is considerably slower due to a weeker nucleophility of the oxygen atom compared with the sulfur. According to TLC, the reaction mixture needed to be heated at reflux for 24 hours before all starting material was consumed. The Trt-protected monomer **46** was isolated as white foam in 87% yield.

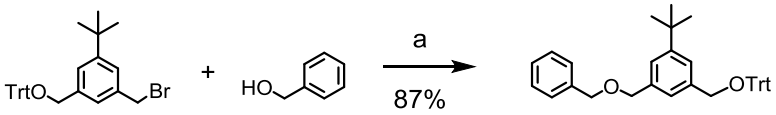

38 **46**

Scheme 36. Synthesis of the Trt-protected monomer 46; a) NaH, THF, reflux, 24 h, 87%.

The next crucial reaction step was the selective cleavage of the Trt-group in the presence of benzylic ether. It is well known,[159] that Trt-group can be cleaved under mild acidic conditions (eg. trifluoroacetic acid) but strong acidic conditions may also cleave the benzylic ethers.[163] Trifluoroacetic acid (TFA) was added to a solution of the Trt-protected **46** and 2.5 equivalents of triethylsilane in dichloromethane (Scheme 37).

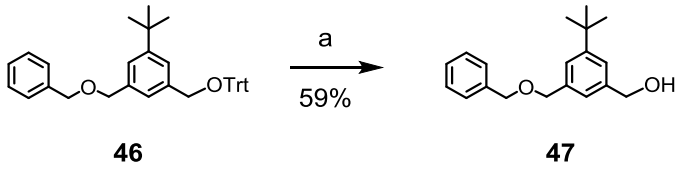

Scheme 37. Deprotection of 46 to47; TFA, Et_3SiH,CH_2Cl_2,rt, 2 h, 59%.

The solution turned yellow directly after the addition of the acid and became colorless again within 10 minutes. The yellow color indicated the formation of the tritylcation. The reaction was stirred for an additional 20 minutes after the yellow color had disappeared and the progress of the reaction was monitored by TLC. No starting material could be detected by TLC and two new spots where found. The deprotection reaction was quenched and extracted with CH_2Cl_2. After purification by column chromatography, the alcohol **47** was obtained as a colorless liquid in 57% yield.

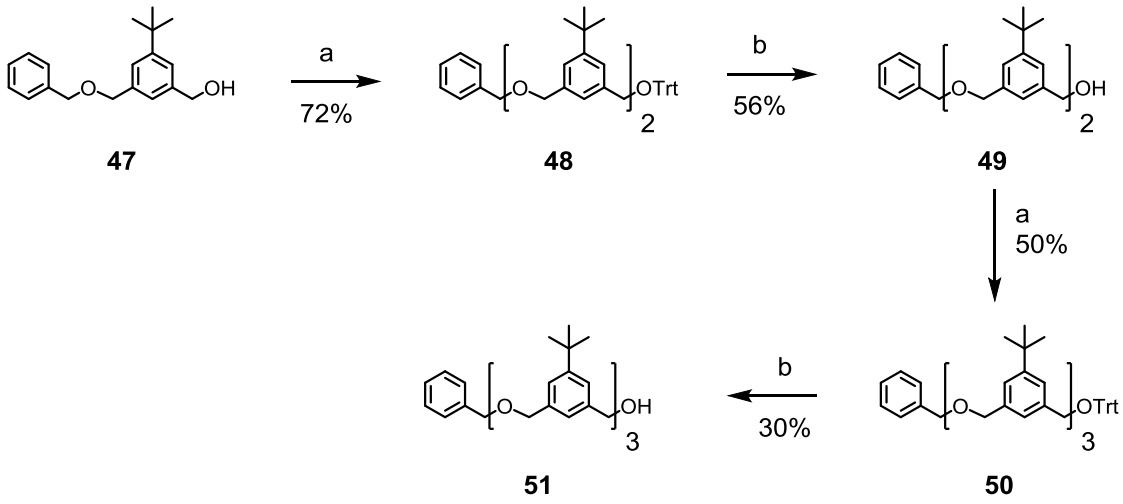

Scheme 38. Synthesis of higher oligomers;a) 38, NaH, THF, reflux, 24 h;b) TFA, Et_3SiH,CH_2Cl_2,rt, 2 h; 48: 72%; 49: 56%; 50: 50%;51: 30%.

The elongation of the oligomer **47** was achieved using the same reaction conditions as applied before, see Scheme 38. The alcohol **47** and the building block **38** were, with an excess of NaH, reacted in refluxing THF. The Trt-protected dimer **48** was obtained in 72% yield after column chromatography. The remaining material turned out to be the byproduct **52**, possessing an aldehyde function instead of an alcohol (Scheme 39). This reaction was further on investigated, see section 6.1.3.

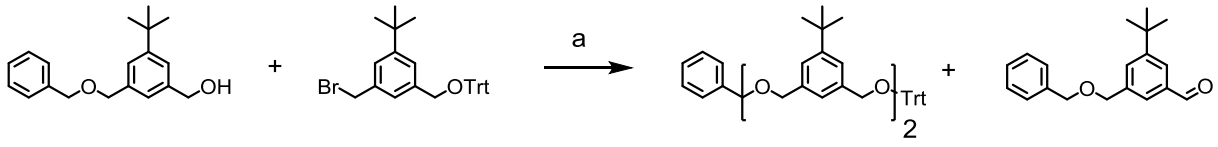

46 **38** **48,** 72% **52**

Scheme 39. Synthesis of the Trt-protected dimer 48; a) NaH, THF, reflux, 24 h, 72%.

The deprotection reaction described above using TFA as an acid was also adopted for the preparation of the dimer **48** to yield the dimer alcohol **49** in 56% after column chromatography.

The elongation of the dimer **49** to the trimer **50** was achieved by reacting the dimer **49** with **38** as described in Scheme 38. The Trt-trimer **50** was purified by column chromatography and gave an off-white solid in 50% yield. The Trt-trimer **50** was further treated with the acidic conditions for the removal of the Trt-protecting group to give the trimer alcohol **51** as a pale yellow oil in 30% yield after column chromatography. In the final step, two equivalents of the trimer **51** were attached to one equivalent of the dibromide **37** in a nucleophilic reaction and the pure heptamer product **33** was isolated as pale yellow oil in 13% yield after chromatographic purification.

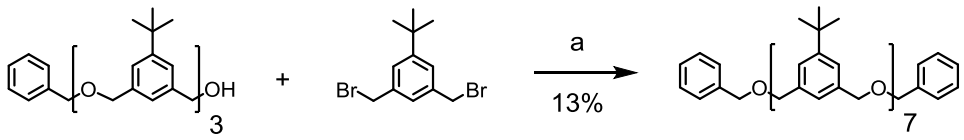

51 **37** **33**

Scheme 40. Synthesis of the heptamer 33. a) NaH, THF, reflux, 24 h, 13%.

A possible explanation for the decreasing yields as the length of the oligomers increases might be the presence of the ether functionalities. Longer oligomers have the potential to fold up and therefore hinder the free alcohol from undergoing the substitution reaction. Alternatively, oligomers might be able to act like a crown-ether, which motif can bind the base cation in close proximity to the benzylic oxygen anion and hamper the substitution reaction.

With regard to the large-scale synthesis of the heptameric ligand **33**, an alternative route was investigated with the aim of synthesizing the desired ligand in as few steps as possible, without using a protecting group. Given that tosylate is known to be a superb leaving group, it was used instead of the bromide (Scheme 41), so that reactions could be conducted at room temperature.

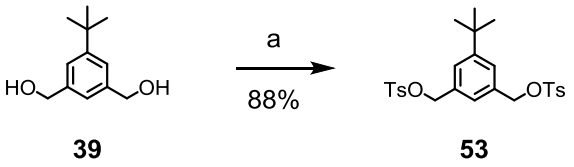

Scheme 41. Synthesis of the the ditosyl building block 53;a) TsCl, NaH, THF, 0°C, 20 min, rt, 18 h, 88%.

In order to decrease the chances of polymer formation, one equivalent of the di-tosylate **53** in THF at room temperature was treated with 10 equivalents of dialcohol **39** and an excess of NaH. TLC showed the consumption of the **53**, the unreacted dimethanol **39** and one new prominent spot with an R_f value above the diol **39**, see Scheme 42. The excess of NaH was carefully quenched with water and an aqueous work-up was performed. The crude product was purified by column chromatography to afford the pure trimerdiol **54** as colorless oil in 60% yield.

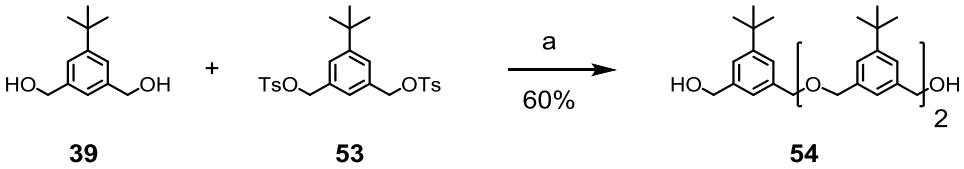

Scheme 42. Synthesis of the trimer building block 54;a) NaH, THF, rt, 16 h, 60%.

The next step towards the synthesis of the heptamer **33** was the statistical endcapping reaction. Since the tosyl group exhibited very good coupling characteristics it was decided to synthesize the benzylic endcapping agent **55** with a Ts-group.

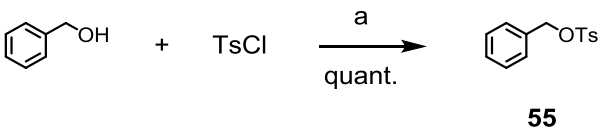

Scheme 43. Synthesis of endcapping agent 54; a) NaH, THF, rt, 2 h, quant.

According to the literature procedure,[242] benzyl alcohol and NaH in THF were stirred at room temperature. An equimolar amount of *p*-toluolsulfonyl chloride (TsCl) was dissolved in THF and added *via* a dropping funnel over 30 minutes to the stirred mixture of benzyl alcohol. After the addition was completed, the reaction was stirred for an additional 2 before the aqueous work-up. The organic solvent was removed under reduced pressure to give the pure desired pure product **55** as white solid in quantitative yield (Scheme 43).

55 was used to perform the statistical endcapping reaction of **54**. To favor the formation of the desired product, the trimerdiol **53** was added in an excess of 1.4:1 with respect to the building block **55**, see Scheme 44. The reaction was stirred for 18 hours at room temperature before aqueous work-up was performed. Column chromatography gave the pure trimer **51** as pale yellow liquid in 58% yield.

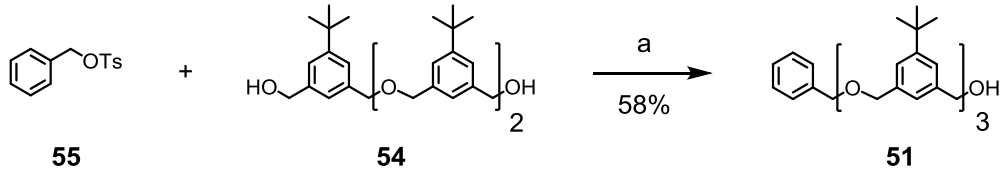

Scheme 44. Synthesis of trimer 51; a) NaH, THF, rt, 18 h, 58%.

The last step of this synthesis was identical with the one described before, using NaH and refluxing the reaction in THF for 24 hours. Unfortunately, the use of ditosyl **53** instead of dibromide **37** could not increase the yield of the final coupling step. In the case of **53** the yield dropped even further down to 11%.

The trimerdiol **54** shows good coupling efficiency, while the coupling of the trimer **51** to the heptamer **33** decreases dramatically. This finding led to the assumption that the coupling efficiency of the oligomers drops with increasing length. For this reason an additional change was made. The endcapping **55** was reacted with the double amount of diol **39** at room temperature for 16 hours. The reaction was quenched with water and the crude product was purified by column chromatography to obtain the alcohol monomer **47** in 37% yield.

In a following step the alcohol **47** was reacted with 4 equivalents of dibromide **37** and 2 equivalents of NaH, see Scheme 45. The dibromide **38** was chosen because previous reactions pointed out that the terminal Ts-group is not very stable towards column chromatography. Column chromatography gave the dimer **56** as colorless liquid in 77% yield.

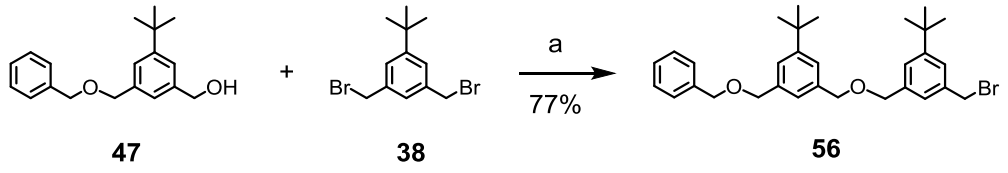

Scheme 45. Synthesis of the intermediate 56;a) NaH, THF,reflux, 24 h, 77%.

In a final step, the diol trimer **54** was reacted with equimolar amounts of dimer **56** and column chromatography gave the final pure ligand **33** in 17% yield.

Monomer **36** was synthesized by the reaction of dibormo building block **37** with benzyl alcohol. The pure product was isolated in 80% yield after column chromatography as oil. In a similar manner trimer **35** was synthesized by the reaction of **47** with dibromo **37** in refluxing THF. Column chromatography using silica and additional gel permeation chromatography (GPC) gave the pure product as colorless oil in 63% yield.

The dimeralcohol **49** was used to synthesize the pentamer **34**. Together with **37**, **49** was dissolved in THF and heated with NaH to reflux over night. Aqueous work-up followed by silica column chromatography and GPC gave the product in 86% as off–white wax.

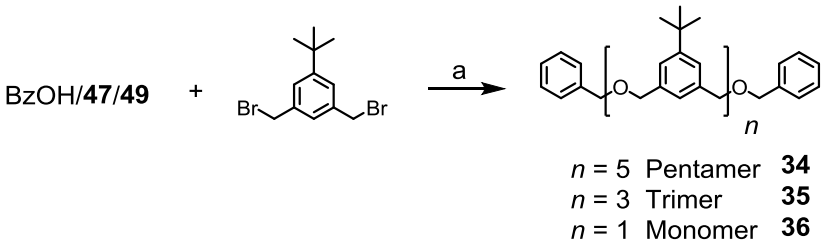

Scheme 46. Synthesis of the linear oligomers; a) NaH, THF, reflux, 24h;34: 86%, 35: 63%; 36: 88%.

6.1.3 Investigations of the Aldehyde Formation

As mentioned already above, see Scheme 39, it was observed that the reaction of the dibromide **37** with benzylic alcohols (**47** and **39**) can lead to the formation of aldehydes. Because the formation of these aldehydes lowered the efficiency of the reaction and where found to have a similar R_f value as the desired products and where therefore hard to remove by column chromatography different investigations towards the formation of aldehyde **57** out of the alcohol under S_N2 reaction conditions were made, see Scheme 47.

In order to investigate the aldehyde formation from alcohol **39** under S_N2 reaction conditions different experiments were carried out, compare Table 6.

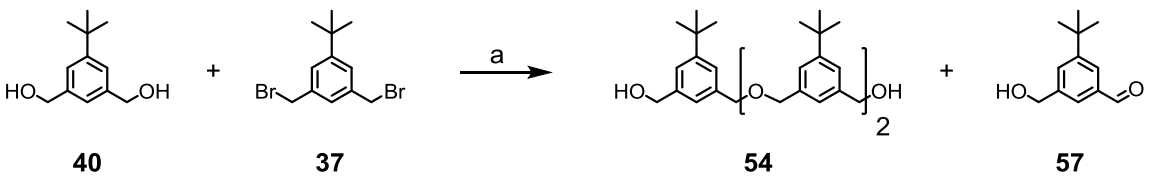

Scheme 47. Synthesis of the trimer 54; a) NaH, THF, reflux, 24 h.

Table 6. Typical reaction conditions: 1 eq of 39, 10 eq of 37 and 3 eq base. Solvent, reaction temperature and time as given. All reactions were performed under inert atmosphere; 18-C-6 = 18-crown-6 ether.

	Solvent	Base	Temp	Time	Prod 53	Prod 56	comment
1	THF	NaH	reflux	20hr	yes	yes	
2	DMF	NaH	70°C	48hr	yes	yes	
3	DMF	Proton sponge	70	24	no	no	
4	DMF	Cs_2CO_3	70°C	24	no	no	
5	THF	Et_3N	reflux	24	no	no	
6	THF	K_2CO_3	reflux	24	no	no	
7	DMF	NaH	70	24	yes	yes	18-C-6
8	THF	NaH	150°C-MW	1hr	yes	yes	
9	DMF	NaH	70	24	no	no	*
10	THF	NaBr	rt	24	no	no	*

*just dialcohol **39**, no dibromide **37**

Entry 1 shows the standard S_N2 reaction conditions described in this thesis. The change of the solvent from THF to DMF did not change the ratio of product **54** to aldehyde **57**. On this account different bases where tried, see entrance 3-6. Neither the use of weaker inorganic bases as Cs_2CO_3 and K_2CO_3 nor the change to organic bases like Et_3N did lead to the formation of **54**. Even with proton sponge (1,8-bis(dimethylamino)naphthalene), which is one of the strongest amine bases known with a pK_a of 12.3[247], no formation of the desired product **54** could be detected by GC-MS or TLC. Hence the investigations were limited to NaH as base. Entry 7 shows that the use of 18-crown-6 could not hinder the formation of undesired side product **57**. Also to lower the reaction time and increase the reaction temperature by using the microwave for irradiation did not lead to promising results.

Due to the fact that none of the different reaction conditions shower promising results it was investigated if the presence of the dibromo building block **37** is crucial for the formation of the aldehyde **57** or if the presence of bromide is sufficient. The entry 9 shows that the presence of the strong base NaH alone is not enough to form the aldehyde. But also the presence of Br^- as sodium bromide does not lead to the formation of the side product **57**, see entry 10.

As conclusion it must be admitted that the reason for the formation of the aldehyde **57** still remains unsolved. This reaction seems to be directly related to the formation of the trimer **54**.

6.1.4 Branched Ether Ligands

To be able to incorporate the PdNPs in any other material, it would be huge a benefit to lower the amount of ligands further down, so every NPs is stabilized by one ligand. To achieve this goal the ligand needs to be redesigned (Figure 46). To increase the length of the ligand was not a very promising consideration not just due to the dropping yields with increasing length of the building blocks. So a branched version of the ether ligand was designed.

It has been shown in previous work that the *tert*-butyl group is crucial for the stability of NPs stabilized with these kinds of ligands due to the steric repulsion.[159,161] Also the size of the symmetric ligand was chosen in agreement with previous works, where it was proved that one of this thioether analogue is able to stabilize a AuNP.[240,248]

The synthetic strategy was similar to the above described synthesis of the linear ligands. The experience made in these syntheses could be adapted. Therefore it was decided not to work with protecting groups but to us the symmetric building blocks that could be synthesized in large scale.

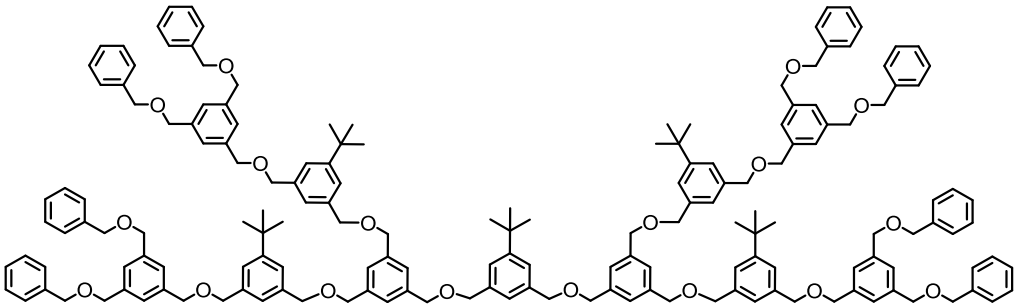

58

Figure 46. Branched target ligand 58.

Two equivalents of benzyl alcohol were reacted with 1 equivalent of 1,3,5-*tris*(bromomethyl)benzene (**59**) in refluxing THF with the use of NaH, see Scheme 48. After aqueous work-up and purification by column chromatography the pure bromo branching **60** was achieved in 41% yield as colorless liquid.

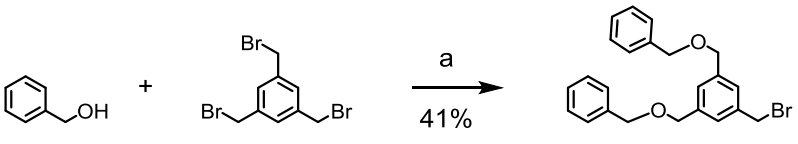

59 **60**

Scheme 48. Synthesis of ligand 60;a) NaH, THF, reflux, 18 h, 41%.

This building block **60** could now be used for two different syntheses. In one the branched ligand **61** could be achieved (Scheme 49). To achieve these 2 equivalents of the building block **60** were reacted with 1 equivalent of trimerdiol **54** and an excess of NaH. Aqueous work-up and column chromatography gave the branched ligand **61** in a considerable low yield of 21% as colorless liquid.

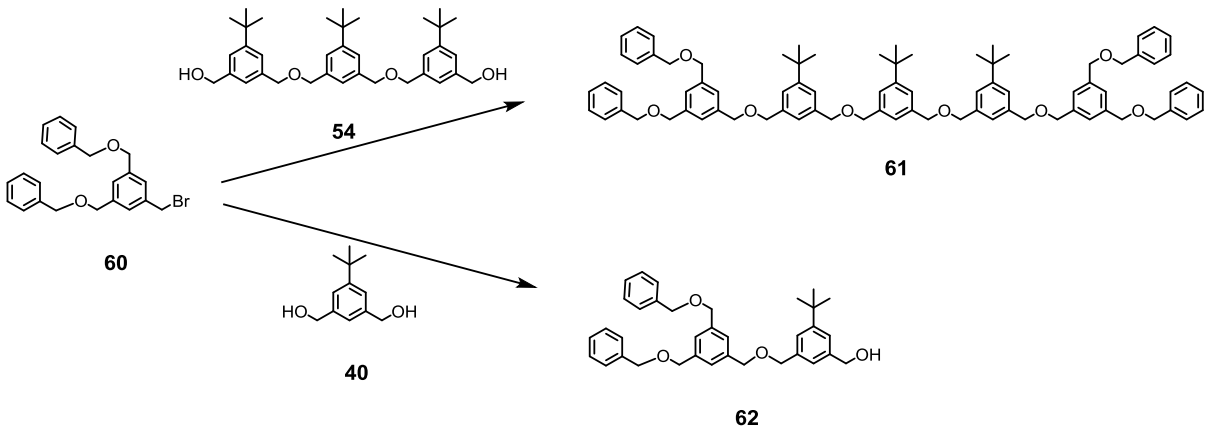

Scheme 49. Synthesis of ligands 61 and 62 starting from building block 60.

The other reaction was the installation of a *tert*-butyl bearing building block to increase the repulsion and with this the stability of the final NPs (Scheme 49). The dialcohol monomer **39** was reacted with the bromo branching **60** in a ratio of 1.8/1 to prevent the formation of double reacted product. The desired pure product **62** was isolated in a good yield of 49% after column chromatography.

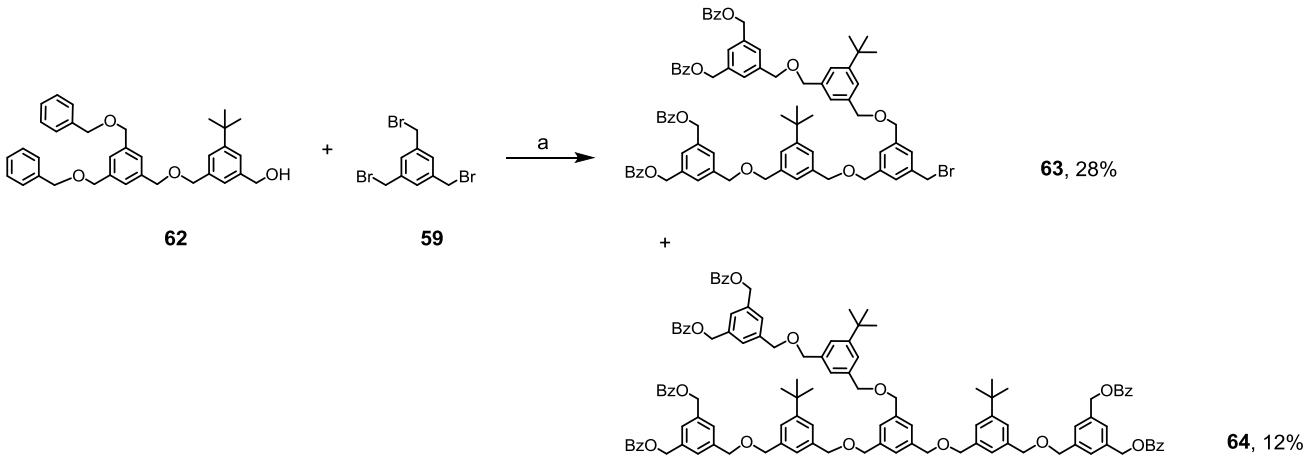

Scheme 50. Synthesis of the ligands63 and 64; a) NaH, THF, reflux,24 h, 63: 28%, 64: 12%.

The introduction of another branching unit led to the formation of the ligand **64** as well as to the formation of the intermediate **63**, see Scheme 50. Column chromatography gave the two products **64** and **63** in 12% and 28%, respectively. The yield of **64** could be increased with increasing the ratio of **60** to **59** up to 3:1.

Finally, two equivalents of building block **63** and one equivalent of **39** were reacted to the ligand **58**. An aqueous work-up was performed followed by column chromatography and GPC to obtain the final pure product in 21% as pale yellow oil.

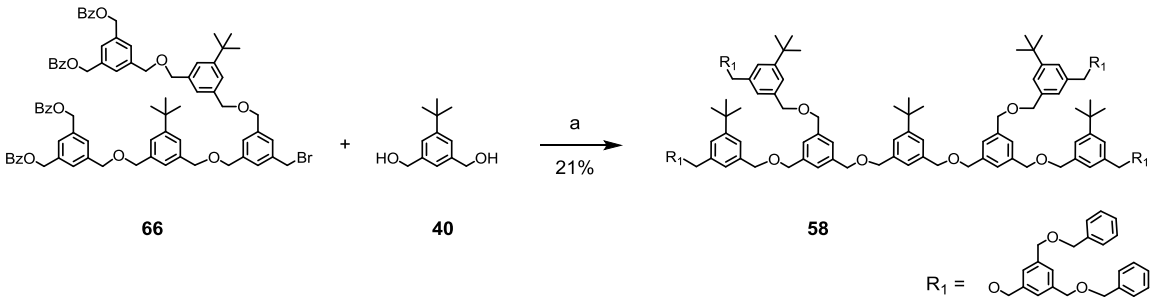

Scheme 51. Synthesis of the biggest ligand 58; a) NaH, THF, reflux, 18 h, 21%.

6.2 Ether coated NPs by Direct Synthesis

Encouraged by the stabilization potential of thioether ligands we decided to synthesize an ether ligand similar to the thioether ligand described by Peterle et al.[159] This ether based ligand should provide the possibility to stabilize other metal particles than gold, such as silver (Ag) NPs in the same way as the thioether stabilizes Au NPs. To gain an idea about the number of ether moieties needed to stabilize a NP, the synthesis of the NPs was performed in the presence of 4 different lengths of ether ligands, namely monomer **36**, trimer **35**, pentamer **34** and heptamer **33**. The synthesis followed the two phase procedure developed by Brust[65] with minor modifications.

6.2.1 Silver NPs

6.2.1.1 Initial Studies

As silver precursor silver nitrate ($AgNO_3$) was used as it was found in literature to be a suitable source for the formation of AgNPs.[249–251]

The ratio of silver ion to oxygen present in the particular ligand used for the stabilization was kept at a 1 to 1 ratio for all the ligands. So for the trimer **35** which bears 8 ether units the ratio of ligand to $AgNO_3$ was 1 to 8. The silver salt was dissolved in NanoPure water and the metal ions were transferred to the organic phase with the use of tetraoctylammonium bromide (TOABr) in dichloromethane. The ligand was also dissolved in dichloromethane and added to the mixture. After stirring for approximately 5 minutes a freshly prepared aqueous solution of sodium borohydride was added to reduce the silver precursor to silver. The organic phase turned dark immediately after the addition of the reducing agent and after a view minutes some precipitation was formed. After 10 minutes the organic phase was separated and dried under a gas stream. Purification was achieved by repeated precipitation and centrifugation using methanol followed by size exclusion chromatography using *Bio-Rad Bio-Beads S-X1 Beads* as solid state and toluene as eluent. The NPs were collected and further analyzed. This procedure was applied for all ligands **35**, **34** and **33**.

It is known that quaternary amines such as TOABr exhibit to a certain extend the possibility to stabilize NPs.[80,84] In the two phase synthesis TOABr encapsulates the metal ion and even very small NPs before the ligand, mainly a thiol takes over the stabilization of the growing particle, see chapter 1.1.3.

To prove the roll of the ligand and the phase transfer catalyst in this synthesis AgNPs were synthesized in the absence of an ether ligand. After the reduction the gray organic phase was collected and concentrated.

6.2.1.2 Investigations

UV/Vis

The concentrated organic phase was dissolved with methanol where upon the color changed into purple. After the centrifugation the formed pellet could not be dissolved in any common organic solvent. Also without the suspension in methanol the TOABr stabilized NPs were not very stable. After storing the NPs solution at ambient conditions for 24 hours a dark film was formed at the glass wall of the storage vial and the solution had become nearly colorless.

All this findings indicate very limited stabilizing efficiency of the TOABr for AgNPs. On the other hand this reveals the stabilizing efficiency of the ether ligands in the synthesis of these AgNPs.

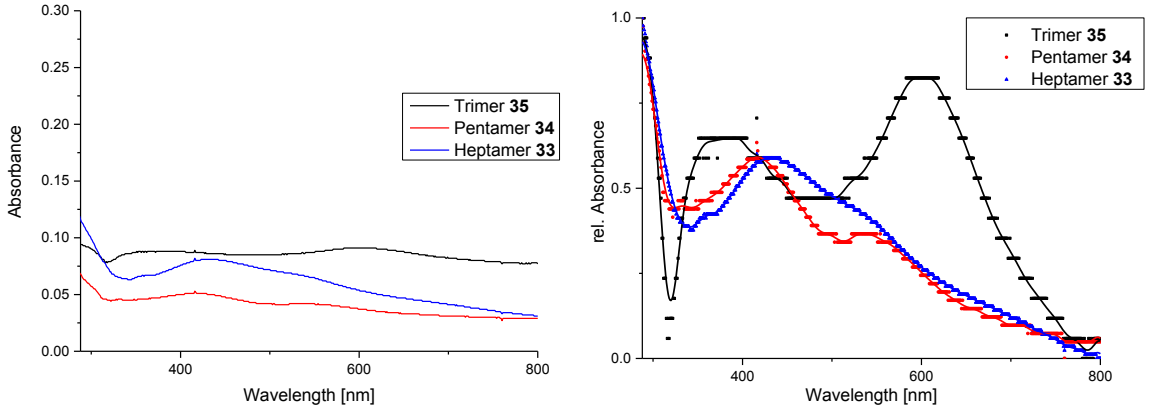

Figure 47. Left absorbance and right relative absorbance of 33, 34 and 35 stabilized Ag NPs. In the right figure the points are fitted due to too low resolution.

Initial UV/Vis measurements of the collected Ag NPs gave the spectrum shown in Figure 47. The left figure shows the spectrum as obtained. In the right figure the measurements were normalized giving a better comparability of the different concentrations. In the normalized spectrum one can clearly see a peak arising in the case of **35** stabilized NPs at 600 nm indicating bigger NPs than 2 nm, the presence of bigger particles was also detected by TEM. In the case of **34** and **33** stabilized NPs no such band is detected indicating that the size of the particles is mainly below 2 nm. The NPs stabilized by the trimer ligand could not be redissolved after the removal of TOABr.

After a view days at ambient conditions also the Ag NPs could not be dissolved anymore in any common solvent regardless of the used size of the ligand indicating that the interaction of the ether ligand and the silver is to week to efficiently stabilize these NPs.

TEM

The ether stabilized AgNPs showed direct after the synthesis a narrow size distribution. After the extraction of the phase transfer catalyst with methanol the size distribution became much broader. This finding suggests that TOABr plays a crucial role in the stabilization of the AgNPs although it could be proven that TOABr alone is not able to stabilize AgNPs for efficiently.

A TEM analysis histogram of **33** stabilized NPs is given in Figure 48. It can be clearly seen that the size of the NPs direct after the synthesis is quite narrow with a maximum peak at 1.5 nm and some bigger particles tailing up to 3.5 nm.

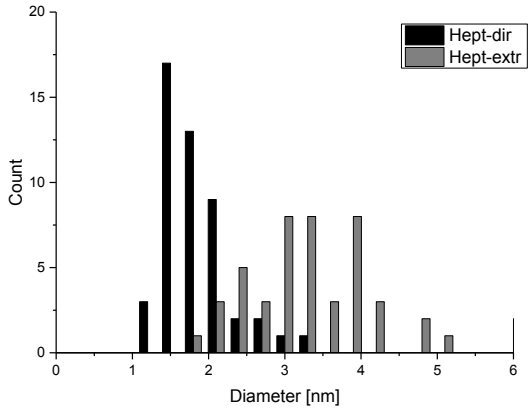

Figure 48. Histogram of the 33 stabilized Ag NPs after synthesis (black) and after removal of TOABr (gray).

After the removal of TOABr the size distribution became much broader with particles size between 2 and 5 nm and no clear maximum can be detected.

6.2.1.3 Conclusion

All the ether ligands show low stabilization ability towards AgNPs. The short ligands like trimer **35** does not exhibit any better stability than the used phase transfer catalyst TOABr. The formed NPs are polydisperse and cannot be purified without the disintegration of the particles. AgNPs stabilized by higher oligomers are monodisperse after formation but become more polydisperse upon removal of the phase transfer catalyst. These particles are more stable than the **35** protected AgNPs but still decompose upon storage in bulk within several days.

The tendency of the ether ligands to interact with the AgNPs could be shown. But it could be also shown that the binding of the ligand to the silver surface is to week to successfully protect the NPs from coagulation.

6.2.2 Palladium NPs

Due to the low stability of the Ag NPs stabilized by the ether ligands the stabilization properties towards other metals was tried. Palladium chloride ($PdCl_2$), nickel acetate tetrahydrate (Ni Ac_2*4 H_2O) copper acetate monohydrate (Cu Ac_2* H_2O) and copper chloride were tried but TOABr was in none of this cases able to transfer the metal ion to the organic phase. This was indicated by the color of the aqueous and the organic phase as well as by the addition of $NaBH_4$. The reduction to the bulk metal took clearly place in the aqueous and not in the organic phase.

Potassium tetrachloropalladate (K_2PdCl_4) was tried as well. TOABr transferred the palladium precursor easily to the organic phase, indicated by the color change. The water phase was first yellow and upon addition of the phase transfer catalyst the color disappeared and the organic phase became dark red. Addition of $NaBH_4$ in water let to a color change of the organic phase to black after about 2 seconds. This is a quite slow reaction in comparison with the reduction of Na_2AuCl_4 which has usually a delay of less than 1 second.

The particles formed in this initial phase transfer study were collected after 10 minutes of stirring and without further purification used for an initial UV/Vis measurement. The rest was dried and redissolved in deuterated chloroform to obtain a ^1H NMR of these particles. Because of the low amount of organic substance present in such already very black samples a long term spectrum had to be recorded over night. The next day the NPs were already completely decomposed leaving a dark, insoluble film on the glass wall of the NMR tube. Therefore it is not known to what extend the NMR shown the TOABr stabilizing the Pd NPs and to how much of the NPs were already decomposed leaving free TOABr in solution.

6.2.2.1 Synthesis and Investigations

After this promising finding the synthesis of PdNPs was conducted in the presence of the ether ligands **33**, **34**, **35** and **36**. See Figure 49. The synthesis was kept the same as reported for the synthesis of Ag particles, beside the metal salt was changed from $AgNO_3$ to K_2PdCl_4.

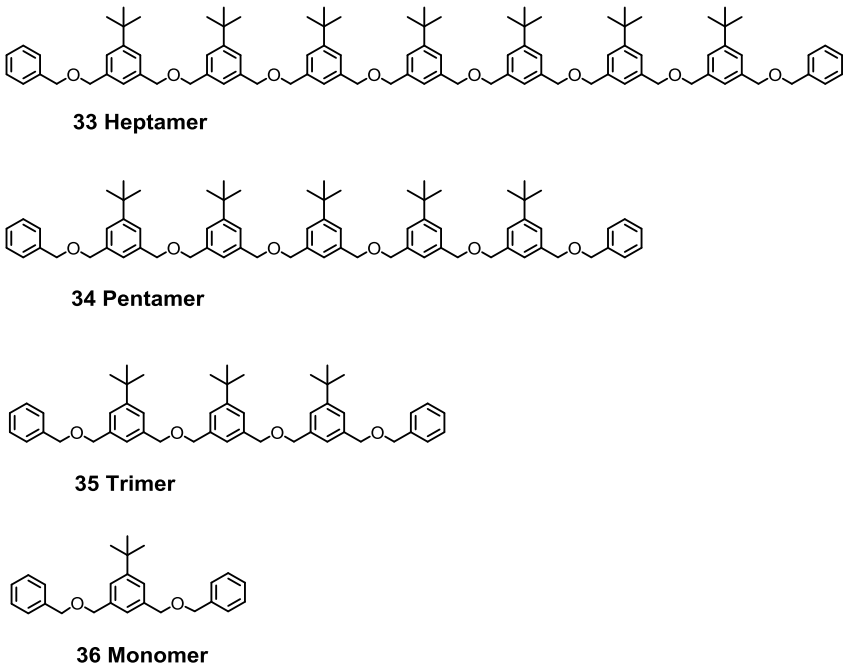

Figure 49. Linear ether ligands 33-36.

The formed PdNPs were collected and the TOABr was removed by repeated precipitation from methanol. This led in the case of TOABr stabilized NPs to the formation of an insoluble precipitate. In the case the NPs were stabilized by monomer **36**, the removal of the TOABr gave partly insoluble NPs. The still soluble monomer protected PdNPs were stable for about one day in solution at ambient conditions. After two days the organic phase had completely lost color and the particles formed an insoluble precipitate at the bottom of the storage vial.

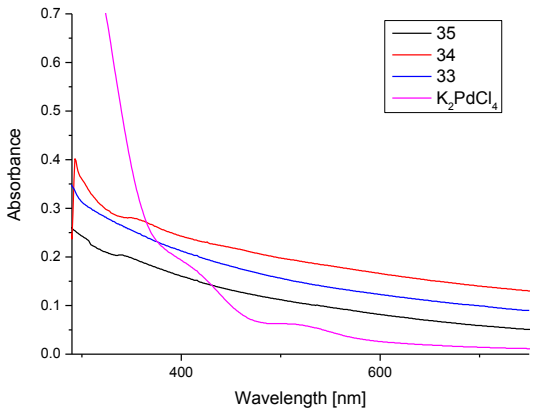

Figure 50. UV/Vis spectrum of Pd NPs stabilized by 35, 34 and 33 ligand and of the Pd-salt.

The PdNPs stabilized with higher oligomeric ethers were synthesized and the TOABr was removed in the same way as mentioned for the monomer **36** stabilized NPs. All of this longer oligomers exhibited

bigger stabilization potential than the ligand **36**. After the removal of the phase transfer catalyst TOABr, the NPs were dissolved in toluene and further purified by GPC using *Bio-Beads SX-3* as packing material. The NPs containing fractions were collected and dried under reduced pressure without the use of a heating bath.

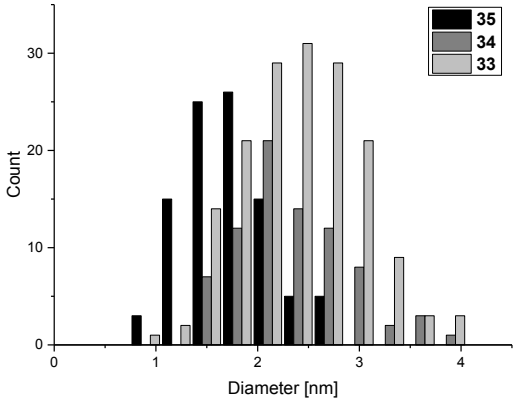

Figure 51. 35, 34 and 33 stabilized Pd NPs size distribution by TEM analysis.

TEM analysis (Figure 51) showed that the size of the Pd NPs increases with the length of the stabilizing ligand. The **35** stabilized NPs exhibit a size with a maximum around 1.5 ± 0.8nm whereupon the **33** stabilized NPs have a size between 1.2 and 3.9 nm with a maximum around 2.4 nm. Trimer stabilized NPs coagulate within a few days leading to an insoluble dark film on the surface of the storage vessel. The same can be observed for the **34** stabilized NPs. **33** stabilized PdNPs show the biggest stability. The UV/Vis of these NPs does not change upon storage over two weeks in solution.

Branched Ligands for Pd NP synthesis

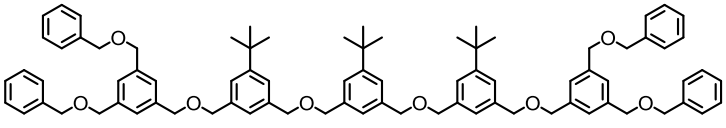

61

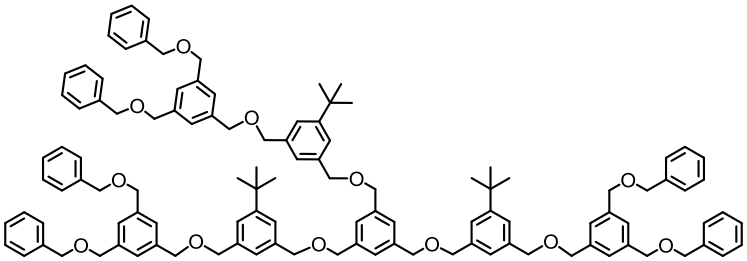

64

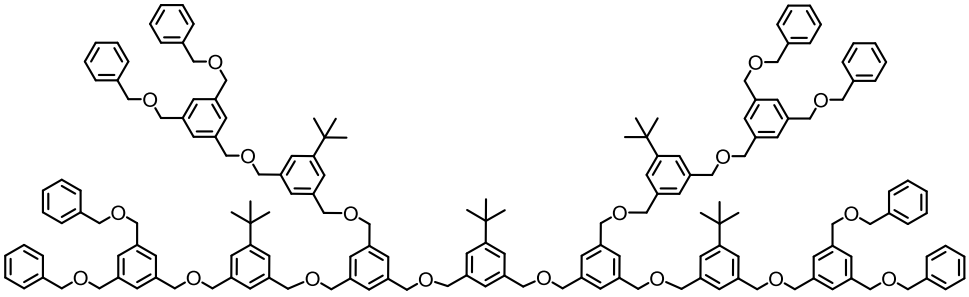

58

Figure 52. Branched ligands 58, 61 and 64 used for the formation of Pd NPs

In the same way as was reported for the synthesis of the PdNPs stabilized with linear ligands also the stabilization potential of the branched ether ligands **61**, **64** and **58** was investigated, see Figure 52. The molar ratio of palladium precursor and oxygen-units was kept at a one to one ratio and the synthesis was performed in dichloromethane. Also in these cases the UV/Vis did not exhibit any plasmon resonance peaks.

61 stabilized NPs were found not to be stable. After the removal of TOABr, just parts of the particles could be redissolved. But even this fraction could not be purified by the *Bio-Beads S-X1* column because the particles did not move on the column.

The NPs stabilized with the bigger branched ligands **64** and **58** could be purified by GPC. TEM measurements of these PdNPs showed similar results (Figure 53). The particle size distribution tails up to 4 nm with a maximum peaks around 1.5 nm.

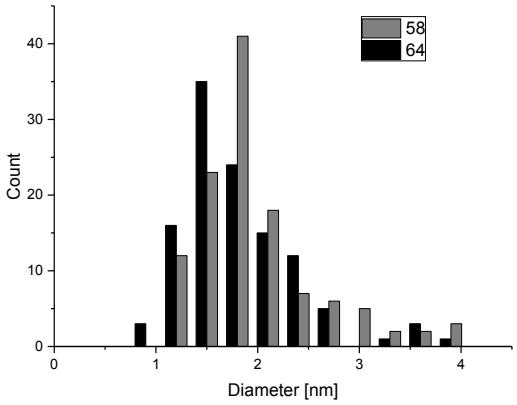

Figure 53. 58 and 64 stabilized Pd NPs size distribution by TEM analysis.

In contrast to the linear ligands stabilized NPs the NPs stabilized by branched ligands do not follow the trend that bigger ligands lead to bigger particles. The size of this particles is closer to the one obtained for the smaller **35** stabilized particles than for bigger **33** stabilized particles. Especially the ligand **58** stabilized NPs seem to exhibit increased stability. These particles stayed in solution unchanged for at least two weeks. Another benefit of the particles stabilized by branched ligands is the more narrow size distribution of the isolated PdNPs.

6.3 Conclusion

It was shown that multidentate ether ligands have the potential to stabilize noble metal NPs. The ability to stabilize AgNPs is rather low and the particles can after several days in bulk not be dissolved any more. PdNPs stabilized by higher ether oligomers show acceptable stability although the stability towards impacts like higher temperatures or chemical reactions needs to be investigated. The NPs were synthesized in a two phase synthetic approach. For the linear ligands the size of the formed NPs is depending of the stabilizing ligand and growing with its length. Also the stability of the PdNPs increased with increasing length of the oligomer. The monomer stabilized NPs were after the removal of the phase transfer catalyst stable for less than one day in solution. For the branched ligands **64** and **58** the size of the formed NPs was similar and mainly particles with a diameter below

3 nm were formed. How many of the bigger ligands are needed for the stabilization of the NPs is not clear yet. TGA has to be investigated from the **34** and **33** and **58** stabilized NPs.

7 Conclusion& Outlook

Several projects concerning the formation and investigation of different metal NPs are reported.

1 X: **2** = C≡C
3 = CH=CH

Figure 54. The three desired ligands of different length and conductivity.

For the synthesis of Au NPs three different conjugated, aromatic ligands, containing a pyridine and a thiol unit, were synthesized (Figure 13). These ligands **1**-**3** were investigated towards their properties of binding to the surface of Au NPs by directly applying the ligand or via ligand exchange reaction.

The size and surface functionalization of the Au NPs can be controlled by the synthetic conditions. It was shown that the amount of ligands, their relative ratio and the order of the addition to the reaction mixture is of crucial importance for the composition of the ligand shell and the size of the formed particles. Furthermore, a straightforward way to separate Au NPs of different size was deployed by using their size-dependent solubility .

Physical measurements like STM and STS confirmed the size of the Au NPs to be around Au_{144}. After finding conditions to deposit the NPs individually on a metal surface, DPV scans displayed several well defined maxima, which indicate that electrons are added or removed from the NP, in a linear dependency to the charge state. Single NPs on a Pt(111) surface can be individually addressed and work in ionic liquid as a multistate electronic switch at room temperature.

These very interesting and promising findings show the potential of these particles to be used as micro/nano electronic devices such as capacitors.

19 X: **20 =** C≡C
21 = CH=CH

Figure 55. Ligands designed for the exchange reaction towards acetylene stabilized AuNPs

The Au–C≡C stabilized NPs exhibit the benefit of a better conductivity over the interface between the ligand and the gold particle compared to thiol stabilized particles. Another benefit of these particles is the synthesis *via* ligand exchange reaction, what gives better control over the size of the formed NPs and can also be used for the preparation of particles bigger than 3-4 nm what can hardly be achieved by direct synthesis with thiol ligands.

Electrochemical and physical investigations of such acetylene stabilized Au NPs are not yet reported in the literature and will, without a doubt, lead to interesting results and better understanding of the behavior of such electrochemical switches.

As a different class of ligands, a set of linear and branched benzyl ethers of different size were synthesized and analyzed towards their ability to stabilize different metal NPs.

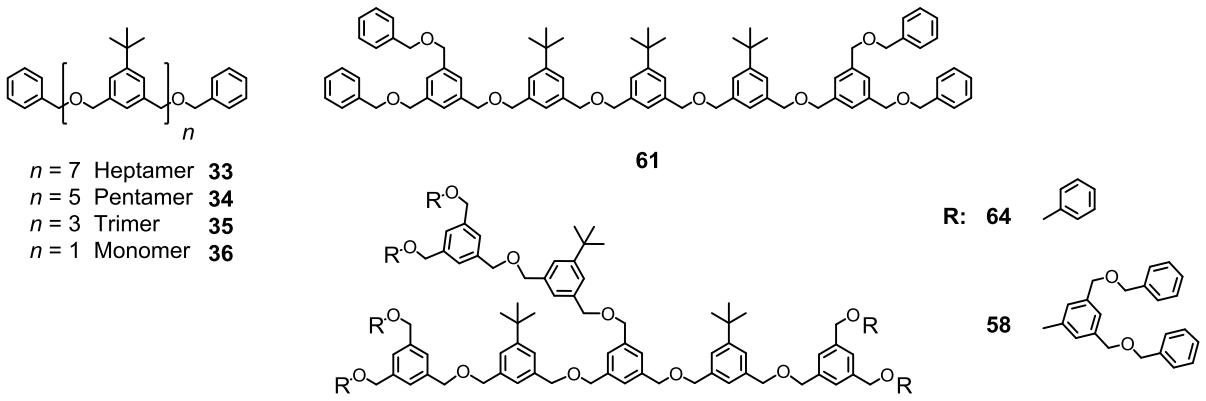

Figure 56. Ether containing ligands designed and investigated for the stabilization of Ag and Pd NPs..

The stability of silver particles formed in the presence of the linear ether ligands was very limited. On the other hand, the ability of these linear ligands to stabilize Pd NPs was higher compared to silver and further investigated.

The synthesis of the Pd NPs is uncomplicated and they exhibit a rather low size distribution. It was shown that a certain size of ligand is necessary to stabilize the formed nanoparticles efficiently. The higher oligomers exhibited not just increasing stability with increasing length of the ether ligand, but also bigger NPs diameters could be observed. This trend of bigger particles resulting from higher oligomeric benzyl ethers was not observed in the case of the branched ligands.

These NPs could for example find application as a easy separable catalyst for reaction types like C–C coupling and hydrogenation or as supermolecular building blocks in wet chemistry due to their low number of ligands per particle.

This thesis did answer fundamental questions but — as commen in science — also raise new issues to be addressed like the distribution of the ligands **1** and hexylthiol on the surface of the Au NPs (Figure 57) or the comparable electrochemical behavior of Au NPs with a similar ligand shell composition but of different core sizes.

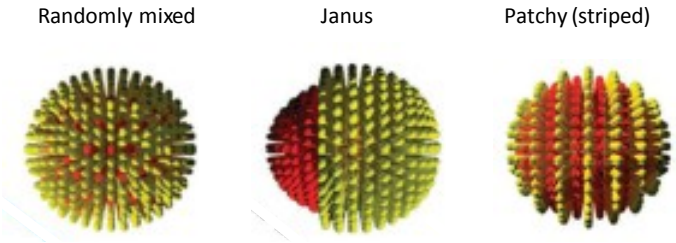

Figure 57. Different types of arrangement of two ligand on a nanoparticle.[252]

In the case of the ether coated Pd NPs further investigations towards the composition of the particles should be performed not least to confirm the hypothesis that the biggest ligand **58** is able to enwrap a NP completely. Such NP compositions, where one single ligand is sufficient to stabilize a particle are very rare and mainly reported for complex structures like DNA.

8 Experimental Part

8.1 Materials and Methods

Reagents and Solvents: All reagents and solvents were obtained either from Sigma-Aldrich, Acros, Fluorochem, Alfa, VWR, Fluka, ABCR, Apollo or TCI and were used as received unless otherwise stated. Dry solvents used for reactions corresponded to the quality purissp. a., abs., over Molecular Sieves from Fluka AG. For an inert atmosphere Argon 4.8 from PanGas AG was used. Oxygen-free solvents for were obtained from commercial sources or *via* bubbling argon through the solvent for 10 minutes. Technical grade solvents were use for extraction and column chromatography distilled prior to usage.

UV/Vis spectroscopy: UV/Vis spectra were recorded on a *Shimadzu* UV spectrometer UV-1800 using optical 1115F-QS *Hellma* cuvettes (10 mm light path). The wavelength of maxima (λ_{max}) are reported in nm.

NMR spectroscopy: Nuclear magnetic resonance (NMR) spectra were recorded using a *Bruker* DPX-NMR(400 MHz for 1H and 100 MHz for 13C) or a *Bruker* DRX-500 (500 MHz for 1H and 125 MHz for 13C) spectrometer at ambient temperature in the solvents indicated. Solvents for NMR were obtained from *Cambridge Isotope Laboratories* (Andover, MA, USA). Chemical shifts are given in ppm relative to tetramethylsilane (TMS). The spectra are referenced to the residual proton signal of the deuterated solvent (CDCl3: 7.26 ppm, CD2Cl2: 5.33 ppm,DMSO-d6: 2.49 ppm) for 1H spectra or the carbon signal of the solvent (CDCl3: 77.0 ppm,CD2Cl2: 55.8 ppm, DMSO-d6: 39.5 ppm) for 13C spectra. The coupling constants (J) are given in Hertz (Hz), the multiplicities are denoted as: *s* (singlet), *d* (duplet), *t* (triplet), *q* (quartet), *m* (multiplet) and *br* (broad).

Mass Spectrometry: Electron spray mass spectrometry was measured on a Bruker amaZon^{TM} X for electrospray ionization (ESI).

Gas chromatography (GC-MS): A Shimadzu GCMS-QP2010 SE gas chromatography system was used, with a ZB-5HT inferno column (30 m x 0.25 mm x 0.25 mm), at 1 mL/min He-flow rate (split = 20:1) with a Shimadzu mass detector (EI 70 eV) for gas chromatography-mass spectrometry (GC/MS).

High-resolution mass spectrum (HRMS) was performed on a HR-ESI-ToF-Ms with a Maxis 4G instrument from *Bruker*.

Direct analysis at real time (DART): The DART®-SVP source (IonSense, MA, USA) was equipped on a Shimadzu LC-MS 2020. The distance between the source orifice and the ceramic transfer tube was approximately 10 mm. The DART source was operated in positive mode with helium gas (5.0) and the substances were desorbed from a glass capillary. The other parameters, including the gas temperature, were optimized for the best performance in the experiments.

Matrix assisted laser desorption ionization – time of flight (MALDI-ToF MS) *Bruker* microflex™, calibrated with CsI_3 and *trans*-2-[3-(4-*tert*-Butylphenyl)-2-methyl-2-propenylidene]malononitrile (DCTB) was used as matrix.

Gel permeation chromatography (GPC) for the purification of gold nanoparticles was performed using *Bio-Rad Bio-Beads S-X1 Beads* (operating range 600 – 14000 g/mol) with toluene a solvent. Or GPC was performed on a *Shimadzu* Prominence System with SDV preparative columns from *Polymer Standards Service* (analytical: two SDV columns in series, 7.5 mm x300 mm each, exclusion limit: 70,000 and 400,000 g/mol; preparative: two Showdex columns in series, 20 mm x 60 cm each, exclusion limit: 30,000 g/mol.

Elementary analysis: The elemental analysis was performed by Mrs. Sylvie Mittelheisser on a *Vario Micro Cube*.

Melting Point: Measurements of melting points were made with a *Will Wetzlar* instrument; the measured temperatures are not corrected.

Thin layer chromatography (TLC) was performed on 0.25 mm precoated glass plates (silica gel 60 F_{254}) from *Merk*. Compounds were detected at 254 nm by fluorescence quenching or at 366 nm by self-fluorescence. If necessary, the plates were stained with KMnO4, vanillin, cerium or ninhydrin.

Thermogravimetric Analysis (TGA) was performed on a *Mettler Toledo TGA/SDTA851e* with a heating rate of 10°C/minute.

Transmission Electron Microscopy (TEM): TEM was performed on a *Philips CM100* transmission electron microscope at 80 kV. The particles were deposited by carefully putting a drop of the nanoparticles dispersion on top of a thin carbon film that spanned a perforated carbon support film covering a copper microscopy grid.

8.2 Synthetic Procedure

8.2.1 Ligands for AuNPs

4-(Pyridin-4-yl)benzenethiol[162] (**1**)

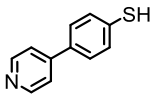

$C_{11}H_9NS$
187.26 g/mol

4-(4-(Methylthio)phenyl)pyridine (**4**) (264 mg, 1.31 mmol, 1 eq) and sodium 2-methyl-2-propanethiolate (411 mg, 3.67 mmol, 2.8 eq) were dissolved in 60 ml dry DMF, put under inert atmosphere and heated up at 160°C for 4 hours. After cooling to room temperature the reaction mixture was poured onto crushed ice and neutralized with 1M HCl. The aqueous solution was extracted with ethyl acetate 3 times. The combined organic fraction was washed with water and once with brine before the solvent was removed under reduced pressure. Further purification was done by column chromatography using EtOAc /CH_2Cl_2 4/1 as solvent to give the product **1** in 51% yield.

Note: The product forms disulfides. This can be observed by color change. The free sulfide is an orange liquid, the disulfide is a yellowish solid.

^{1}H NMR (400 MHz, Chloroform-*d*) δ 7.67 (ddd, *J* = 12.0, 8.3, 1.4 Hz, 4H), 7.58 – 7.52 (m, 2H), 7.50 – 7.42 (m, 4H).

^{13}C NMR (101 MHz, $CDCl_3$) δ 150.21, 147.28, 137.08, 129.65, 127.71, 127.05.

GC-MS (EI) *m/z* (%): 187.0 $[M]^+$.

4-(Pyridin-4-ylethynyl)benzenethiol (**2**)

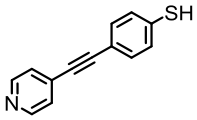

$C_{13}H_9NS$
211.28g/mol

8 (95 mg, 0.37 mmol, 1.0 eq) was dissolved in CH_2Cl_2 and degassed with argon. Pyrrolidine (156 µl, 1.88 mmol, 5.0 eq) was added and the mixture was stirred at room temperature for 3 hours. After aqueous work-up, the solvent was removed under reduced pressure. The crude product was purified by column chromatography with EtOAc /CH_2Cl_2 4/1 as solvent. The product **2** was yielded as yellow solid in 77%.

^{1}H NMR (250 MHz, Methanol-d4) δ 8.82 (d, *J* = 6.9 Hz, 2H), 8.13 (d, *J* = 6.9 Hz, 2H), 7.55 (d, *J* = 8.5 Hz, 2H), 7.43 – 7.36 (m, 2H).

^{13}C NMR (101 MHz, $CDCl_3$) δ 149.80, 132.34, 129.65, 127.01, 120.61, 93.32, 87.57.

(E)-4-(2-(pyridin-4-yl)vinyl)benzenethiol (**3**)

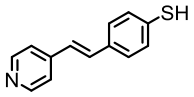

$C_{13}H_{11}NS$
213.30 g/mol

16 (100 mg, 0.41 mmol, 1.0 eq) was dissolved in THF (15 ml) and NH_4OH solution (631 µl, 40.9 mmol, 10.0 eq) was added and the solution was stirred at room temperature for 3 hours. The pH was adjusted to pH 7 with 3M HCl. The aqueous phase was extracted 3-times with ethyl acetate and the combined organic fractions were dried over Na_2SO_4. The solvent was removed under reduced pressure and the pure product **3** was obtained without further purification in 84 % yield.

^{1}H NMR (400 MHz, Chloroform-*d*) δ 8.58 (s, 2H), 7.54 – 7.47 (m, 2H), 7.42 – 7.37 (m, 2H), 7.35 (d, *J* = 5.8 Hz, 2H), 7.22 (d, *J* = 16.3 Hz, 1H), 6.99 (d, *J* = 16.3 Hz, 1H).

^{13}C NMR (101 MHz, $CDCl_3$) δ 150.25, 144.23, 135.34, 135.08, 132.01, 131.87, 128.44, 127.64, 122.68.

MS (ESI-MS) *m/z* (%): 213.0 $[M]^+$.

MS (DART-EI) *m/z* (%): 443.9 $[M+NH_4]^+$.

4-(4-(Methylthio)phenyl)pyridine (**4**)

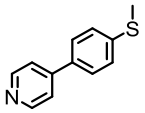

$C_{12}H_{11}NS$
201.29 g/mol

Methode a)[162]

4-Bromopyridine hydrochloride (350 mg, 1.8 mmol, 1 eq), 4-(methylthio)phenylboronic acid (302 mg, 1.8 mmol, 1 eq), potassium phosphate, (1910 mg, 9.0 mmol, 5 eq) and X-Phos (97 mg, 0.2 mmol, 0.1 eq), were placed in a MW tube and dissolved in 5 ml DMF and 2 ml water. This mixture was degassed by bubbling argon through the solution for 10 minutes. $Pd(OAc)_2$ (40 mg, 0.18 mmol, 0.1 eq) was added to the stirred solution and the MW flask was sealed and heated at 140°C for 2 h. The reaction was quenched with saturated NH_4Cl solution and extracted 3 times with Et_2O. The combined organic phases were washed with water and brine and dried over Na_2SO_4. The solvent was removed under reduced pressure and the crude product was purified by column chromatography (Cy/ EtOAc 4/1) or by sublimation to yield the product **4** as white solid in 95%.

Methode b)

4-Iodopyridine (634 mg, 3 mmol, 1 eq), 4-(methylthio)phenylboronicacid (554 mg, 3.3 mmol, 1.1 eq), potassium hydroxide (842 mg, 15 mmol, 5 eq) and tetrabutylammonium bromide (96.7 mg, 0.3 mmol, 0.1 eq) were dissolved in 20 ml THF and 3 ml water. This mixture was degassed by bubbling argon through the solution for 10 minutes. $Pd(PPh)_4$ (208 mg, 0.18 mmol, 6 mol%) was added to the stirred solution, the flask was sealed and heated at 60°C for 3 h. After cooling to room temperature the reaction was quenched with saturated NH_4Cl solution and extracted 3 times with Et_2O. The combined organic phases were washed with water and brine and dried over Na_2SO_4. The solvent was removed under reduced pressure and the crude product was purified by sublimation to yield the product **4** as white solid in 71%.

^{1}H NMR (400 MHz, Chloroform-*d*) δ 8.63 (d, *J* = 6.2 Hz, 2H), 7.56 (d, *J* = 8.5 Hz, 2H), 7.46 (d, *J* = 6.3 Hz, 2H), 7.34 (s, 2H), 2.51 (s, 3H).

^{13}C NMR (101 MHz, $CDCl_3$) δ 150.42, 147.71, 140.45, 134.64, 127.36, 126.79, 121.28, 15.60.

GC-MS (EI) *m/z* (%): 201.0 $[M]^+$, 186.0 $[M\text{-Me}]^+$.

MS (DART-EI) *m/z* (%): 201.8 $[M\text{+H}]^+$, 403.0 $[2M\text{+H}]^+$.

S-(4-iodophenyl) ethanethioate[164] (**6**)

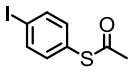

C_8H_7IOS
278.11g/mol

Zinc dust (732 mg, 11.2 mmol, 3.5 eq) and dichlorodimethylsilane (1145 mg, 11.2 mmol, 3.5 eq) were placed in a schlenk tube and suspended in 20 ml 1,2-dichloroethane. To this stirred solution pipsyl chloride (1000 mg, 3.21 mmol, 1 eq) and *N*,*N*-dimethylacetamide (839 mg, 9.63 mmol, 2.9) were added. The reaction mixture was heated up at 75°C until the zinc dust was dissolved (about 2.5 hours). The mixture was cooled at 50°C, acetyl chloride (328 mg, 4.17 mmol, 1.3 eq) was added and the solution was stirred for 20 minutes. After that time the reaction mixture was poured onto crushed ice. The aqueous phase was extracted 3-times with CH_2Cl_2 and the combined organic fraction was dried over Na_2SO_4 followed by evaporation of the solvent under reduced pressure. Column chromatography was performed using Cy/EtOAc 4/1 as solvent to yield the product **6** as white solid in 50% yield.

^{1}H NMR (400 MHz, Chloroform-d) δ 7.74 (d, *J* = 8.5 Hz, 2H), 7.13 (d, *J* = 8.5 Hz, 2H), 2.42 (s, 3H).

^{13}C NMR (101 MHz, $CDCl_3$) δ 193.28, 138.48, 136.08, 127.89, 96.08, 30.38.

GC-MS (EI) *m/z* (%): 277.7 $[M]^+$, 235.8 $[M$-Acetyl$]^+$.

S-(4-Ethynylphenyl) ethane thioate (**7**)

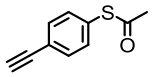

$C_{10}H_8OS$
176.23g/mol

6 (35 mg, 0.126 mmol, 1.0 eq), CuI (2 mg, 0.012 mmol, 0.1 eq) and Et_3N (254 µl, 1.79 mmol, 14.2 eq) were dissolved in 5 ml DMF and degassed for 10 minutes with argon. $Pd(PPh_3)_4$ (15 mg, 0.012 mmol, 0.1 eq) and trimethylsilylacetylene (23 µl, 0.164 mmol, 1.3 eq) were added and the reaction mixture was stirred at room temperature for 40 minutes. The reaction was quenched with saturated NH_4Cl solution and the aqueous phase was 3 times extracted with CH_2Cl_2. The combined organic fractions were once washed with brine and then dried over Na_2SO_4 before the solvent was removed under reduced pressure. The crude product was redissolved in 10 mL THF and 5 mL MeOH. 2 eq K_2CO_3 (35 mg, 0.25 mmol) was added and the mixture was stirred for one hour. The mixture was diluted with water and extracted 3 times with ethyl acetate. The solvent was removed under reduced pressure and the crude product was purified by column chromatography (Cy/EtOAc) 1/1 to give the product **7** in 55% as yellow oil.

^{1}H NMR (400 MHz, Chloroform-*d*) δ 7.48 (d, *J* = 8.3 Hz, 2H), 7.34 (d, *J* = 8.3 Hz, 2H), 2.41 (s, 3H), 0.25 (s, 9H).

^{13}C NMR (101 MHz, $CDCl_3$) δ 193.49, 134.21, 134.01, 132.65, 124.51, 104.30, 96.36, 30.42, 0.04.

S-(4-(Pyridin-4-ylethynyl)phenyl) ethanethioate (**8**)

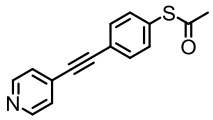

$C_{15}H_{11}NOS$
253.32g/mol

Methode a) starting from **14**

14 (140 mg, 0.45 mmol, 1.0 eq) was dissolved in 10 mL THF and degassed for 10 minutes. 20 eq TBAF was added (9 mL 1M solution) and the solution was stirred for 1 hour before it was cooled at 0°C. Acetyl chloride (843 µL, 11.7 mmol, 26 eq) was added and the reaction mixture was stirred for 20 minutes before 10 mL chloroform and 10 mL EtOH were added. The reaction mixture was extracted with water and DCM. After drying over Na_2SO_4 the solvent was removed under reduced pressure and the crude product was purified by column chromatography (EtOAc/DCM 4/1). Product **8** was yielded as pale yellow solid in 81%.

Methode b) starting from **7**

(4-Ethynylphenyl)ethanethioate (**7**) (100 mg, 0.567 mmol, 1 eq), 4-iodopyridine (121 mg, 0.567 mmol, 1 eq), X-Phos, (34.1 mg, 0.07 mmol, 0.12 eq) and Et_3N (402 µl, 2.83 mmol, 5 eq) were placed in a MW tube and suspended in 2 ml dry DMF. This suspension was degassed by bubbling argon through the solution for 10 minutes. $Pd(OAc)_2$ (13 mg, 0.58 mmol, 0.1 eq) and copper iodide (10.7 mg, 0.056 mmol, 0.1 eq) were added and the tube was sealed immediately. The reaction mixture was heated up at 140°C for 1 hour in the microwave. The reaction was quenched with NH_4Cl solution, extracted with CH_2Cl_2 and the solvent was removed under reduced pressure. The crude product was purified by column chromatography (Cy/EtOAc 2/1) to yield the product as off-white solid in 14% yield.

^{1}H NMR (400 MHz, Chloroform-d) δ 8.61 (d, *J* = 6.1 Hz, 2H), 7.58 (d, *J* = 8.6 Hz, 2H), 7.43 (d, *J* = 8.6 Hz, 2H), 7.38 (d, *J* = 6.1 Hz, 2H), 2.45 (s, 3H), 1.66 (s, 1H).

^{13}C NMR (101 MHz, MeOD) δ 194.46, 150.36, 135.65, 133.43, 131.33, 127.18, 124.16, 101.39, 94.53, 88.48, 30.20.

GC-MS (EI) *m/z* (%): 253.1 $[M]^+$, 211.1 [*M*-Acetyl]$^+$.

MS (DART-EI) *m/z* (%): 253.0 $[M]^+$, 253.8 $[M+H]^+$, 271 $[M+NH_4]^+$.

(2-((4-Bromophenyl)thio)ethyl)trimethylsilane[170] (**10**)

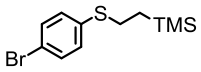

$C_{11}H_{17}BrSSi$
289.31g/mol

4-Bromothiophenol (14 g, 72.5 mmol, 1.0 eq), vinyltrimethylsilane (8.69 g, 84.1 mmol, 1.16 eq) and di-*tert*-butyl peroxide (1.61 g, 10.9 mmol, 0.15 eq) were mixed neat and heated at 100°C over night. Fractionated distillation gave the desired product **10** as colorless liquid in 76% yield.

^{1}H NMR (400 MHz, Chloroform-*d*) δ 7.42 – 7.37 (m, 2H), 7.19 – 7.14 (m, 2H), 2.97 – 2.90 (m, 2H), 0.95 – 0.88 (m, 2H), 0.04 (s, 9H).

^{13}C NMR (63 MHz, $CDCl_3$) δ 136.62, 131.97, 130.61, 119.56, 29.87, 16.95, -1.62.

MS (DART-EI) *m/z* (%): 289.8 $[M+H]^+$.

(2-((4-Iodophenyl)thio)ethyl)trimethylsilane[170] (**11**)

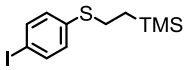

$C_{11}H_{17}ISSi$
336.31g/mol

10 (1.13 g, 3.9 mmol, 1 eq) and iodine (1.29 g, 5.1 mmol, 1.3 eq) were separately dissolved in dry Et_2O (2*30 ml). Both solutions were cooled to -70°C. *tert*-Butyllithium (3.25 mg, 9.4 mmol, 2.4 eq) was added to the solution of **10** and the mixture was stirred for 40 minutes at that temperature. The Iodine solution was slowly added and the reaction mixture was stirred for 10 minutes at -70 °C before it was warmed to 0°C. After stirring for 30 minutes the mixture was quenched with Na-thiosulfate solution, extracted with Et_2O and brine. After drying over Na_2SO_4 the solvent was removed under reduced pressure and the crude product was purified by column chromatography using pentane + 2% EtOAc as solvent. The product **11** was yielded as colorless liquid in 72%.

^{1}H NMR (400 MHz, $CDCl_3$) δ 7.60 – 7.56 (m, 2H), 7.05 – 7.01 (m, 2H), 2.96 – 2.90 (m, 2H), 0.95 – 0.89 (m, 2H), 0.06 – 0.03 (s, 9H).

^{13}C NMR (101 MHz, $CDCl_3$) δ 137.83, 137.55, 130.57, 90.28, 29.53, 16.86, -1.61.

MS (DART-EI) *m/z* (%): 277.8 $[M]^+$, 547 $[2M+NH_4]^+$.

Trimethyl((4-((2-(trimethylsilyl)ethyl)thio)phenyl)ethynyl)silane[170] (**12**)

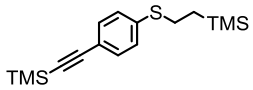

$C_{16}H_{26}SSi_2$
306.61g/mol

11 (626 mg, 1.86 mmol, 1.0 eq) was dissolved in 10 ml Et_2NH and degassed for 10 minutes with argon. $Pd(PPh_3)_2Cl_2$(133 mg, 0.18 mmol, 0.1 eq), CuI (40 mg, 0.20 mmol, 0.11 eq) and at last trimethylsilylacetylene (300 µl, 2.79 mmol, 1.5 eq) were added and the mixture was heated for 1.5 hours at 50°C. After cooling to room temperature the reaction was quenched with NH_4Cl, extracted 3-times with CH_2Cl_2. The combined organic fractions were once washed with brine and the solvent was removed under reduced pressure. Column chromatography (Cy + 10% DCM) gave the product **12** as light yellow solid in quantitative yields.

^{1}H NMR (400 MHz, Chloroform-*d*) δ 7.36 (d, *J* = 8.5 Hz, 2H), 7.22 – 7.15 (m, 2H), 3.00 – 2.91 (m, 2H), 0.96 – 0.87 (m, 2H), 0.24 (s, 9H), 0.04 (s, 9H).

^{13}C NMR (101 MHz, $CDCl_3$) δ 138.68, 132.36, 127.83, 120.03, 105.01, 94.45, 29.03, 16.76, 0.14, -1.62.

MS (DART-EI) *m/z* (%): 306.9 $[M+H]^+$, 613.2 $[2M+H]^+$, 630 $[2M+NH_4]^+$.

(2-((4-Ethynylphenyl)thio)ethyl)trimethylsilane[170] (**13**)

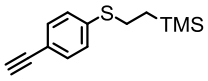

$C_{13}H_{18}SSi$
234.43g/mol

12 (218 mg, 0.71 mmol, 1.0 eq) and potassium carbonate (248 mg, 1.78 mmol, 2.5 eq) were suspended in a mixture of THF (10 ml) and MeOH (10 ml) and the solution was stirred for 1 hour at room temperature. H_2O was added and the product was extracted with EtOAc. After reducing the solvent under reduced pressure the product **13** was yielded in quantitative yields.

^{1}H NMR (400 MHz, Chloroform-d) δ 7.39 (d, *J* = 8.3 Hz, 2H), 7.21 (d, *J* = 8.4 Hz, 2H), 3.07 (s, 1H), 2.97 (d, *J* = 17.5 Hz, 2H), 0.93 (d, *J* = 17.5 Hz, 2H), 0.05 (s, 9H).

^{13}C NMR (101 MHz, $CDCl_3$) δ 137.83, 137.55, 130.57, 90.28, 29.53, 16.86, -1.61.

4-((4-((2-(Trimethylsilyl)ethyl)thio)phenyl)ethynyl)pyridine (**14**)

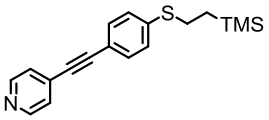

$C_{18}H_{21}NSSi$
311.52g/mol

4-Iodopyridine (357 mg, 1.69 mmol, 1.05 eq) and CuI (31 mg, 0.16 mmol, 0.1 eq) were placed in a round bottle flask and dissolved in 20 ml Et_2NH and 30 ml DMF. The solution was degassed for 15 minutes with argon and cooled to 0°C. $Pd(PPh_3)_2Cl_2$ (115 mg, 0.16 mmol, 0.1 eq) and **13** (377 mg,1.61 mmol, 1 eq) were added and the reaction mixture was stirred at room temperature for 2 hours. The reaction was quenched with NH_4Cl and extracted 3-times with CH_2Cl_2. The combined organic fractions were once washed with brine and the solvent was removed under reduced pressure. Column chromatography (Cy/EtOAc 1/1) gave the product **14** as pale yellow solid in 71% yield.

^{1}H NMR (400 MHz, Chloroform-d) δ 8.59 (dd, *J* = 4.6, 1.5 Hz, 1H), 7.50 – 7.42 (m, 1H), 7.36 (dd, *J* = 4.5, 1.5 Hz, 1H), 3.03 – 2.97 (m, 1H), 0.98 – 0.93 (m, 1H), 0.06 (s, 4H).

^{13}C NMR (101 MHz, CD_2Cl2) δ 150.36, 140.82, 132.64, 131.80, 127.85, 125.87, 119.00, 94.13, 87.34, 29.06, 17.05, -1.58.

GC-MS (EI) *m/z* (%): 305.95 $[M]^+$, 277.95 $[M\text{-}2Me]^+$.

MS (DART-EI) *m/z* (%): 311.9 $[M]^+$.

(E)-4-(4-((2-(Trimethylsilyl)ethyl)thio)styryl)pyridine (**15**)

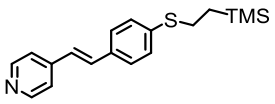

$C_{18}H_{23}NSSi$
313.53g/mol

4-Vinylpyridine (86.9 µl, 0.78 mmol, 1.5 eq), **10** (150 mg, 0.52 mmol, 1.0 eq), potassium carbonate (145 mg, 1.04 mmol, 2.0 eq), triphenylphosphine (68.6 mg, 0.26 mmol, 0.5 eq) and tributylamine (192 mg, 1.04 mmol, 2.0 eq) were suspended in 3 ml H_2O and degassed for 10 minutes before $PdCl_2$ (9.18 mg, 0.05 mmol, 0.1 eq) was added. The suspension was heated at 100°C for 10 hours. After cooling to room temperature the solution was extracted 3-times with ethyl acetate. The combined organic fractions were dried over Na_2SO_4 and the solvent was removed under reduced pressure. The residue was filtered over a silica plug to remove excess vinyl pyridine followed by sublimation at 120°C to give the product **15** as pale yellow solid in 65% yield

^{1}H NMR (400 MHz, Chloroform-*d*) δ 8.57 (d, *J* = 5.7 Hz, 2H), 7.45 (d, *J* = 8.3 Hz, 2H), 7.37 – 7.32 (m, 2H), 7.27 (dd, *J* = 16.8, 9.9 Hz, 3H), 6.97 (d, *J* = 16.3 Hz, 1H), 3.05 – 2.95 (m, 2H), 1.02 – 0.91 (m, 2H), 0.06 (s, 9H).

^{13}C NMR (63 MHz, $CDCl_3$) δ 150.32, 144.76, 138.73, 133.53, 132.69, 128.59, 127.50, 125.52, 120.90, 29.25, 16.91, -1.60.

GC-MS (EI) *m/z* (%): 313.0 $[M]^+$, 285.0 $[M$-Me$]^+$, 270.0 $[M$-3 Me$]^+$.

MS (DART-EI) *m/z* (%): 313.9 $[M]^+$.

(E)-S-(4-(2-(Pyridin-4-yl)vinyl)phenyl) ethanethioate (**16**)

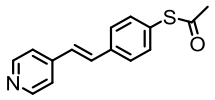

$C_{15}H_{13}NOS$
255.34g/mol

17 (251 mg, 0.96 mmol, 1.0 eq), potassium thioacetate (255 mg, 1.9 mmol, 2.0 eq), Xantphos, (28.5 mg, 0.048 mmol, 5 mol%) and DIPEA (782 µl, 1.93 mmol, 2.0 eq) were added to a MW tube and suspended in 10 ml dioxane. The solution was degassed for 10 minutes with argon. 2.5 mol% $Pd(dba)_2$ (14 mg, 0.024 mmol) was added, the tube was sealed and heated in the micro wave at 160°C for 25 minutes. After cooling to room temperature the reaction mixture was poured into water and extracted with ethyl acetate. The combined organic phase was once washed with brine and dried over Na_2SO_4 before the solvent was removed under reduced pressure. The crude product was purified by column chromatography (EtOAc/CH_2Cl_2 1/1) to yield the product **16** in 30% as yellow solid

^{1}H NMR (400 MHz, Chloroform-d) δ 8.62 – 8.54 (m, 2H), 7.54 – 7.49 (m, 2H), 7.43 – 7.33 (m, 4H), 7.23 (d, *J* = 16.4 Hz, 1H), 7.00 (d, *J* = 16.3 Hz, 1H), 2.44 (s, 3H).

^{13}C NMR (101 MHz, $CDCl_3$) δ 193.76, 150.28, 144.21, 135.08, 134.76, 132.09, 132.01, 131.86, 128.44, 127.62, 127.47, 126.72, 120.94, 120.85, 30.30.

GC-MS (EI) *m/z* (%): 213 $[M\text{-Ac}]^+$.

MS (DART-EI) *m/z* (%): 255.9 $[M]^+$, 256.9 $[M\text{+H}]^+$.

(E)-4-(4-Bromostyryl)pyridine[178] (**17**)

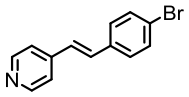

$C_{13}H_{10}BrN$
260.13g/mol

4-Vinylpyridine (1537 µl, 13.7 mmol, 1.2 eq), 1-bromo-4-iodobenzene (3304 mg, 11.4 mmol, 1.0 eq) and triphenylphosphine (6 mg, 0.023 mmol, 0.2 mol%) were placed in a pressure vessel and dissolved in Et_3N(5.7 ml, 40 mmol, 3.5 eq). The solution was degassed for 10 minutes with argon. $Pd(OAc)_2$(2.57 mg, 0.011 mmol, 0.1 mol%) was added, the pressure vessel was closed and the reaction mixture was heated at 110°C for 25 hours. The reaction to room temperature quenched with water and extracted with CH_2Cl_2. The combined organic fraction was dried over Na_2SO_4 and the solvent was removed under reduced pressure. The crude product was purified by column chromatography (Cy/EtOAc 1/2) or sublimated at 100°C to give the product **17** as off white solid in 73% yield.

^{1}H NMR (250 MHz, Chloroform-*d*) δ 8.65 – 8.60 (m, 2H), 7.64 – 7.52 (m, 4H), 7.44 (dd, *J* = 8.6, 2.0 Hz, 3H), 7.36 (s, 1H), 7.07 (d, *J* = 16.3 Hz, 1H).

^{13}C NMR (101 MHz, $CDCl_3$) δ 150.42, 144.36, 135.22, 132.15, 132.01, 128.58, 126.86, 122.81, 120.99.

GC-MS (EI) *m/z* (%): 260.8 $[M]^+$, 179.9 $[M\text{-Br}]^+$.

MS (DART-EI) *m/z* (%): 259.8$[M]^+$, 261.7 $[M\text{+H}]^+$, 539.8 $[2M\text{+Na}]^+$.

4-(4-Ethynylphenyl)pyridine (**19**)

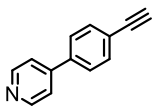

$C_{13}H_9N$
179.22g/mol

The product **23** (170 mg, 0.67 mmol, 1.0 eq) was dissolved in 5 ml MeOH (+ 5% EtOAc). 3 eq K_2CO_3 (280 mg, 2.0 mmol) was added and the mixture was stirred for 30 minutes at room temperature. The mixture was quenched with water and extracted with ethyl acetate. The combined organic layers were dried, filtered and evaporated. The residue was purified by column chromatography on silica to afford the title compound **19** as light brown solid in quantitative yield.

^{1}H NMR (400 MHz, $CDCl_3$) δ 8.68, 8.68, 8.67, 8.67, 7.50, 7.50, 7.49, 7.48, 3.18.

^{13}C NMR (101 MHz, $CDCl_3$) δ 150.54, 147.44, 138.53, 132.97, 127.04, 123.08, 121.59, 83.15, 78.89.

GC-MS (EI) *m/z* (%): 179.0 $[M]^+$.

MS (DART-EI) *m/z* (%): 179.9 $[M]^+$, 180.8 $[M+H]^+$, 197.9 $[M+NH_4]^+$.

(E)-4-(4-Ethynylstyryl)pyridine (**20**)

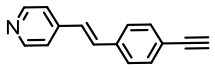

$C_{15}H_{11}N$
205.26g/mol

24 (51.0 mg, 0.18 mmol, 1.0 eq) and potassium carbonate (64.2 mg, 0.46 mmol, 2.5 eq) were suspended in a mixture of THF (3 ml) and MeOH (3 ml) and the solution was stirred for 1 hour at room temperature. H_2O was added and the product was extracted with EtOAc. After reducing the solvent under reduced pressure the product **20** was yielded in quantitative yields.

4-((4-Ethynylphenyl)ethynyl)pyridine[234] (**21**)

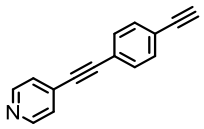

$C_{15}H_9N$
203.24g/mol

27(51.0 mg, 0.18 mmol, 1.0 eq) and potassium carbonate (77.6 mg, 0.56 mmol, 2.5 eq) were suspended in a mixture of THF (3 ml) and MeOH (3 ml) and the solution was stirred for 1 hour at room temperature. H_2O was added and the product was extracted with EtOAc. After reducing the solvent under reduced pressure the product **21** was yielded in quantitative yields.

^{1}H NMR (400 MHz, Chloroform-*d*) δ 8.64 – 8.58 (m, 2H), 7.50 (s, 4H), 7.41 – 7.35 (m, 2H), 3.20 (s, 1H).

^{13}C NMR (101 MHz, $CDCl_3$) δ 149.92, 132.33, 131.90, 131.29, 125.66, 123.10, 122.62, 93.39, 88.56, 83.14, 79.62.

GC-MS (EI) *m/z* (%): 202.95 $[M]^+$.

4-(4-Bromophenyl)pyridine[254,255] (**22**)

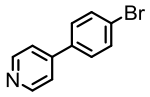

$C_{11}H_8BrN$
234.10g/mol

Pyridine-4-boronic acid (300 mg, 2.44 mmol, 1.0 eq), 1-bromo-4-iodobenzene (705 mg, 2.44 mmol, 1.0 eq) and a 2M solution of potassium carbonate (0.4 ml) were suspended in 10 ml toluene and 2 ml EtOH. The mixture was degassed by bubbling argon through the solution for 10 minutes. $Pd(PPh_3)_4$ (285 mg, 0.24 mmol, 0.1 eq) was added and the reaction mixture was stirred at reflux for 24 hours. After cooling to room temperature, the reaction mixture was poured into water and then extracted with toluene. The combined organic phase was washed with brine and dried over Na_2SO_4. The crude product was purified by column chromatography using $CHCl_3$/EtOAc 3/1 as solvent. The product **22** was yielded in 73% as white solid.

^{1}H NMR (250 MHz, Chloroform-*d*) δ 8.67 (d, *J* = 6.2 Hz, 2H), 7.63 (d, *J* = 8.5 Hz, 2H), 7.51 – 7.44 (m, 2H), 7.23 (d, *J* = 8.6 Hz, 2H).

^{13}C NMR (101 MHz, $CDCl_3$) δ 150.54, 147.25, 137.18, 132.44, 128.68, 123.68, 121.53.

GC-MS (EI) *m/z* (%): 234.1 $[M]^+$.

MS (DART-EI) *m/z* (%): 233.7 $[M]^+$, 235.7 $[M+H]^+$, 466.8 $[2M+H]^+$.

4-(4-((Trimethylsilyl)ethynyl)phenyl)pyridine (**23**)

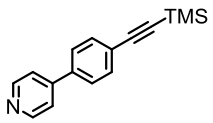

$C_{16}H_{17}NSi$
251.40g/mol

22 (55 mg, 0.218 mmol, 1.0 eq), CuI (6 mg, 0.031 mmol, 0.14 eq), $Pd(PPh_3)_2Cl_2$, (23 mg, 0.033 mmol) were placed in a MW tube under an atmosphere of argon. TMS acetylene (46 µL, 0.327 mmol, 0.15 eq), Et_3N (121 µL, 0.873 mmol, 4.0 eq) and THF (1.1 mL) were added and the mixture was heated at 100°C for 20 min and then cooled to ambient temperature. The mixture was filtered through a silica gel pack and washed with EtOAc. Combined eluents were evaporated under reduced pressure to give crude product as a solid. The combined organic layers were dried and the crude product was purified by sublimation. The product **23** was obtained as solid in quantitative yield.

^{1}H NMR (400 MHz, Chloroform-d) δ 8.63 – 8.53 (m, 2H), 7.47 (s, 4H), 7.38 – 7.32 (m, 2H), 7.25 (d, *J* = 16.3 Hz, 1H), 7.01 (d, *J* = 16.4 Hz, 1H), 0.26 (s, 9H).

^{13}C NMR (101 MHz, $CDCl_3$) δ 150.49, 147.56, 138.08, 132.81, 126.91, 124.18, 121.57, 104.49, 96.27, 0.08.

GC-MS (EI) *m/z* (%): 250.9 $[M]^+$, 235.9 $[M\text{-Me}]^+$.

Note: The shifts in the ^{1}H NMR are concentration depending.

(E)-4-(4-((Trimethylsilyl)ethynyl)styryl)pyridine (**24**)

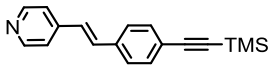

$C_{18}H_{19}NSi$
277.44g/mol

17 (55 mg, 0.21 mmol, 1.0 eq), CuI (5.7 mg, 0.03 mmol, 0.15 eq) and Et_3N (121 µl, 0.85 mmol, 4.0 eq) were dissolved in THF in a MW tube and degassed for 10 minutes with argon. Trimethylsilylacetylene (31.4 mg, 0.32 mmol, 1.5 eq) and $Pd(PPh_3)_2Cl_2$ (22.7 mg, 0.03 mmol, 0.15 eq) were added and the tube was sealed. After heating at 100°C for 20 minutes in the microwave the reaction was quenched with NH_4Cl and extracted 3-times with EtOAc. The combined organic fractions were once washed with brine and the solvent was removed under reduced pressure. Sublimation at 80°C gave the product **24** as yellow solid in 57% yield.

^{1}H NMR (400 MHz, Chloroform-d) δ 8.63 – 8.53 (m, 2H), 7.47 (s, 4H), 7.38 – 7.32 (m, 2H), 7.25 (d, *J* = 16.3 Hz, 1H), 7.01 (d, *J* = 16.4 Hz, 1H), 0.26 (s, 9H).

^{13}C NMR (101 MHz, $CDCl_3$) δ 150.40, 144.42, 136.30, 133.96, 133.77, 132.54, 132.47, 127.02, 126.92, 120.99, 104.93, 96.04, 0.09.

4-((4-Bromophenyl)ethynyl)pyridine[234] (**25**)

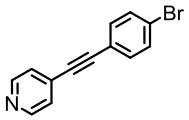

$C_{13}H_8BrN$
258.12g/mol

4-Ethynylpyridine hydrochloride (107 mg, 0.74 mmol, 1.05 eq) was washed with 1M NaOH solution, extracted with CH_2Cl_2 and concentrated to get free 4-ethynylpyridine. 1-Bromo-4-iodobenzene (200 mg, 1.0 eq, 0.707 mmol) and the pyridine derivative were dissolved in Et_3N/DMF (2/2) and degassed for 10 minutes. $Pd(PPh_3)_2Cl_2$ (50 mg, 0.1 eq, 0.07 mmol) and CuI (14.9 mg, 0.11 eq, 0.08 mmol) were added and the reaction mixture was stirred at room temperature for 30 minutes. The reaction was quenched with NH_4Cl solution, extracted with CH_2Cl_2 and the solvent was removed under reduced pressure. The crude product was purified by sublimation at 90°C to yield the product **25** as white solid in 83%.

^{1}H NMR (400 MHz, Chloroform-*d*) δ 8.64 – 8.59 (m, 2H), 7.52 (d, *J* = 8.5 Hz, 2H), 7.41 (d, *J* = 8.5 Hz, 2H), 7.39 – 7.34 (m, 2H).

^{13}C NMR (101 MHz, $CDCl_3$) δ 149.99, 133.40, 131.98, 131.23, 125.61, 123.79, 121.19, 92.90, 87.84.

GC-MS (EI) *m/z* (%): 256.8 $[M]^+$, 178.0 $[M\text{-Br}]^+$.

4-((4-((trimethylsilyl)ethynyl)phenyl)ethynyl)pyridine[234] (**27**)

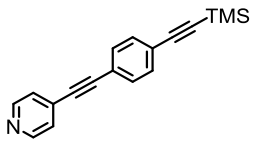

$C_{18}H_{17}NSi$
275.43g/mol

25 (145 mg, 0.56 mmol, 1.0 eq), CuI (10.8 mg, 0.06 mmol, 0.1 eq) and Et_3N (1.1 ml, 7.98 mmol, 14.2 eq) were dissolved in DMF in a MW tube and degassed for 10 minutes with argon. Trimethylsilylacetylene (71.7 mg, 0.73 mmol, 1.3 eq) and $Pd(PPh_3)_4$ (65.6 mg, 0.06 mmol, 0.1 eq) were added and the tube was sealed. After heating at 120°C for 20 minutes in the microwave the reaction was quenched with NH_4Cl and extracted 3-times with EtOAc. The combined organic fractions were once washed with brine and the solvent was removed under reduced pressure. Sublimation at 80°C gave the product **27** as white solid in 80% yield.

^{1}H NMR (400 MHz, Chloroform-*d*) δ 8.64 – 8.58 (m, 2H), 7.47 (d, *J* = 1.7 Hz, 2H), 7.40 – 7.35 (m, 4H), 0.24 (s, 9H).

^{13}C NMR (101 MHz, $CDCl_3$) δ 149.97, 132.15, 131.88, 131.81, 125.62, 124.13, 123.28, 122.17, 104.45, 97.16, 93.59, 88.51, 0.05, 0.04.

S-(4-((4-((Trimethylsilyl)ethynyl)phenyl)ethynyl)phenyl) ethanethioate[257] (**28**)

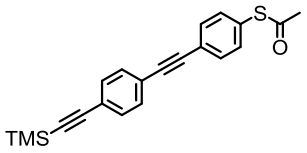

$C_{21}H_{20}OSSi$
348.54g/mol

(4-Iodophenylethynyl)trimethylsilane (252 mg, 0.84 mmol, 1.05 eq) and (4-ethynylphenyl) ethanethioate (**7**) (141 mg, 0.8 mmol, 1.0 eq) were dissolved in 3 ml Et_3N. The solution was degassed for 10 minutes with argon. $Pd(PPh_3)_2Cl_2$ (67.5 mg, 0.096 mmol, 0.12 eq) and CuI (15.2 mg, 0.08 mmol, 0.1 eq) were added and the reaction mixture was heated to reflux for 1.5 h. After cooling to room temperature the reaction was quenched with NH_4Cl solution and 3 times extracted with CH_2Cl_2. The crude product was purified with 2 chromatographic columns using Cy/CH_2Cl_2 1st 2/1, 2nd 1/1 to give the product **28** in 32% yield.

^{1}H NMR (250 MHz, Chloroform-d) δ 7.59 – 7.29 (m, 8H), 2.44 (s, 3H), 0.26 (s, 9H).

^{13}C NMR (63 MHz, $CDCl_3$) δ 182.15, 134.37, 132.31, 132.06, 131.61, 124.39, 123.07, 98.10, 96.62, 90.62, 30.44, 0.06.

GC-MS (EI) *m/z* (%): 347.8 $[M]^+$, 332.8 $[M$-Me$]^+$, 305.9 $[M$-Acetyl$]^+$, 290.9 $[M$-Acetyl-Me$]^+$.

MS (DART-EI) *m/z* (%):348.0 $[M]^+$, 348.8 $[M$+H$]^+$, 697.3 $[2M$+H$]^+$, 714.2 $[2M$+$NH_4]^+$.

4-((4-((4-Bromophenyl)ethynyl)phenyl)ethynyl)pyridine (**29**)

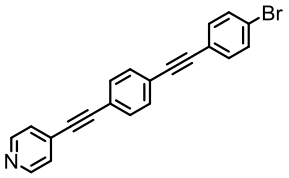

$C_{21}H_{12}BrN$
358.24g/mol

21 (111 mg, 0.54 mmol, 1.0 eq) and 1-bromo-4-iodobenzene (162 mg, 0.57 mmol, 1.05 eq) were dissolved in DMF (10 ml) and Et_3N (2 ml). After degassing the mixture for 10 minutes with argon $Pd(PPh_3)_4$ (64 mg, 0.05 mmol, 0.1 eq) and CuI (10 mg, 0.05 mmol, 0.1 eq) were added and the reaction mixture was stirred at room temperature for 40 minutes. The reaction was quenched with NH_4Cl solution and extracted 3-times with Et_2O. The combined organic phase was washed once with brine and dried over Na_2SO_4. The solvent was removed under reduced pressure and the crude product was purified by column chromatography using pure EtOAc as solvent to give the product **29** as colorless solid in 40% yield.

^{1}H NMR (400 MHz, Acetone-d6) δ 8.64 (d, *J* = 6.1 Hz, 2H), 7.67 – 7.61 (m, 6H), 7.55 – 7.48 (m, 4H).

^{13}C NMR (101 MHz, $CDCl_3$) δ 149.93, 133.19, 132.00, 131.86, 131.77, 125.66, 123.96, 123.06, 122.19, 121.96, 93.64, 90.85, 90.07, 88.59.

GC-MS (EI) *m/z* (%): 356.8 $[M]^+$, 277.0 $[M\text{-Br}]^+$.

MS (DART-EI) *m/z* (%): 357.8 $[M\text{+H}]^+$.

S-(4-((4-(Pyridin-4-ylethynyl)phenyl)ethynyl)phenyl) ethanethioate (**30**)

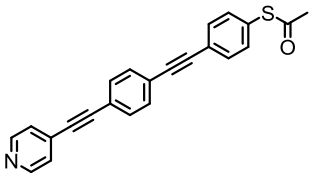

$C_{23}H_{15}NOS$
353.44g/mol

28 was dissolved in a 1:1 mixture of MeOH and THF in the presence of K_2CO_3 and stirred for 1 hour. The mixture was extracted with CH_2Cl_2 and dried to give the free acetyl-compound.

21.3 mg of the free acetyl **28** (0.08 mmol, 1.0 eq) and 4-iodopyridine (17.9 mg, 0.08 mmol, 1.1 eq) were dissolved in a mixture of Et_3N and DMF (3+3 ml). The mixture was degassed for 10 minutes and cooled to 0°C before $Pd(PPh_3)_2$ Cl_2 (6.5 mg, 0.01 mmol, 0.12 eq) and CuI (1.47 mg, 0.01 mmol, 0.1 eq) were added. The reaction mixture was stirred at 0°C for 2 hours before warmed to rt and stirred for another 2 hours. The reaction was quenched with NH_4Cl solution and extracted 3-times with EtOAc. The combined organic phase was washed once with brine and dried over Na_2SO_4. The solvent was removed under reduced pressure and the crude product was purified by column chromatography using pure EtOAc/CH_2Cl_2 (4/1) as solvent mixture to give the product **30** as colorless solid in 75% yield.

^{1}H NMR (400 MHz, Chloroform-*d*) δ 7.74 (d, *J* = 8.4 Hz, 2H), 7.53 (d, *J* = 8.4 Hz, 4H), 7.13 (d, *J* = 8.4 Hz, 2H), 7.04 – 6.98 (m, 4H), 2.42 (s, 3H).

^{13}C NMR (101 MHz, $CDCl_3$) δ 193.47, 149.91, 134.39, 132.34, 131.98, 131.86, 131.35, 128.64, 125.65, 124.21, 123.94, 122.22, 93.65, 91.14, 90.57, 88.60, 30.45.

4-((4-((4-((Trimethylsilyl)ethynyl)phenyl)ethynyl)phenyl)ethynyl)pyridine (**31**)

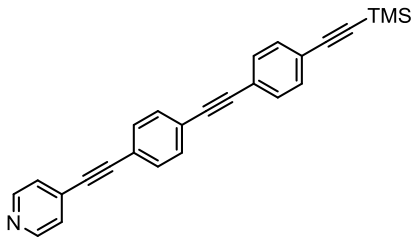

$C_{26}H_{21}NSi$
375.55g/mol

29 (20 mg, 0.056 mmol, 1.0 eq), CuI (8 mg, 0.072 mmol, 1.3 eq), Et_3N (112 µl, 0.79 mmol, 14.2 eq) were placed in a MW tube and dissolved in 4.5 ml DMF. The solution was degassed for 10 minutes with argon before $Pd(PPh_3)_4$ (6.5 mg, 0.005 mmol, 0.1 eq) was added and the reaction mixture was heated at 120°C for 20 minutes in the micro wave. After cooling to room temperature the reaction mixture was poured into water and extracted 3-times with ethyl acetate. The combined organic fraction was dried over Na_2SO_4 and the solvent was removed under reduced pressure. The crude product was purified by column chromatography using pure ethyl acetate as solvent to give the product **31** as white solid in 86% yield.

^{1}H NMR (400 MHz, Chloroform-*d*) δ 8.62 (d, *J* = 6.1 Hz, 2H), 7.53 (s, 4H), 7.46 (d, *J* = 0.9 Hz, 2H), 7.38 (d, *J* = 6.1 Hz, 2H), 0.26 (s, 9H).

^{13}C NMR (101 MHz, $CDCl_3$) δ 149.90, 132.29, 132.19, 132.09, 131.99, 131.78, 131.57, 128.69, 128.57, 125.65, 124.04, 123.45, 123.00, 122.14, 104.65, 96.73, 93.66, 91.58, 90.83, 88.58, 0.05.

GC-MS (EI) *m/z* (%): 374.9 $[M]^+$, 359,9 $[M\text{-Me}]^+$.

MS (DART-EI) *m/z* (%): 376.0 $[M+H]^+$.

4-((4-(*tert*-Butylthio)phenyl)ethynyl)pyridine (**32**)

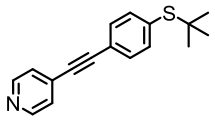

$C_{17}H_{17}NS$
267.39g/mol

tert-Butyl(4-ethynylphenyl)sulfane (100 mg, 0.525 mmol, 1 eq), 4-iodopyridine (112 mg, 0.525 mmol, 1 eq) and potassium phosphate (558 mg, 2.63 mmol, 5.0 eq) were placed in a MW tube and dissolved in 1.5 ml DMF. The solution was degassed with argon for 10 minutes. $Pd(OAc)_2$(11.7 mg, 0.052 mmol, 0.1 eq), 2-(dicyclohexylphosphino)-2',4',6'-triisopropylbiphenyl (30.6 mg, 0.063 mmol, 0.12 eq) and copper iodide (9.9 mg, 0.052 mmol, 0.1 eq) were added and the MW vial was sealed immediately. After heating up at 140°C for 2 h the reaction was quenched with NH_4Cl and extracted 3 times with CH_2Cl_2 and once washed with brine. After drying over Na_2SO_4 the solvent was removed under reduced pressure and the crude product was purified by two column chromatography's (Cy/EtOAc 2/1 and 1/2). Product 32 was yielded in 54% as pale yellow solid.

^{1}H NMR (400 MHz, Chloroform-d) δ 8.65 (s, 2H), 7.51 (d, *J* = 8.6 Hz, 4H), 7.39 (d, *J* = 1.9 Hz, 2H), 1.30 (s, 9H).

GC-MS (EI) *m/z* (%): 243[*M*]$^+$, 187 [*M*-*t*-Bu]$^+$.

MS (DART-EI) *m/z* (%): 267.1 [*M*]$^+$, 267.9 [*M*+H]$^+$.

8.3 Ether Ligands

8.3.1 Linear Ligands

5,5'-((((5-(*tert*-Butyl)-1,3-phenylene)bis(methylene))bis(oxy))bis(methylene))bis(1-(((3-(((3-((benzyloxy)methyl)-5-(*tert*-butyl)benzyl)oxy)methyl)-5-(*tert*-butyl)benzyl)oxy)methyl)-3-(*tert*-butyl)benzene) (**33**)

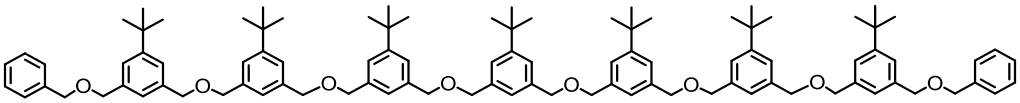

$C_{98}H_{126}O_8$
1432.08g/mol

Methode a) starting from **51**

51 (34.5 mg, 0.05 mmol, 2.0 eq) was placed in a schlenk tube, put under argon and dissolved in dry THF. 2.5 mg NaH (0.06 mmol, 1.0 eq) was added and the mixture was stirred for 10 minutes. 2.3 eq **37** (8.7 mg, 0.03 mmol) were added and the reaction mixture was stirred over night at 60 °C. After cooling to room temperature the reaction was quenched with water and extracted 3 times with ethyl acetate. The combined organic fraction was washed with brine and dried over Na_2SO_4 and the solvent was removed under reduced pressure. The crude product was purified by column chromatography using Cy/EtOAc 10/1 as solvent. The product was further purified by GPC using $CHCl_3$. The product **33** was yielded in 13% as pale yellow oil.

Methode b) starting from **54**

54 (20.9 mg, 0.04 mmol, 1.0 eq) and **56** (40 mg, 0.07 mmol, 2.0 eq) were dissolved in 5 ml of dry THF under an argon atmosphere. NaH (4.6 mg, 0.11 mmol, 3.0 eq) were added and the mixture was heated up to reflux and stirred for 24 hours. After cooling to room temperature the reaction was quenched with water and extracted 3 times with Et_2O. The combined organic layers were washes once with brine before dried over Na_2SO_4.The solvent was removed under reduced pressure. The

crude product was purified by column chromatography (Cy/EtOAc 8/1) to give the product as colorless oil in 17 % yield.

^{1}H NMR (400 MHz, Chloroform-*d*) δ 7.39 – 7.28 (m, 24H), 7.23 – 7.18 (m, 7H), 4.57 – 4.48 (m, 32H), 1.32 (t, *J* = 2.2 Hz, 63H).

^{13}C NMR (101 MHz, $CDCl_3$) δ 151.69, 151.68, 138.26, 138.20, 129.59, 128.54, 128.43, 127.99, 127.76, 124.80, 124.76, 124.36, 72.57, 72.56, 72.54, 72.31, 34.84, 31.55.

MS (MALDI-ToF), *m/z*: 1439.7 $[M+Li]^+$, 1454.9 $[M+Na]^+$.

EA calc: C 82.19, H 8.87%, O 8.94%; found: C 81.85%, H 8.70%, N 0.00%

5,5'-((((5-(*tert*-butyl)-1,3-phenylene)bis(methylene))bis(oxy))bis(methylene))bis(1-(((3-((benzyloxy)methyl)-5-(*tert*-butyl)benzyl)oxy)methyl)-3-(*tert*-butyl)benzene) (**34**)

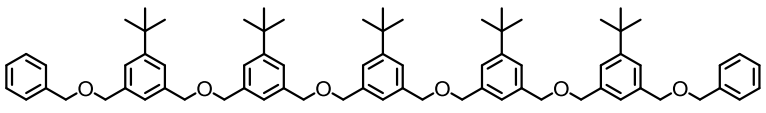

$C_{74}H_{94}O_6$
1079.56g/mol

49 (73.5 mg, 0.16 mmol, 2.0 eq) was dissolved in 5 ml dry THF and put under argon. NaH (8 mg, 0.20 mmol, 2.5 eq) was added and the mixture was stirred for 10 minutes at room temperature before **37** (25 mg, 0.08 mmol, 1.0 eq) was added. The reaction mixture was stirred at reflux for 16 hours. After cooling to room temperature the reaction was quenched with water and extracted 3 times with ethyl acetate. The combined organic fraction was washed with brine and dried over Na_2SO_4 and the solvent was removed under reduced pressure. The crude product was purified by column chromatography suing Cy/EtOAc 5/1 as solvent. The product was further purified by GPC using $CHCl_3$. The product **34** was yielded in 86% as off-white wax.

^{1}H NMR (400 MHz, Chloroform-*d*) δ 7.33 (dq, *J* = 13.6, 7.1, 6.5 Hz, 20H), 7.19 (s, 5H), 4.55 (d, *J* = 2.8 Hz, 24H), 1.35 – 1.30 (m, 45H).

^{13}C NMR (101 MHz, $CDCl_3$) δ 151.69, 151.68, 138.26, 138.24, 129.59, 128.53, 128.43, 127.99, 127.75, 124.80, 124.76, 124.36, 124.33, 72.57, 72.56, 72.54, 72.33, 34.84, 31.55.

MS (MALDI-ToF) *m/z*: 1102.7 $[M+Na]^+$, 975.2 $[M-2t\text{Bu-Me}]^+$.

MS (DART-EI) *m/z* (%): 1097.6 $[M+NH_4]^+$.

EA calc: C 82.33%, H 8.78%, N 0.0%; found: C 81.99%, H 9.08 %, N 0.33 %

5,5'-((((5-(*tert*-Butyl)-1,3-phenylene)bis(methylene))bis(oxy))bis(methylene))bis(1-((benzyloxy)methyl)-3-(*tert*-butyl)benzene) (**35**)

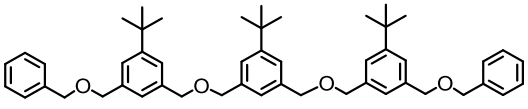

$C_{50}H_{62}O_4$
727.04g/mol

47 (156 mg, 0.55 mmol, 2.05 eq) and **37** (85.6 mg, 0.27 mmol, 1.0 eq) were dissolved in dry THF and degassed for 10 minutes with argon. Sodium hydride (24.6 mg, 0.61 mmol, 2.3 eq) was added and the reaction mixture was heated up to reflux for 24 hours. After cooling to room temperature the reaction was quenched with water and the aqueous phase was extracted with ethyl acetate. The combined organic layers were washed with brine and dried over Na_2SO_4 and then the solvent was removed under reduced pressure. The crude product was purified by column chromatography (Cy/EtOAc 4/1). The product was further purified by GPC using $CHCl_3$to give the product **35** as colorless oil in 63% yield.

^{1}H NMR (400 MHz, Chloroform-d) δ 7.39 – 7.28 (m, 16H), 7.19 (s, 3H), 4.57 – 4.54 (m, 16H), 1.32 (s, 27H).

^{13}C NMR (101 MHz, $CDCl_3$) δ 151.68, 138.48, 138.26, 138.17, 128.54, 128.00, 127.76, 124.81, 124.77, 124.37, 124.34, 72.56, 72.34, 34.85, 31.55.

MS (MALDI-ToF) *m/z*: 711.9 [*M*-Me]$^+$.

MS (DART-EI) *m/z* (%): 744.5 [*M*+NH_4]$^+$, 1471.0 [2*M*+NH_4]$^+$.

EA calc.: C 83.38%, H 8.07%, O 8.54%; found: C 82.11%, H 8.58%, N 0.51%

((((5-(*tert*-Butyl)-1,3-phenylene)bis(methylene))bis(oxy))bis(methylene))dibenzene (**36**)

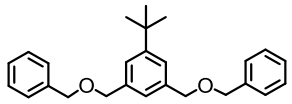

$C_{26}H_{30}O_2$
374.52g/mol

421 µl Benzyl alcohol (439 mg, 4.0 mmol, 2.2 eq) was dissolved in 50 ml dry THF. NaH (221 mg, 5.53 mmol, 3.0 eq) was added and the mixture was stirred for 10 minutes at room temperature. Dibromo **37** (590 mg, 1.84 mmol, 1.0 eq) was added and the reaction mixture was heated up to reflux and stirred at that temperature for 12 hours. After cooling to room temperature the reaction was quenched with water and extracted 3 times with Et_2O. The combined organic layers were washes once with brine before dried over Na_2SO_4.The solvent was removed under reduced pressure. The crude product was purified by column chromatography (Cy/EtOAc 4/1) to give the product **36** as colorless oil in 80 % yield.

^{1}H NMR (400 MHz, Chloroform-*d*) δ 7.41 – 7.27 (m, 12H), 7.21 (d, *J* = 0.7 Hz, 1H), 4.59 – 4.55 (m, 9H), 1.33 (s, 10H).

^{13}C NMR (101 MHz, $CDCl_3$) δ 151.68, 138.48, 138.19, 128.54, 128.00, 127.76, 124.71, 124.36, 72.53, 72.31, 34.84, 31.54.

GC-MS (EI) *m/z* (%): 359.0 [*M*-Me]$^+$, 268.0 [*M*-Me-Bz]$^+$.

MS (DART-EI) *m/z* (%): 392.0 [M+NH_4]$^+$, 766.4 [2M+NH_4]$^+$.

EA calc: C 83.38%, H 8.07%, O 8.54%; found: C 83.08%, H 8.18 %, N 0.00 %

1,3-Bis(bromomethyl)-5-(*tert*-butyl)benzene[159,258] (**37**)

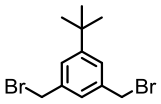

$C_{12}H_{16}Br_2$
320.07g/mol

5-*tert*-Butyl (m-xylene) (25.1 g, 147 mmol, 1 eq), N-bromosuccinimide (NBS) (79.9 g, 444 mmol, 3 eq) and AIBN (2,2'-Azobis(2-methylpropionitrile)) (0.19 g, 1.16 mmol, 8 mol%) were suspended in 400 mL methylformate in a 500 mL round bottom flask. The reaction was stirred and brought to reflux with a 500 W lamp (distance ~ 50 cm).After refluxing for 3 hours the mixture was cooled to room temperature and the solvent was removed under reduced pressure. The residue was redissolved in 300 mL CH_2Cl_2 and was washed twice with 100 mL $NaHCO_{3\ conc.}$ solution, with 100 mL H_2O_{dest} and once with brine. The organic fraction was dried over Na_2SO_4 and then dried under reduced pressure. Recrystallization from hexane (~500 mL) gave the product **37** as a white solid in 71% yield.

mp: 117-120 °C (Lit: 112-119°C)

^{1}H NMR (400 MHz, Chloroform-d) δ 7.34 (d, J = 1.6 Hz, 2H), 7.26 (d, J = 1.4 Hz, 1H), 4.49 (s, 4H), 1.33 (s, 9H).

^{13}C NMR (101 MHz, $CDCl_3$) δ 152.65, 138.11, 126.97, 126.38, 34.92, 33.60, 31.35.

GC-MS (EI) *m/z* (%): 320.0 $[M]^+$, 303.0 $[M\text{-Me}]^+$, 239 $[M\text{-Br}]^+$, 225 $[M\text{-Me-Br}]^+$.

MS (DART-EI) *m/z* (%): 377.8 $[M+NH_4]^+$.

(((3-(Bromomethyl)-5-(*tert*-butyl)benzyl)oxy)methanetriyl)tribenzene (**38**)

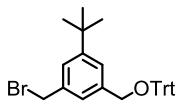

$C_{31}H_{31}BrO$
499.49g/mol

1,3-bis(Bromomethyl)-5-*tert*-butylbenzene (**37**) (6.4 g, 20 mmol, 1 eq) and triphenylmethanol (4.83 g, 18 mmol, 10.9 eq) were, under nitrogen atmosphere, dissolved in 20 mL dry THF. NaH (1.04 g, 26 mmol, 1.3 eq) was added and the reaction was stirred over night at reflux. After cooling to room temperature 100 mL water was added and the mixture was extracted with MTBE (3x 100 mL). The MTBE phase was than washed with brine and dried over Na_2SO_4.
The solvent was removed under reduced pressure and the crude product was purified by column chromatography using Cy/EtOAc 9/1 as solvent to yield the product **38** as white solid in 32%.

^{1}H NMR (400 MHz, Chloroform-d) δ 7.55 – 7.48 (m, 6H), 7.37 – 7.20 (m, 12H), 4.51 (s, 2H), 4.18 (s, 2H), 1.31 (s, 9H).

^{13}C NMR (101 MHz, $CDCl_3$) δ 151.84, 144.20, 139.58, 137.46, 128.87, 128.04, 128.01, 127.19, 125.00, 124.90, 124.35, 87.22, 65.86, 34.87, 34.44, 31.46, 27.06.

(5-(*tert*-Butyl)-1,3-phenylene)dimethanol[224] (**39**)

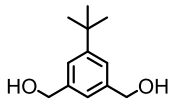

$C_{12}H_{18}O_2$
194.27g/mol

5-*tert*-Butylisophthalic acid (12.9 g, 58 mmol, 1 eq) was dissolved in 300 ml of dry THF using a three neck flask equipped with a mechanic stirrer and a condenser. The solution was cooled to -20°C before $LiAlH_4$ (6.9 g, 174 mmol, 3 eq) was added in portions. The mixture was stirred at that temperature for 4 h and then quenched by the slow addition of ice followed $HCl_{conc.}$ The aqueous phase was extracted with MTBE and the combined extract was washed with brine and dried over Na_2SO_4 and evaporated under reduced pressure to give the product **39** as white waxy solid in quant. Yield.

mp: according to Literature

^{1}H NMR (250 MHz, Chloroform-d) δ 7.31 (s, 2H), 7.18 (s, 1H), 4.67 (s, 4H), 1.98 (s, 2H), 1.33 (s, 9H).

^{13}C NMR (101 MHz, $CDCl_3$) δ 152.10, 141.03, 123.54, 123.05, 65.66, 34.90, 31.50.

GC-MS (EI) *m/z* (%): 194.1 $[M]^+$, 179.1 $[M\text{-Me}]^+$.

MS (DART-EI) *m/z* (%): 211.9 $[M+NH_4]^+$, 406.1 $[2M+NH_4]^+$, 600.3 $[3M+NH_4]^+$.

(3-(*tert*-Butyl)-5-((trityloxy)methyl)phenyl)methanol (**41**)

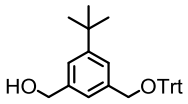

$C_{31}H_{32}O_2$
436.59g/mol

The dialcohol **39** (2.25 g, 11.6 mmol, 1.0 eq) was dissolved in dry THF and cooled to -40°C. NaH (0.7 g, 17.4 mmol, 1.5 eq) was added and the mixture was stirred at that temperature for 15 minutes before triphenylmethyl chloride (3.3 g, 11.6 mmol, 1.0 eq) was added over 10 minutes. The mixture was warmed to room temperature and then heated at 50°C for 14 h. After cooling to room temperature the reaction was quenched with water and extracted with ethyl acetate. The combined organic fraction was dried over Na_2SO_4 and the solvent was removed under reduced pressure. Column chromatography (Cy/ EtOAc 4/1) gave the desired product **41** in 18% as white solid.

^{1}H NMR (400 MHz, Chloroform-d) δ 7.57 – 7.48 (m, 6H), 7.35 – 7.21 (m, 12H), 4.67 (s, 2H), 4.19 (s, 2H), 1.32 (s, 9H).

^{13}C NMR (101 MHz, $CDCl_3$) δ 151.61, 144.26, 140.70, 139.27, 128.88, 128.87, 127.96, 127.14, 123.57, 123.02, 87.16, 66.08, 65.88, 34.85, 31.52, 31.51.

MS (DART-EI) *m/z* (%): 211.9 $[M\text{-Trt}+NH_4]^+$, 242.9 $[Trt]^+$,406.1 $[2M\text{-}2Trt+NH_4]^+$.

3-(*tert*-Butyl)-5-((trityloxy)methyl)benzyl 4-methylbenzenesulfonate (**42**)

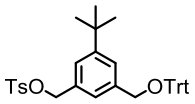

$C_{38}H_{38}O_4S$
590.78g/mol

Methode a) starting from **53**

5.23 g (5-(*tert*-Butyl)-1,3-phenylene)bis(methylene) bis(4-methylbenzenesulfonate) (**53**) (10.4 mmol, 1 eq) and triphenylmethanol (2.79 g, 10.4 mmol, 1 eq) were places in a schlenk tube, put under argon and dissolved in 60 ml dry THF. NaH (0.62 g, 150.6 mmol, 1.5 eq) was added and the mixture was heated to reflux for 24 hours. After cooling to room temperature the reaction was quenched with water. The aqueous phase was 3 times extracted with diethyl ether. The combined organic fraction was washed with brine and dried over Mg_2SO_4 before the solvent was removed under reduced pressure. The crude product was purified by column chromatography using Cy/ EtOAc 4/1 as solvent to give the product **42** as white solid in 34% yield.

Methode b) starting from **41**

1 eq (3-(tert-Butyl)-5-((trityloxy)methyl)phenyl)methanol (**41**) (200 mg, 0.458 mmol) was dissolved in dry THF. NaH (27 mg, 0.68 mmol, 1.5 eq) was added and the mixture was stirred for 10 minutes before p-toluenesulfonyl chloride (106 mg, 0.55 mmol, 1.2 eq), dissolved in 5 ml dry THF were added. The reaction mixture was stirred at room temperature for 20 hours before quenched with water. The aqueous phase was 3 times extracted with diethyl ether. The combined organic fraction was washed with brine and dried over Mg_2SO_4 before the solvent was removed under reduced pressure. The crude product was purified by column chromatography using Cy/EtOAc 4/1 as solvent to give the product **42** as white solid in 68% yield.

This product is not stable under ambient conditions for more than 3 days.

^{1}H NMR (250 MHz, Chloroform-d) δ 7.78 (d, J = 8.3 Hz, 2H), 7.49 (dd, J = 8.2, 1.6 Hz, 6H), 7.35 – 7.23 (m, 20H), 7.10 (s, 1H), 5.08 (s, 2H), 4.12 (s, 2H), 2.38 (s, 3H), 1.26 (s, 9H).

MS (DART-EI) *m/z* (%): 364.9 [*M-Trt* +NH_4]$^+$.

(3-(*tert*-Butyl)-5-(((tert-butyldiphenylsilyl)oxy)methyl)phenyl)methanol (**43**)

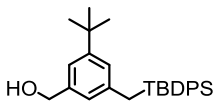

$C_{28}H_{36}OSi$
416.68g/mol

39 (155 mg, 0.8 mmol, 1.0 eq) was dissolved in 5 ml CH_2Cl_2 and cooled to –20°C before N,N-DIPEA (399 µl, 2.4 mmol, 3.0 eq) was added and the mixture was stirred for 5 minutes. *tert*-Butyldiphenyl chlorosilane (254 µl, 0.96 mmol, 1.2 eq) and dimethyl aminopyridin (DMAP) (14.8 mg, 0.12 mmol, 0.15 eq) were added and the reaction mixture was warmed to room temperature and stirred overnight. The mixture was quenched with saturated NH_4Cl and the layers were separated. The aqueous layer was extracted 3 times with ether and the combined organic layers were washed with brine and dried over $MgSO_4$. The solvent was removed under reduced pressure to give the crude product. This was purified using column chromatography (Cy/EtOAc 7/1) yielding the product **43** in 42% as colorless oil.

^{1}H NMR (250 MHz, Chloroform-d) δ 7.70 (dd, *J* = 7.7, 1.8 Hz, 4H), 7.44 – 7.33 (m, 7H), 7.28 (s, 1H), 7.14 – 7.10 (m, 1H), 4.78 (d, *J* = 0.7 Hz, 2H), 4.67 (d, *J* = 5.9 Hz, 2H), 1.32 (s, 9H).

^{13}C NMR (101 MHz, $CDCl_3$) δ 151.69, 141.24, 140.57, 135.76, 135.72, 134.94, 133.71, 129.81, 127.92, 127.86, 127.83, 122.79, 122.15, 65.98, 65.82, 34.90, 31.53, 27.01, 19.48.

(3-(*tert*-Butyl)-5-(((2-methoxyethoxy)methoxy)methyl)phenyl)methanol[245] (**44**)

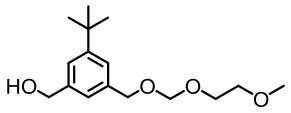

$C_{16}H_{26}O_4$
282.38g/mol

39 (217 mg, 1.11 mmol, 1.0 eq), MEM chloride (127 µl, 1.11 mmol, 1.0 eq) and N,N-DIPEA (278 µl, 1.67 mmol, 1.5 eq) were dissolved in CH_2Cl_2 under inert atmosphere and stirred at room temperature for 2 h. The reaction was quenched with H_2O, extracted twice with ethyl acetate, once with brine, dried over Na_2SO_4 and the solvent was removed under reduced pressure. The crude product was purified by two columns (solvents Cy/EtOAc 1st 2/3, 2nd 1/1) to give the product **44** in 12% yield.

^{1}H NMR (400 MHz, Chloroform-*d*) δ 8.03 (t, *J* = 1.8 Hz, 1H), 7.90 – 7.87 (m, 1H), 7.62 (t, *J* = 1.7 Hz, 1H), 4.81 (s, 0H), 4.74 (d, *J* = 4.3 Hz, 2H), 4.68 (d, *J* = 4.1 Hz, 1H), 4.61 (s, 0H), 3.91 – 3.86 (m, 2H), 3.61 – 3.56 (m, 2H), 3.38 (s, 3H), 1.35 (s, 9H).

(3-(*tert*-Butyl)-5-((1-(2-nitrophenyl)ethoxy)methyl)phenyl)methanol (**45**)

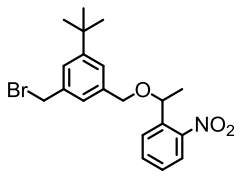

$C_{20}H_{24}BrNO_3$
406.32g/mol

2410 mg **37** (7.53 mmol, 1.0 eq) was dissolved in dry THF in a brown round bottle flask. NaH (361 mg, 9.03 mmol, 1.2 eq) was added ant the reaction mixture was stirred for 10 minutes before 1-(2-nitrophenyl)ethan-1-ol (881 mg, 5.27 mmol, 0.7 eq) was added. The mixture was stirred at room temperature for 20 hours away from light. The reaction was quenched with water and extracted with ethyl acetate. The combined organic fraction was dried over Na_2SO_4 and the solvent was removed under reduced pressure. The crude product was purified by column chromatography (Cy/EtOAc 9/1) with product **45** up to 50% yield.

^{1}H NMR (400 MHz, Chloroform-*d*) δ 7.91 (dd, *J* = 8.2, 1.3 Hz, 1H), 7.85 (dd, *J* = 7.9, 1.5 Hz, 1H), 7.67 (td, *J* = 7.7, 1.3 Hz, 1H), 7.43 (ddd, *J* = 8.0, 7.3, 1.5 Hz, 1H), 7.31 (t, *J* = 1.8 Hz, 1H), 7.20 (t, *J* = 1.7 Hz, 1H), 7.15 (d, *J* = 1.7 Hz, 1H), 5.11 (q, *J* = 6.3 Hz, 1H), 4.39 – 4.29 (m, 2H), 1.58 (d, *J* = 6.3 Hz, 3H), 1.30 (s, 9H).

^{13}C NMR (101 MHz, $CDCl_3$) δ 152.13, 139.81, 138.21, 137.70, 133.71, 128.20, 128.04, 125.69, 125.06, 124.30, 73.06, 71.39, 34.82, 34.11, 31.37, 23.81.

MS (DART-EI) *m/z* (%): 424.9 $[M+NH_4]^+$.

(((3-((Benzyloxy)methyl)-5-(*tert*-butyl)benzyl)oxy)methanetriyl)tribenzene (**46**)

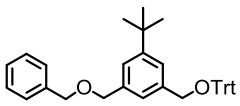

$C_{38}H_{38}O_2$
526.72g/mol

Benzyl alcohol (80.7 mg, 0.74 mmol, 1.2 eq), building block **38** (310 mg, 0.62 mmol, 1.0 eq) and NaH (37 mg, 0.93 mmol, 1.5 eq) were dissolved in 10 ml dry THF. The mixture was heated to reflux for 24 h. After cooling to room temperature the reaction was quenched with water and extracted with MTBE tree times. The organic fraction was dried over Na_2SO_4 and then the solvent was removed under reduced pressure. The crude product was purified by column chromatography using Cy/EtOAc 5/1 as solvent to give the product **46** as white solid in 87%.

^{1}**H-NMR** ($CDCl_3$, 400 MHz):7.51- 7.54 (m, 6 H),7.23-7.34 (m, 17 H),4.62 (s, 2 H),4.24 (s, 2 H),1.37 (s, 9 H).

^{13}**C-NMR** ($CDCl_3$, 100 MHz):128.80, 128.32,127.87,126.81, 123.62,123.42, 72.51,72.05,66.13,31.67.

(3-((Benzyloxy)methyl)-5-(*tert*-butyl)phenyl)methanol (**47**)

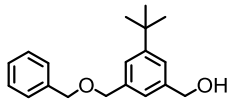

C19H24O2
284.40 g/mol

Methode a) starting from **39**

1240 mg **39** (6.38 mmol, 2 eq) was placed in a round bottom flask and dissolved in 30 ml dry THF and the degassed for 10 minutes. NaH (511 mg, 12.8 mmol, 4 eq) was added and the mixture flask was wrapped in aluminium foil before **55** (837 mg, 3.19 mmol, 1 eq) was added. The reaction mixture was stirred at room temperature for 16 hours before it was quenched by the addition of water and extracted with ethyl acetate. The combined organic fraction was washed with brine and dried over Na_2SO_4 and the solvent was removed under reduced pressure. The crude product was purified by column chromatography using Cy/EtOAc 2/1 as solvent to give the product **47** as colorless liquid in 37% yield.

Methode b) starting from **46**

500 mg of **46** (0.94 mmol, 1.0 eq) was dissolved in 20 ml CH_2Cl_2. Triethylsilane (0.6 ml, 3.8 mmol, 4.0 eq) and trifluoroacetic acid (3.8 ml, 3.8 mmol, 4.0 eq) were added to the solution and the reaction mixture was stirred for 2 hours at room temperature. The reaction was quenched with $NaHCO_3$ and extracted with CH_2Cl_2. The organic fraction was washed with brine and dried over Na_2SO_4 before the solvent was removed under reduced pressure and the crude product was purified by column chromatography (Cy/EtOAc 9/1). The product **47** was obtained in 59% as colorless liquid.

^{1}H NMR (400 MHz, Chloroform-d) δ 7.40 – 7.28 (m, 7H), 7.21 (d, J = 0.7 Hz, 1H), 4.69 (s, 2H), 4.57 (d, J = 8.6 Hz, 4H), 1.34 (s, 9H).

^{13}C NMR (101 MHz, CDCl3) δ 151.90, 140.87, 138.38, 128.54, 127.99, 127.79, 124.37, 123.87, 123.56, 72.48, 72.40, 65.77, 34.87, 31.52.

MS (ESI-DI) *m/z* (%): 323.1 $[M+K]^+$.

MS (DART-EI) *m/z* (%): 302.0 $[M+NH_4]^+$, 586.3 $[2M+NH_4]^+$.

EA: calc.: C 80.24%, H 8.51%, O 11.25%; found: C 79.93%, H 8.58%, N 0.00%.

(((3-(((3-((Benzyloxy)methyl)-5-(*tert*-butyl)benzyl)oxy)methyl)-5-(*tert*
butyl)benzyl)oxy)methanetriyl)tribenzene (**48**)

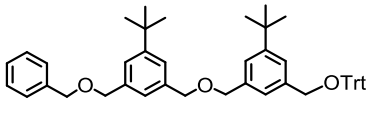

$C_{50}H_{54}O_3$
702.98g/mol

Monomer alcohol (**47**, 372 mg, 1.31 mmol, 1.0 eq), building block **38** (654 mg, 1.31 mmol, 1.0 eq) and NaH (68 mg, 1.7 mmol, 1.3 eq) were dissolved in 30 ml dry THF. The mixture was heated to reflux for 24 h. After cooling to room temperature the reaction was quenched with water and extracted with MTBE tree times. The organic fraction was dried over Na_2SO_4 and then the solvent was removed under reduced pressure. The crude product was purified by column chromatography using Cy/EtOAc 8/1 as solvent to give the product **48** as waxy white solid in 72% yield.

^{1}H NMR (400 MHz, Chloroform-*d*) δ 7.55 – 7.50 (m, 6H), 7.36 – 7.19 (m, 20H), 4.56 (dd, *J* = 14.3, 2.1 Hz, 8H), 4.18 (s, 2H), 1.32 (d, *J* = 4.4 Hz, 18H).

^{13}C NMR (101 MHz, $CDCl_3$) δ 151.69, 151.42, 144.33, 139.06, 138.49, 138.33, 138.19, 138.09, 128.91, 128.53, 127.99, 127.97, 127.74, 127.13, 124.74, 124.34, 124.31, 123.86, 123.79, 123.55, 87.15, 72.67, 72.55, 72.53, 72.32, 66.14, 34.84, 31.55.

(3-(((3-((Benzyloxy)methyl)-5-(*tert*-butyl)benzyl)oxy)methyl)-5-(*tert*-butyl)phenyl)methanol (**49**)

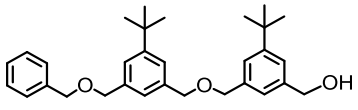

$C_{31}H_{40}O_3$
460.66g/mol

667 mg of **48** (0.95 mmol, 1.0 eq) was dissolved in 15 ml CH_2Cl_2. Triethylsilane (0.23 ml, 1.42 mmol, 1.5 eq) and trifluoroacetic acid (0.14 ml, 1.9 mmol, 2.0 eq) were added to the solution and the reaction mixture was stirred for 2 hours at room temperature. The reaction was quenched with $NaHCO_3$ and extracted with CH_2Cl_2. The organic fraction was washed with brine and dried over Na_2SO_4 before the solvent was removed under reduced pressure. The crude product was purified by column chromatography and yielded the product **49** as colorless oil in 56%.

^{1}H NMR (400 MHz, Chloroform-*d*) δ 7.39 – 7.26 (m, 9H), 7.19 (d, *J* = 1.8 Hz, 2H), 4.67 (s, 2H), 4.58 – 4.54 (m, 8H), 1.33 (d, *J* = 1.1 Hz, 18H).

^{13}C NMR (101 MHz, $CDCl_3$) δ 151.91, 151.69, 140.87, 138.46, 138.42, 138.20, 138.16, 128.54, 128.00, 127.77, 124.78, 124.39, 124.37, 123.95, 123.54, 72.61, 72.52, 72.48, 72.34, 65.78, 34.87, 34.84, 31.53.

(((3-(((3-(((3-((Benzyloxy)methyl)-5-(*tert*-butyl)benzyl)oxy)methyl)-5-(*tert*-butyl)benzyl)oxy)methyl)-5-(*tert*-butyl)benzyl)oxy)methanetriyl)tribenzene (**50**)

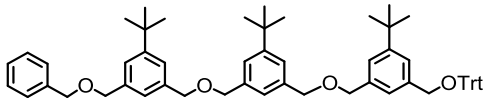

$C_{62}H_{70}O_4$
879.24g/mol

Dimer alcohol (**49**) (169 mg, 0.37 mmol, 1.0 eq), building block **38** (202 mg, 0.40 mmol, 1.0 eq) and NaH (19 mg, 0.48 mmol, 1.3 eq) were dissolved in 30 ml dry THF. The mixture was heated to reflux for 24 h. After cooling to room temperature the reaction was quenched with water and extracted with MTBE tree times. The organic fraction was washed with brine and dried over Na_2SO_4 and then the solvent was removed under reduced pressure. The crude product was purified by column chromatography using Cy/EtOAc 12/1 as solvent to give the product **50** as white solid in 59 % yield.

^{1}H NMR (400 MHz, Chloroform-*d*) δ 7.56 – 7.49 (m, 8H), 7.39 – 7.16 (m, 21H), 4.61 – 4.46 (m, 12H), 4.20 (d, *J* = 4.5 Hz, 2H), 1.35 – 1.29 (m, 27H).

^{13}C NMR (101 MHz, $CDCl_3$) δ 151.86, 151.68, 151.66, 140.89, 138.42, 138.40, 138.21, 138.17, 138.12, 128.52, 127.98, 127.74, 124.82, 124.76, 124.35, 123.93, 123.51, 84.53, 72.59, 72.54, 72.51, 72.49, 72.30, 65.71, 65.37, 34.85, 34.82, 31.53, 31.52.

(3-(((3-(((3-((Benzyloxy)methyl)-5-(*tert*-butyl)benzyl)oxy)methyl)-5-(*tert*-butyl)benzyl)oxy)methyl)-5-(*tert*-butyl)phenyl)methanol (**51**)

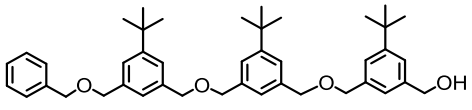

$C_{43}H_{56}O_4$
636.92g/mol

Methode a) starting from **50**

100 mg of **50** (0.11 mmol, 1.0 eq) was dissolved in 15 ml CH_2Cl_2. Triethylsilane (37 µl, 0.23 mmol, 2.0 eq) and trifluoroacetic acid (17 µl, 0.23 mmol, 2.0 eq) were added to the solution and the reaction mixture was stirred for 2 hours at room temperature. The reaction was quenched with $NaHCO_3$ and extracted with CH_2Cl_2. The organic fraction was washed with brine and dried over Na_2SO_4 before the solvent was removed under reduced pressure and the crude product was purified by column chromatography to give the product **51** in 30% yield as colorless liquid.

Methode b) starting from **54**

115 mg Diol-trimer **54** (0.21 mmol, 1.4 eq) was dissolved in dry THF, degassed for 10 minutes by bubbling argon through. NaH (12 mg, 0.3 mmol, 2.0 eq) was added and the mixture was stirred for 15 minutes before **55** (39 mg, 0.15 mmol, 1.0 eq) was added. The reaction mixture was stirred at room temperature over night. It was quenched with water before the aqueous phase was extracted with ethyl acetate. The combined organic fraction was washed with brine and dried over Na_2SO_4 and the solvent removed under reduced pressure. The crude product was purified by column chromatography using Cy/EtOAc 4/1 to give the product **51** as slightly yellow liquid in 58% yield.

^{1}H NMR (400 MHz, Chloroform-d) δ 7.38 – 7.30 (m, 11H), 7.20 (s, 3H), 4.67 (s, 2H), 4.56 (d, J = 2.2 Hz, 12H), 1.33 (d, J = 1.4 Hz, 27H).

^{13}C NMR (101 MHz, CDCl3) δ 151.91, 151.71, 151.69, 140.87, 138.47, 138.43, 138.24, 138.19, 138.15, 129.96, 129.16, 128.78, 128.68, 128.53, 128.11, 128.00, 127.76, 124.84, 124.78, 124.40, 124.38, 123.96, 123.55, 72.63, 72.57, 72.54, 72.52, 72.51, 72.33, 72.02, 65.78, 34.84, 31.55, 31.53.

MS (DART-EI) *m/z* (%): 654.4 $[M+NH_4]^+$.

EA calc: C 81.09%, H 8.86%, N 0.0 %; found: C 80.71 %, H 9.07 %, N 0.31 %.

(5-(*tert*-Butyl)-1,3-phenylene)bis(methylene) bis(4-methylbenzenesulfonate) (**53**)

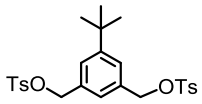

$C_{26}H_{30}O_6S_2$
502.64g/mol

The dialcohol (**39**) (2 g, 10.3 mmol, 1 eq) was dissolved in dry THF under argon atmosphere. NaH (1.24 g, 30.9 mmol, 3.0 eq) was added to the diol solution and the mixture was stirred for some minutes than cooled to 0°C. p-Tosylsulfonyl chloride (4.3, 22.6 mmol, 2.2 eq) dissolved in 20mL dry THF was added over 20 min. The reaction mixture was stirred overnight, quenched with cold H_2O, extracted with Et_2O, washed with brine and dried over Na_2SO_4. The solvent was removed under reduced pressure and the residue was recrystallized from pentane and ethyl acetate to give the product **53** as white solid in 88% yield

mp: 97°C (decomposition)

^{1}H NMR (400 MHz, Chloroform-*d*) δ 7.79 – 7.74 (m, 4H), 7.35 – 7.29 (m, 4H), 7.16 (d, *J* = 1.6 Hz, 2H), 6.91 (s, 1H), 4.99 (s, 4H), 2.44 (s, 6H), 1.21 (s, 9H).

^{13}C NMR (101 MHz, $CDCl_3$) δ 152.36, 144.89, 133.51, 133.25, 129.87, 127.94, 126.23, 125.86, 71.78, 34.68, 31.10, 21.64.

MS (DART-EI) *m/z* (%): 520.0 $[M+NH_4]^+$, 1022.4 $[2M+NH_4]^+$.

(((((5-(*tert*-Butyl)-1,3-phenylene)bis(methylene))bis(oxy))bis(methylene))bis(3-(*tert*-butyl)-5,1-phenylene))dimethanol (**54**)

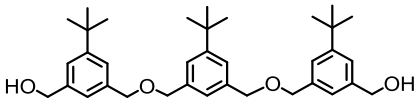

$C_{36}H_{50}O_4$
546.79g/mol

1319 mg Dialcohol **39** (6.79 mmol, 10 eq) was dissolve in 50 ml dry THF and degassed for 10 min. NaH (326 mg, 8.15 mmol, 12 eq) was added and the solution was stirred at room temperature for 10 minutes. Ditosyl **53** (341 mg, 0.68 mmol, 1 eq) was dissolved in 10 ml dry THF and added via a dropping funnel over 10 minutes. The mixture was stirred at room temperature for 16 hours. Water was added and the aqueous solution was extracted with ethyl acetate and the combined organic fraction was washed with brine and dried over Na_2SO_4 before the solvent was removed under reduced pressure. The crude product was purified by column chromatography (Cy/EtOAc 4/1) to give the product **53** as colorless oil in 60% yield.

^{1}H NMR (400 MHz, Chloroform-d) δ 7.32 (dd, J = 2.1, 0.9 Hz, 6H), 7.23 – 7.15 (m, 3H), 4.66 (s, 4H), 4.56 (d, J = 2.9 Hz, 8H), 1.33 (d, J = 2.5 Hz, 27H).

^{13}C NMR (101 MHz, CDCl3) δ 151.94, 140.90, 138.49, 138.23, 124.43, 124.40, 123.98, 123.58, 72.65, 72.55, 65.81, 34.89, 31.56, 31.54.

MS (ESI-DI) *m/z* (%): 585.3 $[M+K]^+$.

HRMS (ESI *m/z*): 569.36 $[M+Na]^+$, 585.33 $[M+K]^+$, 1125.73$[2M+Na]^+$,1131.70 $[2M+K]^+$.

MS (DART-EI) *m/z* (%): 564.3 $[M+NH_4]^+$, 1110.7, 1111.7 $[2M+NH_4]^+$.

EA calc: C 78.96%, H 9.67%, O 11.37%; found: C 79.08%, H 9.22%, N 0.00 %

Benzyl 4-methylbenzenesulfonate (**55**)

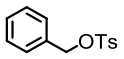

$C_{14}H_{14}O_3S$
262.32g/mol

Benzyl alcohol (1.0 ml, 9.63 mmol, 1 eq) was, together with NaH (0.58 g, 14.5 mmol, 1.5 eq), dissolved in dry THF (10 ml) and stirred at room temperature. p-Toluolsulfonyl chloride (2.2 g, 11.6 mmol, 1.2 eq) was dissolved in 15 ml dry THF and added to the stirred solution with a dropping funnel over 30 minutes. The reaction mixture was stirred for 2 h at room temperature before it was quenched with water and extracted with ethyl ether. The organic fraction was dried over Na_2SO_4 and the solvent was distilled off under reduced pressure to give the desired product **55** as white solid in quant. yield.

mp: 72-75°C (Lit: 54-55°C)

^{1}H NMR (400 MHz, Chloroform-d) δ 7.80 (d, J = 8.3 Hz, 2H), 7.35 – 7.29 (m, 5H), 7.26 – 7.23 (m, 2H), 5.05 (s, 2H), 2.44 (s, 3H).

^{13}C NMR (101 MHz, $CDCl_3$) δ 144.92, 133.40, 129.95, 129.14, 128.76, 128.66, 128.08, 72.02, 21.77.

MS (DART-EI) *m/z* (%): 279.8 $[M+NH_4]^+$, 542.1 $[2M+NH_4]^+$.

1-((Benzyloxy)methyl)-3-(((3-(bromomethyl)-5-(*tert*-butyl)benzyl)oxy)methyl)-5-(*tert*-butyl)benzene (**56**)

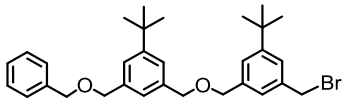

$C_{31}H_{39}BrO_2$
523.55g/mol

Monomer alcohol **47** (100 mg, 0.35 mmol, 1.0 eq) was dissolved in 10 ml dry THF. NaH (28.1 mg, 0.70 mmol, 2.0 eq) was added and the mixture was stirred for 10 minutes at room temperature. 450.0 mg **37** (1.41 mmol, 4.0 eq) was added and the reaction mixture was heated up to reflux for 24 hours before cooled down to room temperature. After quenching with H_2O and extracting with CH_2Cl_2 the combined organic fraction was washed with brine and dried over Na_2SO_4 and the solvent was removed under reduced pressure. The product was purified by column chromatography using Cy/ EtOAc 12/1 as solvent. The product **56** was yielded as colorless liquid in 77% yield.

^{1}H NMR (400 MHz, Chloroform-d) δ: 7.40 – 7.27 (m, 9H), 7.23 (s, 1H), 7.20 (s, 1H), 4.59 – 4.54 (m, 7H), 4.50 (s, 2H), 4.49 (s, 1H), 1.33 (d, J = 4.7 Hz, 18H).

^{13}C NMR (101 MHz, CDCl3) δ: 152.15, 151.74, 138.80, 138.45, 138.22, 138.09, 137.66, 128.55, 128.00, 127.77, 125.82, 125.53, 125.13, 124.78, 124.43, 124.39, 72.67, 72.53, 72.37, 72.18, 34.88, 34.86, 34.20, 31.55, 31.45.

MS (DART-EI) *m/z* (%): 540.2, 542.1 $[M+NH_4]^+$, 1062.5, 1064.3 $[2M+NH_4]^+$.

8.3.2 Branched Ligands

Branched 2 ligand (**58**)

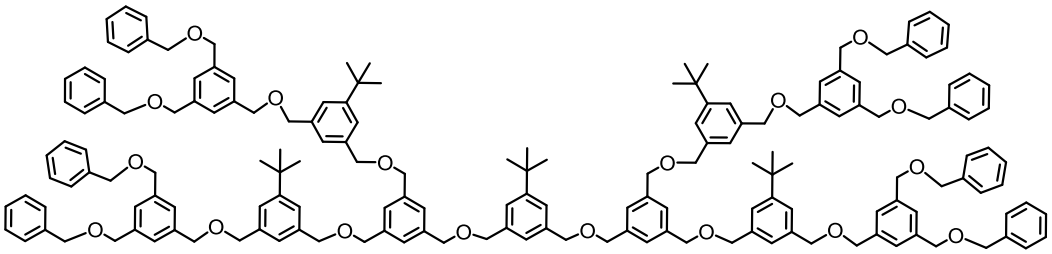

$C_{170}H_{190}O_{18}$
2521.37g/mol

39 (4.51 mg, 0.23 mmol, 1.0 eq) placed in a round bottom flask and put under argon atmosphere. Dry THF (10 ml) and NaH (2.32 mg, 0.058 mmol, 2.5 eq) were added and the mixture was stirred for 10 minutes before **63** (57.8 mg, 0.046 mmol, 2.0 eq) was added and the mixture was heated to reflux for 18 h. After cooling to room temperature the reaction was quenched with water and extracted 3 times with ethyl acetate. The combined organic fraction was washed with brine and dried over Na_2SO_4 and the solvent was removed under reduced pressure. The crude product was purified by column chromatography using Cy/EtOAc 5/1 as solvent. The product **58** was yielded in 21% as colorless liquid.

^{1}H NMR (400 MHz, Chloroform-d) δ 7.39 – 7.27 (m, 68H), 7.18 (s, 5H), 4.56 (d, *J* = 1.8 Hz, 76H), 1.31 (d, *J* = 1.2 Hz, 45H).

MS (MALDI-ToF) *m/z*: 2538.4 $[M+NH_4)]^+$.

((((5-(Bromomethyl)-1,3-phenylene)bis(methylene))bis(oxy))bis(methylene))dibenzene (**60**)

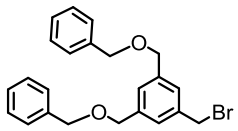

$C_{23}H_{23}BrO_2$
411.34g/mol

1,3,5-Tris(bromomethyl)benzene (**59**) (1501 mg, 4.08 mmol, 1.0 eq) and benzyl alcohol (884 mg, 8.16 mmol, 2.0 eq) were dissolved in dry THF and put under argon. Sodium hydride (490 mg, 12.2 mmol, 3.0 eq) was added and the reaction mixture was heated to reflux over night. After cooling to room temperature the reaction was quenched with water and extracted 3 times with CH_2Cl_2. The combined organic fraction was washed with brine and dried over Na_2SO_4 and the solvent was removed under reduced pressure. The crude product was purified by column chromatography using Cy/EtOAc 8/1 as solvent. The product **60** was yielded in 41% as colorless liquid.

^{1}H NMR (400 MHz, Chloroform-*d*) δ 7.39 – 7.27 (m, 13H), 4.58 (s, 4H), 4.55 (s, 4H), 4.50 (s, 2H).

^{13}C NMR (101 MHz, $CDCl_3$) δ 139.39, 138.16, 128.59, 127.99, 127.88, 127.66, 127.11, 72.56, 71.78, 33.48.

MS (DART-EI) *m/z* (%): 429.9 $[M+NH_4]^+$, 838.1 $[2M+NH_4]^+$.

Branched 1 ligand (**61**)

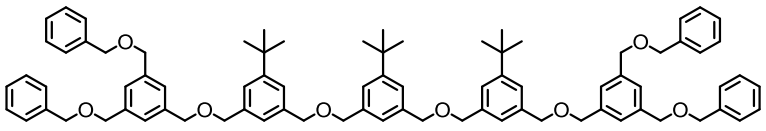

$C_{82}H_{94}O_8$
1207.65g/mol

54 (23 mg, 0.04 mmol, 1 eq) placed in a round bottom flask and put under argon atmosphere. Dry THF (5 ml) and NaH (4 mg, 0.11 mmol, 2.5 eq) were added and the mixture was stirred for 10 minutes before **60** (35 mg, 0.08 mmol, 2.0 eq) was added and the mixture was heated to reflux for 18 h. After cooling to room temperature the reaction was quenched with water and extracted 3 times with ethyl acetate. The combined organic fraction was washed with brine and dried over Na_2SO_4 and the solvent was removed under reduced pressure. The crude product was purified by column chromatography using Cy/EtOAc 5/1 as solvent. The product **61** was yielded in 21% as colorless liquid.

^{1}H NMR (400 MHz, Chloroform-d) δ 7.38 – 7.27 (m, 32H), 7.18 (s, 3H), 4.56 (d, *J* = 1.7 Hz, 32H), 1.31 (s, 27H).

^{13}C NMR (101 MHz, $CDCl_3$) δ 151.71, 138.91, 138.87, 138.34, 138.29, 138.25, 138.10, 128.55, 127.95, 127.79, 126.61, 124.79, 124.34, 72.57, 72.44, 72.14, 34.85, 31.56.

MS (MALDI-ToF) *m/z*: 889.8 $[M\text{-}(C_{23}H_{23}O_2\text{+}NH_4)]^+$ 1231 $[M\text{+}Na]^+$, 1247 $[M\text{+}K]^+$.

(3-(((3,5-Bis((benzyloxy)methyl)benzyl)oxy)methyl)-5-(*tert*-butyl)phenyl)methanol (**62**)

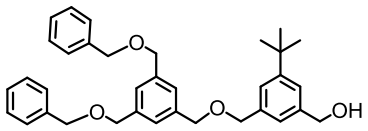

$C_{35}H_{40}O_4$
524.70g/mol

132 mg **60** (0.32 mmol, 1.0 eq) and 112 mg **39** (0.58 mmol, 1.8 eq) were dissolved in dry THF and degassed for 10 minutes. NaH (25 mg, 0.64 mmol, 2.0 eq) was added and the reaction mixture was heated to reflux over night. After cooling to room temperature the reaction was quenched with water and extracted 3 times with ethyl acetate. The combined organic fraction was washed with brine and dried over Na_2SO_4 and the solvent was removed under reduced pressure. The crude product was purified by column chromatography suing Cy/EtOAc 2/1 as solvent. The product **62** was yielded in 49% as colorless liquid.

^{1}H NMR (400 MHz, Chloroform-*d*) δ 7.37 – 7.28 (m, 15H), 7.19 (s, 1H), 4.66 (s, 2H), 4.56 (dt, *J* = 4.7, 2.3 Hz, 12H), 1.32 (d, *J* = 1.3 Hz, 9H).

^{13}C NMR (101 MHz, $CDCl_3$) δ 151.92, 140.92, 138.87, 138.34, 138.32, 128.56, 127.97, 127.81, 126.65, 126.55, 124.43, 123.97, 123.60, 72.64, 72.47, 72.24, 72.12, 65.78, 34.88, 31.53.

MS (DART-EI) *m/z* (%): 542.2 $[M+NH_4]^+$, 1066.5 $[2M+NH_4]^+$.

EA calc: C 80.12%, H 7.68 %, O 12.20%; found: C 80.07 %, H 7.62 %, N 0.00 %

Half branched 2 ligand (**63**)

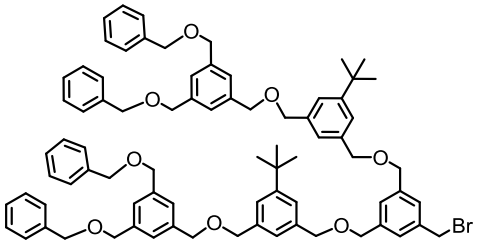

$C_{79}H_{87}BrO_8$
1244.46g/mol

59 (132 mg, 0.37 mmol, 1.0 eq) and **62** (387 mg, 0.74 mmol, 2.0 eq) were dissolved in dry THF and put under argon. NaH (34 mg, 0.85 mmol, 2.3 eq) was added and the reaction mixture was heated to reflux over night. After cooling to room temperature the reaction was quenched with water and extracted 3 times with ethyl acetate. The combined organic fraction was washed with brine and dried over Na_2SO_4 and the solvent was removed under reduced pressure. The crude product was purified by column chromatography using Cy/EtOAc 5/1 as solvent. The product **63** was yielded in 28% as colorless liquid and the product **64** in 12%

63

^{1}H NMR (400 MHz, Chloroform-*d*) δ 7.38 – 7.27 (m, 32H), 7.19 (s, 2H), 4.53 (s, 32H), 4.46 (s, 2H), 1.32 (s, 18H).

^{13}C NMR (101 MHz, $CDCl_3$) δ 151.75, 139.42, 138.87, 138.33, 138.18, 137.97, 128.55, 127.94, 127.78, 127.71, 126.60, 126.52, 124.80, 124.46, 72.82, 72.67, 72.44, 72.22, 72.12, 71.83, 34.85, 31.55, 27.06.

1,3,5-Tris(((3-(((3,5-bis((benzyloxy)methyl)benzyl)oxy)methyl)-5-(*tert*-butyl)benzyl)oxy)methyl)benzene (**64**)

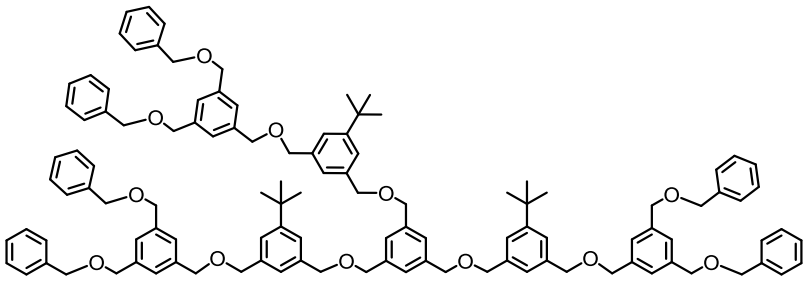

$C_{114}H_{126}O_{12}$
1688.25g/mol

59 (132 mg, 0.37 mmol, 1.0 eq) and **62** (387 mg, 0.74 mmol, 2.0 eq) were dissolved in dry THF and put under argon. NaH (34 mg, 0.85 mmol, 2.3 eq) was added and the reaction mixture was heated to reflux over night. After cooling to room temperature the reaction was quenched with water and extracted 3 times with ethyl acetate. The combined organic fraction was washed with brine and dried over Na_2SO_4 and the solvent was removed under reduced pressure. The crude product was purified by column chromatography using Cy/EtOAc 5/1 as solvent. The product **63** was yielded in 28% as colorless liquid and the product **64** in 12%

64

^{1}H NMR (400 MHz, Chloroform-*d*) δ 7.38 – 7.26 (m, 48H), 7.18 (d, *J* = 1.5 Hz, 3H), 4.55 (q, *J* = 2.1 Hz, 48H), 1.30 (s, 27H).

^{13}C NMR (101 MHz, $CDCl_3$) δ 151.68, 138.90, 138.86, 138.34, 138.13, 128.54, 127.94, 127.78, 126.67, 126.60, 126.50, 124.76, 124.37, 72.75, 72.68, 72.43, 72.25, 72.18, 72.12, 34.83, 31.54.

3-(*tert*-Butyl)-5-(hydroxymethyl)benzyl 4-methylbenzenesulfonate (**65**)

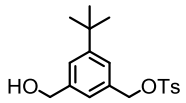

$C_{19}H_{24}O_4S$
348.46g/mol

39 (93 mg, 0.48 mmol, 1.0 eq) was dissolved in 5 ml dry THF and cooled to –40°C. NaH (19 mg, 0.48 mmol, 1.0 eq) was added and the reaction mixture was stirred for 10 minutes. p-Toluenesulfonyl chloride (92 mg, 0.48 mmol, 1.0 eq) was dissolved in dry THF and added to the stirred reaction mixture and slowly warmed to room temperature. After stirring for 5 hours the reaction mixture was quenched with water and extracted 3 times with ethyl acetate. The combined organic fraction was washed with brine and dried over Na_2SO_4 and the solvent was removed under reduced pressure. The crude product **65** was purified by column chromatography.

1-(Bromomethyl)-3-(*tert*-butoxymethyl)-5-(*tert*-butyl)benzene (**66**)

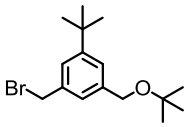

$C_{16}H_{25}BrO$
313.28g/mol

37 (301 mg, 0.94 mmol, 1.0 eq) was dissolved in 5 ml dry DMF and stirred at room temperature. Potassium *tert*-butoxide (108 mg, 0.94 mmol, 1.0 eq) was added and the mixture was stirred at room temperature for 2 hours. The reaction was quenched with H_2O, extracted twice with CH_2Cl_2 and once with brine, dried over Na_2SO_4 and the solvent was removed under reduced pressure. The crude product was purified by column chromatography (Pentane/EtOAc 50/1) to yield the product **66** in 43%.

^{1}H NMR (400 MHz, Methylene Chloride-d2) δ 7.34 – 7.28 (m, 2H), 7.22 (t, *J* = 1.7 Hz, 1H), 4.54 (s, 2H), 4.42 (d, *J* = 0.8 Hz, 2H), 1.34 (d, *J* = 1.4 Hz, 9H), 1.29 (s, 9H).

^{13}C NMR (101 MHz, $CDCl_3$) δ 151.83, 140.21, 137.47, 125.51, 125.14, 124.86, 73.62, 64.26, 34.83, 34.41, 31.44, 27.85.

5,5'-((((5-(*tert*-Butyl)-1,3-phenylene)bis(methylene))bis(oxy))bis(methylene))bis(1-(*tert*-butyl)-3-((1-(2-nitrophenyl)ethoxy)methyl)benzene) (**67**)

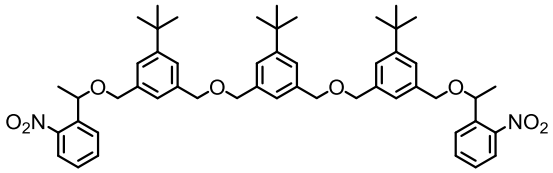

$C_{52}H_{64}N_2O_8$
845.09g/mol

37 (45 mg, 0.23 mmol, 1.0 eq) and NaH (21 mg, 0.53 mmol, 2.3 eq) were dissolved in 6 ml dry THF and stirred for 5 minutes. **45** (188 mg, 0.46 mmol, 2.0 eq) was added and the reaction mixture was stirred at 60°C for 8 hours. After cooling to room temperature the reaction was quenched with water. The aqueous phase was extracted 3 times with ethyl acetate. The combined organic layer was washed with brine and dried over Na_2SO_4 before the solvent was removed under reduced pressure. The crude product was purified using Cy/EtOAc 9/1 and yielded 11% of product **67**.

^{1}H NMR (400 MHz, Chloroform-*d*) δ 7.94 – 7.81 (m, 5H), 7.72 – 7.60 (m, 3H), 7.55 (t, *J* = 1.8 Hz, 1H), 7.48 – 7.39 (m, 2H), 7.35 – 7.30 (m, 2H), 7.23 – 7.10 (m, 3H), 5.12 (dd, *J* = 12.4, 6.2 Hz, 2H), 4.60 (d, *J* = 11.6 Hz, 2H), 4.55 (s, 2H), 4.40 – 4.29 (m, 3H), 1.60 (d, *J* = 6.3 Hz, 5H), 1.38 – 1.29 (m, 27H).

8.4 AuNP Experiments

8.4.1 Au_{144}Pure Hexylthiol and Mixed Ligands

Hexylthiol Au_{144}

Au_{144}NPs where successfully synthesized according to literature[188].

$HAuCl_4$ (118 mg, 0.35 mmol, 1.0 eq) and TOABr (232 mg, 0.42 mmol, 1.2 eq) were dissolved in 15 ml MeOH and stirred at rt for 15 minutes. Hexanthiol (270 µl, 1.74 mmol, 5.3 eq) was added and after an additional stirring time of 3-5 minutes $NaBH_4$ (131 mg, 3.47 mmol, 10 eq) dissolved in water was added to form NPs. The reaction mixture turned black immediately and was stirred at room temperature for 4 hours. The particles were collected and concentrated at room temperature. To remove the excess hexylthiol the residue was suspended in methanol and centrifuged at 4000 rpm for 10 minutes. This was repeated 4 times. The precipitate was dissolved in acetone and centrifuged. The supernatant was containing the Au_{25} particles. The pellet was suspended in CH_2Cl_2 and centrifuged. This supernatant was containing mainly Au_{144} particles. The third and minor fraction contained particles bigger than 2 nm and was obtained by extracting with pentane or heptane.

The obtained fractions were dried and analyzed by TEM, UV/Vis and NMR.

Au_{144} mixed ligands

$HAuCl_4$ (226 mg, 0.66 mmol, 1.0 eq) and TOABr (396 mg, 0.71 mmol, 1.07 eq) were dissolved in 15 ml DCM and stirred at rt for 5 minutes. Ligand **1** (132 mg, 0.74 mmol, 1.06 eq) was added and the mixture was stirred for 10 minutes. $NaBH_4$ (251 mg, 6.64 mmol, 10 eq) dissolved in water and hexanthiol (413 µl, 2.82 mmol, 4.24 eq) were added at the same time. The reaction mixture turned black within a view seconds and was stirred at room temperature for 4 hours. The particles were collected and concentrated at room temperature. To remove the excess ligands the residue was suspended in methanol and centrifuged at 4000 rpm for 10 minutes. This was repeated 4 times. The precipitate was dissolved in acetone and centrifuged. The supernatant was containing the Au_{25} particles. The pellet was suspended in CH_2Cl_2 and centrifuged. This supernatant was containing mainly Au_{144} particles. The third and minor fraction contained particles bigger than 2 nm and was obtained by extracting with pentane or heptane.

Yield: Au_{25} 12.2 mg. = 9%

Au_{144} 115.6 mg = 88%

The obtained fractions were dried and analyzed by TEM, UV/Vis, NMR, (TGA just Au_{144}) and MALDI-ToF MS.

8.4.2 F-Alkyl protected AuNPs[210]

$HAuCl_4$ (309 mg, 0.91 mmol, 1 eq) and F-octanethiol (427 µl, 1.82 mmol, 2.0 eq) were dissolved in 10 ml EtOH and stirred for 10 minutes. 3 eq $NaBH_4$ (103 mg, 2.73 mmol) was dissolved in water and added at once. The solution turned black and was stirred for 3 hours at room temperature. The formed NPs precipitated out of the solution and where collected. The particles where washed with water, EtOH and cold and hot $CHCl_3$ by sonication and centrifugation until the supernatant stayed colorless. The particles were obtained as black powder in 66% yield (226mg) calculated to pure gold.

The obtained fractions were dried and analyzed by TEM, UV/Vis, NMR, TGA and MALDI-ToF MS.

8.4.3 Acetylene ligands

Au:PVP[235,236]

$HAuCl_4$ (80 mg, 0.235 mmol, 1 eq) and 8558 mg PVP (100 eq calculated on monomeric units) with a molecular weight of 40kDa were dissolved in water 250 mL water and stirred for 30 minutes at 0°C. An aqueous solution of $NaBH_4$ (92.85 mg, 2.35 mmol, 10 eq) was added ad once. This reaction mixture was stirred for 30 minutes, after that it was freezed with liquid nitrogen and dried by lyophilization. The NPs were yielded as brownish powder due to the excess of PVP. No yield is given due to the lag of purification.

Exchange with acetylene[40,226]

The reaction conditions were kept constant for all exchange reactions with PVP stabilized AuNPs.

The freeze-dried particles were redissolved in NonoPure water and an excess of the free acetylene ligand was dissolved in toluene. The acetylene ligand has to be added in excess referred to the NPs. Both solutions were mixed and heated up to 60°C under vigorous stirring for 2 hours. The phases were separated, dried and further analyzed.

Inverse acetylene exchange

6 mg (0.16 µmol Au, 1 eq) of the Au-PVP lyophilisate was dissolved in 1 ml pure water. Pyridine acetylene-TMS ligand **23** (15.2 mg, 58.6 µmol, 360 eq) was dissolved in 2 ml toluene and added to the aqueous solution. The mixture was under vigorous stirring heated to 60°C for 8 hours.

After that time the phases were separated and the organic phase was dried. No exchange occurred in this reaction. The water phase did not lose any color and also the organic phase stayed the same.

8.5 Ag and PdNPs Experiments

Formation of NPs stabilized by Oxygen Ligands, General Procedure

The synthesis of the NPs was carried out with respect to the number *n* of ether moieties present in the ligand. *n* eq of the metal salt ($AgNO_3$ or K_2PdCl_4) was dissolved in NanoPure water (2-3 ml). A solution of 2*n* eq TOABr in dichloromethane (3 ml) was added and the mixture was stirred until all metal ions were transferred to the organic phase and the water phase was colorless. The respective ether ligand (1 eq) was added in 3-4 ml dichloromethane and the mixture was stirred for about 3 minutes before a freshly prepared aqueous solution of $NaBH_4$ (8*n* eq) was added. The organic phase was separated from the water phase after 10 minutes of stirring. The organic phase was concentrated to ~1 ml in a gas stream at room temperature. Ethanol (10-15 ml) was added to precipitate the particles. This mixture was centrifuged for 10 minutes and the colorless supernatant was discarded. The precipitation procedure was repeated twice to remove TOABr. After that the particles were further purified by Gel Permeation Chromatography using *Bio-Rad Bio-Beads S-X1 Beads* with toluene as solvent. The NPs containing fractions could be easily detected due to the strong color of the NPs. The solvent was removed by reduced pressure at ambient temperature.

9 Appendix: TEM Pictures and Calculations

9.1 Au_{144}NPs with Hexylthiol and Ligand 1

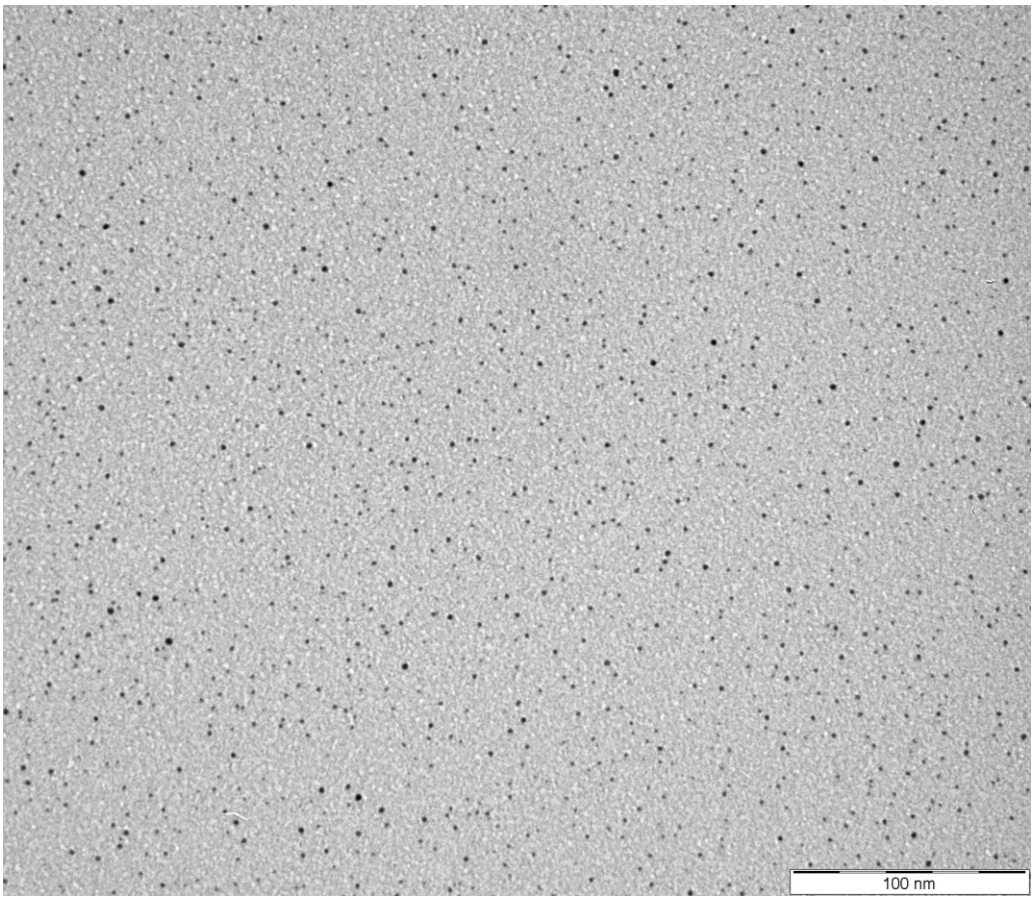

Figure 58.TEM micrograph of Au_{144}NPs with hexylthiol and 1. Scale bar indicates 100 nm.

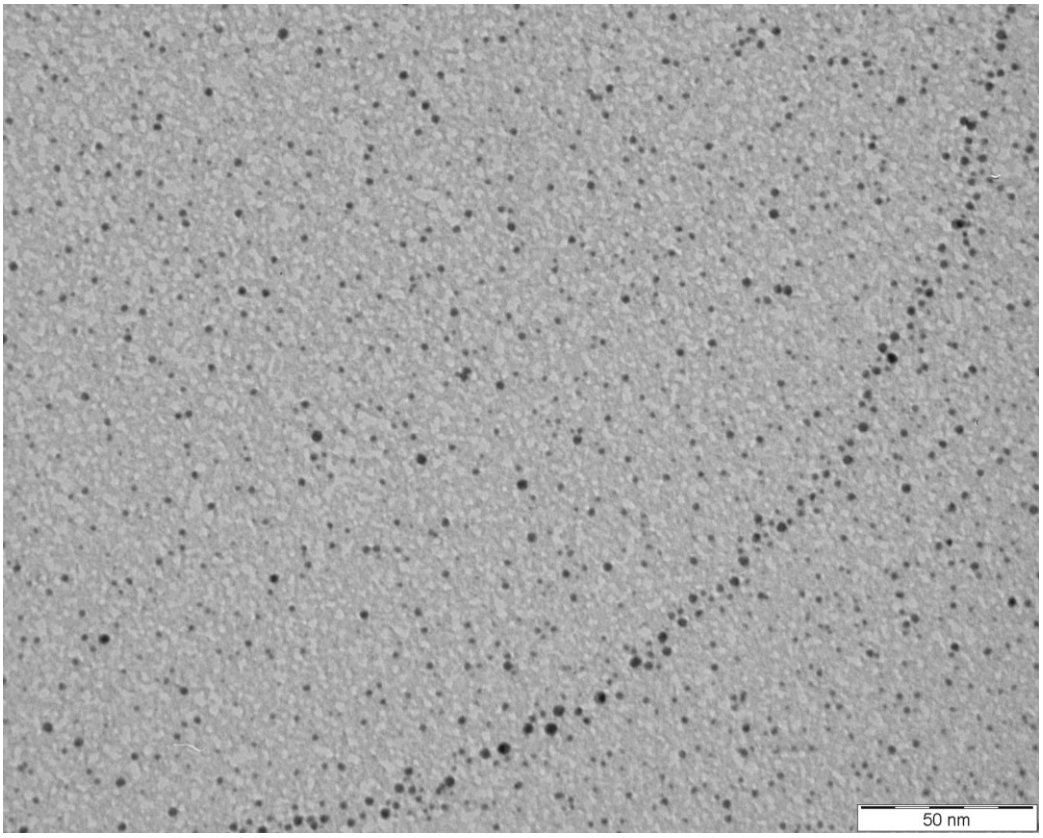

Figure 59.TEM micrograph of Au_{144}NPs with hexylthiol and 1. Scale bar indicates 50 nm.

9.2 Hexyne stabilized Au NPs

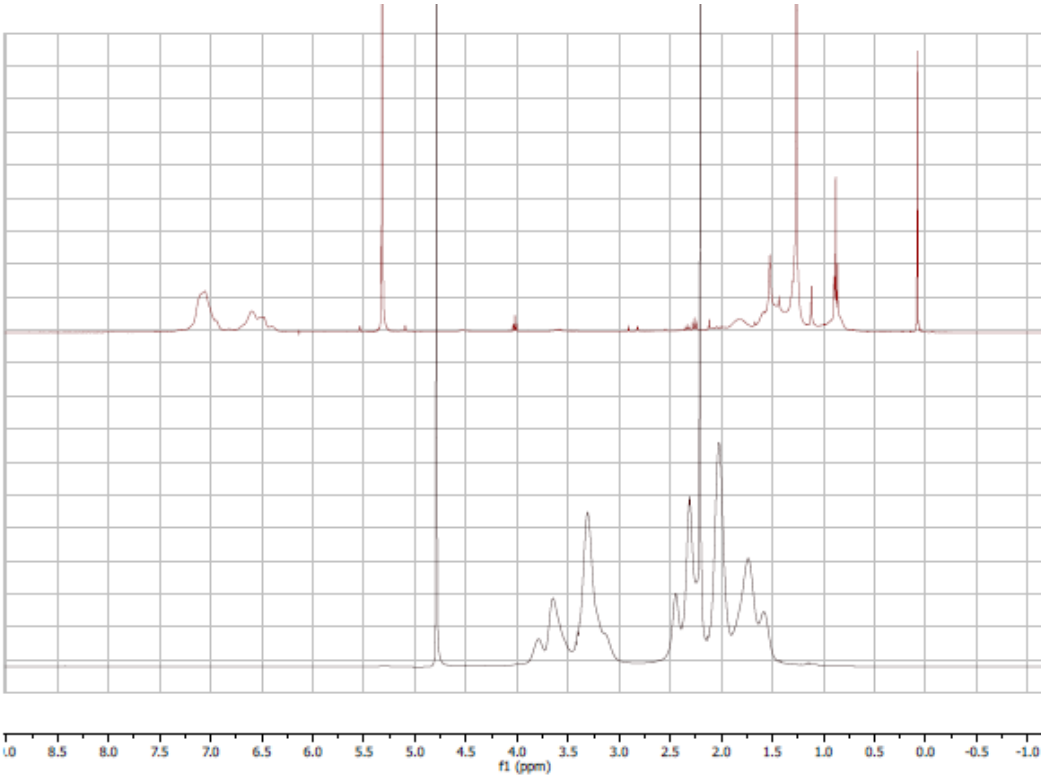

Figure 60. ^{1}H NMR spectra of Au NP:PVP (lower) and Au NP:hexyne (upper).

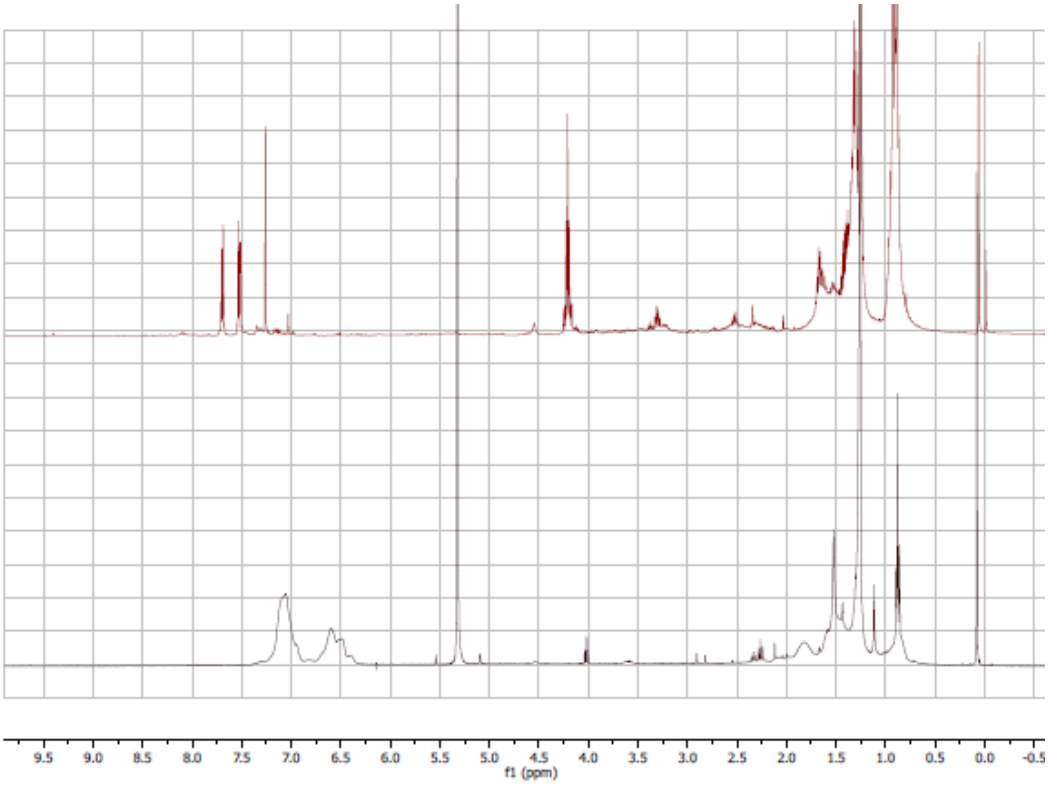

Figure 61. ^{1}H NMR spectra of hexyne (upper) and Au NP:hexyne (lower).

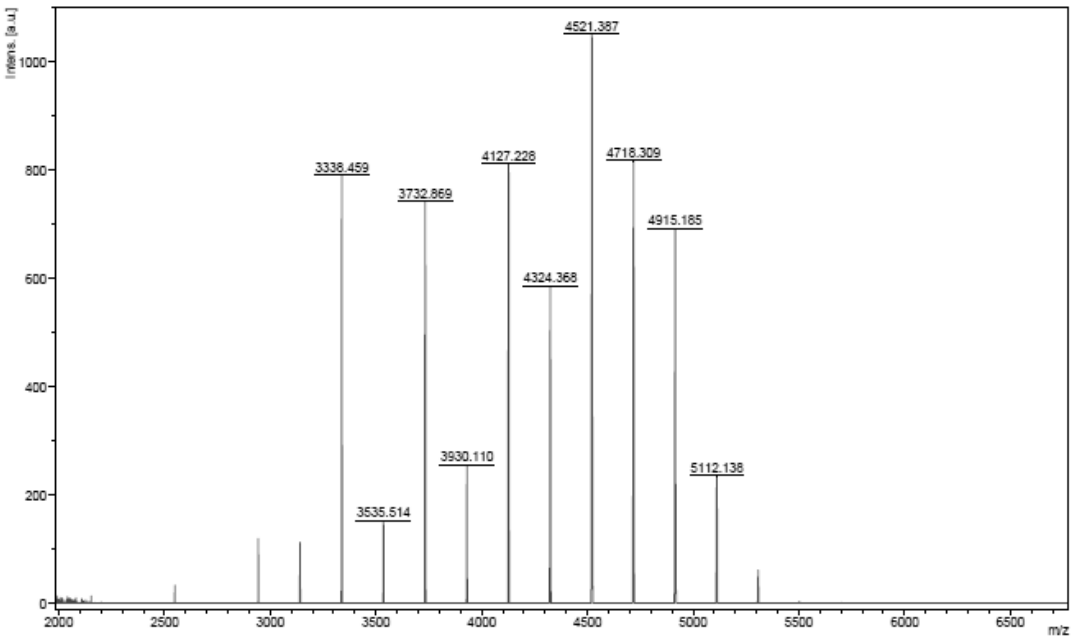

Figure 62. MALDI-ToF MS of Au NP:26.

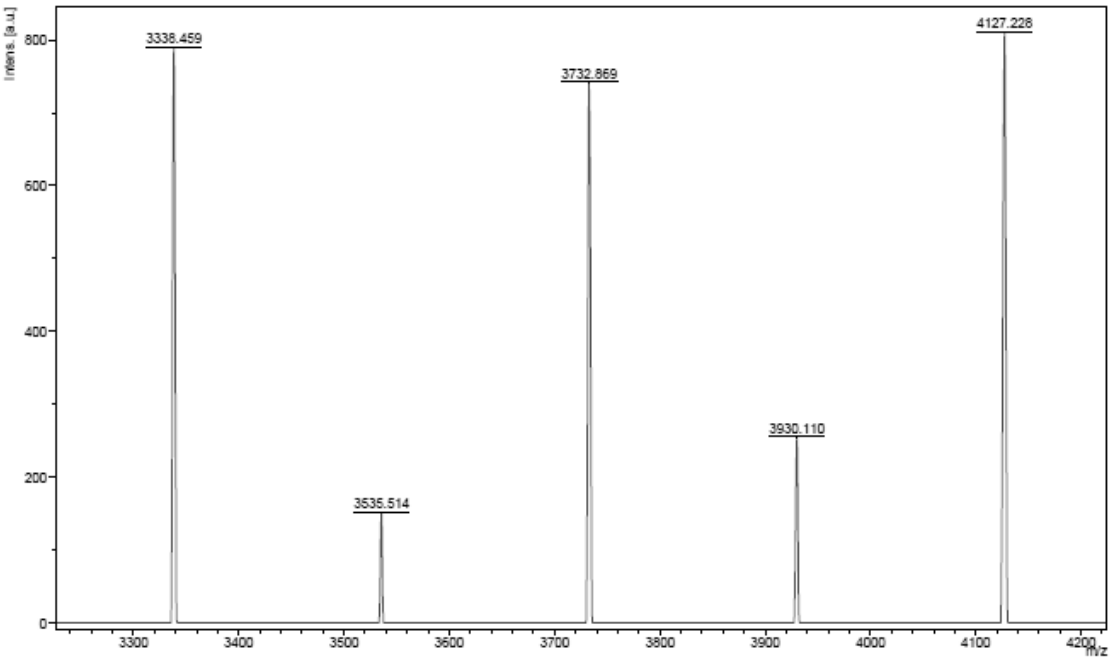

Figure 63. Close up of MALDI-ToF MS of Au NP:26.

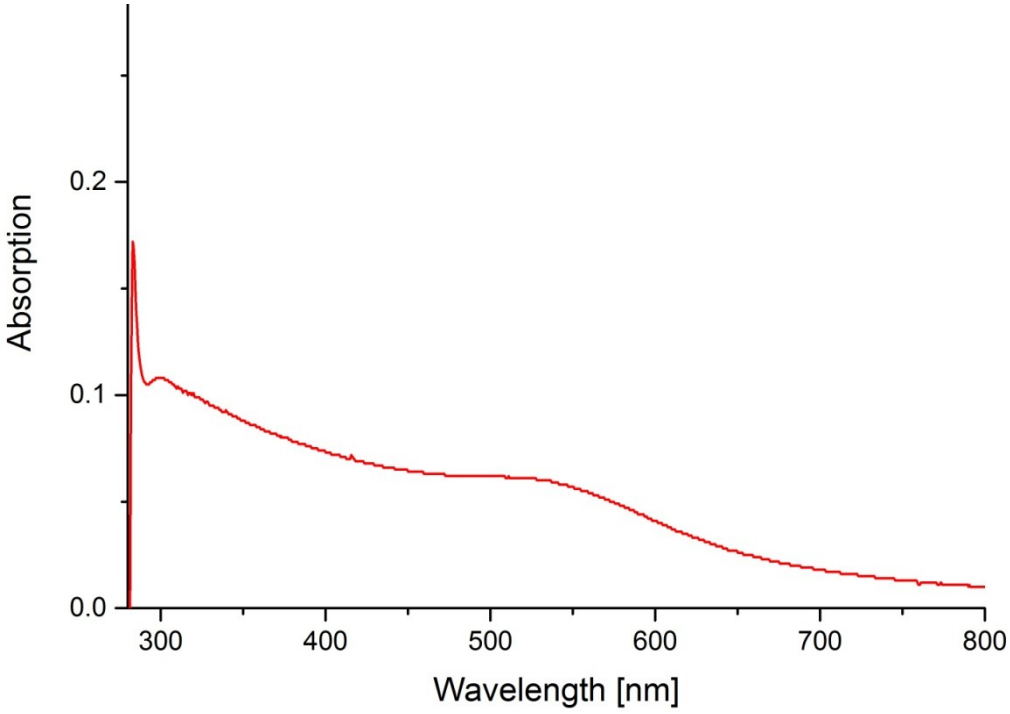

Figure 64. UV/Vis spectra of Au NP:26.

Hexyne→ Au	5	6	7	8	9	10	11	12	13	14	15	16	17	18
1	602.7	683.8	764.9	846.1	927.2	1008.4	1089.5	1170.6	1251.8	1332.9	1414.1	1495.2	1576.3	1657.5
2	799.6	880.8	961.9	1043.1	1124.2	1205.3	1286.5	1367.6	1448.8	1529.9	1611	1692.2	1773.3	1854.5
3	996.6	1077.7	1158.9	1240	1321.2	1402.3	1483.4	1564.6	1645.7	1726.9	1808	1889.1	1970.3	2051.4
4	1193.6	1274.7	1355.8	1437	1518.1	1599.3	1680.4	1761.5	1842.7	1923.8	2005	2086.1	2167.2	2248.4
5	1390.5	1471.7	1552.8	1634	1715.1	1796.2	1877.4	1958.5	2039.7	2120.8	2201.9	2283.1	2364.2	2445.4
6	1587.5	1668.6	1749.8	1830.9	1912.1	1993.2	2074.3	2155.5	2236.6	2317.8	2398.9	2480	2561.2	2642.3
7	1784.5	1865.6	1946.7	2027.9	2109	2190.2	2271.3	2352.4	2433.6	2514.7	2595.9	2677	2758.1	2839.3
8	1981.4	2062.6	2143.7	2224.9	2306	2387.1	2468.3	2549.4	2630.6	2711.7	2792.8	2874	2955.1	3036.3
9	2178.4	2259.5	2340.7	2421.8	2503	2584.1	2665.2	2746.4	2827.5	2908.7	2989.8	3070.9	3152.1	3233.2
10	2375.4	2456.5	2537.6	2618.8	2699.9	2781.1	2862.2	2943.3	3024.5	3105.6	3186.8	3267.9	3349	3430.2
11	2572.3	2653.5	2734.6	2815.8	2896.9	2978	3059.2	3140.3	3221.5	3302.6	3383.7	3464.9	3546	3627.2
12	2769.3	2850.4	2931.6	3012.7	3093.9	3175	3256.1	3337.3	3418.4	3499.6	3580.7	3661.8	3743	3824.1
13	2966.3	3047.4	3128.5	3209.7	3290.8	3372	3453.1	3534.2	3615.4	3696.5	3777.7	3858.8	3939.9	4021.1
14	3163.2	3244.4	3325.5	3406.7	3487.8	3568.9	3650.1	3731.2	3812.4	3893.5	3974.6	4055.8	4136.9	4218.1
15	3360.2	3441.3	3522.5	3603.6	3684.8	3765.9	3847	3928.2	4009.3	4090.5	4171.6	4252.7	4333.9	4415
16	3557.2	3638.3	3719.4	3800.6	3881.7	3962.9	4044	4125.1	4206.3	4287.4	4368.6	4449.7	4530.8	4612
17	3754.1	3835.3	3916.4	3997.6	4078.7	4159.8	4241	4322.1	4403.3	4484.4	4565.5	4646.7	4727.8	4809
18	3951.1	4032.2	4113.4	4194.5	4275.7	4356.8	4437.9	4519.1	4600.2	4681.4	4762.5	4843.6	4924.8	5005.9
19	4148.1	4229.2	4310.3	4391.5	4472.6	4553.8	4634.9	4716	4797.2	4878.3	4959.5	5040.6	5121.7	5202.9
20	4345	4426.2	4507.3	4588.5	4669.6	4750.7	4831.9	4913	4994.2	5075.3	5156.4	5237.6	5318.7	5399.9
21	4542	4623.1	4704.3	4785.4	4866.6	4947.7	5028.8	5110	5191.1	5272.3	5353.4	5434.5	5515.7	5596.8
22	4739	4820.1	4901.2	4982.4	5063.5	5144.7	5225.8	5306.9	5388.1	5469.2	5550.4	5631.5	5712.6	5793.8
23	4935.9	5017.1	5098.2	5179.3	5260.5	5341.6	5422.8	5503.9	5585	5666.2	5747.3	5828.5	5909.6	5990.7
24	5132.9	5214	5295.2	5376.3	5457.5	5538.6	5619.7	5700.9	5782	5863.2	5944.3	6025.4	6106.6	6187.7
25	5329.9	5411	5492.1	5573.3	5654.4	5735.6	5816.7	5897.8	5979	6060.1	6141.3	6222.4	6303.5	6384.7

Table 7.Systematic calculations of the mass of Au NP by # Au-atoms *vs*. amount of hexyne ligand 26.

9.3 Ether Ligands stabilized NPs

9.3.1 Ag NPs

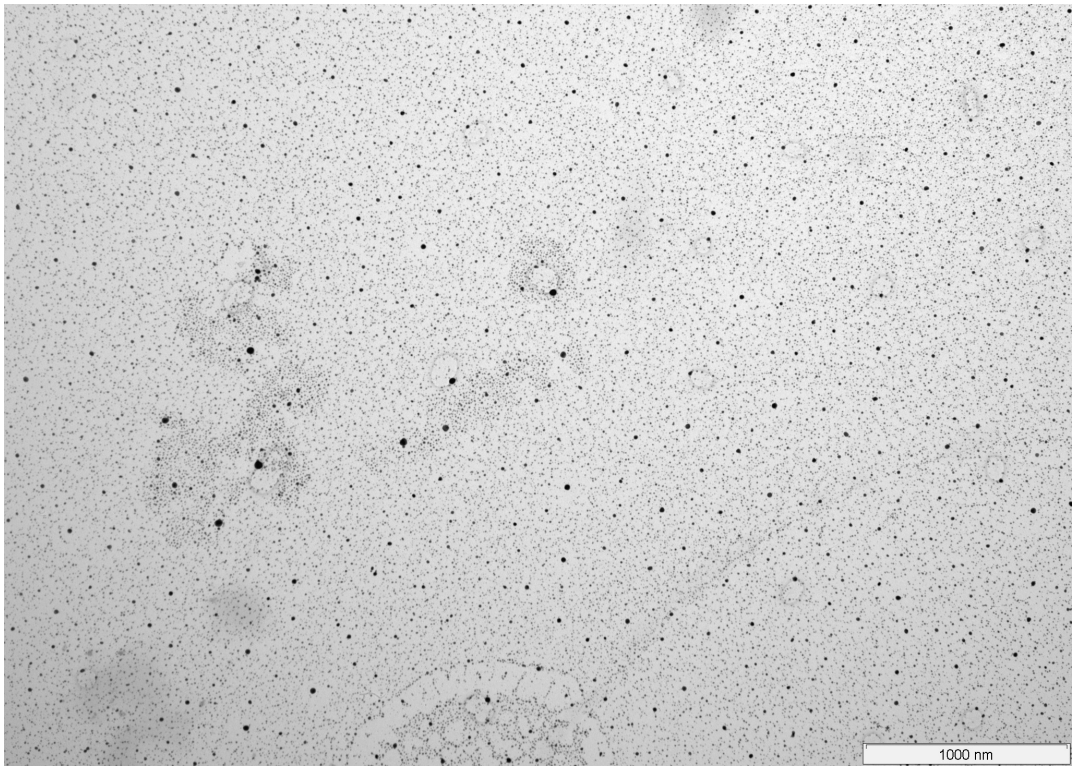

Figure 65.TEM micrograph of Ag NP:35. Scale bar indicates 1000 nm.

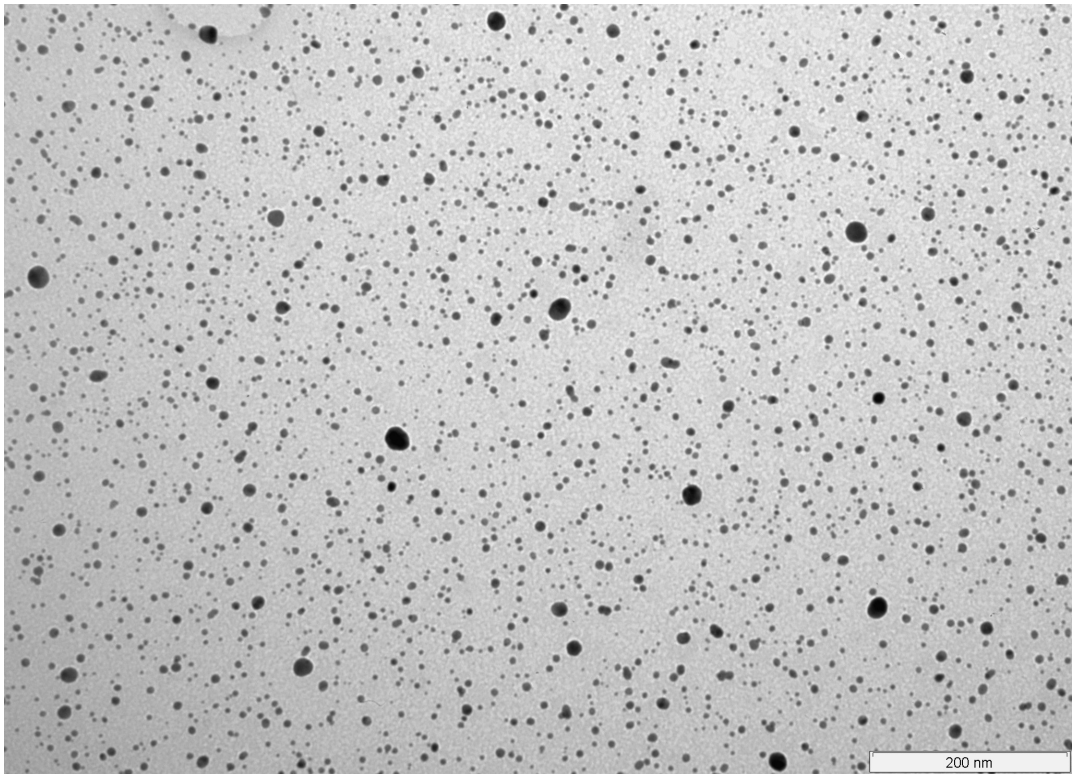

Figure 66. TEM micrograph of Ag NP:35. Scale bar indicates 200 nm.

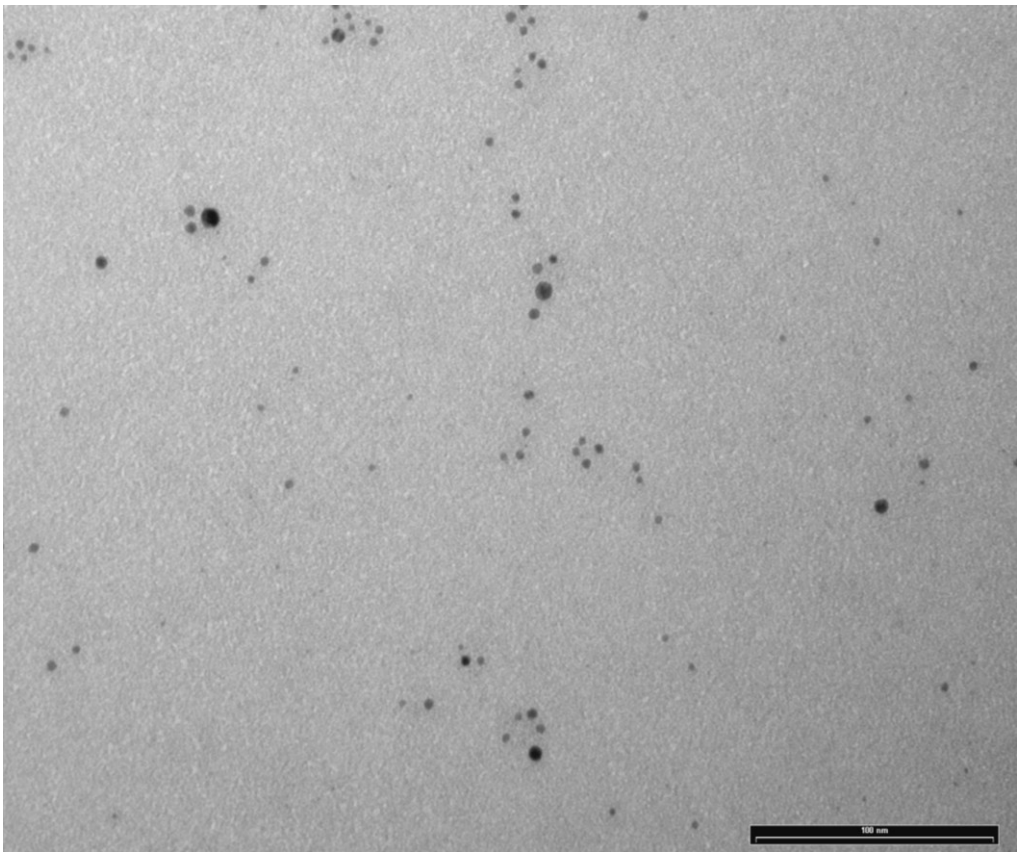

Figure 67. TEM micrograph of Ag NP:33. Scale bar indicates 100 nm.

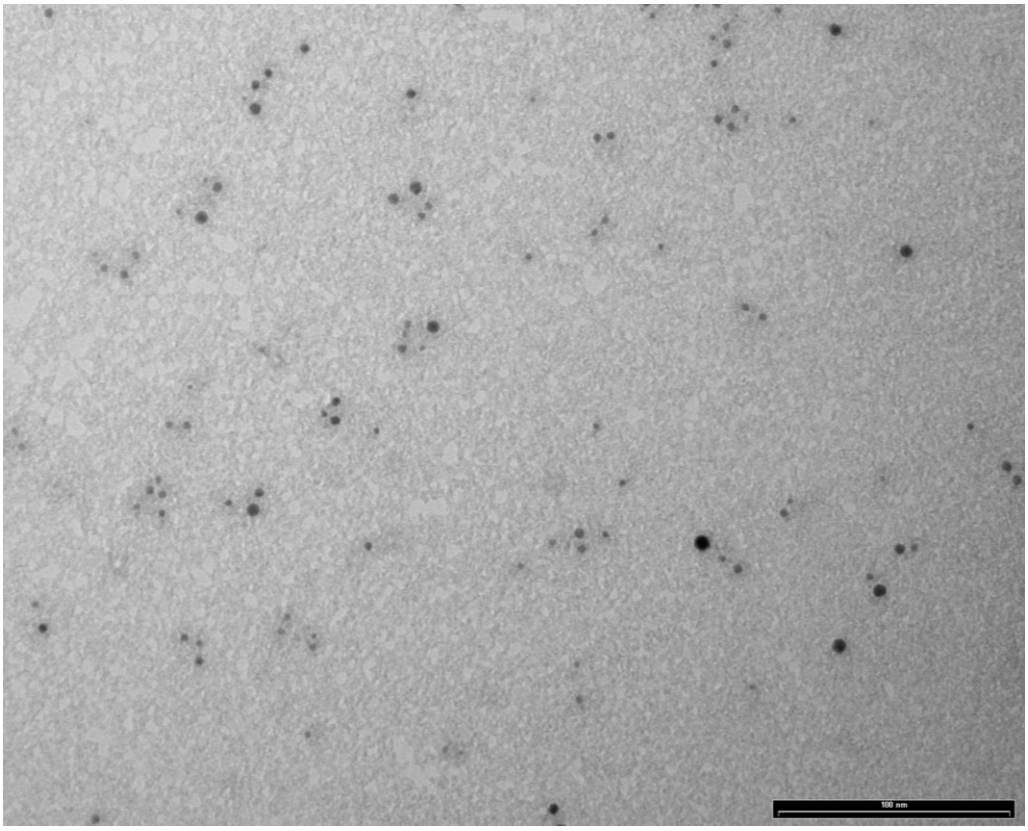

Figure 68. TEM micrograph of Ag NP:33. Scale bar indicates 100 nm.

9.3.2 Pd NPs

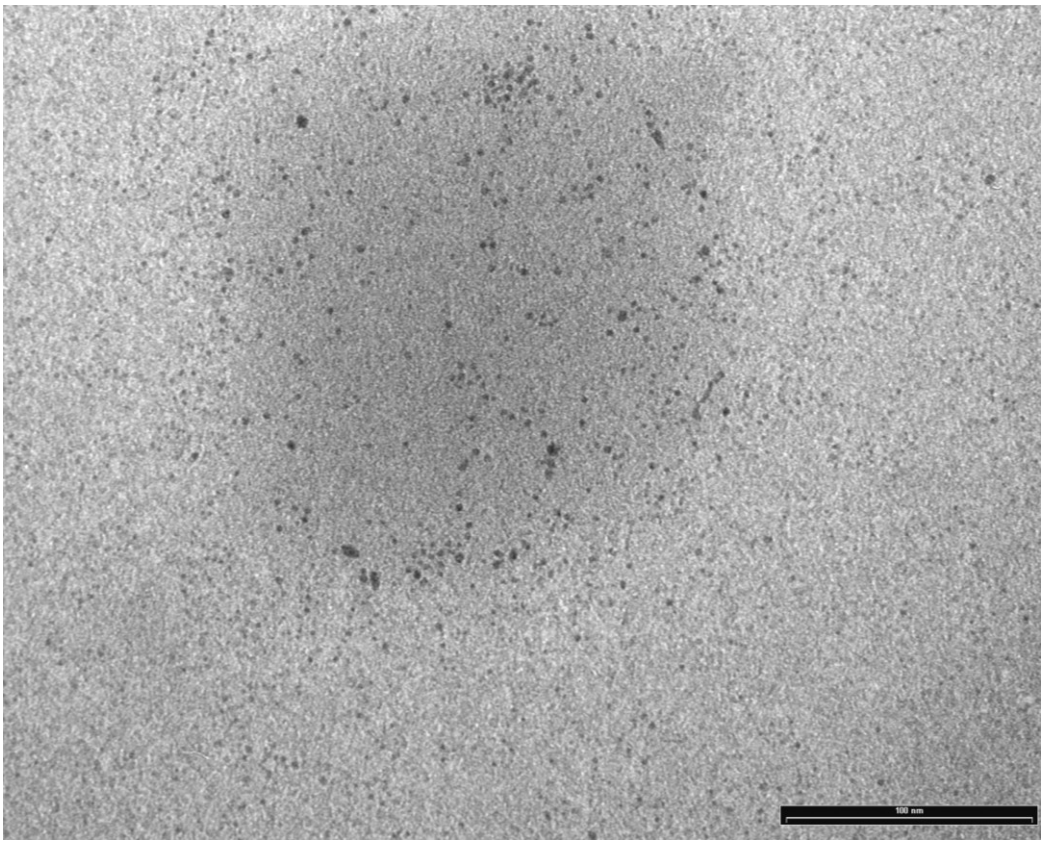

Figure 69. TEM micrograph of Pd NP:35. Scale bar indicates 100 nm.

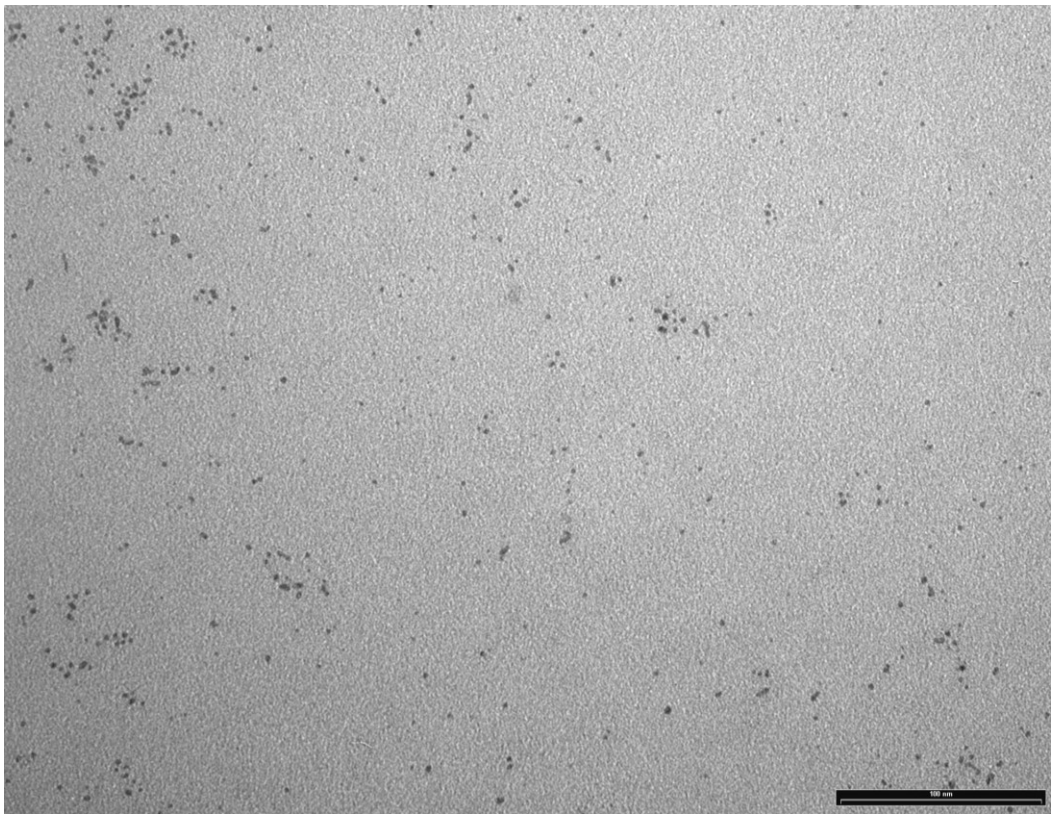

Figure 70. TEM micrograph of Pd NP:34. Scale bar indicates 100 nm.

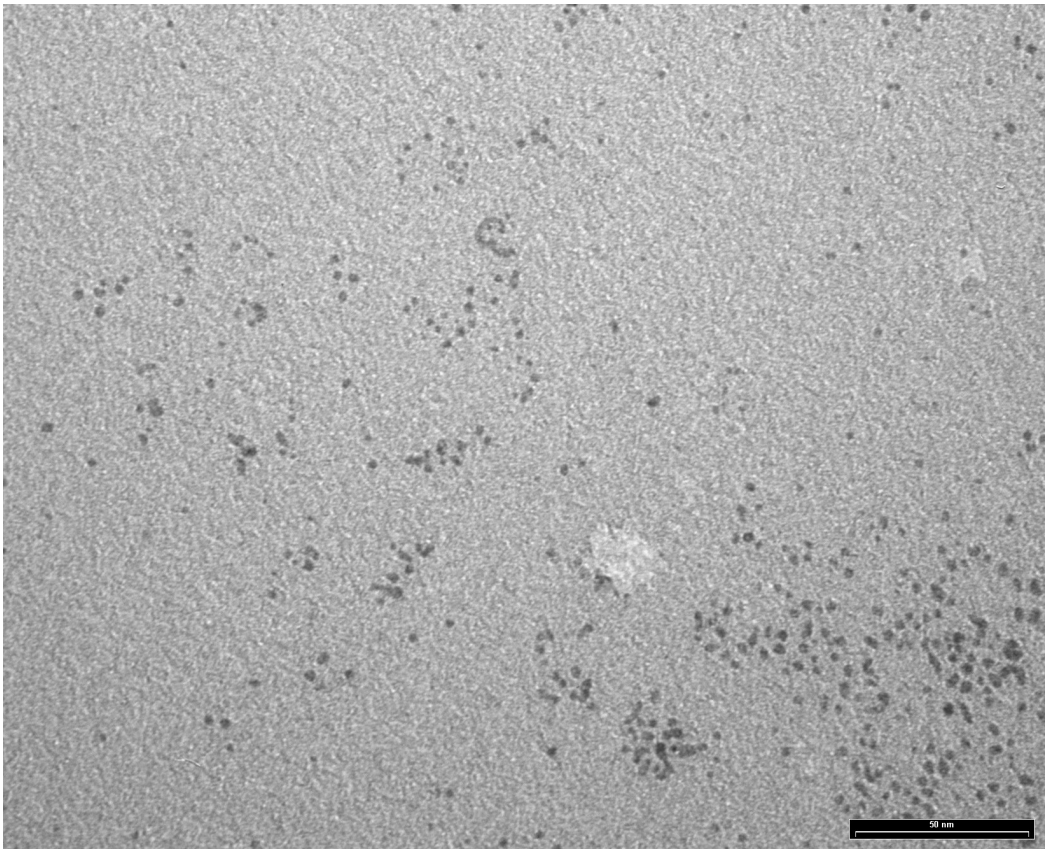

Figure 71. TEM micrograph of Pd NP:34. Scale bar indicates 50 nm.

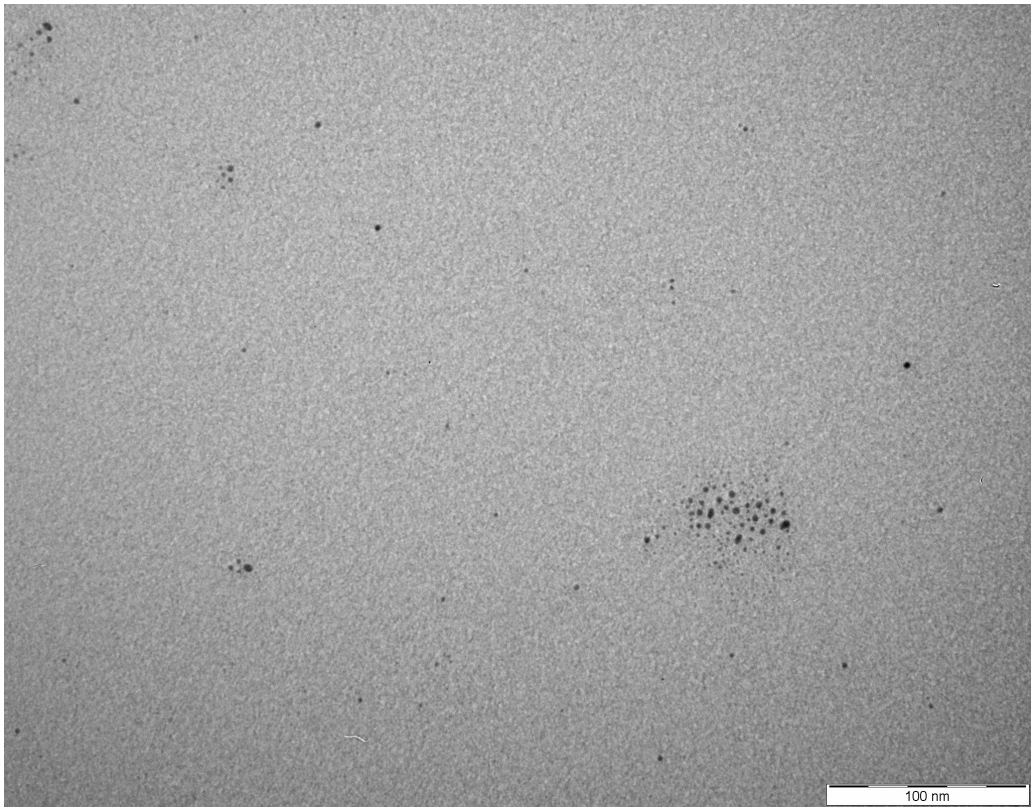

Figure 72. TEM micrograph of Pd NP:64. Scale bar indicates 100 nm.

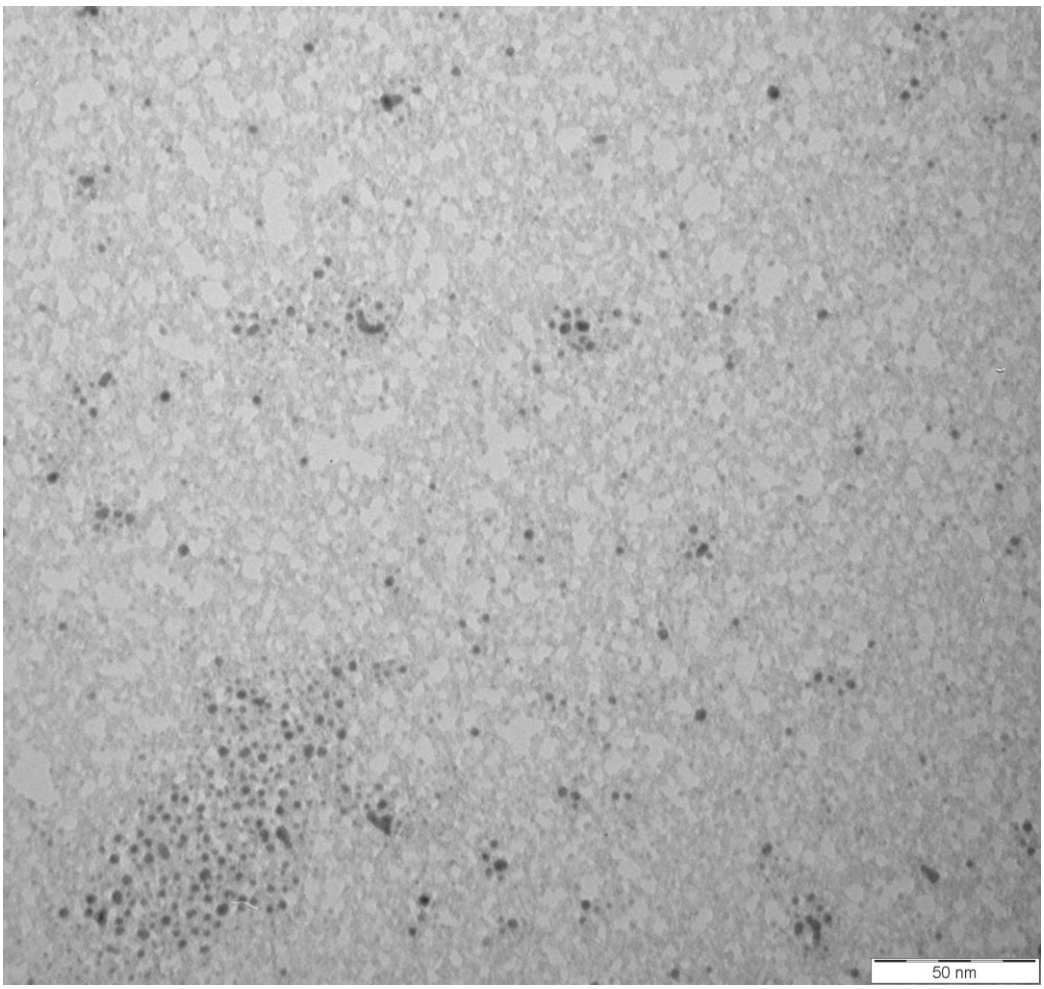

Figure 73. TEM micrograph of Pd NP:58. Scale bar indicates 50 nm.

10 Abbreviations

18-C-6	1,4,7,10,13,16-Hexaoxacyclooctadecane
18-Crown-6	1,4,7,10,13,16-Hexaoxacyclooctadecane
Ac	Acetyl
acac	Acetylacetone
AIBN	2,2'-Azobis(2-methylpropionitrile)
aq.	aqueous
Bn	Benzyl
br	broad
Bu	Butyl
Cy	Cyclohexane
d	duplet
DBU	1,8-Diazabicyclo[5.4.0]undec-7-en
DCTB	*trans*-2-[3-(4-*tert*-Butylphenyl)-2-methyl-2-propenylidene]malononitrile
DIBAL-H	Diisobutylaluminium hydride
DIPEA	Diisopropylethylamine
DMI	1,3-Dimethyl-2-imidazolidinone
DMAP	Dimethyl aminopyridine
DMF	*N,N*-Dimethylformamide
DMSO	Dimethylsulfoxide
DNA	2'-Deoxyribonucleic acid

EA	Elemental Analysis
EI	Electron Impact
eq.	equivalent
ESI	Electron Spray Ionization
Et_3N	Triethyl amine
Et_2NH	Diethyl amine
EtOAc	Ethyl acetate
FG	Functional group
F-octylthiol	3,3,4,4,5,5,6,6,7,7,8,8,8-tridecafluorooctane-1-thiol
GPC	Gel Permeation Chromatography
HRSTEM	High Resolution Scanning Transmission Electron Microscopy
h	hour
h*v*	light
m	multiplet
m/z	mass per charge
MALDI	Matrix-Assisted Laser Desorption/Ionization
Me	Methyl
MEM	2-Methoxyethoxymethyl
MEM-Cl	methoxyethoxymethyl chloride
MP	Melting point
MPC	Monolayer protected cluster
MS	Mass Spectrometry
MTBE	*t*-Butyl methyl ether
MW	Micro wave

NBS	*N*-Bromosuccinimide
NMR	Nuclear Magnetic Resonance
OPE	Oligophenyleneethynyl
OPV	Oligophenylenevinyl
PAMAM	Poly(amidoamine)
PG	Protecting group
Ph	Phenyl
ppm	parts per million
Proton sponge	*N,N,N',N'*-Tetramethylnaphthalin-1,8-diamin
PVP	Polyvinylpyrrolidone
q	quartet
quant.	quantitative
R_f	retention factor
rt	Room temperature
s	singlet
STM	Scanning Tunneling Microscopy
STS	Scanning Tunneling Spectroscopy
t	triplet
TBAF	*tetra*-*n*-Butylammonium fluoride
$TBAPF_6$	Tetrabutylammonium hexafluorophosphate
*t*BDPS	*tert*-Butyldiphenylsilyl
TEM	Transmission Electron Microscopy
TFA	Trifluoroacetic acid
TGA	Thermogravimetric Analysis

THF	Tetrahydrofuran
TIPS	tri-*iso*-propylsilyl
TLC	Thin layer chromatography
TMS	Trimethylsilyl
TMS	Tetramethylsilane
TOABr	tetra-*n*-octylammonium bromide
ToF	Time of Flight
Trt	Trityl
Ts	Tosly
UV/Vis	Ultraviolet and visible
v/v	Volume per volume
X-Phos	2-Dicyclohexylphosphino-2',4',6'-triisopropylbiphenyl
Xantphos	4,5-Bis(diphenylphosphino)-9,9-dimethylxanthene

11 Literature

1. P. Mulvaney, *MRS Bull.*, 2001, **26**, 1009–1014.
2. *Lycurgus Cup*, 1988.
3. M. Faraday, *Philos. Trans. R. Soc. Lond.*, 1857, **147**, 145–181.
4. J. M. Thomas, *Pure Appl. Chem.*, 1988, **60**, 1517–1528.
5. B. L. Cushing, V. L. Kolesnichenko, and C. J. O'Connor, *Chem. Rev.*, 2004, **104**, 3893–3946.
6. G. Mie, *Ann. Phys.*, **25**, 377.
7. G. Schmid and B. Corain, *Eur. J. Inorg. Chem.*, 2003, **2003**, 3081–3098.
8. G. Schmid, *Angew. Chem. Int. Ed.*, 2008, **47**, 3496–3498.
9. K. J. Klabunde, J. Stark, O. Koper, C. Mohs, D. G. Park, S. Decker, Y. Jiang, I. Lagadic, and D. Zhang, *J. Phys. Chem.*, 1996, **100**, 12142–12153.
10. P. Buffat and J.-P. Borel, *Phys. Rev. A*, 1976, **13**, 2287–2298.
11. C. Burda, X. Chen, R. Narayanan, and M. A. El-Sayed, *Chem. Rev.*, 2005, **105**, 1025–1102.
12. J. Zheng, J. T. Petty, and R. M. Dickson, *J. Am. Chem. Soc.*, 2003, **125**, 7780–7781.
13. P. Mulvaney, *Langmuir*, 1996, **12**, 788–800.
14. S. Chen, R. S. Ingram, M. J. Hostetler, J. J. Pietron, R. W. Murray, T. G. Schaaff, J. T. Khoury, M. M. Alvarez, and R. L. Whetten, *Science*, 1998, **280**, 2098–2101.
15. A. C. Templeton, W. P. Wuelfing, and R. W. Murray, *Acc. Chem. Res.*, 2000, **33**, 27–36.
16. L. M. Liz-Marzán, *Mater. Today*, 2004, **7**, 26–31.
17. N. W. Ashcroft, *Solid state physics*, Holt, Rinehart and Winston, New York, 1976.
18. G. Schmid, in *Nanoscale Materials in Chemistry*, ed. K. J. Klabunde, John Wiley & Sons, Inc., New York, USA, pp. 15–59.
19. M. M. Alvarez, J. T. Khoury, T. G. Schaaff, M. N. Shafigullin, I. Vezmar, and R. L. Whetten, *J. Phys. Chem. B*, 1997, **101**, 3706–3712.
20. M. J. Hostetler, J. E. Wingate, C.-J. Zhong, J. E. Harris, R. W. Vachet, M. R. Clark, J. D. Londono, S. J. Green, J. J. Stokes, G. D. Wignall, G. L. Glish, M. D. Porter, N. D. Evans, and R. W. Murray, *Langmuir*, 1998, **14**, 17–30.
21. C. F. Bohren and D. R. Huffman, in *Absorption and Scattering of Light by Small Particles*, Wiley-VCH Verlag GmbH, 2007, pp. 1–11.
22. *Optical Properties of Metal Clusters*, .
23. *Sigma-Aldrich*.
24.
25. J. A. A. J. Perenboom, P. Wyder, and F. Meier, *Phys. Rep.*, 1981, **78**, 173–292.
26. R. L. Johnston, *Philos. Trans. R. Soc. Lond. Ser. Math. Phys. Eng. Sci.*, 1998, **356**, 211–230.
27. G. Schmid, *Adv. Eng. Mater.*, 2001, **3**, 737–743.
28. E. Hutter and J. H. Fendler, *Adv. Mater.*, 2004, **16**, 1685–1706.
29. T. Laaksonen, V. Ruiz, P. Liljeroth, and B. M. Quinn, *Chem. Soc. Rev.*, 2008, **37**, 1836–1846.
30. E. Hartmann, P. Marquardt, J. Ditterich, P. Radojkovic, and H. Steinberger, *Appl. Surf. Sci.*, 1996, **107**, 197–202.
31. T. Sato and H. Ahmed, *Appl. Phys. Lett.*, 1997, **70**, 2759–2761.
32. L. Guo, E. Leobandung, and S. Y. Chou, *Science*, 1997, **275**, 649–651.

33. M. Amman, R. Wilkins, E. Ben-Jacob, P. D. Maker, and R. C. Jaklevic, *Phys. Rev. B*, 1991, **43**, 1146–1149.
34. W. Hofstetter and W. Zwerger, *Phys. Rev. Lett.*, 1997, **78**, 3737–3740.
35. R. S. Ingram, M. J. Hostetler, R. W. Murray, T. G. Schaaff, J. T. Khoury, R. L. Whetten, T. P. Bigioni, D. K. Guthrie, and P. N. First, *J. Am. Chem. Soc.*, 1997, **119**, 9279–9280.
36. J. Turkevich, P. C. Stevenson, and J. Hillier, *Discuss. Faraday Soc.*, 1951, **11**, 55–75.
37. W. W. Weare, S. M. Reed, M. G. Warner, and J. E. Hutchison, *J. Am. Chem. Soc.*, 2000, **122**, 12890–12891.
38. L. O. Brown and J. E. Hutchison, *J. Am. Chem. Soc.*, 1999, **121**, 882–883.
39. U. Chatterjee and S. K. Jewrajka, *J. Colloid Interface Sci.*, 2007, **313**, 717–723.
40. P. Maity, H. Tsunoyama, M. Yamauchi, S. Xie, and T. Tsukuda, *J. Am. Chem. Soc.*, 2011, **133**, 20123–20125.
41. R. Schreiber, J. Do, E.-M. Roller, T. Zhang, V. J. Schüller, P. C. Nickels, J. Feldmann, and T. Liedl, *Nat. Nanotechnol.*, 2014, **9**, 74–78.
42. X. Zhang, T. Gouriye, K. Göeken, M. R. Servos, R. Gill, and J. Liu, *J. Phys. Chem. C*, 2013, **117**, 15677–15684.
43. Z. Wang, R. Lévy, D. G. Fernig, and M. Brust, *Bioconjug. Chem.*, 2005, **16**, 497–500.
44. R. Lévy, N. T. K. Thanh, R. C. Doty, I. Hussain, R. J. Nichols, D. J. Schiffrin, M. Brust, and D. G. Fernig, *J. Am. Chem. Soc.*, 2004, **126**, 10076–10084.
45. C. Mangeney, F. Ferrage, I. Aujard, V. Marchi-Artzner, L. Jullien, O. Ouari, E. D. Rékaï, A. Laschewsky, I. Vikholm, and J. W. Sadowski, *J. Am. Chem. Soc.*, 2002, **124**, 5811–5821.
46. X. Peng, J. Wickham, and A. P. Alivisatos, *J. Am. Chem. Soc.*, 1998, **120**, 5343–5344.
47. L. Naldini, F. Cariati, and G. Simonetta, *Chem. Commun.*, 1966, 647.
48. L. Malatesta, L. Naldini, G. Simonetta, and F. Cariati, *Coord. Chem. Rev.*, 1966, **1**, 255.
49. M. McPartlin, L. Malatesta, and R. Mason, *J. Chem. Soc. Chem. Commun.*, 1969, 334.
50. Q. Zhang, J. Xie, Y. Yu, and J. Y. Lee, *Nanoscale*, 2010, **2**, 1962–1975.
51. M. K. Harbola, *Proc. Natl. Acad. Sci.*, 1992, **89**, 1036–1039.
52. M. Walter, J. Akola, O. Lopez-Acevedo, P. D. Jadzinsky, G. Calero, C. J. Ackerson, R. L. Whetten, H. Grönbeck, and H. Häkkinen, *Proc. Natl. Acad. Sci.*, 2008, **105**, 9157–9162.
53. M. Zhu, C. M. Aikens, F. J. Hollander, G. C. Schatz, and R. Jin, *J. Am. Chem. Soc.*, 2008, **130**, 5883–5885.
54. M. W. Heaven, A. Dass, P. S. White, K. M. Holt, and R. W. Murray, *J. Am. Chem. Soc.*, 2008, **130**, 3754–3755.
55. J. Akola, M. Walter, R. L. Whetten, H. Häkkinen, and H. Grönbeck, *J. Am. Chem. Soc.*, 2008, **130**, 3756–3757.
56. D. Jiang, W. Luo, M. L. Tiago, and S. Dai, *J. Phys. Chem. C*, 2008, **112**, 13905–13910.
57. Y. Pei, Y. Gao, and X. C. Zeng, *J. Am. Chem. Soc.*, 2008, **130**, 7830–7832.
58. O. Toikkanen, V. Ruiz, G. Rönnholm, N. Kalkkinen, P. Liljeroth, and B. M. Quinn, *J. Am. Chem. Soc.*, 2008, **130**, 11049–11055.
59. A. Dass, *J. Am. Chem. Soc.*, 2009, **131**, 11666–11667.
60. Y. Gao, N. Shao, and X. C. Zeng, *ACS Nano*, 2008, **2**, 1497–1503.
61. P. D. Jadzinsky, G. Calero, C. J. Ackerson, D. A. Bushnell, and R. D. Kornberg, *Science*, 2007, **318**, 430–433.
62. O. Lopez-Acevedo, J. Akola, R. L. Whetten, H. Grönbeck, and H. Häkkinen, *J. Phys. Chem. C*, 2009, **113**, 5035–5038.
63. H. Qian and R. Jin, *Nano Lett.*, 2009, **9**, 4083–4087.
64. C. A. Fields-Zinna, R. Sardar, C. A. Beasley, and R. W. Murray, *J. Am. Chem. Soc.*, 2009, **131**, 16266–16271.
65. M. Brust, M. Walker, D. Bethell, D. J. Schiffrin, and R. Whyman, *J. Chem. Soc. Chem. Commun.*, 1994, 801.

66. R. L. Whetten and R. C. Price, *Science*, 2007, **318**, 407–408.
67. H. Häkkinen, *Nat. Chem.*, 2012, **4**, 443–455.
68. M. Brust, J. Fink, D. Bethell, D. J. Schiffrin, and C. Kiely, *J. Chem. Soc. Chem. Commun.*, 1995, 1655.
69. P. J. G. Goulet and R. B. Lennox, *J. Am. Chem. Soc.*, 2010, **132**, 9582–9584.
70. Y. Li, O. Zaluzhna, B. Xu, Y. Gao, J. M. Modest, and Y. J. Tong, *J. Am. Chem. Soc.*, 2011, **133**, 2092–2095.
71. E. Pensa, E. Cortés, G. Corthey, P. Carro, C. Vericat, M. H. Fonticelli, G. Benítez, A. A. Rubert, and R. C. Salvarezza, *Acc. Chem. Res.*, 2012, **45**, 1183–1192.
72. C. J. Ackerson, P. D. Jadzinsky, and R. D. Kornberg, *J. Am. Chem. Soc.*, 2005, **127**, 6550–6551.
73. Y. Negishi, K. Nobusada, and T. Tsukuda, *J. Am. Chem. Soc.*, 2005, **127**, 5261–5270.
74. N. K. Chaki, Y. Negishi, H. Tsunoyama, Y. Shichibu, and T. Tsukuda, *J. Am. Chem. Soc.*, 2008, **130**, 8608–8610.
75. H. Qian, W. T. Eckenhoff, Y. Zhu, T. Pintauer, and R. Jin, *J. Am. Chem. Soc.*, 2010, **132**, 8280–8281.
76. A. C. Templeton, M. J. Hostetler, C. T. Kraft, and R. W. Murray, *J. Am. Chem. Soc.*, 1998, **120**, 1906–1911.
77. A. C. Templeton, M. J. Hostetler, E. K. Warmoth, S. Chen, C. M. Hartshorn, V. M. Krishnamurthy, M. D. E. Forbes, and R. W. Murray, *J. Am. Chem. Soc.*, 1998, **120**, 4845–4849.
78. D. Li, G. L. Jones, J. R. Dunlap, F. Hua, and B. Zhao, *Langmuir*, 2006, **22**, 3344–3351.
79. F. Hua, M. T. Swihart, and E. Ruckenstein, *Langmuir*, 2005, **21**, 6054–6062.
80. G. H. Woehrle, L. O. Brown, and J. E. Hutchison, *J. Am. Chem. Soc.*, 2005, **127**, 2172–2183.
81. M. J. Hostetler, S. J. Green, J. J. Stokes, and R. W. Murray, *J. Am. Chem. Soc.*, 1996, **118**, 4212–4213.
82. J. Yang, J. Y. Lee, and J. Y. Ying, *Chem. Soc. Rev.*, 2011, **40**, 1672–1696.
83. G. Schmid, R. Pfeil, R. Boese, F. Bandermann, S. Meyer, G. H. M. Calis, and J. W. A. van der Velden, *Chem. Ber.*, 1981, **114**, 3634–3642.
84. G. H. Woehrle, M. G. Warner, and J. E. Hutchison, *J. Phys. Chem. B*, 2002, **106**, 9979–9981.
85. G. Schmid, R. Pugin, J.-O. Malm, and J.-O. Bovin, *Eur. J. Inorg. Chem.*, 1998, **1998**, 813–817.
86. G. Schmid, R. Pugin, W. Meyer-Zaika, and U. Simon, *Eur. J. Inorg. Chem.*, 1999, **1999**, 2051–2055.
87. H. Qian, W. T. Eckenhoff, M. E. Bier, T. Pintauer, and R. Jin, *Inorg. Chem.*, 2011, **50**, 10735–10739.
88. Lon A. Porter, D. Ji, S. L. Westcott, M. Graupe, R. S. Czernuszewicz, N. J. Halas, and T. R. Lee, *Langmuir*, 1998, **14**, 7378–7386.
89. A. Manna, P.-L. Chen, H. Akiyama, T.-X. Wei, K. Tamada, and W. Knoll, *Chem. Mater.*, 2003, **15**, 20–28.
90. J. B. Schlenoff, M. Li, and H. Ly, *J. Am. Chem. Soc.*, 1995, **117**, 12528–12536.
91. D. M. Collard and M. A. Fox, *Langmuir*, 1991, **7**, 1192–1197.
92. C. D. Bain, J. Evall, and G. M. Whitesides, *J. Am. Chem. Soc.*, 1989, **111**, 7155–7164.
93. J. R. Scott, L. S. Baker, W. R. Everett, C. L. Wilkins, and I. Fritsch, *Anal. Chem.*, 1997, **69**, 2636–2639.
94. M. J. Hostetler, A. C. Templeton, and R. W. Murray, *Langmuir*, 1999, **15**, 3782–3789.
95. R. L. Donkers, Y. Song, and R. W. Murray, *Langmuir*, 2004, **20**, 4703–4707.
96. J. C. Love, L. A. Estroff, J. K. Kriebel, R. G. Nuzzo, and G. M. Whitesides, *Chem. Rev.*, 2005, **105**, 1103–1170.

97. M. H. Schoenfisch and J. E. Pemberton, *J. Am. Chem. Soc.*, 1998, **120**, 4502–4513.
98. J. D. Aiken III and R. G. Finke, *J. Mol. Catal. Chem.*, 1999, **145**, 1–44.
99. J. Cookson, *Platin. Met. Rev.*, 2012, **56**, 83–98.
100. D. Astruc, *Inorg. Chem.*, 2007, **46**, 1884–1894.
101. A. T. Bell, *Science*, 2003, **299**, 1688–1691.
102. N. Semagina, A. Renken, and L. Kiwi-Minsker, *J. Phys. Chem. C*, 2007, **111**, 13933–13937.
103. O. M. Wilson, M. R. Knecht, J. C. Garcia-Martinez, and R. M. Crooks, *J. Am. Chem. Soc.*, 2006, **128**, 4510–4511.
104. N. Dimitratos, F. Porta, and L. Prati, *Appl. Catal. Gen.*, 2005, **291**, 210–214.
105. Z. Hou, N. Theyssen, A. Brinkmann, and W. Leitner, *Angew. Chem. Int. Ed.*, 2005, **44**, 1346–1349.
106. M. Beller, H. Fischer, K. Kühlein, C.-P. Reisinger, and W. A. Herrmann, *J. Organomet. Chem.*, 1996, **520**, 257–259.
107. R. Narayanan and M. A. El-Sayed, *J. Catal.*, 2005, **234**, 348–355.
108. S. Horinouchi, Y. Yamanoi, T. Yonezawa, T. Mouri, and H. Nishihara, *Langmuir*, 2006, **22**, 1880–1884.
109. M. Yamauchi, R. Ikeda, H. Kitagawa, and M. Takata, *J. Phys. Chem. C*, 2008, **112**, 3294–3299.
110. S. Mubeen, T. Zhang, B. Yoo, M. A. Deshusses, and N. V. Myung, *J. Phys. Chem. C*, 2007, **111**, 6321–6327.
111. P. Tobiška, O. Hugon, A. Trouillet, and H. Gagnaire, *Sens. Actuators B Chem.*, 2001, **74**, 168–172.
112. B. Lim, M. Jiang, J. Tao, P. H. C. Camargo, Y. Zhu, and Y. Xia, *Adv. Funct. Mater.*, 2009, **19**, 189–200.
113. Y. Xiong and Y. Xia, *Adv. Mater.*, 2007, **19**, 3385–3391.
114. B. P. S. Chauhan, J. S. Rathore, and T. Bandoo, *J. Am. Chem. Soc.*, 2004, **126**, 8493–8500.
115. F. Lu, J. Ruiz, and D. Astruc, *Tetrahedron Lett.*, 2004, **45**, 9443–9445.
116. J. Alvarez, J. Liu, E. Román, and A. E. Kaifer, *Chem. Commun.*, 2000, 1151–1152.
117. I. Quiros, M. Yamada, K. Kubo, J. Mizutani, M. Kurihara, and H. Nishihara, *Langmuir*, 2002, **18**, 1413–1418.
118. F. Dassenoy, K. Philippot, T. O. Ely, C. Amiens, P. Lecante, E. Snoeck, A. Mosset, M.-J. Casanove, and B. Chaudret, *New J. Chem.*, 1998, **22**, 703–712.
119. T. Teranishi and M. Miyake, *Chem. Mater.*, 1998, **10**, 594–600.
120. C. K. Yee, R. Jordan, A. Ulman, H. White, A. King, M. Rafailovich, and J. Sokolov, *Langmuir*, 1999, **15**, 3486–3491.
121. S. Chen, K. Huang, and J. A. Stearns, *Chem. Mater.*, 2000, **12**, 540–547.
122. A. C. Templeton, D. E. Cliffel, and R. W. Murray, *J. Am. Chem. Soc.*, 1999, **121**, 7081–7089.
123. D. Dorokhin, N. Tomczak, A. H. Velders, D. N. Reinhoudt, and G. J. Vancso, *J. Phys. Chem. C*, 2009, **113**, 18676–18680.
124. M. Ganesan, R. G. Freemantle, and S. O. Obare, *Chem. Mater.*, 2007, **19**, 3464–3471.
125. V. Huc and K. Pelzer, *J. Colloid Interface Sci.*, 2008, **318**, 1–4.
126. I. Hussain, S. Graham, Z. Wang, B. Tan, D. C. Sherrington, S. P. Rannard, A. I. Cooper, and M. Brust, *J. Am. Chem. Soc.*, 2005, **127**, 16398–16399.
127. S.-W. Kim, J. Park, Y. Jang, Y. Chung, S. Hwang, T. Hyeon, and Y. W. Kim, *Nano Lett.*, 2003, **3**, 1289–1291.
128. S. U. Son, Y. Jang, K. Y. Yoon, E. Kang, and T. Hyeon, *Nano Lett.*, 2004, **4**, 1147–1151.
129. M. Tamura and H. Fujihara, *J. Am. Chem. Soc.*, 2003, **125**, 15742–15743.
130. R. Tatumi, T. Akita, and H. Fujihara, *Chem. Commun.*, 2006, 3349–3351.
131. V. Mazumder and S. Sun, *J. Am. Chem. Soc.*, 2009, **131**, 4588–4589.

132. Z. Li, J. Gao, X. Xing, S. Wu, S. Shuang, C. Dong, M. C. Paau, and M. M. F. Choi, *J. Phys. Chem. C*, 2010, **114**, 723–733.
133. A. A. Athawale, S. V. Bhagwat, P. P. Katre, A. J. Chandwadkar, and P. Karandikar, *Mater. Lett.*, 2003, **57**, 3889–3894.
134. T. Mayer-Gall, A. Birkner, and G. Dyker, *J. Organomet. Chem.*, 2008, **693**, 1–3.
135. D. I. Gittins and F. Caruso, *Angew. Chem. Int. Ed.*, 2001, **40**, 3001–3004.
136. C. J. Serpell, J. Cookson, D. Ozkaya, and P. D. Beer, *Nat. Chem.*, 2011, **3**, 478–483.
137. D. H. Turkenburg, A. A. Antipov, M. B. Thathagar, G. Rothenberg, G. B. Sukhorukov, and E. Eiser, *Phys. Chem. Chem. Phys.*, 2005, **7**, 2237–2240.
138. W. Chen, J. R. Davies, D. Ghosh, M. C. Tong, J. P. Konopelski, and S. Chen, *Chem. Mater.*, 2006, **18**, 5253–5259.
139. F. Mirkhalaf, J. Paprotny, and D. J. Schiffrin, *J. Am. Chem. Soc.*, 2006, **128**, 7400–7401.
140. D. Ghosh and S. Chen, *J. Mater. Chem.*, 2008, **18**, 755–762.
141. J. S. Bradley, in *Clusters and Colloids*, ed. G. Schmid, Wiley-VCH Verlag GmbH, Weinheim, Germany, pp. 459–544.
142. B. Corain, K. Jerabek, P. Centomo, and P. Canton, *Angew. Chem. Int. Ed.*, 2004, **43**, 959–962.
143. L. D. Rampino and F. F. Nord, *J. Am. Chem. Soc.*, 1941, **63**, 3268–3268.
144. N. Toshima and T. Yonezawa, *New J. Chem.*, 1998, **22**, 1179–1201.
145. Y. Yu, Y. Zhao, T. Huang, and H. Liu, *Pure Appl. Chem.*, 2009, **81**, 2377–2385.
146. W. Tu and H. Liu, *Chem. Mater.*, 2000, **12**, 564–567.
147. B. Thiébaut, 2004.
148. V. Calò, A. Nacci, A. Monopoli, and F. Montingelli, *J. Org. Chem.*, 2005, **70**, 6040–6044.
149. P. D. Stevens, G. Li, J. Fan, M. Yen, and Y. Gao, *Chem. Commun.*, 2005, 4435–4437.
150. S. Pande, M. G. Weir, B. A. Zaccheo, and R. M. Crooks, *New J. Chem.*, 2011, **35**, 2054–2060.
151. *Dendrimers and other dendritic polymers*, Wiley, Chichester ; New York, 2001.
152. L. Balogh and D. A. Tomalia, *J. Am. Chem. Soc.*, 1998, **120**, 7355–7356.
153. L. K. Yeung and R. M. Crooks, *Nano Lett.*, 2001, **1**, 14–17.
154. M. V. Gomez, J. Guerra, A. H. Velders, and R. M. Crooks, *J. Am. Chem. Soc.*, 2009, **131**, 341–350.
155. R. Andrés, E. de Jesús, and J. C. Flores, *New J. Chem.*, 2007, **31**, 1161–1191.
156. L. Wu, B.-L. Li, Y.-Y. Huang, H.-F. Zhou, Y.-M. He, and Q.-H. Fan, *Org. Lett.*, 2006, **8**, 3605–3608.
157. R. M. Crooks, M. Zhao, L. Sun, V. Chechik, and L. K. Yeung, *Acc. Chem. Res.*, 2001, **34**, 181–190.
158. M. Zhao, L. Sun, and R. M. Crooks, *J. Am. Chem. Soc.*, 1998, **120**, 4877–4878.
159. T. Peterle, A. Leifert, J. Timper, A. Sologubenko, U. Simon, and M. Mayor, *Chem. Commun.*, 2008, 3438–3440.
160. F. Sander, T. Peterle, N. Ballav, F. von Wrochem, M. Zharnikov, and M. Mayor, *J. Phys. Chem. C*, 2010, **114**, 4118–4125.
161. J. P. Hermes, F. Sander, T. Peterle, R. Urbani, T. Pfohl, D. Thompson, and M. Mayor, *Chem. – Eur. J.*, 2011, **17**, 13473–13481.
162. A. Gallardo-Godoy, M. I. Torres-Altoro, K. J. White, E. L. Barker, and D. E. Nichols, *Bioorg. Med. Chem.*, 2007, **15**, 305–311.
163. P. G. M. Wuts, *Greene's protective groups in organic synthesis*, Wiley-Interscience, Hoboken, N.J, 4th ed., 2007.
164. D. T. Gryko, C. Clausen, K. M. Roth, N. Dontha, D. F. Bocian, W. G. Kuhr, and J. S. Lindsey, *J. Org. Chem.*, 2000, **65**, 7345–7355.
165. S. Grunder, R. Huber, V. Horhoiu, M. T. González, C. Schönenberger, M. Calame, and M. Mayor, *J. Org. Chem.*, 2007, **72**, 8337–8344.

166. H. Valkenier, E. H. Huisman, P. A. van Hal, D. M. de Leeuw, R. C. Chiechi, and J. C. Hummelen, *J. Am. Chem. Soc.*, 2011, **133**, 4930–4939.
167. A. García-Rubia, M. Á. Fernández-Ibáñez, R. Gómez Arrayás, and J. C. Carretero, *Chem. – Eur. J.*, 2011, **17**, 3567–3570.
168. D. Nagarathnam, J. Dumas, H. Hatoum-Mokdad, S. Boyer, and H. Pluempe, 2003.
169. J. Dumas, U. Khire, T. Lowinger, H. Paulsen, B. Riedl, W. Scott, R. Smith, J. Wood, H. Hatoum-Mokdad, J. Johnson, W. Lee, and A. Redman, 1999.
170. C. J. Yu, Y. Chong, J. F. Kayyem, and M. Gozin, *J. Org. Chem.*, 1999, **64**, 2070–2079.
171. A. K. Flatt and J. M. Tour, *Tetrahedron Lett.*, 2003, **44**, 6699–6702.
172. Y. Shirai, L. Cheng, B. Chen, and J. M. Tour, *J. Am. Chem. Soc.*, 2006, **128**, 13479–13489.
173. Y. Shirai, J. M. Guerrero, T. Sasaki, T. He, H. Ding, G. Vives, B.-C. Yu, L. Cheng, A. K. Flatt, P. G. Taylor, Y. Gao, and J. M. Tour, *J. Org. Chem.*, 2009, **74**, 7885–7897.
174. G. J. Rowlands and R. J. Seacome, *Beilstein J. Org. Chem.*, 2009, **5**.
175. F. Maya, S. H. Chanteau, L. Cheng, M. P. Stewart, and J. M. Tour, *Chem. Mater.*, 2005, **17**, 1331–1345.
176. J. W. Ciszek, M. P. Stewart, and J. M. Tour, *J. Am. Chem. Soc.*, 2004, **126**, 13172–13173.
177. D.-K. Bučar, A. Sen, S. V. S. Mariappan, and L. R. MacGillivray, *Chem. Commun.*, 2012, **48**, 1790.
178. J. Burdeniuk and D. Milstein, *J. Organomet. Chem.*, 1993, **451**, 213–220.
179. C. Lai and B. J. Backes, *Tetrahedron Lett.*, 2007, **48**, 3033–3037.
180. K. Rößler, T. Rüffer, B. Walfort, R. Packheiser, R. Holze, M. Zharnikov, and H. Lang, *J. Organomet. Chem.*, 2007, **692**, 1530–1545.
181. B. de Boer, H. Meng, D. F. Perepichka, J. Zheng, M. M. Frank, Y. J. Chabal, and Z. Bao, *Langmuir*, 2003, **19**, 4272–4284.
182. A. C. Templeton, S. Chen, S. M. Gross, and R. W. Murray, *Langmuir*, 1999, **15**, 66–76.
183. D. E. Cliffel, F. P. Zamborini, S. M. Gross, and R. W. Murray, *Langmuir*, 2000, **16**, 9699–9702.
184. K. V. Sarathy, G. Raina, R. T. Yadav, G. U. Kulkarni, and C. N. R. Rao, *J. Phys. Chem. B*, 1997, **101**, 9876–9880.
185. V. R. Jupally, R. Kota, E. V. Dornshuld, D. L. Mattern, G. S. Tschumper, D. Jiang, and A. Dass, *J. Am. Chem. Soc.*, 2011, **133**, 20258–20266.
186. S. Knoppe, A. C. Dharmaratne, E. Schreiner, A. Dass, and T. Bürgi, *J. Am. Chem. Soc.*, 2010, **132**, 16783–16789.
187. T. G. Schaaff and R. L. Whetten, *J. Phys. Chem. B*, 1999, **103**, 9394–9396.
188. H. Qian and R. Jin, *Chem. Mater.*, 2011, **23**, 2209–2217.
189. R. L. Wolfe and R. W. Murray, *Anal. Chem.*, 2006, **78**, 1167–1173.
190. S. Chen and K. Kimura, *Chem. Lett.*, 1999, **28**, 1169–1170.
191. P. Christian and M. Bromfield, *J. Mater. Chem.*, 2010, **20**, 1135–1139.
192. P. R. Nimmala and A. Dass, *J. Am. Chem. Soc.*, 2011, **133**, 9175–9177.
193. A. Helfrich and J. Bettmer, *Int. J. Mass Spectrom.*, 2011, **307**, 92–98.
194. A. Dass, A. Stevenson, G. R. Dubay, J. B. Tracy, and R. W. Murray, *J. Am. Chem. Soc.*, 2008, **130**, 5940–5946.
195. H. A. Biebuyck and G. M. Whitesides, *Langmuir*, 1993, **9**, 1766–1770.
196. H. Grönbeck, A. Curioni, and W. Andreoni, *J. Am. Chem. Soc.*, 2000, **122**, 3839–3842.
197. T. G. Schaaff, M. N. Shafigullin, J. T. Khoury, I. Vezmar, and R. L. Whetten, *J. Phys. Chem. B*, 2001, **105**, 8785–8796.
198. H. Qian, M. Zhu, Z. Wu, and R. Jin, *Acc. Chem. Res.*, 2012, **45**, 1470–1479.
199. R. L. Wolfe, R. Balasubramanian, J. B. Tracy, and R. W. Murray, *Langmuir*, 2007, **23**, 2247–2254.
200. K. Salorinne, T. Lahtinen, J. Koivisto, E. Kalenius, M. Nissinen, M. Pettersson, and H. Häkkinen, *Anal. Chem.*, 2013, **85**, 3489–3492.

201. D. Lee, R. L. Donkers, J. M. DeSimone, and R. W. Murray, *J. Am. Chem. Soc.*, 2003, **125**, 1182–1183.
202. J.-P. Choi and R. W. Murray, *J. Am. Chem. Soc.*, 2006, **128**, 10496–10502.
203. A. M. Ricci, E. J. Calvo, S. Martin, and R. J. Nichols, *J. Am. Chem. Soc.*, 2010, **132**, 2494–2495.
204. P. Salvatore, A. G. Hansen, K. Moth-Poulsen, T. Bjørnholm, R. J. Nichols, and J. Ulstrup, *Phys. Chem. Chem. Phys.*, 2011, **13**, 14394–14403.
205. T. Albrecht, K. Moth-Poulsen, J. B. Christensen, J. Hjelm, T. Bjørnholm, and J. Ulstrup, *J. Am. Chem. Soc.*, 2006, **128**, 6574–6575.
206. Y. Hu, O. Uzun, C. Dubois, and F. Stellacci, *J. Phys. Chem. C*, 2008, **112**, 6279–6284.
207. S. F. L. Mertens, K. Blech, A. S. Sologubenko, J. Mayer, U. Simon, and T. Wandlowski, *Electrochimica Acta*, 2009, **54**, 5006–5010.
208. S. F. L. Mertens, G. Mészáros, and T. Wandlowski, *Phys. Chem. Chem. Phys.*, 2010, **12**, 5417–5424.
209. M. Brust, M. Walker, D. Bethell, D. J. Schiffrin, and R. Whyman, *J. Chem. Soc. Chem. Commun.*, 1994, 801.
210. T. Yonezawa, S. Onoue, and N. Kimizuka, *Langmuir*, 2001, **17**, 2291–2293.
211. S. Eibenberger, S. Gerlich, M. Arndt, M. Mayor, and J. Tüxen, *Phys. Chem. Chem. Phys.*, 2013, **15**, 14696–14700.
212. P. Schmid, F. Stöhr, M. Arndt, J. Tüxen, and M. Mayor, *Mass Spectrom.*, **24**, 602–608.
213. W. Hong, H. Li, S.-X. Liu, Y. Fu, J. Li, V. Kaliginedi, S. Decurtins, and T. Wandlowski, *J. Am. Chem. Soc.*, 2012, **134**, 19425–19431.
214. F. Chen, X. Li, J. Hihath, Z. Huang, and N. Tao, *J. Am. Chem. Soc.*, 2006, **128**, 15874–15881.
215. L. Venkataraman, J. E. Klare, I. W. Tam, C. Nuckolls, M. S. Hybertsen, and M. L. Steigerwald, *Nano Lett.*, 2006, **6**, 458–462.
216. A. Mishchenko, L. A. Zotti, D. Vonlanthen, M. Bürkle, F. Pauly, J. C. Cuevas, M. Mayor, and T. Wandlowski, *J. Am. Chem. Soc.*, 2011, **133**, 184–187.
217. Y. S. Park, A. C. Whalley, M. Kamenetska, M. L. Steigerwald, M. S. Hybertsen, C. Nuckolls, and L. Venkataraman, *J. Am. Chem. Soc.*, 2007, **129**, 15768–15769.
218. C. A. Martin, D. Ding, J. K. Sørensen, T. Bjørnholm, J. M. van Ruitenbeek, and H. S. J. van der Zant, *J. Am. Chem. Soc.*, 2008, **130**, 13198–13199.
219. C. Li, I. Pobelov, T. Wandlowski, A. Bagrets, A. Arnold, and F. Evers, *J. Am. Chem. Soc.*, 2008, **130**, 318–326.
220. M. S. Hybertsen, L. Venkataraman, J. E. Klare, A. C. Whalley, M. L. Steigerwald, and C. Nuckolls, *J. Phys. Condens. Matter*, 2008, **20**, 374115.
221. S. Y. Quek, M. Kamenetska, M. L. Steigerwald, H. J. Choi, S. G. Louie, M. S. Hybertsen, J. B. Neaton, and L. Venkataraman, *Nat. Nanotechnol.*, 2009, **4**, 230–234.
222. B. Xu and N. J. Tao, *Science*, 2003, **301**, 1221–1223.
223. M. J. Ford, R. C. Hoft, and A. McDonagh, *J. Phys. Chem. B*, 2005, **109**, 20387–20392.
224. D. Naveen Kumar, N. Sudhakar, B. V. Rao, K. H. Kishore, and U. S. Murty, *Tetrahedron Lett.*, 2006, **47**, 771–774.
225. N. Griffete, F. Herbst, J. Pinson, S. Ammar, and C. Mangeney, *J. Am. Chem. Soc.*, 2011, **133**, 1646–1649.
226. P. Maity, S. Takano, S. Yamazoe, T. Wakabayashi, and T. Tsukuda, *J. Am. Chem. Soc.*, 2013, **135**, 9450–9457.
227. S. Zhang, K. L. Chandra, and C. B. Gorman, *J. Am. Chem. Soc.*, 2007, **129**, 4876–4877.
228. X. Kang, N. B. Zuckerman, J. P. Konopelski, and S. Chen, *Angew. Chem. Int. Ed.*, 2010, **49**, 9496–9499.
229. S.-W. Joo and K. Kim, *J. Raman Spectrosc.*, 2004, **35**, 549–554.

230. M. Boronat, D. Combita, P. Concepción, A. Corma, H. García, R. Juárez, S. Laursen, and J. de Dios López-Castro, *J. Phys. Chem. C*, 2012, **116**, 24855–24867.
231. M. L. Patterson and M. J. Weaver, *J. Phys. Chem.*, 1985, **89**, 5046–5051.
232. Q. Li, C. Han, M. Fuentes-Cabrera, H. Terrones, B. G. Sumpter, W. Lu, J. Bernholc, J. Yi, Z. Gai, A. P. Baddorf, P. Maksymovych, and M. Pan, *ACS Nano*, 2012, **6**, 9267–9275.
233. S.-J. Su, D. Tanaka, Y.-J. Li, H. Sasabe, T. Takeda, and J. Kido, *Org. Lett.*, 2008, **10**, 941–944.
234. M. A. Bartucci, P. M. Wierzbicki, C. Gwengo, S. Shajan, S. H. Hussain, and J. W. Ciszek, *Tetrahedron Lett.*, 2010, **51**, 6839–6842.
235. H. Tsunoyama, H. Sakurai, N. Ichikuni, Y. Negishi, and T. Tsukuda, *Langmuir*, 2004, **20**, 11293–11296.
236. H. Tsunoyama and T. Tsukuda, *J. Am. Chem. Soc.*, 2009, **131**, 18216–18217.
237. J.-M. Song, G.-D. Chiou, W.-T. Chen, S.-Y. Chen, T.-H. Kao, I.-G. Chen, and H.-Y. Lee, *Phys. Chem. Chem. Phys.*, 2011, **13**, 5099–5104.
238. J. Gao, J. Fu, C. Lin, J. Lin, Y. Han, X. Yu, and C. Pan, *Langmuir*, 2004, **20**, 9775–9779.
239. P.-L. Kuo, C.-C. Chen, and S.-M. Yuen, *J. Phys. Chem. B*, 2004, **108**, 5541–5546.
240. D. Thompson, J. P. Hermes, A. J. Quinn, and M. Mayor, *ACS Nano*, 2012, **6**, 3007–3017.
241. H. B. Lee, M. Pattarawarapan, S. Roy, and K. Burgess, *Chem. Commun.*, 2003, 1674–1675.
242. J. K. Kochi and G. S. Hammond, *J. Am. Chem. Soc.*, 1953, **75**, 3443–3444.
243. H. Gilman and N. J. Beaber, *J. Am. Chem. Soc.*, 1925, **47**, 518–525.
244. R. Fazaeli, S. Tangestaninejad, and H. Aliyan, *Can. J. Chem.*, 2006, **84**, 812–818.
245. R. C. Larock, M. J. Doty, and S. Cacchi, *J. Org. Chem.*, 1993, **58**, 4579–4583.
246. D. A. Pearson, M. Blanchette, M. L. Baker, and C. A. Guindon, *Tetrahedron Lett.*, 1989, **30**, 2739–2742.
247. R. W. Alder, P. S. Bowman, W. R. S. Steele, and D. R. Winterman, *Chem. Commun. Lond.*, 1968, 723–724.
248. J. P. Hermes, F. Sander, U. Fluch, T. Peterle, D. Thompson, R. Urbani, T. Pfohl, and M. Mayor, *J. Am. Chem. Soc.*, 2012, **134**, 14674–14677.
249. S. Chen and K. Kimura, *Chem. Lett.*, 1999, **28**, 1169–1170.
250. C. Weiping and Z. Lide, *J. Phys. Condens. Matter*, 1997, **9**, 7257.
251. S. Link, Z. L. Wang, and M. A. El-Sayed, *J. Phys. Chem. B*, 1999, **103**, 3529–3533.
252. X. Liu, M. Yu, H. Kim, M. Mameli, and F. Stellacci, *Nat. Commun.*, 2012, **3**, 1182.
253. D.-K. Bučar, A. Sen, S. V. S. Mariappan, and L. R. MacGillivray, *Chem. Commun.*, 2012, **48**, 1790–1792.
254. S.-J. Su, D. Tanaka, Y.-J. Li, H. Sasabe, T. Takeda, and J. Kido, *Org. Lett.*, 2008, **10**, 941–944.
255. Y. M. Choi-Sledeski, D. G. McGarry, D. M. Green, H. J. Mason, M. R. Becker, R. S. Davis, W. R. Ewing, W. P. Dankulich, V. E. Manetta, R. L. Morris, A. P. Spada, D. L. Cheney, K. D. Brown, D. J. Colussi, V. Chu, C. L. Heran, S. R. Morgan, R. G. Bentley, R. J. Leadley, S. Maignan, J.-P. Guilloteau, C. T. Dunwiddie, and H. W. Pauls, *J. Med. Chem.*, 1999, **42**, 3572–3587.
256. C. Fischer, J. Methot, H. Zhou, A. Schell, B. Munoz, A. Rivkin, S. Ahearn, S. Chichetti, R. Maccoss, S. Kattar, M. Christopher, C. Li, A. Rosenau, and W. C. Brown, 2010.
257. A. K. Flatt, Y. Yao, F. Maya, and J. M. Tour, *J. Org. Chem.*, 2004, **69**, 1752–1755.
258. E. Weber, H. P. Josel, H. Puff, and S. Franken, *J. Org. Chem.*, 1985, **50**, 3125–3132.
259. T. R. Hoye, P. E. Humpal, and B. Moon, *J. Am. Chem. Soc.*, 2000, **122**, 4982–4983.
260. C. Sund, O. Belda, D. Wiktelius, C. Sahlberg, L. Vrang, S. Sedig, E. Hamelink, I. Henderson, T. Agback, K. Jansson, N. Borkakoti, D. Derbyshire, A. Eneroth, and B. Samuelsson, *Bioorg. Med. Chem. Lett.*, 2011, **21**, 358–362.

261. A. Martinez, C. Hemmert, H. Gornitzka, and B. Meunier, *J. Organomet. Chem.*, 2005, **690**, 2163–2171.